Modulation of the texture and tissue fragmentation of fruits during thermal treatments by the methods of cultivation and maturation : impact on the texture of the purees

Alexandra Büergy

THÈSE DE DOCTORAT D'AVIGNON UNIVERSITÉ

École Doctorale N° 536
Agrosciences & Sciences

Spécialité / Discipline de doctorat :
Chimie

INRAE UMR 408 « Sécurité et Qualité des Produits d'Origine Végétale »

Présentée par
Alexandra Bürgy

MODULATION DE LA TEXTURE ET DE LA FRAGMENTATION TISSULAIRE DE FRUITS LORS DE TRAITEMENTS THERMIQUES PAR LES MODES DE CULTURE ET LA MATURATION : IMPACT SUR LA TEXTURE DES PURÉES

Modulation of the texture and tissue fragmentation of fruits during thermal treatments by the methods of cultivation and maturation: impact on the texture of the purees

---

Soutenue publiquement le 26/01/2021 devant le jury composé de :

M. Marc Lahaye, Directeur de Recherche-HDR, INRAE Nantes **Rapporteur**

M. Paul Menut, Professeur-HDR, AgroParisTech Paris **Rapporteur**

M. Pierre Picouet, Maître de conférences-HDR, ESA Angers **Examinateur**

Mme Catherine M.G.C. Renard, Directrice de Recherche-HDR, INRAE Nantes **Directrice de thèse**

Mme Agnès Rolland-Sabaté, Ingénieure d'étude-Dr, INRAE Avignon **Co-encadrante de thèse**

M. Alexandre Leca, Chargé de recherche, INRAE Avignon **Co-encadrant de thèse**

agropolis fondation
Supporting agricultural research for sustainable development

SQPOV
UMR408

INRAE
la science pour la vie, l'humain, la terre

To my parents Martina & Hans

Acknowledgements

Carla, thank you for our friendship from the first day of my arrival. I was lucky not only to share the same office but also a lot of time, good times and hard times, with you. I also thank Béa, Miarka, Alexandre do Brasil, Armand, Gaëtan and Thibault for making the time in Avignon unforgettable.

During my PhD thesis, I had the chance to count with three trainees, Tanagra, Hanen and Adam, who contributed with some excellent work to this thesis. I was happy to be charged with their co-supervision, a really enriching task.

I sincerely thank my family, especially my parents, for their endless love, for being always there for me and their high support. Without you, I would never have decided to go to France! I also thank Gitti, my godmother (what a nice word in English – it sums up what you are for me, a second mother), who always believed in me.

And as I always save the best for the end, I thank Hervé, who supported me with his simple presence, his motivating words and his excellent cuisine. *Je t'aime !*

Thank you, merci & danke!

Table of contents

List of figures

20

List of tables

28

List of abbreviations

A

AceA	Aceric Acid
ADP	Adenosine-5-diphosphate
AF	Arabinofuranosidase
AFM	Atomic Force Microscopy
AG I	Arabinogalactan I
AG II	Arabinogalactan II
AGP	Arabinogalactan Proteins
AIS	Alcohol Insoluble Solid
ANOVA	Analysis of Variance
ANPP	Association Nationale Pommes Poires
ANR	Agence Nationale de la Recherche (**English**: French National Agency)
Api	Apiose
Ara	Arabinose
ATP	Adenosine-5-triphosphate

B

BR	Braeburn
BRM	Mealy Braeburn

C

CAS	Chemical Abstracts Service
CB	Cold Break
CDTA	Cyclohexanediaminetetraacetic Acid
CIE	Commission Internationale de l'éclairage (English: International Commission on Illumination)
CIRAD	Centre de Coopération Internationale en Recherche Agronomique pour le Développement (**English**: Agricultural Research Centre for International Development)
CNRS	Centre National de la Recherche Scientifique (**English**: French National Centre for Scientific Research)
CPMG	Carr-Purcell-Meiboom-Gill
CTCPA	Centre Technique de la Conservation des Produits Agricoles (**English**: Technical Centre for the Conservation of Agricultural Products)
CW	Cell Wall

D

DAc	Degree of Acetylation
DAD	Diode Array Detector
DB	Degree of Blockiness
Dha	2-keto-3-deoxy-lyxo-heptulosaric Acid
DM	Degree of Methylation
DW	Dry Weight

E

eA	Endo-Arabinanase
EDTA	Ethylenediaminetetraacetic Acid
eG	Endo-β-1,4-galactanase
EC	Enzyme Commission
EGase	Endo-β-D-(1→4)-glucanase
EI	Electron Ionization
ESEM	Environmental Scanning Electron Microscopy
ET	Echo Time

F

FAO	Food and Agriculture Organization of the United Nations
FCP	Free-Choice Profiling
FID	Flame Ionization Detector
Frc	Fructose
FT-IR	Fourier-Transform Infrared
Fuc	Fucose
FW	Fresh Weight

G

G'	Storage Modulus
G''	Loss Modulus
G*	Complex Shear Modulus
GA	Gala
Gal	Galactose
β-Gal	β-Galactosidase
GalA	Galacturonic Acid
GC	Gas Chromatography
GD	Golden Delicious
GD1	Golden Delicious, reduced fruit load
GD2	Golden Delicious, high fruit load
Glc	Glucose
GlcA	Glucuronic Acid
GoS	Golden Smoothee
GPA	Generalized Procrustes Analysis
GS	Granny Smith

H

HB	Hot Break
HCl	Hydrochloric Acid
HG	Homogalacturonan
HPLC	High Pressure Liquid Chromatography
HPSEC	High Performance Size Exclusion Chromatography

I

ID	Inner Diameter
ILT	Inverse Laplace Transformation
INRAE	Institut National de Recherche pour l'Agriculture, l'Alimentation et l'Environnement (**English**: National Research Institute for Agriculture, Food and Environment)

K

Kdo	2-keto-3-deoxy-manno-octulosonic Acid
KOH	Potassium hydroxide

L

LDA	Linear Discriminant Analysis
LVER	Linear Viscoelastic Range

M

MALLS	Multi-Angle Laser Light Scattering
Man	Mannose
MeOH	Methanol
MeS	Measuring System
MS	Mass Spectrometry

N

N_A	Avogadro Number
NaCl	Sodium Chloride
NADPH	Nicotinamide Adenine Dinucleotide Phosphate
NaN_3	Sodium Azide
NaOH	Sodium Hydroxide
NeC	Negative Control
NMR	Nuclear Magnetic Resonance
NR	Not Refined

O

OAc	O-acetyl Ester
OMAFRA	Ontario Ministry of Agriculture, Food and Rural Affairs

P

PAE	Pectin acetylesterase
PAL	Pectate Lyase
PC	Principal Component
PCA	Principal Component Analysis
PG	Polygalacturonase
PL	Pectin Lyase
PME	Pectin Methylesterase
PoC	Positive Control
PPO	Polyphenol Oxidase
PSD	Pooled Standard Deviation
PWM	Pulp Wet Mass

R

RA	Refined at 1.8 mm
RA1	Refined at 1.0 mm
RA2	Refined at 0.5 mm
RgAE	Rhamnogalacturonan Acetylesterase
RGH	Rhamnogalacturonan Galacturonohydrolase
RG I	Rhamnogalacturonan I
RG II	Rhamnogalacturonan II
RH	Rhamnogalacturonan Hydrolase
Rha	Rhamnose
RID	Refractive Index Detector
RL	Rhamnogalacturonan Lyase

S

SEM	Scanning Electron Microscopy
SQPOV	Sécurité et Qualité des Produits d'Origine Végétale (**English**: Safety and Quality of Processed Fruit and Vegetables)
Suc	Sucrose

T

T_2	Transverse Relaxation Time
TA	Titratable Acidity
TEM	Transmission Electron Microscopy

U

UERI	Unité Expérimentale de Recherches Intégrées (**English**: Experimental Unit of Integrated Research)

W

WHO	World Health Organization
WIS	Water Insoluble Soldis
WP	Work Package
WRC	Water Retention Capacity

X

XGA	Xylogalacturonan
Xyl	Xylose

Y

YS	Yield Stress

Résumé

À ce jour, il y a peu de connaissance sur les facteurs qui affectent l'aptitude à la transformation des fruits et légumes et sur la façon dont les procédés peuvent être utilisés pour obtenir des produis alimentaires de qualité constante à partir de fruits et légumes hétérogènes. L'interface entre la production et la transformation est donc un point clé pour la durabilité de la chaîne alimentaire. C'est pourquoi le projet « Interfaces » (« L'interface entre production et transformation, un point clé pour relier la variabilité des matières premières et l'adaptabilité des transformations pour des systèmes alimentaires innovants ») a été créé. Il vise à comprendre l'impact d'une part des variétés, des conditions de culture, de la maturité des fruits (pommes, mangues et raisins) et d'autres part des paramètres des procédés et de leurs interactions sur les caractéristiques sensorielles, notamment la texture, des produits transformés (purées de pommes, mangues séchées et vins).

Cette thèse s'intègre dans le lot de travail 2 intitulé « Gérer la variabilité et l'hétérogénéité pendant le procédé ». La transformation des pommes en purées a été choisie en raison du grand nombre de cultivars de pomme, présentant une large gamme de caractéristiques en termes de taille et texture, mais aussi en raison de leur grande importance économique, de leur valeur nutritionnelle et de leur disponibilité sur le marché tout au long de l'année. Les purées de pommes ont gagné en importance ces dernières années avec une production de presque 350 000 tonnes par an en France. La texture des purées est un attribut de qualité majeur et donc essentiel pour un achat répété de ces produits. Bien qu'il existe certaines possibilités de moduler la texture des purées en utilisant des facteurs technologiques, la texture dépend principalement de la structure tissulaire de la matière première et des propriétés de la paroi cellulaire. Les pectines semblent jouer un rôle clé dans les mécanismes au niveau structurel puisqu'elles assurent l'adhésion cellulaire et contribuent à la résistance mécanique de la paroi cellulaire. Une meilleure compréhension de la façon dont la matière première et les conditions de traitement modifient la texture des purées aidera à concevoir des produits « naturels » sans l'ajout d'agents de texture tels que les amidons, les gommes ou les stabilisants. De plus, les caractéristiques texturales pourront ainsi être prédites et mieux contrôlées.

Au niveau scientifique, la microstructure du tissu des pommes a déjà été bien étudiée. Les pectines ont été identifiées comme les polysaccharides pariétaux qui sont responsables de l'adhésion cellulaire et qui contribuent fortement à la résistance de la

paroi végétale. La texture des purées de fruits et légumes est également bien connue. Elle est déterminée par certains facteurs structuraux, comprenant la proportion et la taille des particules ainsi que la viscosité du sérum. En revanche, le lien entre la microstructure des fruits et la texture des purées n'est pas encore compris. La manière dont le procédé peut être utilisé pour moduler les caractéristiques structurelles de la matière première afin d'obtenir la texture souhaitée demande aussi à être approfondie.

L'objectif de cette thèse est donc de mieux comprendre comment les facteurs structuraux des fruits peuvent être liés aux facteurs structuraux des purées (et donc de la texture) après cuisson et fragmentation. Un deuxième objectif porte sur la compréhension des mécanismes qui déterminent la fragmentation tissulaire.

Pour modifier la taille des cellules et la microstructure des parois cellulaires dans la matière première, plusieurs variétés et modes de culture ont été choisis. La maturation des pommes a aussi été utilisée pour moduler l'adhésion cellulaire. Pendant la transformation en purée, la microstructure de la paroi cellulaire est encore modifiée et la fragmentation tissulaire favorisée. Pour étudier l'impact du procédé sur les facteurs structuraux des fruits, la vitesse de broyage, la température et la durée de cuisson ont donc été modulées. Les facteurs structuraux des purées, comprenant la proportion et la taille des particules ainsi que la viscosité du sérum, ont ensuite été analysés et comparés en fonction des matières premières et des conditions du procédé. De la même manière, afin de clarifier la contribution des pectines sur la microstructure de la paroi cellulaire et la fragmentation tissulaire, les pectines ont été extraites, puis leur composition et leur structure ont été déterminées et comparées en fonction de la matière première et les conditions du procédé. L'impact des facteurs structuraux sur la texture des purées a également été décrit et hiérarchisé.

L'impact de la matière première sur la structure et donc la texture des purées est l'objet du premier chapitre. La microstructure des pommes a d'abord été modifiée par l'utilisation de deux variétés différentes, la modulation des pratiques culturales (irrigation et éclaircissage des fruits) et de la maturation. Toutes les pommes ont ensuite été transformées dans les mêmes conditions, seuls plusieurs niveaux de raffinage ont été appliqués. La maturité post-récolte des pommes s'est avérée être le premier facteur modulant la structure des purées, principalement par la variation de la taille des particules. Ceci pouvait s'expliquer par une dégradation des pectines, surtout une hydrolyse des chaînes latérales des rhamnogalacturonanes I, entraînant une

diminution de l'adhésion cellulaire. La fragmentation tissulaire pendant la transformation était donc facilitée et les particules dans la purée plus petites. En conséquence, la viscosité et le seuil d'écoulement des purées diminuait avec la maturité des pommes. La viscosité et le seuil d'écoulement des purées ont également été réduits par le raffinage à cause d'une réduction mécanique de la taille des particules. La taille des particules s'est ainsi montrée être le facteur structural principal qui expliquait les différences de propriétés rhéologiques des purées. Les autres facteurs structuraux des purées n'impactaient la texture qu'à taille de particules constante. Ceci était le cas dans les purées produites avec des pommes à maturité avancée.

Dans une deuxième étude, quatre variétés de pommes aux caractéristiques contrastées ont été transformées et la structure ainsi que la texture des purées ont été comparées. L'impact de l'éclaircissage des fruits et de la farinosité ont également été évalués. Deux procédés de transformation contrastés ont été utilisés afin de vérifier si la structure de la purée pouvait être liée aux caractéristiques structurelles des pommes, quel que soit le procédé appliqué. Cela a permis de montrer que la matière première modulait en effet la structure et donc la texture de la purée de manière plus importante que le procédé. Cependant, une combinaison de température et de vitesse de broyage (70 °C, 3000 tour/min versus 95 °C, 400 tour/min) pouvait augmenter l'hétérogénéité des caractéristiques structurelles et texturales des purées.

Le deuxième chapitre met l'accent sur la manière dont le procédé peut modifier les facteurs structuraux apportés par la matière première. Plusieurs études préliminaires ont été menées, dans lesquelles la vitesse de broyage, la température et la durée de cuisson ont été modulées. L'évolution de la structure et de la texture des purées a été suivie au cours du procédé afin de mieux comprendre son impact sur ces paramètres. Deux paramètres clés ont été identifiés, la température et la vitesse de broyage. Cela a été validé par une étude à grande échelle, combinant trois régimes de température et trois vitesses de broyage. Ici, une seule variété de pomme a été transformée. Par contre, les procédés ont été réalisés sur des pommes stockées en froid positif pendant un et six mois, puisque les études sur la matière première avaient montré que la maturité post-récolte des pommes est un facteur important affectant la texture des purées. Il a ainsi été prouvé que le broyage était le déterminant principal de la fragmentation tissulaire pendant le procédé. La température (entre 70 °C et 95 °C)

n'avait qu'un impact limité sur la texture de la purée de pommes. En revanche, le traitement thermique a favorisé l'hydrolyse des pectines à haute température (95 °C). Ceci a réduit l'adhésion cellulaire et donc favorisé la fragmentation tissulaire pendant le broyage, produisant des particules plus petites. Cet effet était comparable à celui entraîné par la maturation des pommes. La proportion des particules et la viscosité du sérum ont également été modifiées par le traitement thermique. Ceci s'expliquait par une meilleure solubilisation des pectines provoquant à la fois une augmentation de la viscosité du sérum et une augmentation de la proportion du volume de purée occupé par les particules. Cette augmentation était probablement due à la formation de pores plus grands dans la paroi végétale ayant entraîné de meilleures capacités de rétention d'eau. Étant donné que les pectines ainsi que la structure des purées ont été considérablement modifiées par le traitement thermique des pommes stockées pendant un mois mais pas des pommes stockées pendant six mois, l'interaction durée de stockage x température a eu un impact majeur sur les pectines. Par contre, les traitements mécaniques ont un impact mineur sur la composition et la structure des pectines.

Afin d'évaluer l'impact du procédé sur la texture perçue des purées de pommes, les échantillons issus de l'étude précédente ont été analysés par un panel sensoriel. La taille des particules est là aussi montrée être le facteur principal décrivant les différences de texture entre les purées. Par ailleurs, les purées homogènes ont été décrites comme « plus sucrées » par rapport aux purées granuleuses qui ont été perçues plus « acides », mais ces résultats pourraient être influencés par l'aspect visuel des purées.

Dans un troisième chapitre, tous les résultats ont été rassemblés et confrontés par des analyses en composantes principales. La taille des particules a été identifiée comme principal déterminant de la texture des purées de pommes. Ce facteur structural peut être modulé principalement par le broyage et la maturité des pommes. Le raffinage a pu diminuer la taille des particules et donc la viscosité des purées, excepté pour les purées produites avec des pommes à maturité avancée car la taille des cellules individuelles avait été atteinte.

En conclusion, la taille des particules a été identifiée comme le facteur majeur déterminant la texture de la purée de pomme en l'absence de concentration ou dilution. Ceci a été confirmé par une analyse sensorielle. D'autres facteurs structurels, tels que la proportion de particules et la viscosité du sérum, ont contribué à la texture de la purée à taille des particules constante. Le broyage était le facteur principal affectant la fragmentation tissulaire, et donc la taille des particules, pendant le procédé. Cette fragmentation tissulaire est facilitée par la maturation post-récolte des pommes et le traitement thermique. Ceci a pu être corrélé à une solubilisation et une dégradation des pectines, en particulier l'hydrolyse des chaînes latérales, entraînant une réduction de l'adhésion cellulaire.

Cette étude a approfondi la compréhension de la fragmentation tissulaire et des changements de texture pendant la transformation des pommes en purées. Il a également pu fournir des directives à l'industrie afin de mieux gérer la diversité et l'hétérogénéité des fruits grâce à une meilleure connaissance de la manière dont la matière première et le procédé peuvent être utilisés pour moduler la texture de la purée de pommes. Ceci va faciliter la conceptualisation de produits alimentaires innovants et plus naturels (sans agent de texture) et la mise en place d'une transformation durable (pas de reconstitution des purées).

I. Introduction

How to deal with the growing diversity and heterogeneity of agricultural raw materials and how to optimize their processing into food products, which satisfy consumer expectations and enable constant quality? These questions arise for all food processors. Especially fruits and vegetables present a large range of variability and heterogeneity, resulting from varietal effects, agronomic and pedoclimatic conditions, maturity stage and differences between individual fruits due to the position on the tree, for example. Climate change and new agricultural systems (less petrochemicals and fertilizers, development of organic production) increase variability (co-existence of different agricultural systems) and heterogeneity (more abiotic and biotic stresses) additionally and may require new varieties with improved resistance to pests or adapted to new pedoclimatic conditions. This impacts fruit quality (sugars, acids, micronutrients, colour, texture…) and causes high uncertainties on the availability of the raw material. In addition, more durable production systems induce new risks in the food chains due to the presence of mycotoxins or thermophilic bacteria on raw fruits. Processing conditions thus have to be adapted to produce safe food products. However, constant quality in the end products is important for consumer acceptance and a relevant factor for trade.

Until now, food industry manages variability and heterogeneity of raw materials by increasing standardization. A common strategy is to fractionate the raw materials and then recompose the food, sometimes by using additional ingredients. This energy-, matter- and water-intensive strategy generates pollution and thus negatively impacts sustainability.

It is known but not mastered by industry that the characteristics of the processed product mainly depend on the composition of the raw material. While sugars and acids are almost quantitatively retrieved in the processed product (Yi, et al., 2017), extractability of micronutrients, such as polyphenols, is more complex. During juice production, for example, extractability depends not only on the polyphenolic composition but also on fruit acidity, cell walls, maturity (Brahem, Eder, Renard, Loonis, & Le Bourvellec, 2017a) and external factors such as pressing temperature (Renard, et al., 2011). The question of how the raw material influences textural characteristics in the end product is the least understood as the relation is not straightforward. Although pectin polysaccharides seem to play a major role (Sila, et al., 2009), the mechanisms are little investigated. In addition, there is little knowledge on the factors

that affect the processability of fruits and vegetables and how processing can be used to diminish or enhance heterogeneity.

The collaborative project named "The interfaces between agricultural raw material and processing, a key point for bridging variability of raw materials and versatility of processing for innovative food systems" ("Interfaces") thus aims to create a research continuum between fruit production and processing in order to define possibilities during processing to best deal with variability of raw material. The questions of how fruits respond to processing and how they can be characterized in order to be used to obtain specific characteristics in the end product are thus investigated.

The "Interfaces" project is publicly funded through ANR (the French National Agency) under the "Investissements d'avenir" program with the reference ANR-10-LABX-001-01 Labex Agro and coordinated by Agropolis Fondation under the reference ID 1603-001. It is directed by Véronique Broussolle and Dominique Pallet and includes several units (**Fig. 1**) of the research institutes INRAE (Institut National de Recherche pour l'Agriculture, l'Alimentation et l'Environnement) and CIRAD (Centre de Coopération Internationale en Recherche Agronomique pour le Développement).

Fig. 1. Sponsors, partners and research units involved in the "Interfaces" project.

The project is structured into five work packages (WPs), dealing with the search for indicators and tools to better characterize the heterogeneity and processability of fruits (WP 1), the interaction between raw material and process conditions (WP 2), fruit microbiota (WP 3) and relations between physiological and transformation models (WP 4). WP 5 aims to better understand how knowledge of processability can impact relationships between different actors in the food chain.

This PhD thesis, carried out in the joined research unit SQPOV (Sécurité et Qualité des Produits d'Origine Végétale) between Avignon University and INRAE, is embedded in WP 2 entitled "Managing variability and heterogeneity in processing". This WP aims to elucidate the impact of fruit variety, growing conditions, storage duration and processing of raw fruits (apples, mangos and grapes) on the quality of end products (apple purees, dried mangos and wine) concerning textural and nutritional characteristics. The aim of this thesis was to study the impact of diversity and heterogeneity of apples during processing into puree.

Apples (*Malus x domestica* Borkh.) were selected as a model of choice not only because of their high number of cultivars displaying a wide range of fruit characteristics for size and texture, but also because of their great economic importance and availability on the market throughout the year (Ebermann & Elmadfa, 2011; Rimbach, Möhring, & Erbersdobler, 2010). In addition, epidemiological studies show that the consumption of apples reduces the risk of some cancers, cardiovascular diseases and Alzheimer's due to the high content of polyphenols and dietary fibres (Aprikian, et al., 2003; Boyer & Liu, 2004). Apples are also of high economic importance since they are the most produced fruit in whole Europe (Eurostat, 2017).
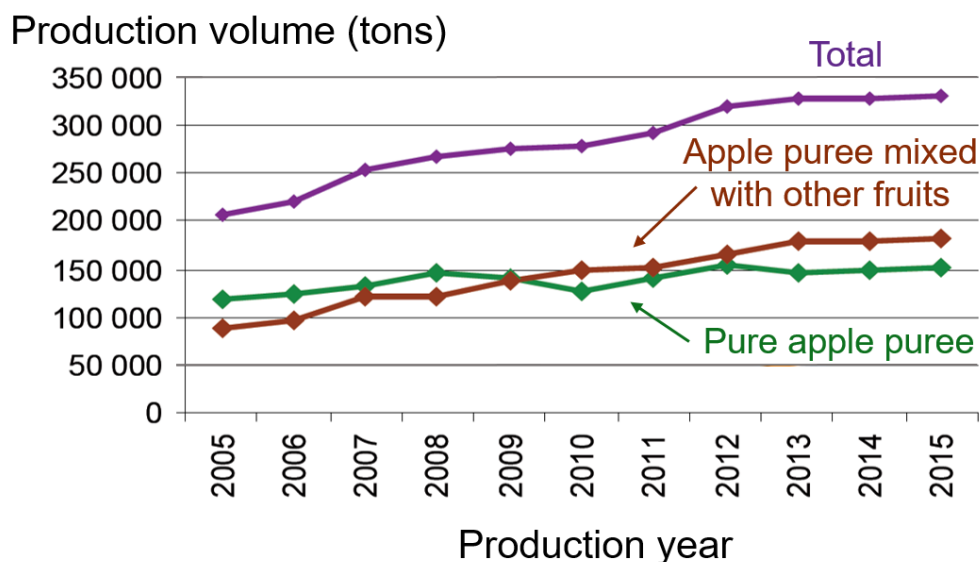
Fig. 2. Evolution of industrial production of apple puree.
Adapted from FranceAgriMer (2017).

In France, apples are also the most processed fruits (ANPP, 2020). Apart from cider production, which represents an individual industrial sector, nearly 20% of the apple stock is processed into puree (72%) and juice (17%). Since purees are appealing products that can be easily eaten and help to increase the recommended daily intake of 400 g of fruit and vegetables (WHO, 2003), consumers' demand increased in the last years. This is why the production of apple puree rose constantly over the last years (**Fig. 2**). In 2015, industrial production was split between pure apple purees (46%) and mixed purees (54%), containing apples and other fruits (FranceAgriMer, 2017).

Modulation of puree's texture by both the raw material and process conditions was considered since texture is a major quality attribute of pureed fruits and vegetables and thus a key for the liking and, in turn, repeated purchase of these products (Szczesniak & Kahn, 1971). Although there exist some possibilities to modulate puree's texture using technological factors and/or texturizing agents, puree's texture depends primarily on the original tissue structure and cell wall properties (Waldron, Smith, Parr, Ng, & Parker, 1997). Pectic polysaccharides seem to play a key role in understanding mechanisms at the structural level since they ensure cell adhesion and contribute to mechanical strength of the cell wall. A better comprehension of how the raw material and process conditions combine to create puree's texture will help to decrease losses and to valorise the resources at its best. It will also help to design both innovative and "natural" products without the addition of texture-controlling agents such as starches, gums and stabilizers. In addition, it will facilitate prediction and control of the texture of pureed food.

Thesis structure

In a first, introductive chapter, this thesis gives an **overview of existing literature** concerning raw apple characteristics, structure and function of plant cell wall components with a main focus on pectins, followed by rheological properties of apple purees. It clarifies why raw material and process conditions might influence puree's texture and why pectins could explain mechanisms at a structural level.

This points out that knowledge about how variations in the raw fruits' cellular and molecular structure determine the rheological behaviour of purees is still missing, leading to the **scientific objectives** and **research strategies** of this thesis.

The background and detailed protocols of all methods applied during this study, including information about raw materials and process conditions, are assembled in the **material and methods** section.

Results are mainly presented in the form of three research articles, studying the impact of i) apple maturation, ii) varietal effects and iii) processing on puree's texture. A first chapter is focused on the impact of raw material on puree's texture (research article I and II), whereas the second one studies the impact of processing (research article III). Exploration of process variables and a sensory study of contrasted apple purees are also included in this part. A third chapter is dedicated to the comprehension of how structural factors, altered by both raw material and process conditions, modulate apple puree's texture. It also depicts the most important parameters to alter puree's texture and summarizes the mechanisms at a microstructural level.

The results are summarized in the **conclusions** and **perspectives** are given at the end of the manuscript.

Publications and participation in congresses

The main results of this work led to three research articles:

> Buergy, A., Rolland-Sabaté, A., Leca, A., & Renard, C.M.G.C. (2020). Pectin modifications in raw fruits alter texture of plant cell dispersions. *Food Hydrocolloids*, 107, 105962.

> Buergy, A., Rolland-Sabaté, A., Leca, A., & Renard, C.M.G.C. Apple puree's texture is independent from fruit firmness. (Submitted to LWT – Food Science and Technology)

> Buergy, A., Rolland-Sabaté, A., Leca, A., Falourd, X., Foucat, L., & Renard, C.M.G.C. Pectin degradation explains tissue fragmentation of fruits during thermomechanical processes for puree production. (In preparation for submission to Food Hydrocolloids)

Development of contrasted purees made it possible to collaborate with WP 1 of the "Interfaces" project. This work was also valorised in a research article:

> Lan, W., Renard, C.M.G.C., Jaillais, B., Buergy, A., Leca, A., Chend, S., Bureau, S. Mid-infrared technique to forecast puree properties from raw apples: a potential strategy towards sustainability and precision processing. (In preparation for submission to Food Chemistry)

Two reports were prepared for the "Interfaces" project:

> INTERFACES Deliverable 2.1 – Report on impact of drought stress, fruit load and storage on plant tissue fragmentation (2018).

> INTERFACES Deliverable 2.2 – Report of modulation of apple puree texture through process variables (2019).

The results obtained during this PhD thesis allowed the participation in national and international congresses through oral presentations:

➢ Buergy, A., Rolland-Sabaté, A., Leca, A., Le Bourvellec, C., & Renard, C.M.G.C. Molecular size of soluble pectins in apple fruits is not affected by heat processing into puree. *12th International Conference on Agrophysics*. 17-19 September 2018, Lublin (Poland).

➢ Buergy, A., Rolland-Sabaté, A., Leca, A., & Renard, C.M.G.C. Modulation de la texture et la fragmentation tissulaire de fruits lors de traitements thermiques en interaction avec la matière première et sa maturation : impact sur la texture des purées. *1er colloque du GDR SLAMM*. 12-15 November 2018, Hyères (France).

➢ Buergy, A., Rolland-Sabaté, A., Leca, A., & Renard, C.M.G.C. Impact of different pre- and post-harvest treatments of apple fruits on puree's texture and on pectic polysaccharides. *12èmes Journées du Réseau Français des Parois*. 14-16 May 2019, Roscoff (France).

➢ Buergy, A., Rolland-Sabaté, A., Leca, A., & Renard, C.M.G.C. Modulation of apple puree's texture through process variables. *Fruit & Veg Processing*. 24-25 November 2020, Avignon (France).

Some results were also presented as posters:

➢ Buergy, A., Rolland-Sabaté, A., Le Bourvellec, C., & Renard, C.M.G.C. Impact of storage and process on the cell wall composition of apple purees. *Biopolymers*. 29 November-1 December 2017, Nantes (France).

➢ Buergy, A., Rolland-Sabaté, A., Leca, A., Le Bourvellec, C., & Renard, C.M.G.C. Modulating the texture of apple purees. *5th Summer Course Glycosciences*. 24-28 Juin 2018, Wageningen (The Netherlands).

I was happy that my work was further appreciated when I got a scholarship from the Provence-Alpes-Côte d´Azur (PACA) region in 2018 in form of a "bourse d´excellence entrante" (excellence scholarship for international mobility). For my presentation held at the *12th International Conference on Agrophysics* (17-19 September 2018, Lublin, Poland), I obtained the 1st price for the best oral presentation for young scientists.

II. Literature review

1. Apple fruits

1.1. Basic and economic data

Apple fruits, botanically referred to as pomes, are members of the *Rosaceae* family whereby the cultivated apples (*Malus x domestica* Borkh.) are the most common type. Their origin is supposed to be in Central Asia where they were first grown for human diet around 8000 to 2000 BC. Via the Silk Road, apple seeds finally got to China and Europe (Cornille, et al., 2012; Velasco, et al., 2010).

Today, apples are cultivated in all countries with temperate climate and they are, with more than 85 million metric tons per year, one of the most produced and consumed fruits all over the world (FAO, 2018). Behind China, Europe is the second largest apple producer worldwide (**Fig. 3**). In Europe, Poland is the leading apple producer with nearly four million metric tons in 2018, followed by Italy (2.4 million metric tons) and France (1.7 million metric tons).
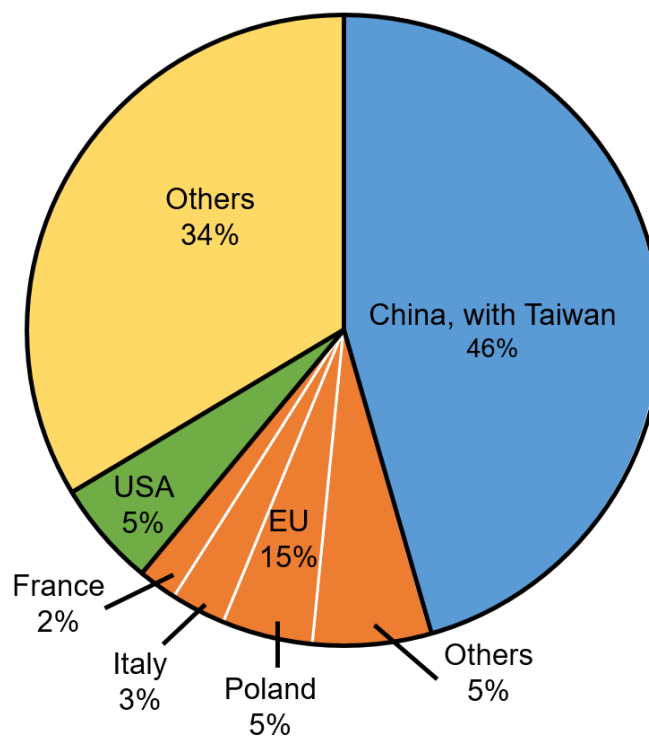
Fig. 3. Worldwide apple production in 2018.
Data from FAO (2018).

Extensive breeding of apples led to more than 7000 cultivars with many different fruit characteristics, affecting flesh texture, skin colour or taste. About 100 cultivars are grown commercially, including the most popular cultivars Fuji, Delicious, Golden Delicious, Gala, Granny Smith, Idared, Jonagold, Braeburn, Cripps Pink, Jonathan, Elstar and McIntosh (Jackson, 2003). In France, Golden Delicious (29%), Gala (20%), Granny Smith (10%), Fuji (4%) and Braeburn (4%) are the most produced cultivars (ANPP, 2020).

The leading regions in French apple production are Provence-Alpes-Côte d'Azur (25%), Midi-Pyrénées (16%) and Pays de la Loire (16%) as the climate conditions are especially favorable (FranceAgriMer, 2015). Around 50% of the French apple production are designated for fresh consumption, whereas 19% are processed. The rest is exported (ANPP, 2020).

1.2. Fruit composition

With only 54 kcal/100 g, apples are low in calories (Anses, 2020). Their chemical composition (**Table 1**) depends on the cultivar, maturity level, growing area, climate, and cultural practices (Downing, 1989).

Table 1. Averaged composition of raw apples with skin.

Component	g/100 g raw apple
Water	85.4
Carbohydrates	11.9
Therefrom monosaccharides	9.4
Therefrom fibre	2.5
Organic acids	0.5
Lipids	0.3
Proteins	0.3
Minerals	0.2

Data from Anses (2020).

Apples mainly consist of water, followed by carbohydrates, comprising simple sugars (monosaccharides), dietary fibre and starch. Starch is a polymeric carbohydrate that counts as the major energy reserve in unripe apples. Starch is composed of amylose and amylopectin, both polymers of α-D-glucose units. In amylose, those units are linked in a linear way with α-(1→4) glycosidic bonds whereas amylopectin shows α-(1→4) linked glucose chains that are branched through α-(1→6) bonds (Pérez & Bertoft, 2010). In apple fruits, the amylose content varies between 22–26% depending on the variety (Singh, Inouchi, & Nishinari, 2005). During fruit growth, apples accumulate starch to a total amount of 3–4% (fresh weight). It is then gradually hydrolysed into simple sugars, mainly fructose (6.0 g/100 g raw apple), glucose (2.0 g/100 g raw apple) and sucrose (1.4 g/100 g raw apple), during ripening (Anses, 2020).

Apples are a good source of dietary fibre. In 2009, the CODEX Alimentarius Commission defined dietary fibres as oligo- and polysaccharides that are resistant to digestion by human enzymes. They are often classified in soluble (pectins) and insoluble fibres (celluloses and hemicelluloses) but could also be grouped by their flow behaviour, fermentation rate or binding potential (Gidley & Yakubov, 2019).

The total acidity of apples depends on climate and the length of the growing period (Downing, 1989). Variations between cultivars are also considerable, with pH values ranging from 3.4 to 4.2 and the average pH lying around 3.7 (Eisele & Drake, 2005). With up to 90%, malic acid is the predominant acid in apples but citric, tartaric, lactic and oxalic acid are also present (Wu, et al., 2007; Zhang, Li, & Cheng, 2010).

Apples contain low amounts of lipids, proteins and minerals. The main mineral is potassium (119 mg/100 g raw apples with skin), followed by considerably less amounts of phosphorus (14 mg/100 g), magnesium (6 mg/100 g) and calcium (5 mg/100 g) (Anses, 2020).

The only vitamin with considerable amounts in raw apples with skin is ascorbic acid (vitamin C) with an average content of 12.8 mg/100 g (Lee, Kim, Kim, Lee, & Lee, 2003). However, apples are rich in polyphenols. These secondary plant metabolites consist of phenol structural units and are considered to interact with the plant's environment, either as attractant for pollinators or in the defence against light or pathogenic aggression. They are also potent antioxidants (Beckman, 2000).

The major class of polyphenols in apples are flavanols (**Fig. 4**A). They comprise the monomeric (+)-catechin (**Fig. 4**A$_1$) and (-)-epicatechin (**Fig. 4**A$_2$) as well as their oligo- and polymers, the procyanidins, and represent more than 80% of the total polyphenol content in apple (Le Bourvellec, et al., 2011; Wojdyło, Oszmiański, & Laskowski, 2008). Hydroxycinnamic acids (1–31%) (**Fig. 4**D), flavonols (2–10%) (**Fig. 4**B) and dihydrochalcones (0.5–5%) (**Fig. 4**E) are also present in variable amounts, depending on the cultivar. In red apples, anthocyanins (1%), the glycosides of anthocyanidins (**Fig. 4**C) are additionally found.
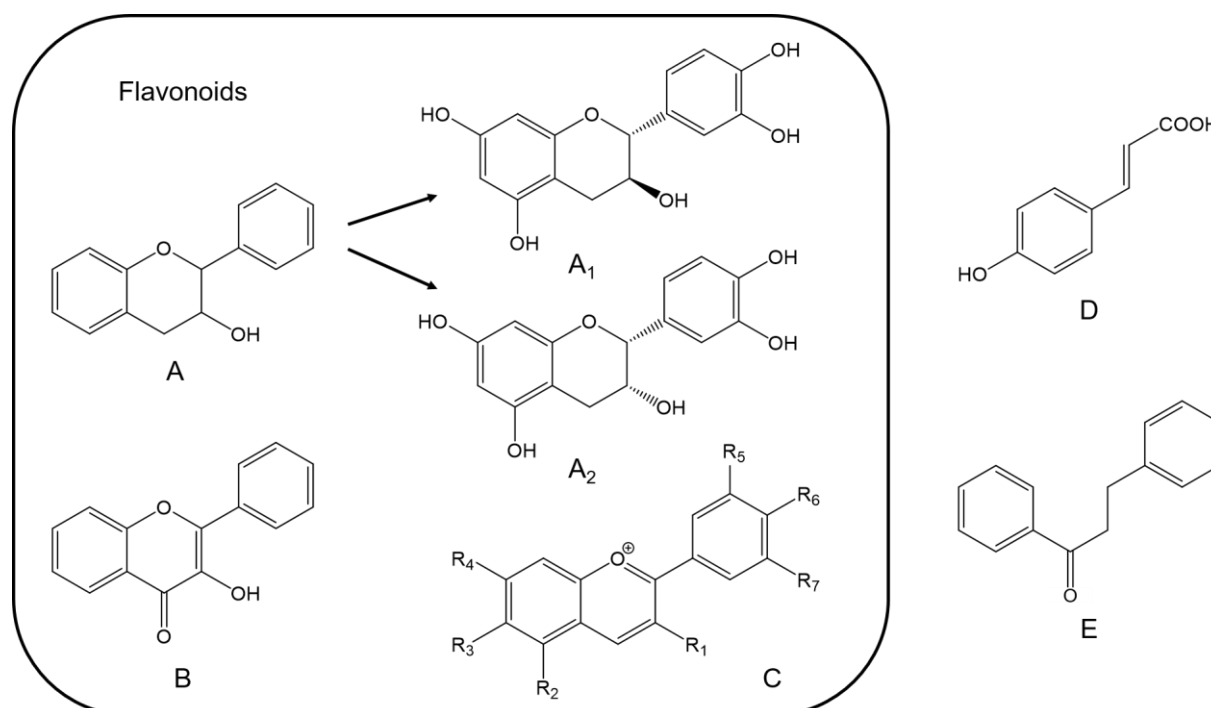
Fig. 4. Chemical structure of common polyphenols in apples.
A: Flavanol; A$_1$: (+)-Catechin; A$_2$: (-)-Epicatechin; B: Flavonol; C: Anthocyanidin; D: Hydroxycinnamic acid; E: Dihydrochalcone. Framed polyphenols are members of the flavonoid family.

Polyphenols are concentrated in the apple skin but also present in the flesh (Guyot, Marnet, Laraba, Sanoner, & Drilleau, 1998; Le Bourvellec, et al., 2011). They are responsible for the colour, flavour, taste and metabolic activity as well as enzymatic browning when they come in contact with air oxygen. Furthermore, they are associated with several health benefits in humans.

1.3. Health benefits

Several studies show evidence that a long term consumption rich in plant-based food helps to protect against cancer development and cardiovascular diseases (Bondonno, Bondonno, Ward, Hodgson, & Croft, 2017; Wang, et al., 2014).

In apples, health benefits are not only linked to the high concentration of free polyphenols (Sun, Chu, Wu, & Liu, 2002), but also to their high amount of dietary fibre. Dietary fibres are not hydrolysed in the human small intestine but fermented by the microbiota in the colon into short chain fatty acids. They consist predominantly of acetate, propionate and butyrate and are supposed to protect against intestinal cancer (Cummings, 1983). In addition, dietary fibres add bulk to the diet and the stool, reducing appetite and constipation, respectively (Dhingra, Michael, Rajput, & Patil, 2012). Increased fibre intake was also associated with a reduction of several risk factors for cardiovascular diseases such as blood pressure, cholesterol and overweight (Lairon, et al., 2005).

The health benefit of polyphenols was a long time associated with their direct antioxidative effect, able to inactivate free radicals in the human body. Recent studies negate this as it is now well known that polyphenols are metabolised after ingestion and that concentrations of polyphenols and their metabolites are not high enough in human tissues and blood plasma to exhibit significant antioxidative activity *in vivo* (Del Rio, Costa, Lean, & Crozier, 2010; Manach, Williamson, Morand, Scalbert, & Rémésy, 2005). Their interaction with the human colonic microflora is now considered more important. Aprikian, et al. (2003) showed that dietary fibres and polyphenols in apples are more effective together (whole fruit or pomaces) than separately (food supplements). This seems to be due to the higher bioaccessibility of polyphenols when linked to dietary fibres (Gidley, 2013). The ability of some polyphenols, especially procyanidins, to bind to dietary fibre is well established (Le Bourvellec, Bouchet, & Renard, 2005; Le Bourvellec, Guyot, & Renard, 2009; Renard, Baron, Guyot, & Drilleau, 2001). Together, they pass through the small intestine and reach the colon, where polyphenols are fermented into diverse phenolic acids (Bazzocco, Mattila, Guyot, Renard, & Aura, 2008). They are either absorbed or help to increase the number of beneficial microorganisms in the gut (Del Rio, et al., 2010; Tomás-Barberán, Selma, & Espín, 2016). Several bioactive effects of the absorbed metabolites are now

discussed in literature, including cell signalling and their ability to modulate the synthesis of inflammatory mediators (Fraga, Oteiza, & Galleano, 2018).

1.4. Fruit development

Apples are so called accessory or false fruits, which means that the edible flesh does not derive from the ovary but from the enlarged hypanthium of the flower (Esau, 1977). This tissue connects sepals, petals and stamen and surrounds the floral ovary that becomes the apple core during ripening (**Fig. 5**).
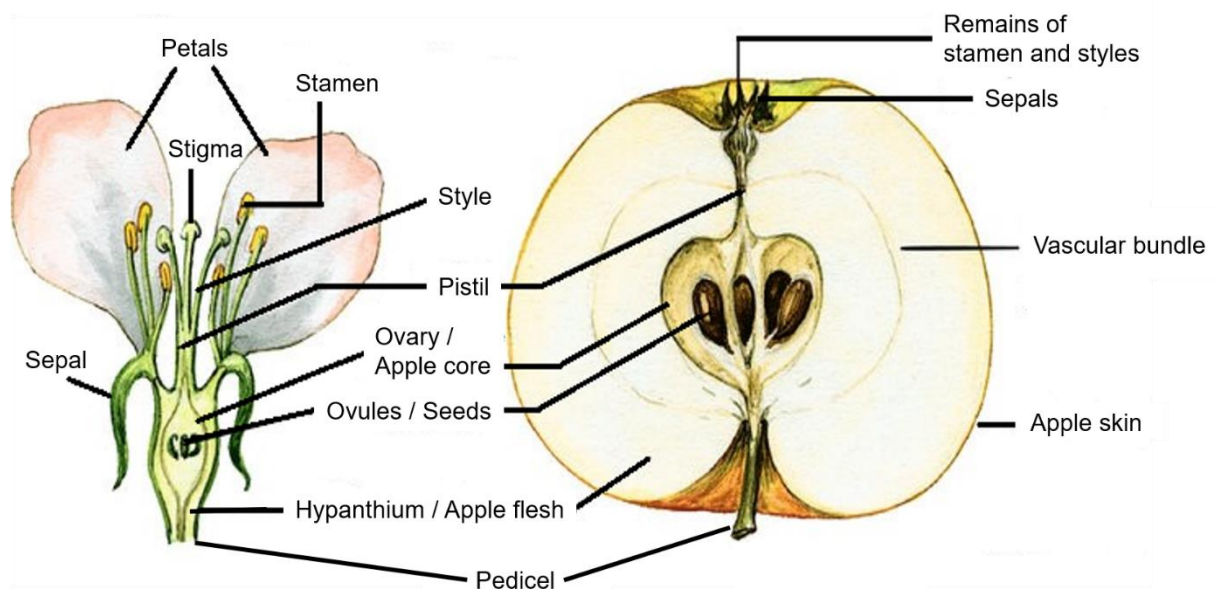
Fig. 5. Anatomy of an apple flower and a ripe apple.
Adapted from Duden (2017).

Apple fruits reach maturation about 150 days after pollination (Denne, 1963). Cell division dominates during the first period of fruit growth but ceases within three weeks after pollination. Cell expansion (Bain & Robertson, 1951; Tukey & Young, 1942), and, unlike other fruits, enlargement of air gaps between cells (Esau, 1977) then account for fruit growth (**Fig. 6**). Cellular respiration is high in the beginning of fruit development since a lot of energy is needed for cell division. The respiration rate then declines before showing a pronounced increase that marks the beginning of ripening. At the same time, ethylene is produced. This hormone controls the expression of ripening-related genes and seems to be necessary to develop skin colour and typical flavor components (Schaffer, et al., 2007). This sudden increase of cellular respiration and ethylene production is typical for climacteric fruits. Also during ripening, accumulated starch converts into simple sugars (Brookfield, Murphy, Harker, & MacRae, 1997) and the flesh softens due to cell wall changes, induced by different enzymes (Toivonen & Brummell, 2008).
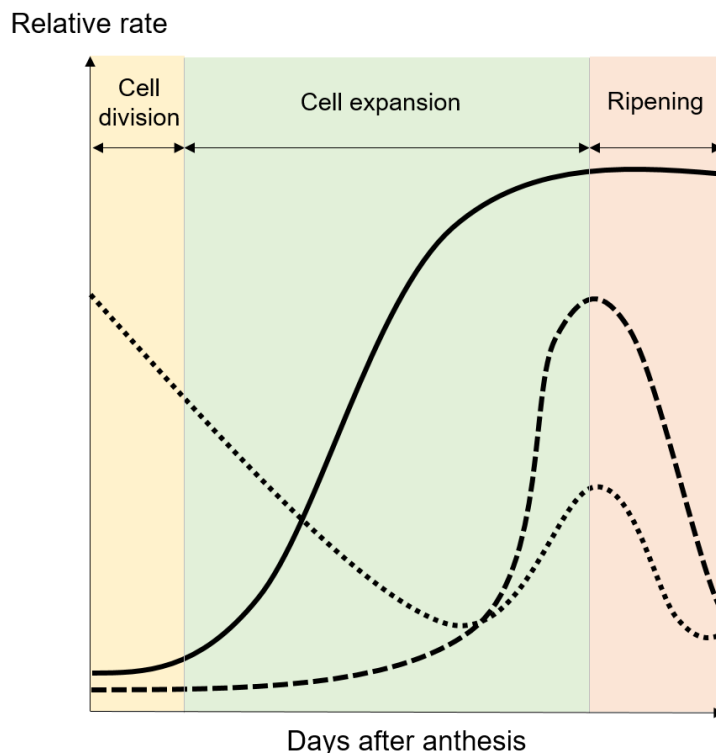
Fig. 6. Events during apple fruit development.
Adapted from Wills, McGlasson, Graham, and Joyce (2007). Continuous line represents apple fruit growth, dotted line respiration rate and dashed line ethylene production.

1.4.1. Impact of fruit thinning

The final fruit size depends mainly on the cell numbers, which are produced during the cell division period (Bain & Robertson, 1951). The fruit size can be increased when some of the apple fruitlets are removed (fruit thinning) during the first period of apple development. This can be done manually (hand thinning), or most commonly, by chemical treatment. This improves the cell division rate (Goffinet, Robinson, & Lakso, 1995) as the tree expends its energy on the fewer remaining apples. As a result, they grow larger and healthier. Depending on the apple cultivar and the thinning treatment, cell expansion can also be improved by fruit thinning (Milić, et al., 2017; Wismer, Proctor, & Elfving, 1995).

1.4.2. Impact of irrigation

Cell expansion of apples occurs mainly by carbohydrate accumulation and water uptake (Lakso, Robinson, & Pool, 1989; Pavel & Dejong, 1995). This explains why deficit irrigation reduces the final fruit size (Ebel, Proebsting, & Patterson, 1993; Lötter, Beukes, & Weber, 1985).

1.5. Parenchyma cells

The soft and edible flesh of fruits and vegetables is mainly composed of parenchyma cells (Esau, 1977). These plant cells do not only store nutrients, but also digest and metabolize them in order to gain energy and eliminate waste out of the cell to assure the functioning of the larger organism.

Apple parenchyma cells are polyhedral in shape and highly heterogeneous (**Fig. 7**A). Their morphology varies depending on the axis of observation, a phenomenon known as anisotropy (Khan & Vincent, 1990). The size of apple parenchyma cells are distributed over a wide range; cells immediately underneath the skin are small and radially flattened with a maximal diameter of 50 µm. Towards the apple core, cells become radially elongated and size increases to diameters between 200 and 300 µm (Khan & Vincent, 1990).

More recent studies confirm this range with size distributions between 50 and 150 μm in the outer section of apple tissue (Gálvez-López, Laurens, Devaux, & Lahaye, 2012) and up to 300 μm, depending on the cultivar (Hou, et al., 2016). The volume of individual cells also depends on the cultivar and ranges between 16 and 48 x 10^5 μm^3 (Smith, 1950; Volz, Harker, & Lang, 2003). Air spaces between individual cells are observed in apple parenchyma tissue (**Fig. 7**A). The volume of these air spaces accounts for 20–27% of the volume of the apple tissue (Bain & Robertson, 1951; Sterling, 1963).
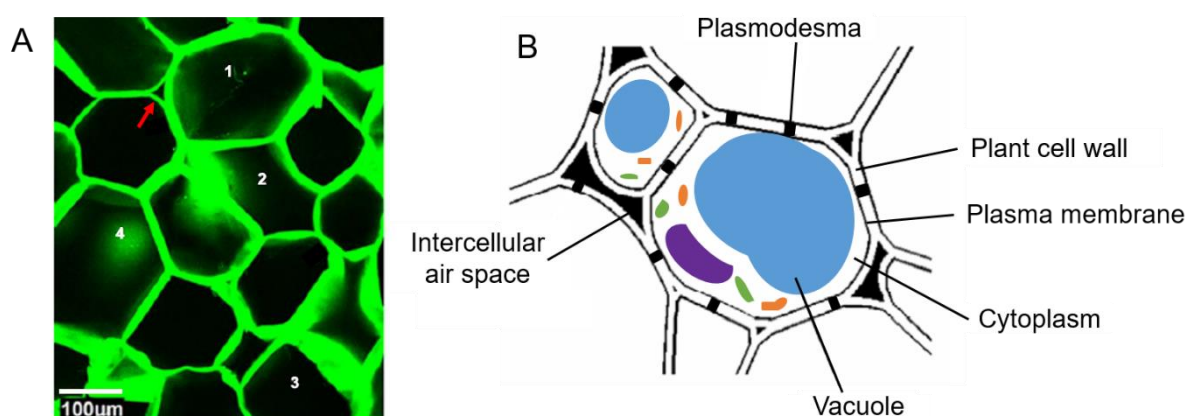
Fig. 7. Confocal laser scanning microscopy image of Fuji parenchyma tissue (A) and a scheme of apple parenchyma cells (B).

Adapted from Hou, et al. (2016) and Mebatsion, et al. (2006). 1: Cell with smooth outlines; 2: Cell with acute angles on the outline; 3: Incomplete cell on the border of the image; 4: Cell in a different layer. The red arrow indicates an intercellular air space.

The main compartment of parenchyma cells is the large central vacuole (**Fig. 7**B) which occupies up to 80–90% of the total cell volume. It allows the cell to store water as well as a variety of organic and inorganic substances such as sugars, organic acids, proteins, several vitamins and mineral nutrients. Secondary metabolites like phenolic compounds or terpenoids are also stored in the vacuole (Wink, 1997). The gel-like cytoplasm surrounds the vacuole and contains different organelles. Microscopic channels (plasmodesma) through the plant cell wall connect the cytoplasm of adjacent cells in order to transport nutrients and to enable intercellular communication. The cytoplasm creates a turgor pressure, which acts against the plasma membrane. Due to the semipermeable character of the plasma membrane, osmosis is allowed.

A thin (0.1 to 10 µm) and semi-rigid cell wall surrounds this complex (Cosgrove, 2005). The detailed function, components and structure of plant cell walls will be discussed in the next section.

2. Plant cell wall

2.1. Generalities

The plant cell wall is a complex macromolecular layer, which encloses the plasma membrane. It forms a strong network, supporting the plasma membrane and preventing it from bursting under the turgor pressure contained osmotically within the cell (Cosgrove, 2005; Fricke, Jarvis, & Brett, 2000). It also provides a structural barrier that helps to protect against pest and pathogen invasion (Darvill, McNeil, Albersheim, & Delmer, 1980).

The cell wall of apple parenchyma cells consists of two layers, the middle lamella and primary cell wall (**Fig. 8**). The colloidal middle lamella is situated between primary cell walls of adjacent cells, holding them together and thus, ensuring cohesion of the tissue (Thakur, Singh, & Handa, 1997). The middle lamella is almost only composed of pectic polysaccharides, accompanied by proteins (Carpita & Gibeaut, 1993; Jarvis, 1984), but without cellulose (Guillemin, et al., 2005; Knox, 2008). During cytoplasmic division, it is the first cell wall layer that is formed, allowing room for expansion during growth (Heredia, Jimenez, & Guillen, 1995).
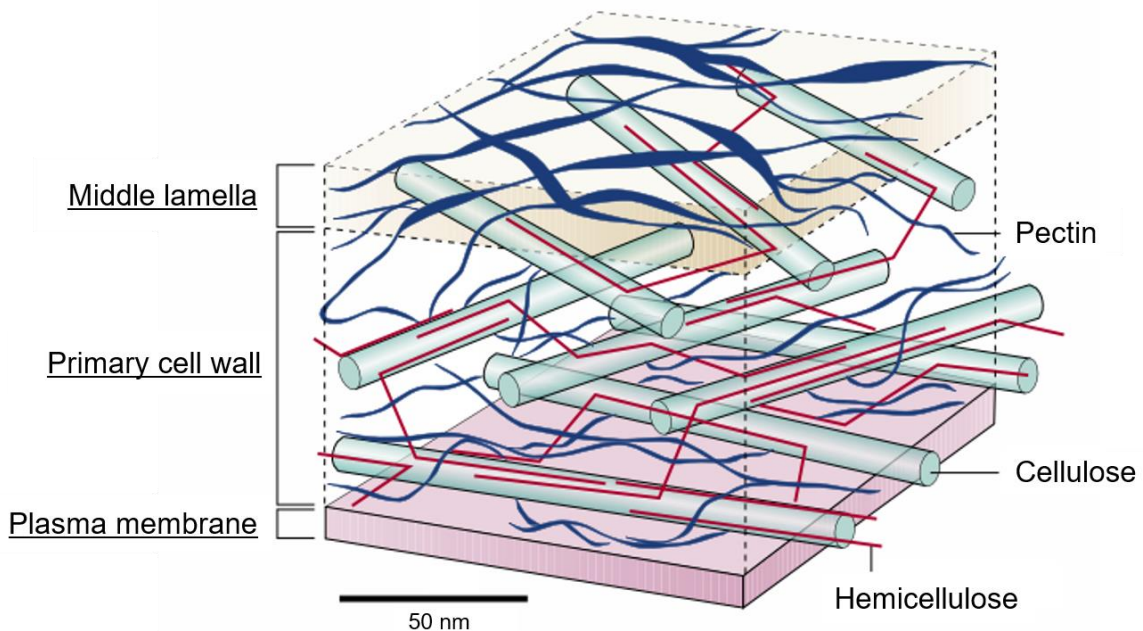
Fig. 8. Scheme of a plant cell wall.
Adapted from Smith (2001).

Primary cell walls are located between the plasma membrane and the middle lamella. They are thin, flexible and non-lignified but thicken during cell growth and thus represent the structural skeleton of the fruit (Gibson, 2012). Long microfibrils of cellulose run through a hydrated matrix of hemicellulose and pectins (Carpita & Gibeaut, 1993; Mohnen, 2008), allowing cell expansion during fruit growth (Cosgrove, 2005; Taylor, 2008).

The edible part of fruit parenchyma has, except conductive tissues, only a primary cell wall (Gibson, 2012; Renard, 1989). Some other plant cells, for example in wood, also have a secondary cell wall. This supplementary layer is synthesised between the primary cell wall and the plasma membrane when cell growth has stopped (Cosgrove, 2005; Taylor, 2008). It is thicker than the primary cell wall and contains a higher amount of cellulose but no pectins and proteins (Raven, Evert, & Eichhorn, 1999; Ridley, O'Neill, & Mohnen, 2001). Furthermore, it is lignified (Heredia, Guillen, Jimenez, & Fernandez-Bolanos, 1993; Jiménez, Labavitch, & Moreno, 1994), providing additional strength and structural support to the plant and forming a barrier against pathogen invasion (Wilson, Jarvis, & Duncan, 1989).

Two sorts of proteins are present in the plant cell wall, being enzymes and structural proteins. Enzymes catalyse a series of chemical reactions that are important for cell growth and fruit ripening. Structural proteins probably further strengthen the cell wall and might be involved in regulatory pathways (Caffall & Mohnen, 2009). Structural proteins are typically rich in hydroxyproline (Caelles, Delseny, & Puigdomenech, 1992), but high amounts of alanine, serine and threonine were also found (Showalter, 1993). Extensin and arabinogalactan proteins (AGP) are members of the hydroyproline-rich glycoproteins. AGPs are anchored to the plasma membrane and could be a good candidate to link the cell wall to the plasma membrane (Leszczuk, Chylinska, & Zdunek, 2019).

2.2. Plant cell wall polysaccharides

Cellulose (15–40% of cell wall dry weight), hemicelluloses (20–30%) and pectins (30–50%) are the three main classes of polysaccharides that have been detected in the complex primary plant cell wall (Cosgrove & Jarvis, 2012; Fischer & Bennett, 1991; Jarvis, 2011). Together, they make up about 80% of the primary cell wall of apple fruits (Renard & Thibault, 1993). The remaining 20% are composed of proteins and phenolic compounds.

2.2.1. Cellulose

Cellulose is an important structural and supporting polysaccharide of primary plant cell walls. Due to its crystalline and para-crystalline structure, it is much more ordered than any other component of the primary cell wall and thus provides both elasticity and tear strength. Consequently, it affects textural characteristics of plant based food, such as crispness of apple tissue (Cybulska, Zdunek, Psonka-Antonczyk, & Stokke, 2013; Jarvis, 2011).
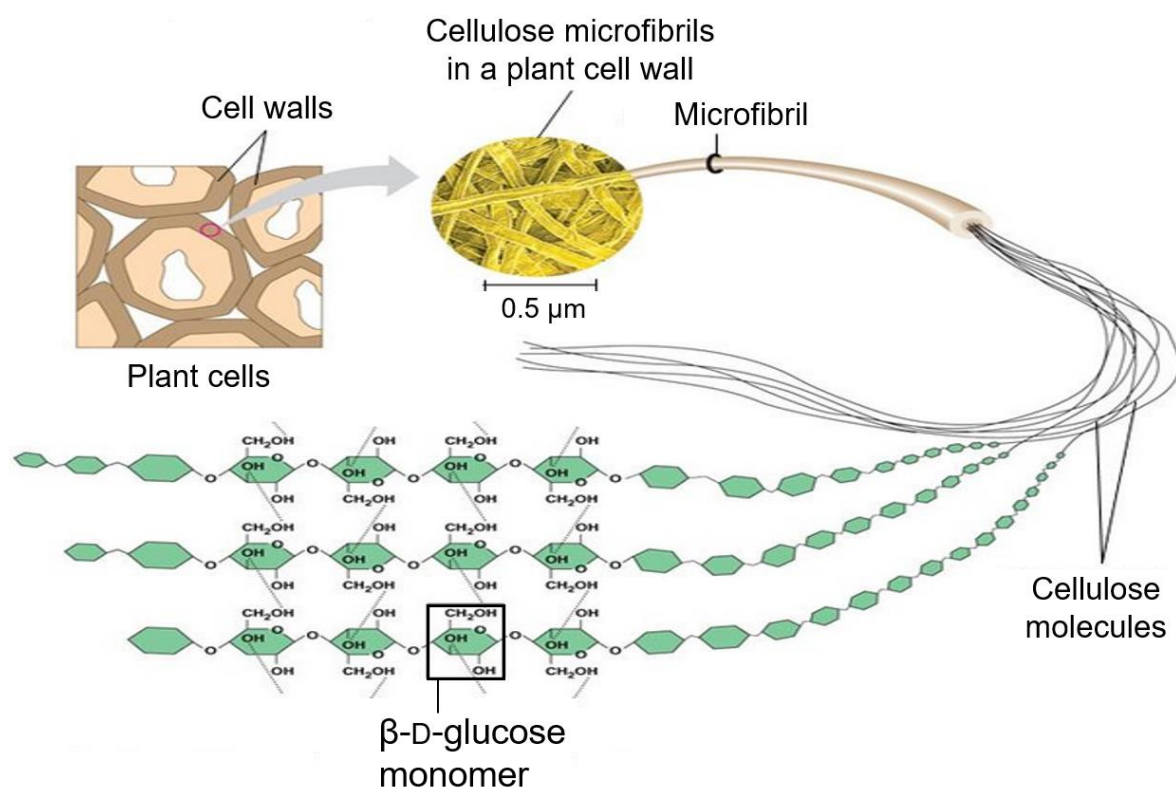
Fig. 9. Chemical structure of cellulose.

Adapted from Pearson-Education (2005).

From a structural perspective, a cellulose molecule (**Fig. 9**) consists of a linear chain of several thousand β-(1→4)-linked D-glucose units. Glucose chains form extremely long and narrow cellulose microfibrils, each about 3 nm in diameter (Jarvis, 2011). They are densely packed and thus extremely firm due to extensive intra- and intermolecular hydrogen bonds, helping to exclude water from between cellulose chains (Taylor, 2008).

2.2.2. Hemicellulose

Hemicelluloses are a very complex group of polysaccharides. They stabilize the cellulose network in plant cell walls as they are able to cross-link cellulose microfibrils by hydrogen bonds and, probably, other interaction mechanisms (Fujino, Sone, Mitsuishi, & Itoh, 2000; Martinez-Sanz, Mikkelsen, Flanagan, Gidley, & Gilbert, 2017; McCann, Wells, & Roberts, 1990). This results in cell strengthening and a high resistance to enzymatic digestion (Cosgrove, 2005).

From a chemical point of view, hemicelluloses are branched polysaccharides with a mixed sugar content showing a β-(1→4)-linked D-pyranosyl backbone that have the O-4 in the equatorial position (O'Neill & York, 2003). The chemical structure of hemicellulose molecules include mannose, xylose, glucose, galactose and arabinose as the most important but not the only monomers (Ebermann & Elmadfa, 2011).

The detailed structure of hemicelluloses differs depending on plant species and cell types. The most representative hemicelluloses found in primary cell walls of apples are xyloglucans, glucomannans and arabinoxylans (Dheilly, et al., 2016; Ray, Vigouroux, Quémener, Bonnin, & Lahaye, 2014; Voragen, Schols, & Pilnik, 1986b).

The backbone of xyloglucans (**Fig. 10**A) is composed of β-(1→4) linked D-glucose residues, most of which are substituted by side chains with (1→6) linked xylose. The xylose residues are often connected to a galactose residue, which can be followed by a fucose residue. In the primary cell wall of apple fruits, fucogalactoxyloglucan is the main hemicellulose, showing a sugar molar distribution of fucose:galactose:xylose:glucose of 1:1.5:3.5:7 (Renard, Voragen, Thibault, & Pilnik, 1990).

Glucomannans (**Fig. 10**B) consist of a chain of irregularly linked β-1,4-mannose and β-1,4-glucose units (Heredia, et al., 1995).

Arabinoxylans (**Fig. 10**C) show a backbone of β-(1→4) linked xylopyranoses, which are mainly linked to α-L-arabinose in the (1→2) or (1→3) position. Some xylose residues can be acetylated.
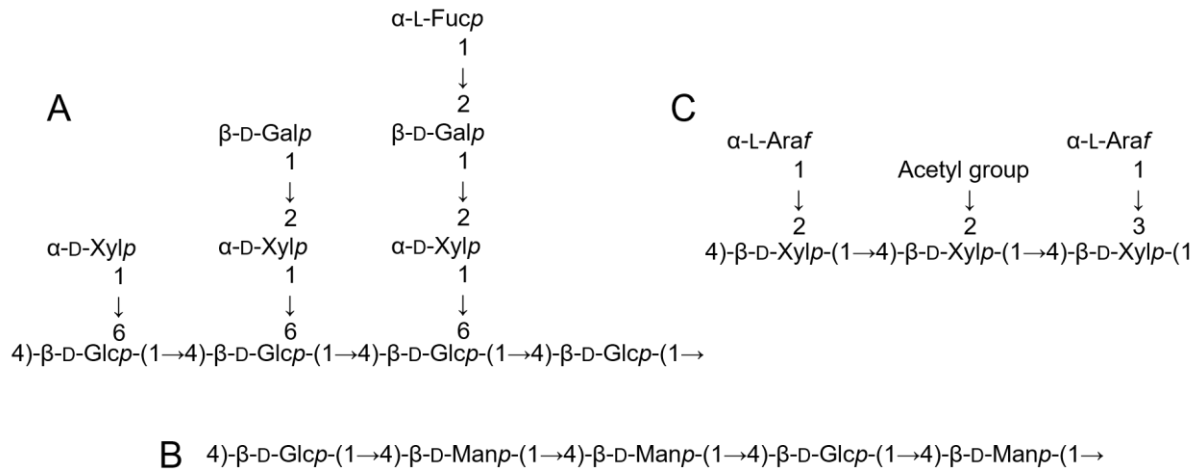
Fig. 10. Chemical structure of xyloglucan (A), glucomannan (B) and arabinoxylan (C). Ara: Arabinose; Gal: Galactose; Glc: Glucose; Man: Mannose; Xyl: Xylose.

2.2.3. Pectins

Pectins are a group of extremely complex and structurally diverse polysaccharides, rich in covalently linked D-galacturonic acid. Their biosynthesis requires specific nucleotide-sugar substrates and several glycosyltransferase enzymes. It is supposed to occur in the Golgi apparatus since some pectin biosynthetic enzymes and active sites were located in the Golgi (Geshi, Jørgensen, & Ulvskov, 2004; Nunan & Scheller, 2003; Sterling, Quigley, Orellana, & Mohnen, 2001). Pectins may then be transported by Golgi vesicles to the plasma membrane before insertion into the cell wall (Caffall & Mohnen, 2009).

Depending on their composition, which differs between the middle lamella and the primary cell wall (Jarvis, Briggs, & Knox, 2003; Selvendran, 1985), they exhibit different functions. They affect not only mechanical properties of the plant tissue, but are also implicated in defence mechanisms of the primary cell wall. Through several interactions between themselves and other cell wall polysaccharides, they contribute to intercellular adhesion and regulate cell wall porosity and water content (Bidhendi & Geitmann, 2016; Caffall & Mohnen, 2009).

Until now, three main pectic polysaccharides have been isolated from plant cell walls and structurally characterized, comprising homogalacturonan, rhamnogalacturonan I and substituted galacturonans (O'Neill, Albersheim, & Darvill, 1990; Visser & Voragen, 1996).

2.2.3.1. Structure

Homogalacturonan (HG)

HGs are the most abundant fraction, as they account for around 60% of pectin molecules (Voragen, Coenen, Verhoef, & Schols, 2009). They are composed of a long, linear chain of α-D-(1→4)-galacturonic acids (**Fig. 11**). HG stretches were estimated to contain a minimum of 72–100 galacturonic acid residues (Thibault, Renard, Axelos, Roger, & Crepeau, 1993). Some of the carboxyl groups in the galacturonic acid backbone are methyl-esterified at C6, and can also be O-acetylated at O-3 or O-2 (Ishii, 1995, 1997).
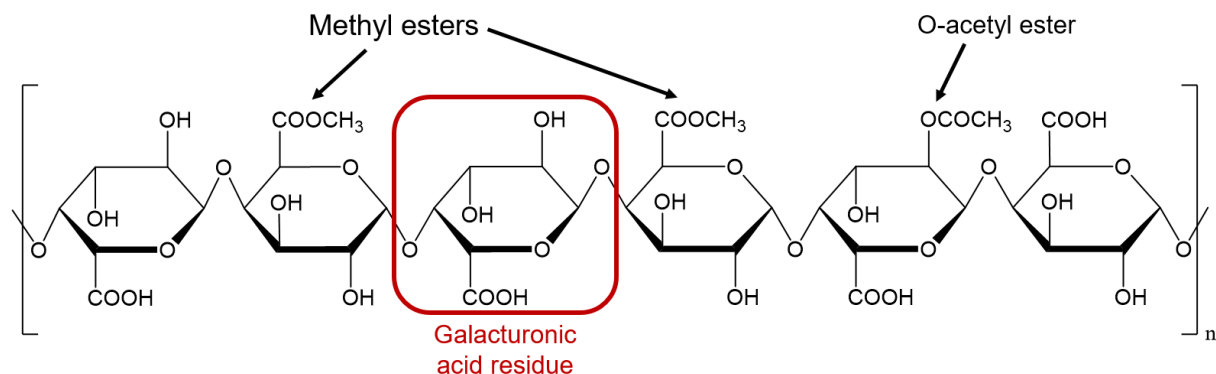
Fig. 11. The primary structure of homogalacturonan.

The degree of methylation (DM) of HG molecules is described as the proportion between methyl-esterified galacturonic acids to 100 galacturonic acid residues. Apple pectins possess a high DM, which means that more than 50% of the galacturonic acids are methylated (Billy, et al., 2008; Fischer & Amado, 1994). The degree of acetylation (DAc) describes the number of acetyl groups in 100 galacturonic acid residues. It is rather low (2–6%) in apples (Billy, et al., 2008; Voragen, Schols, & Pilnik, 1986a) but can be up to 43% in sugar beet pectins (Levigne, Thomas, Ralet, Quéméner, & Thibault, 2002).

Depending on the DM, HG chains may self-associate; an unmethylated and negatively charged C6 position of the HG backbone may ionically interact with calcium-ions to form a stable gel with other HG molecules (**Fig. 12**) if more than 10 consecutive unmethyl-esterified galacturonic acid residues are coordinated (Kohn & Luknár, 1977). This hypothetical conformation was named "egg-box"-model (Grant, Morris, Rees, Smith, & Thom, 1973) but nobody has isolated this conformation so far. The anionic cross-links between individual HG chains are discussed to be involved in cell wall porosity and strengthening. In addition, HGs, together with some structural proteins, are the sole pectin fraction present in the middle lamella. Especially low methyl-esterified HGs were found in this region and could contribute to intercellular adhesion via calcium cross-links (Ridley, et al., 2001; Thakur, et al., 1997; Wolf, Mouille, & Pelloux, 2009).
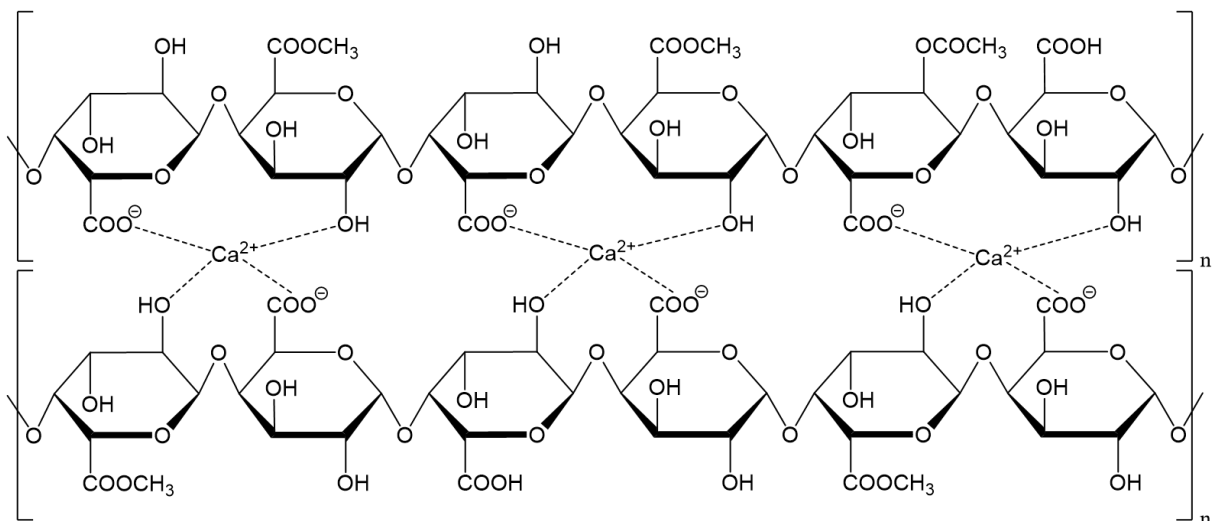
Fig. 12. "Egg-box"-model induced by calcium cross-links of homogalacturonan molecules.

In food industry, knowledge of the DM and DAc is crucial as the extent of methylation and acetylation affects the gelling properties of pectins. Solutions of low methylated HG pectins start gelling with calcium ions according to the "egg-box"-model. High methylated pectins need low pH and water activity to induce gelling. Low pH reduces electrostatic repulsions through protonation of carboxylate residues, while low water activity promotes chain-chain interactions. Dissolved sugars such as sucrose, glucose or fructose are usually used to reduce water activity. High-methylated HGs then assemble through intermolecular hydrogen bonds and hydrophobic interactions

between methyl esters (Chan, Choo, Young, & Loh, 2017). This mechanism is, for example, used in the production of jams.

The way in which the methoxy-esters are distributed over the galacturonan backbone is called "degree of blockiness" (DB). It was proposed by Daas, Meyer-Hansen, Schols, De Ruiter, and Voragen (1999) and describes the percentage of non-esterified mono-, di- and tri- galacturonic acid residues, liberated from enzymatic degradation of pectin, to the total number of non-esterified galacturonic acid residues in pectin. This characteristic also influences the gelling properties of HG pectins (Chan, et al., 2017). For example, high methylated citrus pectins show shorter gelation times when the methyl esters are distributed in a blockwise way (Löfgren, Guillotin, Evenbratt, Schols, & Hermansson, 2005).

Traditionally, the linear HGs are illustrated as "smooth" regions in the pectin molecule (**Fig. 13**). The "hairy" regions represent a pectin fraction with long and numerous side chains (De Vries, Rombouts, Voragen, & Pilnik, 1982; Padayachee, Day, Howell, & Gidley, 2017; Voragen, Pilnik, Thibault, Axelos, & Renard, 1995). They will be detailed in the next section.
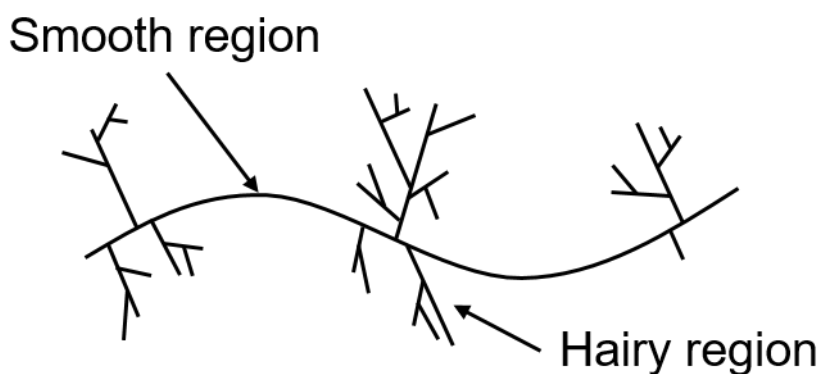
Fig. 13. Scheme of "smooth" and "hairy" regions in pectin molecules.

Rhamnogalacturonan I (RG I)

RG I makes up about 20–35% of the pectin molecule (Mohnen 2008). It exhibits a backbone of repeating α-D-(1→4)-galacturonic acid and α-L-(1→2)-linked rhamnosyl residues (**Fig. 14**A), present in a ratio of approximately 1:1 (Ridley, et al., 2001). The alternating order of galacturonic acid and rhamnose residue induces a "kink" in the RG I backbone (Rees & Wight, 1971). In long sequences, however, the extended chain

conformation of pectin is little affected since the kinking effects of consecutive rhamnose units are cancelled out, leading to a loose spiral (Cros, Garnier, Axelos, Imberty, & Perez, 1996; Pérez, Mazeau, & Hervé du Penhoat, 2000).

A variable portion (20-80%) of the rhamnosyl units are substituted at O-4 (mainly) and/or O-3 (scarcely) with neutral or acidic oligosaccharide side chains (O'Neill, et al., 1990). The extent and detailed structure of the lateral chains depend both on the pectin source and the isolation method (Albersheim, Darvill, O'Neill, Schols, & Voragen, 1996; Ridley, et al., 2001; Vincken, et al., 2003). The galacturonic acid residues are usually not linked to lateral chains. However, a minor part of galacturonic acid (2%) was found to be substituted with a single glucuronic acid in the RG I backbone of sugar beet pectin (Renard, Crepeau, & Thibault, 1999).

The predominant side chains are linear and branched α-L-arabinofuranosyl, and/or β-D-galactopyranosyl residues leading to α-L-(1→5)-arabinans (**Fig. 14**B), β-D-(1→4)-galactans (**Fig. 14**C), arabinogalactan I (AG I) (**Fig. 14**D), arabinogalactan II (AG II) (**Fig. 14**E), and possibly galacto-arabinans (**Fig. 14**F) (Obro, Harholt, Scheller, & Orfila, 2004; Tharanathan, Changala Reddy, Muralikrishna, Susheelamma, & Ramadas Bhat, 1994; Yapo, Lerouge, Thibault, & Ralet, 2007). The galacturonic acid residues in the RG I backbone may be O-acetylated on O-2 and/or O-3 (Komalavilas & Mort, 1989). Although methylation of the RG I backbone is rare and unexpected as this type of pectin is not degraded by β-elimination (Kravtchenko, Arnould, Voragen, & Pilnik, 1992), a fraction of flax RG I showed 40% methyl esters (Rihouey, et al., 1995).

RG I pectins are generally absent or in low amounts in the middle lamella, but high amounts are found in the primary cell wall. There, they bind non-covalently to cellulose (Zykwinska, Ralet, Garnier, & Thibault, 2005) and hemicellulose (Popper & Fry, 2005) via their side chains. The close association of RG I side chains with the cell wall may restrict the access of cell wall-modifying enzymes and thus improve the structural integrity of the cell wall (Ng, et al., 2015). Actually, decreased amounts of RG I side chains were shown to correlate positively with loss of apple fruit firmness (Lahaye, Bouin, Barbacci, Le Gall, & Foucat, 2018; Pena & Carpita, 2004; Winisdorffer, et al., 2015) and elevated levels of galactan side chains were associated with reduced cell wall porosity (Ng, et al., 2015).
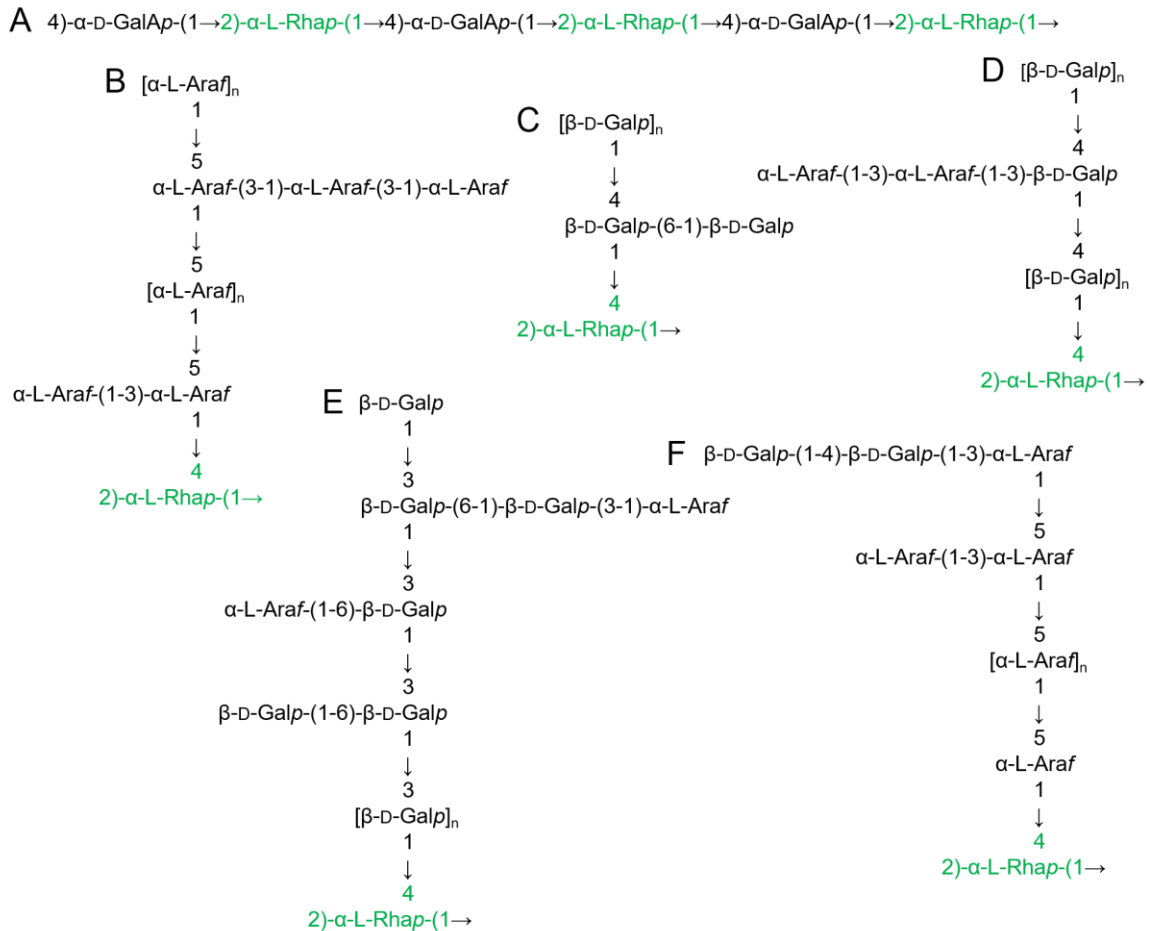
Fig. 14. Structure of the RG I backbone (A) and examples of representative side chains arabinan (B), galactan (C), arabinogalactan I (D), arabinogalactan II (E) and galacto-arabinan (F).

Ara: Arabinose; Gal: Galactose; GalA: Galacturonic acid.

Substituted Galacturonans

Substituted galacturonans possess the same linear backbone of α-D-(1→4)-linked galacturonic acid residues as in HGs (O'Neill, et al., 1990). Unlike HG, the backbone is decorated by several neutral sugars, which can lead to extremely complex pectin fractions. Rhamnogalacturonan II (RG II), xylogalacturonan (XGA) and apiogalacturonan are the most important substituted galacturonans.

The galacturonic acid backbone of RG II is partially methyl-esterified at C6 and carries six (A–F) complex oligosaccharide chains consisting of 12 different glycosyl residues in over 20 different linkages (**Fig. 15**). RG II contains some rare sugars such as D-apiose, L-aceric acid or L-galactose (Mohnen, 2008). Side chains comprise an

octasaccharide, a nonasaccharide, both attached to the C2 position of some of the galacturonic acid residues, two structurally different disaccharides and two monosaccharides, all attached to C3 of the backbone (Hervé du Penhoat, Gey, Pellerin, & Perez, 1999; Ndeh, et al., 2017; Vidal, et al., 2000).
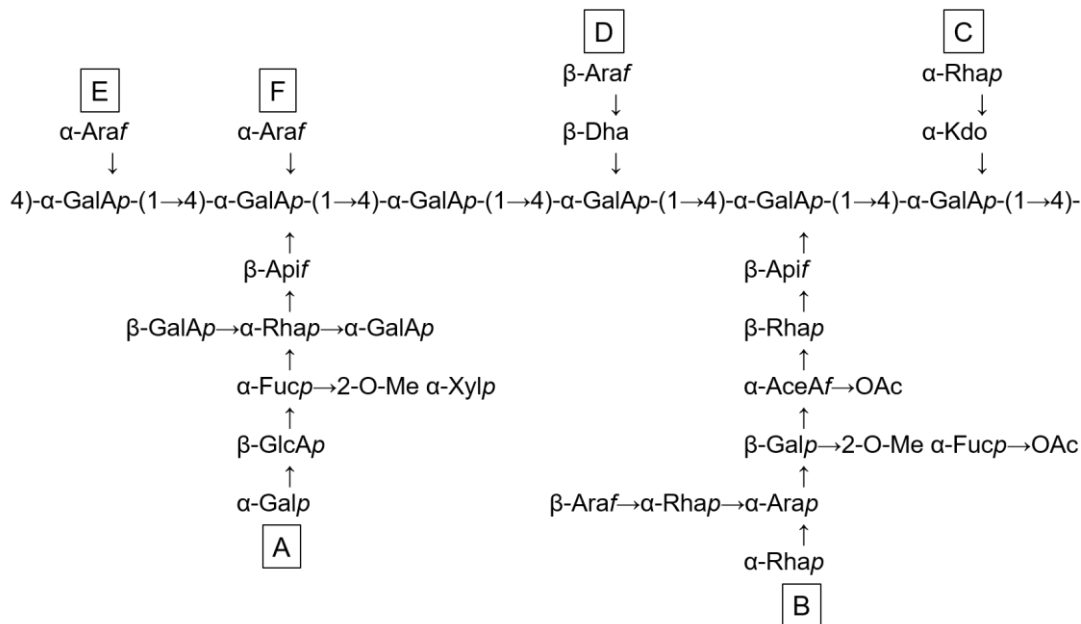
Fig. 15. The primary structure of rhamnogalacturonan II with side chains A–F. AceA: Aceric acid; Api: Apiose; Ara: Arabinose; Dha: 2-keto-3-deoxy-lyxo-heptulosaric acid; Fuc: Fucose; Gal: Galactose; GalA: Galacturonic acid; GlcA: Glucuronic acid; Kdo: 2-keto-3-deoxy-manno-octulosonic acid; Rha: Rhamnose; OAc: O-acetyl ester; 2-O-Me Fuc: 2-O-methyl fucose; 2-O-Me Xyl: 2-O-methyl xylose.

Together with HGs and RG I, RG II are found in the primary cell wall, where they exist predominantly as RG II dimers (**Fig. 16**). The apiosyl residues of side chain A in each monomeric RG II subunit can cross-link between the OH-2 and OH-3 position by a 1:2 borate-diol ester in a self-assembled process (Ishii, et al., 1999; Kobayashi, Matoh, & Azuma, 1996; O'Neill, Ishii, Albersheim, & Darvill, 2004). The formation of two diastereomers is possible (**Fig. 16**) although the natural occurrence of one or both is not clarified (Ishii & Ono, 1999; O'Neill, et al., 1996). *In vitro*, the optimum pH for dimer formation is between pH 3 and 4 (O'Neill, et al., 1996) and di- and trivalent cations with an ionic radius higher than 1 Å increase the reaction rate (Ishii, et al., 1999).
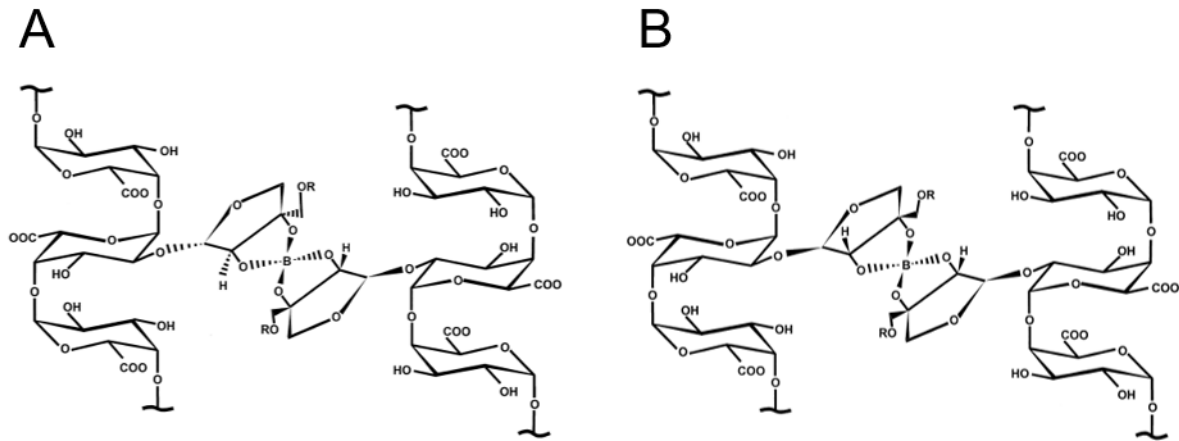
Fig. 16. Borate 1:2 diol ester between apiosyl residues of two monomeric units of RG II in two isoforms A and B.
Taken from Ridley, et al. (2001).

RG II presents up to 10% of the entire pectic polysaccharide, but the ubiquitous character of RG II indicates that it must play a specific role *in planta* (O'Neill, et al., 2004). Borate cross-links were shown to play a key role in normal plant growth and development (O'Neill, Eberhard, Albersheim, & Darvill, 2001) and cell adhesion (Iwai, Masaoka, Ishii, & Satoh, 2002). The porosity of the pectic network could also be affected by dimer formation (Brummell & Harpster, 2001).

In the cell walls of apples (Schols, Bakx, Schipper, & Voragen, 1995) but also in pea hulls (Renard, Weightman, & Thibault, 1997) and carrots (Kikuchi, Edashige, Ishii, & Satoh, 1996), another substituted galacturonan, XGA is found. In this fraction, β-D-xylosyl residues are attached to the C3 position of the linear backbone composed of α-D-(1→4)-galacturonic acid residues. In apples, the degree of xylosidation is around 75% in this specific fraction (Schols, et al., 1995).

Apiogalacturonans are rare and were only found in the primary cell wall of aquatic plants of the subfamilies Lemnoideae (duckweed) and Zosteraceae (eelgrass). Apiogalacturonans are reported to contain side chains of single and (1→5)-linked D-apiofuranose residues, which are attached to the backbone of α-D-(1→4)-galacturonic acid molecules (Patova, Golovchenko, & Ovodov, 2014). Their functions are not yet understood but a high amount of apiogalacturonan was associated with rapid growth (Pagliuso, Grandis, Igarashi, Lam, & Buckeridge, 2018).

2.2.3.2. Pectin conformation in solution

Pectins generally exhibit a semi-flexible conformation in solution (Cros, et al., 1996; Hourdet & Muller, 1991; Morris, Ralet, Bonnin, Thibault, & Harding, 2010). The extend of flexibility depends on their DM, HG proportion and RG I side chains (Axelos & Thibault, 1991; Morris & Ralet, 2012). HG domains are less flexible (Cros, et al., 1996) than RG I domains because of the higher flexibility due to greater conformational freedom of rhamnose residues (Ralet, et al., 2008). Pectin flexibility thus increases generally with the amount of RG I and HG chain flexibility generally increases with DM and at acidic pH values, where galacturonic acid residues are fully protonated (Alba, Bingham, Gunning, Wilde, & Kontogiorgos, 2018).

2.2.3.3. Pectin domain linkage

Although the structure of different pectin fractions is rather well described, the linkage between them is still under debate. In primary cell walls, the pectin elements seem to be covalently linked since harsh chemical treatments or digestion by pectin-degrading enzymes are required to isolate them individually (Mohnen, 2008). Several models thus exist in literature.

Traditional model (De Vries, et al., 1982; Schols & Voragen, 1996; Voragen, et al., 1995)

After enzymatic degradation of apple pectins and subsequent fractionation, De Vries, et al. (1982) proposed a model, in which linear blocks of homogalacturonan ("smooth" regions) alternate with branched RG I blocks ("hairy" regions). Later, covalent bonds between both HG and XGA to RG I via α-(1→2) linkages were shown for the first time by controlled acid hydrolysis of apple pectin, followed by LC-MS and NMR approaches (Coenen, Bakx, Verhoef, Schols, & Voragen, 2007).

Until today, the representation of consecutive blocks composed of HG, XGA, RG I and RG II (**Fig. 17**A) represents the most cited model of the pectic fractions linkages.
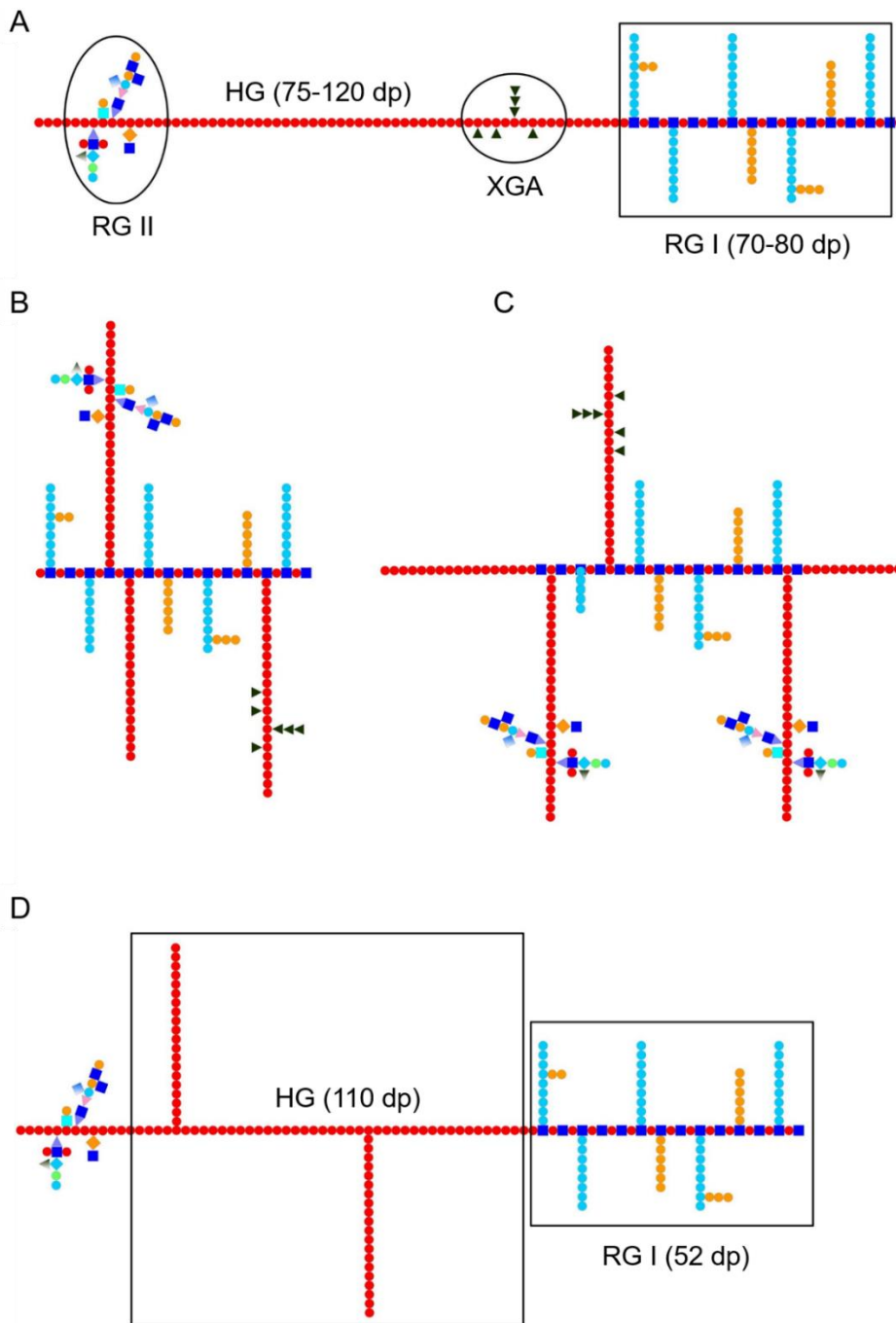
Fig. 17. Schematic representation of the different models proposed for organisation of the different pectin domains: Traditional model (A), RG I backbone model (B), "living thing" model (C) and a hypothetical pectin linkage assessed by atomic force microscopy (D).

Adapted from Paniagua, et al. (2017a). Galacturonic acid (⬤), arabinose (⬤), galactose (⬤), rhamnose (■), apiose (▲), fucose (◆), glucuronic acid (⬤), methyl-xylose (▲), 2-keto-3-deoxy-lyxo-heptulosaric acid (▢), aceric acid (▲), methyl-fucose (◆), 2-keto-3-deoxy-D-manno-octulosonic acid (◆), xylose (▲), dp: Degree of polymerization.

RG I backbone model (Somerville, et al., 2004; Vincken, et al., 2003)

The studies performed by Coenen, et al. (2007), however, could not completely exclude the hypothesis that HG represents a side chain of RG I. This would support another hypothetical model that is completely of a "hairy" type. According to this model, HG, XGA and RG II are attached to a RG I backbone (**Fig. 17**B). HG chains could either be directly linked to the RG I backbone or "grafted" to RG I side chains. However, nobody ever isolated a rhamnose molecule, carrying a galacturonic acid residue on its secondary alcohol function on O-4 or O-3, which would be necessary to validate this model.

"Living thing" model (Yapo, 2011)

Yapo (2011) pointed out that the two before-mentioned models might be only a partial representation of the complex pectin *in muro*. Additionally, the author tried to explain the possible dimerization of RG II blocks and the fact that there exist more HG than RG I fractions in most pectins. Thus, he proposed a backbone that contains two linear HG elements and one RG I core (**Fig. 17**C). Some RG II blocks are linearly connected to the reducing ends of the HG side chains. The RG I backbone carries both side chains of neutral sugars, HG and XGA. Whereas the neutral sugars are linked to rhamnose units, HG and XGA are branched to galacturonic acid residues. The latter branching points, however, seem to be very unlikely. Except for substitution by a single glucuronic acid (Renard, et al., 1999), no branching of the galacturonic acid in the RG I backbone and another molecule was ever detected.

Hypothetical pectin linkage assessed by atomic force microscopy (AFM) (Paniagua, et al., 2017a)

Pectins extracted from tomato tissue showed a long backbone with numerous branches in AFM images (Round, Rigby, MacDougall, Ring, & Morris, 2001). Mild acid hydrolysis (0.1 M HCl, 80 °C) strongly decreased the amount of the neutral sugars arabinose, galactose and rhamnose but neither the pectin size nor branches were significantly altered (Round, Rigby, MacDougall, & Morris, 2010). In contrast to previous models, they concluded that both the backbone and the branches seem to be HG polymers, interlinked with an as yet undetermined covalent bond. The neutral sugars seem to be present as short branches, which were not detected at the

resolution achieved by AFM. These results are supported by subsequent AFM experiments on pectins from apples (Zareie, Gökmen, & Javadipour, 2003) and strawberries (Pose, Kirby, Mercado, Morris, & Quesada, 2012) but no chemical analysis ever confirmed the proposed structure.

Zhang, Cui, Xiao, and Wang (2014) observed a reduced length of both the main backbone and branches in citrus pectin when subjected to mild acid hydrolysis. This indicates the presence of rhamnose molecules in the pectic backbone.

Paniagua, et al. (2017a) used an enzymatic approach in order to cleave the HG backbone and thus try to unravel the pectin structure. The digestion of strawberry pectins with fungal endo-polygalacturonase provoked indeed both a reduction in the pectin chain length and branches. These results support the hypothesis of a HG backbone that is branched with further HG molecules (**Fig. 17**D). They proposed a model, in which the pectin backbone could comprise both HG and RG I molecules. The HG unit possess unbranched regions and a few number of HG branches. RG II could be linked to the HG backbone, allowing the formation of pectin aggregates through borate diester bridges between two RG II blocks from different pectic molecules.

But again, the trisaccharide that could constitute the branching point for covalently linked HG chains has never been identified. This branching point observed by AFM may be due to sublayers or non-covalent linkages such as ionic bonds or dehydration artefacts that occurred during sample preparation. Hence, the images obtained by AFM should always be interpreted with caution.

The proposed RG I backbone model, the "living thing" model and the new model assessed by AFM (**Fig. 17**B-D) lack in explicit knowledge of the hypothesized branching points and are thus little reliable. Hence, the traditional model (**Fig. 17**A) remains the most plausible one and will be referred to in this work.

2.3. Structural organization of the plant cell wall

The "tethered network" (cf. **Fig. 8**), proposed by Carpita and Gibeaut (1993), was for a long time the dominating model of the structural organization within the plant cell wall. In this model, the primary cell wall consists of three independent but interacting domains. Cellulose microfibrils form a network that is coated and linked by, mainly, xyloglucan and some other hemicellulose polymers. This load-bearing network is embedded in an independent matrix composed of pectins. Structural proteins form the third independent domain in this model.

Indeed, hemicelluloses, especially xyloglucans, form cross-links between cellulose microfibrils (Fujino, et al., 2000; Martinez-Sanz, et al., 2017). Pectins could be interconnected to cellulose by hemicellulose cross-links as RG I side chains are able to link with xyloglucans in several suspension-cultured cells (Popper & Fry, 2005; Popper & Fry, 2008; Thompson & Fry, 2000).

However, several studies found evidence that pectin does not form an individual network but interlinks with cellulose both *in vitro* (Lin, Lopez-Sanchez, & Gidley, 2015, 2016; Zykwinska, et al., 2007; Zykwinska, et al., 2005) and *in planta* (Broxterman & Schols, 2018; Dick-Pérez, et al., 2011; Wang, Park, Cosgrove, & Hong, 2015; Wang, Zabotina, & Hong, 2012). Pectins show similar affinities for cellulose as xyloglucans, with weak interactions *in vitro* but rather extensive ones *in planta*. This supposes an important role for pectins, together with hemicelluloses, in maintaining mechanical strength and other functions in plant cell walls. Proposed interactions between pectin molecules and cellulose microfibrils include associations with RG I side chains, probably by hydrogen bonds (Lin, et al., 2015; Zykwinska, et al., 2007; Zykwinska, et al., 2005) and anionic bridges through HG regions (Lin, et al., 2016), although the type and extent of these interactions seem to depend on the fruit species (Broxterman & Schols, 2018).

In addition, Lopez-Sanchez, et al. (2016) and Lopez-Sanchez, et al. (2017) demonstrated in bacterial cellulose hydrogels that pectins fill up the spaces between cellulose microfibrils and thus reduce porosity of the cellulose-network. This could be recently confirmed in onion, carrot and apple cell walls (Lopez-Sanchez, et al., 2020). Due to the densification effect of pectins in the cell wall, it seems even more possible that they contribute significantly to mechanical characteristics of the cell wall.

Since the pectin network seems to be more integrated in the cell wall than previously thought, the polysaccharides present in plant cell walls should be considered to form a single instead of several individual networks.

2.4. Changes in cell wall structure during apple fruit ripening and storage

2.4.1. Observed modifications of cell wall composition and structure

Apples and other climacteric fruits soften during ripening and thus become suitable for human diet. However, over-softening, implying an excessive texture loss, may occur during post-harvest storage. Some apple cultivars may develop undesired mealy textures, which highly diminish fruit quality. In crisp apples, intercellular adhesion is stronger than cell walls. When biting into this apple, cells break and their content is released, what we perceive as crunchy and juicy textures. In mealy apples, the cell walls are stronger than intercellular adhesion. So when biting into this apple, cells separate without being broken and no juice is released (Harker & Hallett, 1992).

Besides a reduction in turgor pressure due to transpirational water loss and increasing solute concentrations in cell wall spaces, modifications in the composition and structure of parenchyma cells are responsible for texture loss during fruit ripening and storage. These cell wall changes promote a decrease in cell wall thickness, strength and intercellular adhesion, leading to reduced mechanical strength and thus texture deterioration (Mercado, Matas, & Posé, 2019; Shackel, Greve, Labavitch, & Ahmadi, 1991).

The major changes in the cell wall structure during fruit ripening and storage are related to pectic molecules. Many studies considered this subject in the last decades but diverse mechanisms are still under discussion. In most fruits and vegetables, pectin depolymerization and solubilisation, as well as the loss of pectin RG I side chains decrease both cell adhesion and cell wall disassembly, resulting in cell separation and thus tissue softening (Brummell & Harpster, 2001; Thakur, et al., 1997; Voragen, et al., 1995).

The most reported pectin modifications that are related to texture loss in apple fruits are listed in **Table 2**.

Table 2. Overview over most important phenomena occurring at the cellular level during apple fruit ripening and storage.

Phenomenon	References
Amount of water soluble pectins ↗ (pectin solubilisation)	Ben and Gaweda (1985); Billy, et al. (2008); Gwanpua, et al. (2014); Gwanpua, et al. (2016); Knee (1973); Massiot, Baron, and Drilleau (1996); Nara, Kato, and Motomura (2001); Ng, et al. (2015); Szymańska-Chargot, et al. (2016); Yoshioka, Aoba, and Kashimura (1992)
Amount of other cell wall pectins ↘	Gwanpua, et al. (2014); Massiot, et al. (1996); Nara, et al. (2001); Ng, et al. (2015); Szymańska-Chargot, et al. (2016); Yoshioka, et al. (1992)
Neutral RG I side chains arabinose and galactose ↘	De Vries, Voragen, Rombouts, and Pilnik (1981); Fischer and Amado (1994); Fischer, Arrigoni, and Amado (1994); Gross and Sams (1984); Gwanpua, et al. (2014); Knee (1973); Massiot, et al. (1996); Nara, et al. (2001); Ng, et al. (2015); Ng, et al. (2013); Pena and Carpita (2004); Redgwell, Fischer, Kendal, and MacRae (1997)
Macromolecular size of soluble pectins ↘	Gwanpua, et al. (2014); Gwanpua, et al. (2016)
Little pectin depolymerization	Fischer, et al. (1994); Yoshioka, et al. (1992)
DM constant (65–100%)	Billy, et al. (2008); De Vries, et al. (1981); Fischer and Amado (1994); Gwanpua, et al. (2014); Gwanpua, et al. (2016); Massiot, et al. (1996)
Water status ↘ through evaporation	Fischer and Amado (1994); Gwanpua, et al. (2016); Massiot, et al. (1996)

Most studies reported an increase of water soluble pectins at the expense of cell-wall associated pectins (Gwanpua, et al., 2014; Szymańska-Chargot, et al., 2016; Yoshioka, et al., 1992), a loss of RG I side chains arabinose and galactose (Fischer & Amado, 1994; Massiot, et al., 1996; Ng, et al., 2013) and a decrease in the macromolecular size of pectins (Gwanpua, et al., 2014; Gwanpua, et al., 2016), although only little depolymerization occurs (Fischer, et al., 1994; Yoshioka, et al., 1992).

High pectin solubilisation can be directly related to decreased cell wall integrity and thus an increased softening rate (Gwanpua, et al., 2016; Ng, et al., 2015). Ng et al. (2015) also linked a reduced amount of RG I galactose to poor cell wall strength. As RG I side chains anchor pectins to the cell wall through bounds with both hemicellulose (Popper & Fry, 2008) and cellulose (Zykwinska, et al., 2005), their degradation may loosen the cell wall structure, resulting in increased cell wall porosity and reduced cell adhesion. Several other studies also attributed a loss in arabinose and galactose side chains to reduced apple firmness (Lahaye, et al., 2018) or development of mealiness (Nara, et al., 2001; Pena & Carpita, 2004). Some studies report different extents of galactose and arabinose loss, maybe depending on the cultivar or the developmental stage (Knee, 1973; Nara, et al., 2001; Pena & Carpita, 2004; Redgwell, et al., 1997). RG I side chain loss was correlated with the (over-)ripening in many other fruits and vegetables, inter alia, in tomatoes, nectarines and pears (Brahem, Renard, Gouble, Bureau, & Le Bourvellec, 2017b; Gross & Sams, 1984).

Gwanpua, et al. (2014) and Gwanpua, et al. (2016) link a decrease in macromolecular size of water soluble pectins to apple softening. This could be due to pectin depolymerization by polygalacturonase and/or the extensive loss of RG I side chains, although only little depolymerization was observed in apples (Fischer, et al., 1994; Yoshioka, et al., 1992) and other *Rosaceae* such as pears (Brahem, et al., 2017b).

Calcium cross-links could additionally enhance cell adhesion in the middle lamella. Indeed, calcium cross-linked HG pectins can be detected in tricellular junction zones by immunofluorescence labelling and they disappear during ripening in the apple cultivar showing intense softening (Ng, et al., 2013). Nevertheless, neither this study nor others (Lahaye, Falourd, Laillet, & Le Gall, 2020) could link improved cell adhesion and apple firmness to a reduced DM, although this is a prerequisite of forming effectively calcium cross-links. As the DM does not change during apple ripening and

storage (Billy, et al., 2008; De Vries, et al., 1981; Gwanpua, et al., 2014), an implication of calcium cross-links in apple fruit firmness and cell adhesion is doubtful.

A decrease in arabinogalactan proteins during apple storage was also reported recently (Leszczuk, et al., 2018). As they possibly anchor the plasma membrane to the cell wall, their decrease could weaken the cell wall structure.

The rate and dimension of fruit softening do not only differ between fruit species but also between cultivars of the same species (Brummell & Harpster, 2001; Gross & Sams, 1984). This is due to different amounts and activity rates of diverse cell wall-modifying enzymes.

2.4.2. Pectin degrading enzymes

Cell wall-modifying enzymes are mainly hydrolases, lyases and oxidoreductases and are implicated in fruit ripening, softening and plant defence (Heredia, et al., 1995).

Degradation of pectin, a complex polysaccharide, involves various enzymes, generally summarised as pectinases. An ordered series of modifications induced by a range of different pectinases is necessary for fruit softening. Depending on their substrate in the pectic polymer, pectin-degrading enzymes can be classified in HG- and RG I-degrading enzymes. The exact roles of the different pectinases as well as their interactions during fruit softening are complex and still considered controversial since enzyme activity seems to depend on the fruit species (Paniagua, et al., 2014).

2.4.2.1. Homogalacturonan-degrading enzymes

Pectin methylesterase (PME)

Pectin methylesterase **(PME**; EC 3.1.1.11) deesterifies the galacturonic acid backbone of HG units by removing the methyl groups from the C6 position of high-molar-mass pectin releasing methanol and H_3O^+ (**Fig. 18**). PMEs were isolated from apples (Denes, Baron, & Drilleau, 2000) and many other fruits such as tomatoes (Tucker, Robertson, & Grierson, 1982) or strawberries (Neal, 1965). At neural pH values, PMEs originating from plants cause blockwise pectin deesterification, whereas microbial PMEs create random deesterification patterns (Limberg, et al., 2000). The progressive demethylesterification induces large negatively charged regions in the HG backbone. If more than 10 consecutive unmethyl-esterified galacturonic acid residues (Kohn &

Luknár, 1977) occur with an elevated level of calcium ions in the cell wall, cross-linking of unesterified HG chains by ionic interactions according to the before mentioned "egg-box"-model is promoted (Grant, et al., 1973). This conformation is supposed to increase cell wall stiffness and to limit the access of other enzymes to the pectin backbone, which therefore prevents enzymatic pectin degradation (Micheli, 2001). Without calcium ions, a loosening of the cell wall structure through electrostatic repulsion of the negatively charged pectins is favoured (Brummell, 2006). In addition, the enzymatic cleavage by polygalacturonase and pectate lyase, which act on deesterified pectins, is enhanced (Micheli, 2001).

During post-harvest softening of apples, PMEs seem to play a minor role as the DM is not modified during post-harvest storage (Gwanpua, et al., 2014).
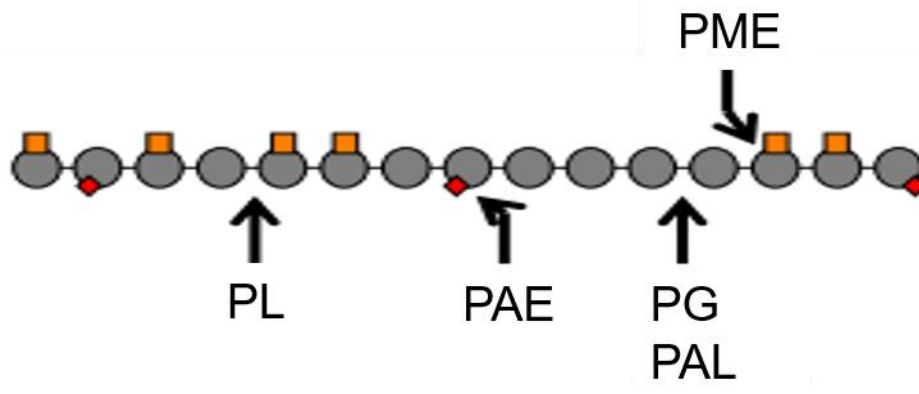
Fig. 18. Enzymes degrading homoglacturonan.

Adapted from Bonnin, Garnier, and Ralet (2014). PME: Pectin methylesterase; PAE: Pectin acteylesterase; PG: Polygalacturonase; PL: Pectin lyase; PAL: Pectate lyase. Galacturonic acid (◯); methanol (▪); O-acetyl (◆).

Pectin acetylesterase (PAE)

Pectin acetylesterase (**PAE**; EC 3.1.1.6) removes acetyl-esters from HG units (**Fig. 18**). They can influence the functional properties of pectins as acetyl groups impede the association between pectic polymers (Ralet, Crepeau, Buchholt, & Thibault, 2003) and hinder the access of pectin-depolymerizing enzymes to their substrates (Bonnin, Le Goff, van Alebeek, Voragen, & Thibault, 2003; Chen & Mort, 1996).

Polygalacturonase (PG)

Polygalacturonases (**PG**) promotes the hydrolytic cleavage of galacturonide linkages in the HG backbone (**Fig. 18**). The exo-type (EC 3.2.1.67) removes single galacturonic acid units from the non-reducing end of HG units whereas the endo-type (EC 3.2.1.15) cleaves these polymers randomly. Previous deesterification of the substrate is mandatory (Carpita & Gibeaut, 1993; Jarvis, 1984) since PG activity decreases with increasing DM. The enzyme involved in fruit ripening in higher plants is generally of the endo-type and has more than one isoform. Both endo- (Wu, Szakacsdobozi, Hemmat, & Hrazdina, 1993) and exo-PG (Bartley, 1978) were extracted from apple tissue, although their amounts and thus activity are relatively little compared to avocados, tomatoes or peaches (Hobson, 1962; Yoshioka, et al., 1992). During fruit ripening and storage, PG depolymerizes probably covalently bound pectin and solubilises it into a water soluble fraction (Carrington, Greve, & Labavitch, 1993). Despite the low amounts of PG in apples, the down-regulation of endo-PG reduced apple softening due to enhanced intercellular adhesion, cell wall strength and reduced transpirational water loss (Atkinson, et al., 2012).

Pectate (PAL) and pectin lyase (PL)

Pectin and pectate lyases (**Fig. 18**) both split the glycosidic linkage between two galacturonic acid units by catalysing a β-elimination reaction, thus introducing a double bond on the newly formed non-reducing end.

Pectate lyases (**PAL**; EC 4.2.2.2) act preferably on non-methylated substrates since their activity decreases with increasing DM. They are found in several fruits, but no activity or gene expression was detected in ripening apple fruits. In tomatoes, however, PAL seems to highly contribute to fruit softening (Wang, Yeats, Uluisik, Rose, & Seymour, 2018).

Pectin lyases (**PL**; EC 4.2.2.10) are mainly found in pathogen microorganisms and act specifically on highly methylated substrates, showing a decreased activity with a decreasing DM (Mutenda, Korner, Christensen, Mikkelsen, & Roepstorff, 2002; Ralet, et al., 2012).

2.4.2.2. Rhamnogalacturonan I-degrading enzymes

a) <u>RG I backbone</u>

Three exo- and two endo-enzymes as well as one esterase are known to degrade the RG I backbone (Bonnin, et al., 2014). These enzymes (**Fig. 19**) do not naturally occur in plants. They are only produced by pathogens after invasion and are thus less important in fruit softening.
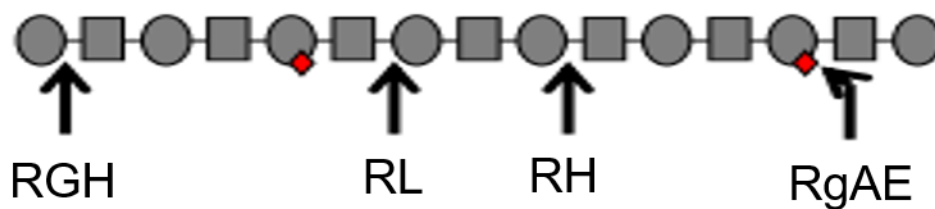
Fig. 19. Enzymes degrading rhamnogalacturonan I (RG I) backbone.
Adapted from Bonnin, et al. (2014). RGH: RG galacturonohydrolase; RL: RG lyase; RH: RG hydrolase; RgAE: RG acetylesterase. Galacturonic acid (⬤); Rhamnose (▦); O-acetyl (◆).

Exo-acting enzymes

RG-galacturonohydrolase (**RGH**; EC 3.2.1.173) was found in fungi and removes specifically the terminal non-reducing galacturonic acid unit from the RG I backbone (Azadi, O'Neill, Bergmann, Darvill, & Albersheim, 1995; Mutter, Beldman, Pitson, Schols, & Voragen, 1998). RG-rhamnohydrolase (EC 3.2.1.174), in contrast, specifically removes the terminal non-reducing rhamnosyl unit from the RG I backbone (Mutter, Beldman, Schols, & Voragen, 1994; Pitson, Mutter, van den Broek, Voragen, & Beldman, 1998). Rhamnogalacturonyl hydrolase (EC 3.2.1.172) acts on unsaturated RG I polymers that were treated with RG lyases, releasing an unsaturated galacturonic acid monomer from the substrate.

Endo-acting enzymes

Among the endo-acting enzymes, rhamnogalacturonan hydrolase (**RH**; EC 3.2.1.171) was isolated from fungi and releases oligosaccharides with a reducing β-D-galacturonic acid during RG I hydrolysis. Rhamnogalacturonan lyases (**RL**; EC 4.2.2.23) also cleave the RG I backbone but very few RG lyases are reported in literature.

Esterase

RG acetylesterases (**RgAE**; EC 3.1.1.86) are required for the deacetylation of the RG I backbone.

b) RG I side chains

For a complete degradation of RG I, also the side chains have to be cleaved by the following enzymes (**Fig. 20**).
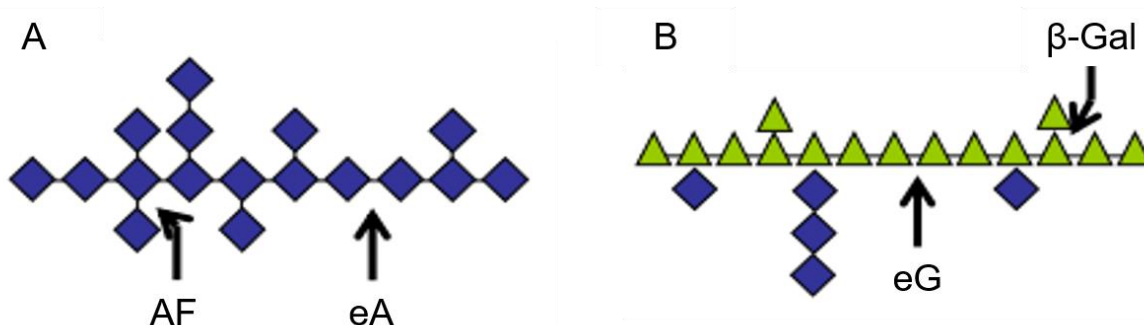
Fig. 20. Arabinan (A) and arabinogalactan I (B) degrading enzymes.
Adapted from Bonnin, et al. (2014). AF: Arabinofuranosidase; eA: Endo-arabinanase; eG: Endo-galactanase; β-Gal: β-galactosidase. Galactose (▲); Arabinose (◆).

Enzymes cleaving arabinose linkages

Endo-arabinanases (**eA**; EC 3.2.1.99) cleave randomly the α-1,5-linkages of the arabinan backbone. In contrast, exo-arabinanases (no EC number) hydrolyse arabinan from the non-reducing end to release arabinose dimers (Sakamoto & Thibault, 2001). α-L-Arabinofuranosidases (**AF**; EC 3.2.1.55) act on α-L-arabinofuranosides, α-L-arabinans containing (1→3)- and/or (1→5)-linkages, arabinoxylans, and arabinogalactans. This enzyme was found in apples and other fruits and could be linked to fruit softening (Nobile, et al., 2011; Wang, et al., 2018).

Enzymes cleaving galactose linkages

Endo-β-1,4-galactanases (**eG**; EC 3.2.1.89) act randomly on the covalent linkage between galactose molecules, whereas exo-β-1,4-galactanases (no EC number) release galactose or galactobiose from the non-reducing end of β-1,4-linked galactans. Galactanases do not belong to the endogenous enzymes of fruits and vegetables. Exo-β-Galactosidases (**β-Gal**; EC 3.2.1.23) are found in a wide range of fruits and

vegetables (Wang, et al., 2018), also in apples (Gwanpua, et al., 2014). They cleave the terminal non-reducing β-D-galactose from various substrates of low molar mass such as galacto-oligosaccharides.

In vivo, only the endogenous enzymes α-L-arabinofuranosidase (**AF**) and β-galactosidase (**β-Gal**) have an effect on fruit ripening and softening. Indeed, Yoshioka, Kashimura, and Kaneko (1995) reported that the activity of AF and β-Gal appeared and increased during post-harvest storage of apples. Due to their ability to cleave RG I side chains, pectin solubilisation may be enhanced, leading to increased cell wall porosity. This allows the access of other pectinases to their substrates. On the other hand, the reduction of steric hindrance by pectic debranching may favour the formation of calcium cross-links between HG chains (Brummell & Harpster, 2001).

2.4.3. Other enzymes involved in fruit ripening

Unlike pectin, the overall hemicellulose and cellulose composition and structure are not significantly affected during apple fruit ripening (Percy, Melton, & Jameson, 1997). Nevertheless, some endogenous enzymes affecting these polysaccharides were found in plant cell walls.

Endo-β-D-(1→4)-glucanase (EGase; EC 3.2.1.4) hydrolyses the internal linkages of β-D-(1→4)-linked glucan chains that are linked to unsubstituted residues and are found in several fruit species (Brummell, Lashbrook, & Bennett, 1994). The substrates probably include some hemicelluloses such as glucomannans and the integral and peripheral regions of non-crystalline cellulose. Certain endo-glucanases also degrade xyloglucan. As xyloglucan coats the cellulose surface, an extensive degradation of xyloglucan facilitates the enzymatic cleavage of cellulose (Vincken, Beldman, & Voragen, 1994; Vincken, de Keizer, Beldman, & Voragen, 1995)

Expansin is a non-enzymatic, small protein that is localized in plant cell walls. It disrupts reversibly the hydrogen bonds between cellulose microfibrils and xyloglucans. This results in cell wall loosening (Cosgrove, 2000, 2016; McQueen-Mason and Cosgrove, 1994, 1995; Whitney et al., 2000), which may be necessary to allow pectinases access to their substrates.

2.5. Analysis of the plant cell wall structure

It is an important issue to elucidate the macromolecular organization within the cell wall since the chemical composition and structure as well as polymer interactions determine the functional characteristic of the whole network. As the main changes during cell wall development and fruit softening occur in the pectic fraction, this polymer is of high interest and both analytical and microscopic techniques are required to clarify its structure-function relation. This section aims to give an overview of some common methods. Although some more techniques exist, only the methods that I came in contact with during my PhD thesis are presented hereinafter.

2.5.1. Cell wall extraction

Traditional chemical methods have been developed to extract and purify polysaccharides from plant cell walls. Several methods exist, all aiming to remove the cell content and inactivate endogenous enzymes while retaining polysaccharides and starch. Renard (2005b) summarized and evaluated the existing methods. The most common one is based on the cell wall extraction by ethanol and acetone to obtain the "Alcohol Insoluble Solids" (AIS). This method was identified as the easiest and less time-consuming with a weak toxic risk for the operator. However, proteins and some polyphenols co-precipitate, making an evaluation of these intracellular macromolecules impossible. Soluble cell wall components can also be extracted by water or buffer, although broad modifications in the cell wall material are expected due to the activity of endogenous enzymes. A solution of buffer and phenol is recommended for cell wall extraction if a subsequent structural analysis is aspired. However, the toxic risk of phenol has to be kept in mind and should potentially be replaced by 1-propanol (Mafra, et al., 2001).

A drawback of all these methods is the destructuration of the cells, making observation of cell wall structure impossible. Hence, only the chemical composition of the cell wall polysaccharides can be studied.

After extraction of the whole cell wall, it can be sequentially extracted (**Fig. 21**). This allows the chemical analysis of different fractions that are enriched in particular cell wall polysaccharides (Brett & Waldron, 1996; Brummell & Harpster, 2001; Selvendran, 1985; Selvendran & O'Neill, 1987).

91

| Water or phenol:acetic acid:water | → | Extraction of already solubilized pectins by processes occurring *in vivo* |

| Chelating agents (CDTA or EDTA) | → | Removal of calcium ions:
→ Extraction of pectins held in the cell wall by ionic bonds
→ Fraction enriched in HG from middle lamella |

| Sodium carbonate | → | De-esterification:
→ Extraction of pectins covalently bound by ester bonds
→ Fraction enriched in RG I from primary cell wall |

| Weak alkali (0.7 M or 1 M KOH) | → | Solubilization of hemicelluloses loosely bound in the cell wall:
→ Mainly matrix glycans (glucomannan, glucuronoarabinoxylan)
→ Small amounts of xyloglucans |

| Strong alkali (4 M or 4.3 M KOH)* | → | Solubilization of hemicelluloses strongly bound in the cell wall through hydrogen bonds:
→ Xyloglucans
→ No dissolution of cellulose microfibrils |

| Residue | → | → Mainly cellulose as insoluble in water
→ Some hemicelluloses and pectins, strongly associated with cellulose |

*The pectin fraction that is only extractable by alkali or hot dilute acid solutions is called protopectin (Renard, 1989).

Fig. 21. Steps during sequential extraction of the plant cell wall.

Adapted from Brummell and Harpster (2001).

2.5.2. Microstructural analysis

2.5.2.1. Electron microscopy

In order to examine the cell wall structure, microscopy is a useful tool (Kirby, Gunning, & Morris, 1995). Transmission electron microscopy (TEM) (Voiniciuc, Pauly, & Usadel, 2018; Xia, et al., 2015) as well as scanning electron microscopy (SEM) (Stokes, 2001), are widely used in cell wall analysis. Both provide information about the sample's surface topography and composition but the need of a carbon (TEM) or metal (SEM) coating limits their application. Apart from the fact that the coating procedure is challenging and thus time consuming, the coating may create artefacts and risks hiding fine structural details. In addition, the samples must be viewed under vacuum, so that they have to be fixed chemically, by dehydration or freezing (cryofixation) prior to analysis. In conclusion, plant material can never be observed in their native state and no dynamic experiments can be conducted.

Environmental scanning electron microscopy (ESEM) overcomes these limitations. As neither coating nor high vacuum are required, the samples can be imaged directly in their native state, allowing *in situ* experiments (Stokes, 2001). Hence, the impact of, for example, mechanical deformation, dynamic processes such as hydration and dehydration or thermal treatments on plant cell walls and other materials can be followed. Cardenas-Perez, et al. (2017) employed ESEM to visualize modifications in the microstructure of apple tissue during post-harvest storage. They clearly showed cell wall contraction and shrinkage as well as loss of turgor pressure (**Fig. 22**). Another study used ESEM to estimate the thickness of apple cell walls (Leverrier, Moulin, Cuvelier, & Almeida, 2017b).
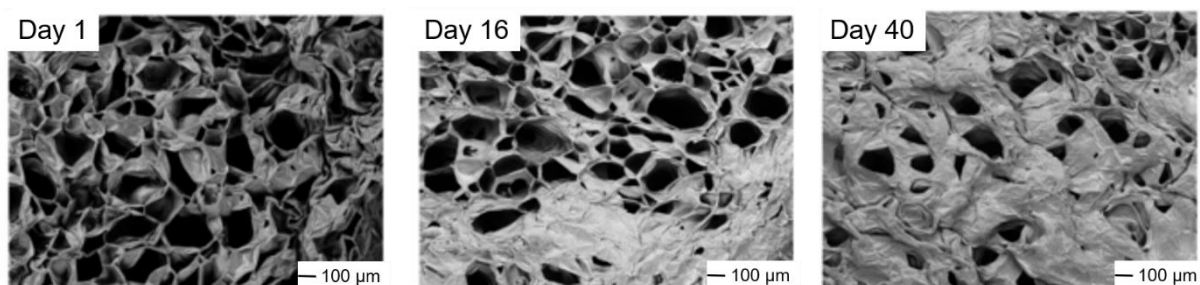
Fig. 22. ESEM images showing evolution of apple tissue during post-harvest storage at 25 °C during 40 days.

Adapted from Cardenas-Perez, et al. (2017).

Conventional microscopic techniques only show the overall structure of the plant cell wall. Immunolabeling, in combination with electron or light microscopy, enables the detection and localization of various polysaccharides within the cell wall (Verhertbruggen, Walker, Guillon, & Scheller, 2017; Willats, et al., 2000). Most immunolabeling techniques are indirect and based on a "two step" procedure. This means that the primary probe, which recognizes specific structural features of pectins and other cell wall polysaccharides, is detected by the use of a secondary antibody that is coupled to a fluorophore (Verhertbruggen, et al., 2017). Although this method is expensive and requires complicated sample preparation (Ralet, Tranquet, Poulain, Moise, & Guillon, 2010; Verhertbruggen, et al., 2017), it is crucial for increasing our understanding about the cell wall organization.

For example, Willats, et al. (2001) showed that the methylation degree and pattern of HG pectins in pea stem parenchyma differ depending on the localization in the cell wall (**Fig. 23**).
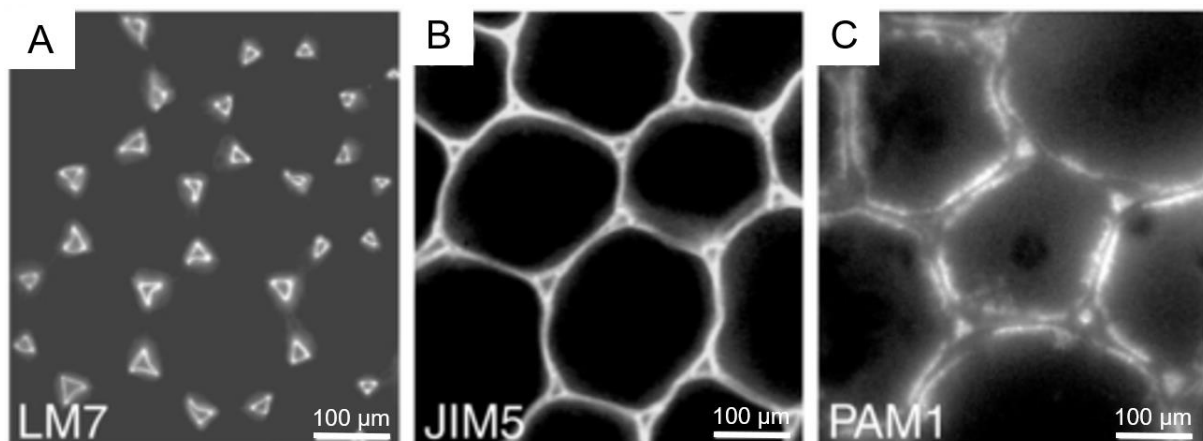
Fig. 23. Immunolabeling images of pea stem parenchyma with monoclonal antibodies LM7 (A), JIM5 (B) and PAM1 (C).
Adapted from Willats, et al. (2001).

HG pectins with a random distribution of methyl-esters (identified by LM7, **Fig. 23**A) are restricted to regions around intercellular spaces, whereas partially methylated HGs (identified by JIM5, **Fig. 23**B) bind throughout the cell wall. In contrast, fully esterified HGs (identified by PAM1, Fig. **23**C) are abundant in intercellular spaces and bind to regions close to the plasma membrane.

Changes occurring in the spatial distribution of different pectin domains during fruit ripening and storage, processing or induced by chemicals or cell wall-degrading enzymes can also be followed by immunolabeling. Ng, et al. (2013) observed a decrease of non- and low-methylated HGs, abundant in the middle lamella and corners of tricellular junctions, during apple storage. Other studies compared the spatial distribution of several pectin domains in firm and soft apples (Ng, et al., 2015; Ng, et al., 2013) (**Fig. 24**).
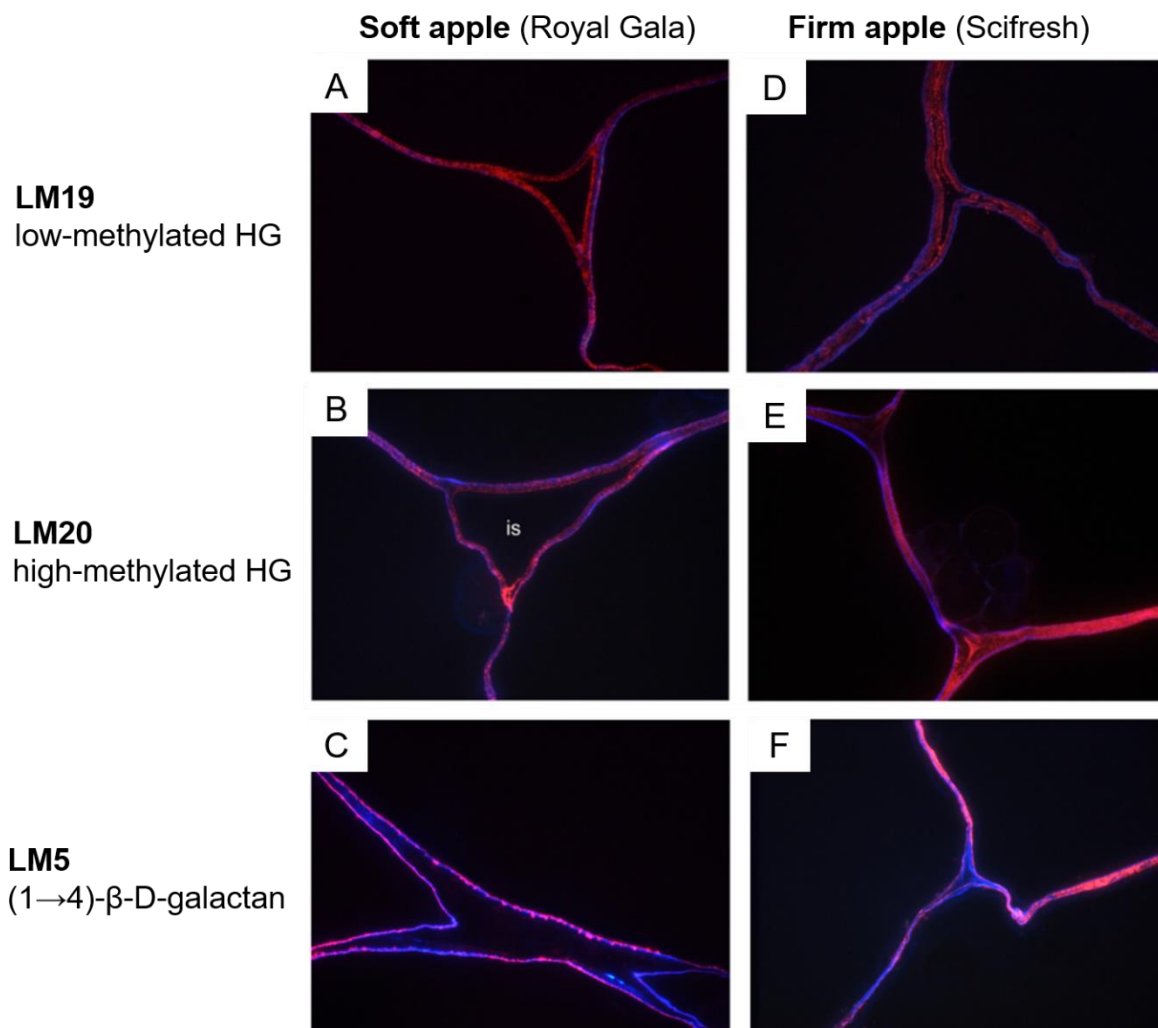
Fig. 24. Immunofluorescence labelling of low-methylated homogalacturonan (HG) by LM19, high-methylated HG by LM20 and (1→4)-β-d-galactan by LM5 in mature soft (A–C) and firm (D–F) apples.

Adapted from Ng, et al. (2013) (A, B, D and E) and Ng, et al. (2015) (C and F). Pectin epitopes are labelled in pink. Cellulose is stained by calcofluor (blue).

They reported that intercellular spaces of firm apples are filled with low-methylated HG in fruitlet and expanding apples but labelling patterns are similar in mature fruits of both firm and soft apples. Highly methylated pectins are mainly present in corners of tricellular junctions in soft apples, while they are more abundant throughout the junction zones and the middle lamella in firm apples. In addition, firm apples show more intense labelling of RG I side chains β-D-(1→4)-galactans in the outer regions of the cell wall. This highlights the contribution of both HG pectins and RG I side chains to cell adhesion and fruit firmness.

2.5.2.2. Raman imaging

In contrast to the immunolabeling technique, in which dead cells are viewed and the staining is complex, Raman imaging allows to follow dynamic processes on living cells as it is a non-destructive method. In addition, the spatial distribution of all cell wall polymers are visualised on the same sample (Gierlinger, Keplinger, & Harrington, 2012). Although sample preparation and imaging are relatively simple, data analysis can be challenging and thus time-consuming (Chylińska, Szymańska-Chargot, & Zdunek, 2014).

Raman imaging is an effective tool to follow changes in plant cell wall polysaccharides during fruit development, ripening or processing. Szymańska-Chargot, et al. (2016) visualized the cell wall of apple parenchyma tissue during fruit development (not shown) and post-harvest storage (**Fig. 25**).

While cellulose and pectin could be viewed separately, the observation of hemicellulose was not possible as the characteristic bands overlap with those from cellulose and pectin. In addition, middle lamella and primary cell wall cannot be distinguished because of limited spatial resolution of Raman imaging. In ripe apples, pectins were concentrated in cell corners but dispersed along the cell wall when apples were stored for three months at 4 °C. Dispersion of pectin polysaccharides during prolonged post-harvest storage suggests a loosening of the cell wall structure and thus decreased cell wall integrity.
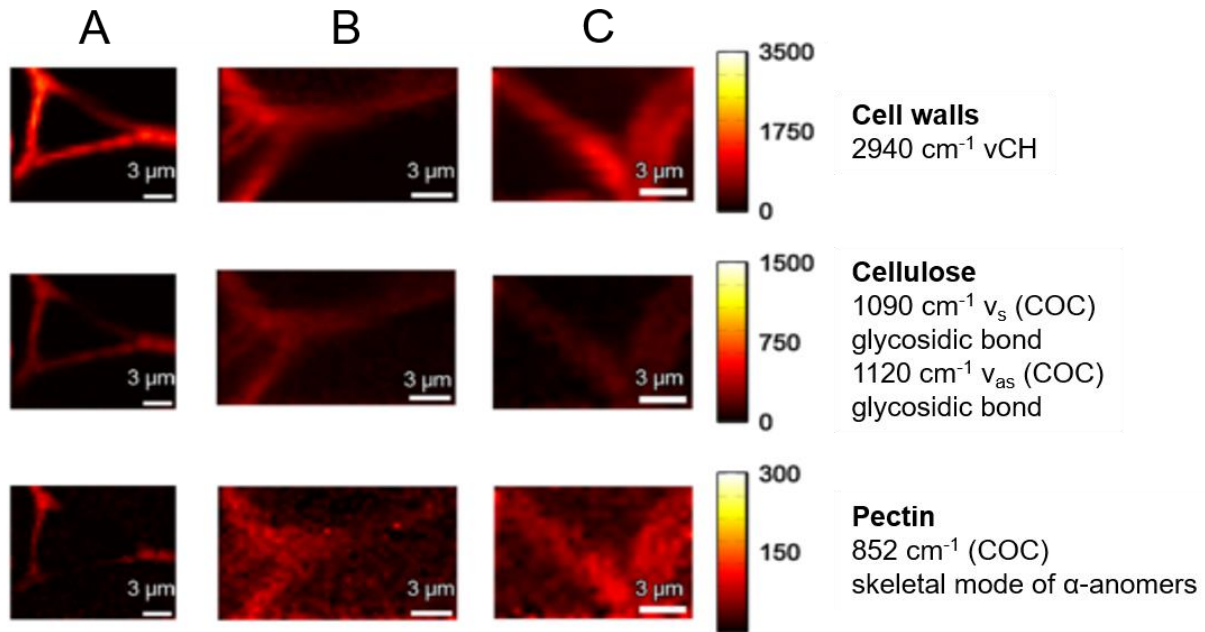
Fig. 25. Raman maps of the cell wall in apple parenchyma tissue during one (A), two (B) and three (C) months storage at 4°C.

Adapted from Szymańska-Chargot, et al. (2016).

2.5.3. Nanostructural analysis

2.5.3.1. High-performance size-exclusion chromatography (HPSEC)

HPSEC fractionates the molecules in solution depending on their hydrodynamic volume (molecular size). The molecules are eluted in columns filled with porous spheres (stationary phase). During analysis, molecules that are too large to enter the pores of the stationary phase, are eluted in the total exclusion volume V_0, whereas molecules that are sufficiently small to freely diffuse in and out of the pores are eluted in the total column volume ($V_t = V_0 + V_p$, with V_p the pore volume), following the expression:

$$V_i = V_0 + K_{sec}V_p \tag{1}$$

$$K_{SEC} = {c_p}/{c_0} \tag{2}$$

Where V_i is the elution volume, K_{SEC} the distribution coefficient, c_p and c_0 the mean concentrations of the polymer in the pores and in the interstitial volume, respectively.

When a pure SEC mechanism occurs, the separation is based only on size, and $0 < K_{SEC} < 1$. A $K_{SEC} = 0$ corresponds to an elution in the total exclusion volume, and when $K_{SEC} = 1$, the solute is eluted in the total volume in the order of decreasing size. If $K_{SEC} > 1$, the separation is controlled by enthalpic interactions, which depend on the chemical composition of the polymer.

A refractive index detector (RID) determines the molecules' concentration and their molar mass can be estimated by comparing the elution profile to those of molar mass standards with the same chemical and molecular structure, such as pullulans.

SEC experiments have been widely employed to qualitatively analyse degradation of different pectin fractions in plant-based food during thermal processing. In carrots, for example, heat treatment induced pectin solubilisation, followed by a decrease in high molecular size pectins with prolonged processing duration (Sila, Doungla, Smout, Van Loey, & Hendrickx, 2006a; Sila, Smout, Elliot, Van Loey, & Hendrickx, 2006b).

HPSEC can also provide insights into depolymerization mechanisms of pectins during post-harvest storage of fruits and vegetables. In apples, a decrease in molar mass of soluble pectins was attributed to firmness loss during post-harvest storage (Gwanpua, et al., 2014).

However, the use of dextran or pullulan standards results in approximate molar mass since the standards' structure differs significantly from the structure of the studied pectins. In order to obtain more accurate molar mass values, HPSEC must be coupled to an absolute molar mass determination method like a multi-angle laser light scattering (MALLS) detector (**Fig. 26**), in combination with a RID. This allows not only the determination of molar mass but also the radius of gyration distributions. Thus, the macromolecule's conformation can be assessed at each elution volume of the chromatogram (Rolland-Sabaté, 2017; Wyatt, 1993). During the experiment, a laser between 400 and 700 nm passes through a diluted solution of macromolecules and is scattered by the macromolecules. In MALLS coupled with HPSEC, the intensity of the scattered light is simultaneously measured at different fixed angles around the sample, allowing the calculation of molar mass (M_i) and radius of gyration (R_{gi}).
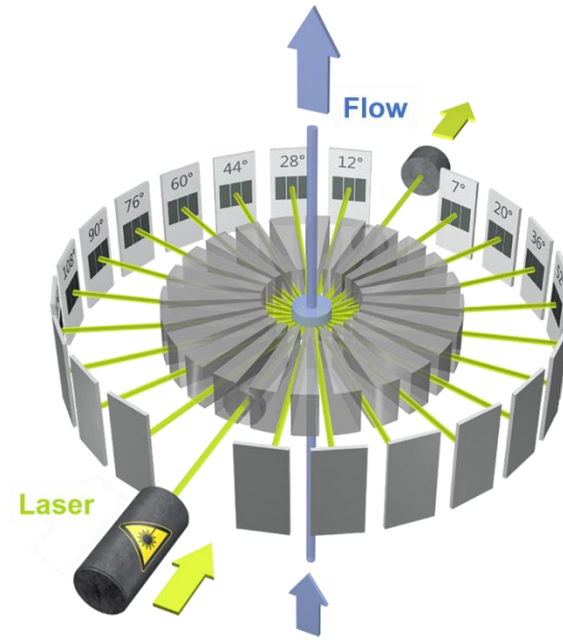
Fig. 26. Scheme of a multi-angle laser light scattering detector.
Adapted from Postnova (2020).

For a polymer solution at a concentration c, the scattered intensity at each angle θ is expressed by the fundamental light scattering relation (Rolland-Sabaté, 2017; Wyatt, 1993), at each slice i of the chromatogram:

$$^{Kc_i}/_{\Delta R_\theta} = ^{1}/_{M_i P_i(\theta)} \tag{3}$$

ΔR_θ is the Rayleigh ratio:

$$\Delta R_\theta = ^{(I_0 - I_s)R^2}/_{I_0} \tag{4}$$

With I_θ the scattering intensity at the angle θ, I_s the scattering intensity of the solvent and I_0 the incident light intensity.

K is the optical constant:

$$K = ^{4\pi^2}/_{\lambda_0^4 N_A} \cdot n^2 (dn / dc)^2 \tag{5}$$

With λ_0 the wavelength of the incident beam, N_A the Avogadro number, dn/dc the refractive index increment of the solution and n the refractive index of the solution.

$$P_i(\theta) = 1 - ^1/_3 q^2 R_{gi} + _{...} \tag{6}$$

With q the scattering vector:

$$q = \frac{4\pi n_0}{\lambda_0} \sin\left(\frac{\theta}{2}\right) \qquad\qquad (7)$$

Where n_0 is the refractive index of the pure solvent.

The molar mass and radius of gyration are then determined by a graphical extrapolation of the data at a null angle thanks to the fundamental light scattering relation by using different diagrams depending on the nature of the polymer to be characterized. For pectins, the Zimm diagram (Zimm, 1948), i.e. $Kc/\Delta R_\theta$ plotted versus $\sin^2(\theta/2)$ is generally used. The slope of the curve gives R_{gi}^2, whereas the intersection of this curve with the y-axis gives $1/M_i$.

Knowing the exact pectin conformation in solution is important as it controls pectin functionality in several food products such as juices or purees by controlling the molecular interactions. For example, during concentration of tomato juice into paste by evaporation, the viscosity of the liquid phase highly decreases. HPSEC-MALLS measurements showed that this is not only due to pectin depolymerization occurring during thermal processing but rather to conformational changes in the pectin polymer (Diaz, Anthon, & Barrett, 2009).

However, it must be taken into consideration during analysis of HPSEC-MALLS experiments that the measured values do not characterize only single pectin chains but could also represent several assembled pectins as they tend to aggregate in solution (Fishman, Gillespie, Sondey, & Barford, 1989; Fishman, Pfeffer, Barford, & Doner, 1984; Sorochan, Dzizenko, Bodin, & Ovodov, 1971). The formation of pectin aggregates is mostly due to hydrogen bonds between carboxyl and hydroxyl groups of galacturonic acids (Alba, et al., 2018), but also hydrophobic interactions and RG I side chains. The DM also influences pectin size in buffered solutions by affecting the strength of ionic repulsions and attractive forces between pectin chains (Fishman, et al., 1984).

2.5.3.2. Atomic force microscopy (AFM)

During AFM measurement, a sharp stylus, attached to a flexible cantilever, is scanned over the sample surface. Attractive forces between the stylus and the sample are detected and the signal is transformed into an image.

Complementary to HPSEC measurements, AFM is capable of imaging individual atoms and molecules as well as their associations at high resolution and under natural conditions, thus providing deeper insights into the molecule´s size, shape, height, contour length distribution and branching (Kirby, et al., 1995; Morris, et al., 2001; Posé, et al., 2018). AFM is further capable of creating 3D images of the sample´s topography with nanometre resolution (Paniagua, et al., 2014). Nanoindentation studies on the surface of, for example, apple tissue and cells are also possible. Thereby, the Young's modulus is calculated and can be correlated to fruit firmness and microstructural cell wall changes (Cardenas-Perez, et al., 2017).

AFM is a promising tool to study complex food materials and their components, such as pectins, since nanostructural features (pectin length, intermolecular agglomeration …) are important to understand their functionalities such as gelling behaviour (Morris, et al., 1997; Zdunek, Koziol, Pieczywek, & Cybulska, 2014). So could, for example, the network of pectin with calcium ions be visualized by AFM (Zareie, et al., 2003).

Pectin linkage and structure is also elucidated by AFM (Round, et al., 2010). **Fig. 27** shows the nanostructure of apple pectin in different fractions (Gawkowska, Cybulska, & Zdunek, 2018). Water soluble pectins (**Fig. 27**A) are visualized as small polymers, whereas chelator soluble pectins (**Fig. 27**B) present both short and polymer chains. Diluted alkali pectins (**Fig. 27**C) show a self-organized network in AFM images.
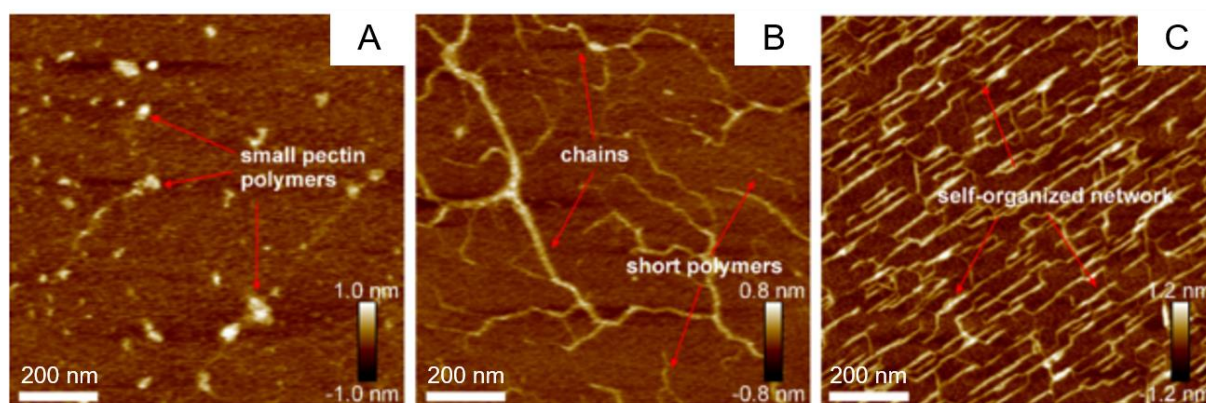
Fig. 27. AFM images of water (A), chelator (B) and diluted alkali (C) soluble pectins of apples.

Adapted from Gawkowska, et al. (2018).

The nanostructure of plant cell wall polysaccharides could be correlated to fruit texture. Pears were firmer when pectins were less degraded, thicker and more branched (Zdunek, et al., 2014). In apples, thicker cellulose microfibrils were correlated to firmer fruits (Cybulska, et al., 2013).

AFM was also shown to be a useful tool to study enzymatic pectin breakdown. In strawberries, a higher polymerization degree, more branched chains and increased aggregation were observed in several pectin fractions due to pectinase silencing (Posé, et al., 2015). Also in strawberries, AFM experiments, together with CW analysis, revealed that pectin complexity decreased during fruit development as branches and aggregates decreased, probably due to enzymatic activity (Paniagua, et al., 2017b).

However, attention has to be payed to the results obtained by AFM. The images generally show aggregated instead of single pectin molecules as the viewed height and width correspond to laterally aggregated molecules (Fishman, Cooke, Chau, Coffin, & Hotchkiss, 2007). Drying artefacts are also possible. That is why AFM studies should always include analysis of chemical composition in order to compare structural and chemical findings (Imaizumi, et al., 2017).

2.5.3.3. Nuclear magnetic resonance (NMR) spectroscopy

Liquid NMR spectroscopy can determine the fine structure of organic molecules, but the sample has to be pure and the concentration high in order to get evaluable spectra. Solid state NMR spectroscopy is also a valuable tool for analysing the molecular structure of, for example, plant cell wall components. Data of these experiments thus provide information on the local chemical environment and structure (Jarvis & McCann, 2000).

Knowledge of the DM in pectin molecules is important in food industry to predict gelling. Although the most common method to determine the DM is based on the individual analysis of galacturonic acid (colorimetric method) and methanol (chromatography), spectroscopic techniques could also provide this value. They are more trouble-free as they limit the interference of neutral sugars in, for example, colorimetric galacturonic acid determination. Besides Fourier-transform infrared (FT-IR) spectroscopy (Filippov & Kohn, 1975; Kyomugasho, Christiaens, Shpigelman, Van Loey, & Hendrickx, 2015), NMR spectroscopy determines directly the DM of pectins.

Tjan, Voragen, and Pilnik (1974) determined the DM as well as β-elimination products of galacturonic acid molecules by ^{1}H-NMR. Furthermore, they determined the complete structure and conformation of homologous series of several (un)-saturated, non, partly and fully esterified oligo-galacturonic acids of up to five galacturonic acid residues in order to study enzymatic action patterns. Later, the protocol was extended to quantify DM in high molar mass pectins (Rosenbohm, Lundt, Christensen, & Young, 2003). Traditionally, NMR analyses for DM determination are performed at elevated temperatures (60–90 °C) to shift the HDO peak from the region for anomeric protons and to reduce the viscosity of pectin samples. This allows improvement of the poor spectral resolution. The DM is then obtained by integration of the proton signals next to free or esterified carboxylate (Grasdalen, Einar Bakøy, & Larsen, 1988; Rosenbohm, et al., 2003). Since the maximum temperature of many NMR probes is 80 °C, Müller-Maatsch, Caligiani, Tedeschi, Elst, and Sforza (2014) proposed an alternative method for DM determination by NMR after pectin saponification. Although highly resolved NMR spectra are obtained even at room temperature, only the amount of methanol is quantified. The DM is obtained indirectly by calculating the molar ratio of methanol to galacturonic acid, which has to be determined separately.

The degree of blockiness in pectins can also be assessed by ^{1}H-NMR spectroscopy, whereas random deesterification can be better predicted than blockwise one (Winning, Viereck, Nørgaard, Larsen, & Engelsen, 2007).

NMR relaxation experiments (Time Domain NMR, TD-NMR) provide information about water mobility within a porous system such as biological tissue and macromolecular matrices (Foucat & Lahaye, 2014; Musse, et al., 2009). The heterogeneous microstructure of these systems affects water diffusion and interactions, resulting in complex longitudinal (T_1) and transverse (T_2) exponential relaxations of the NMR signal decay. These parameters were, amongst others, used to determine apple mealiness (Marigheto, Venturi, & Hills, 2008) and microstructural modifications during cooking of potatoes (Mortensen, Thybo, Bertram, Andersen, & Engelsen, 2005). Estimation of both the pore size and distribution in lignocellulose (Meng, et al., 2013), cellulose (Zhang, et al., 2016) and the cell wall from *Arabidopsis thaliana* (Rondeau-Mouro, Defer, Leboeuf, & Lahaye, 2008) is also possible. Basically, an increase of water mobility in the system is reflected in an increase of the T_2 relaxation time. This can be roughly linked to the porosity of the material since an increase in T_2 relaxation times involves, amongst others, an increase in average pore size (Meng & Ragauskas, 2014). The average T_1 relaxation time of the adsorbed water also provides information about porosity.

3. Plant-based purees

3.1. Definition of apple puree

The European Legislation (Directive 2012/127EU) defines apple and other fruit purees as "the fermentable but unfermented product obtained by suitable physical processes such as sieving, grinding, milling the edible part of whole or peeled fruit without removing the juice". In addition, the fruits have to be "sound [and] appropriately mature". According to the *Codex Alimentarius* (Codex Stan 17-1981, Review 1-2001), canned apple puree has to be prepared from washed apples that do not present any health risk and confirm the characteristics of the fruit of *Malus x domestica* Borkh. The product is obtained from ground apples, which may have been peeled. Furthermore, it can be prepared with or without supplementary ingredients such as sodium chloride, spices, sugars, honey or water. Sweetened apple puree has to contain not less than 16.5% total soluble solids (16.5° Brix) and unsweetened apple puree not less than 9.0% total soluble solids (9.0° Brix). Before or after being processed by heat, the puree has to be hermetically sealed in a proper vessel in order to avoid spoilage.

3.2. Physical structure

Apple and other plant-based purees (**Fig. 28**) are concentrated dispersions of soft and deformable insoluble particles (pulp) in an aqueous medium, the so called serum (Rao, 1992). The pulp is primarily composed of cell clusters, individual cells or cell fragments from the parenchyma of the original fruit. The pulp´s particle size ranges between some hundred µm and some mm (Espinosa, et al., 2011; Leverrier, Almeida, Espinosa-Munoz, & Cuvelier, 2016; Rao, 2007). The serum contains the cell content that was emptied during processing. It is mainly composed of water (85%) and soluble sugars (12%), containing only minor amounts of organic acids, proteins, lipids and salts (Ebermann & Elmadfa, 2011). Some pectins are solubilised during processing but generally represent less than 0.5% (Le Bourvellec, et al., 2011).
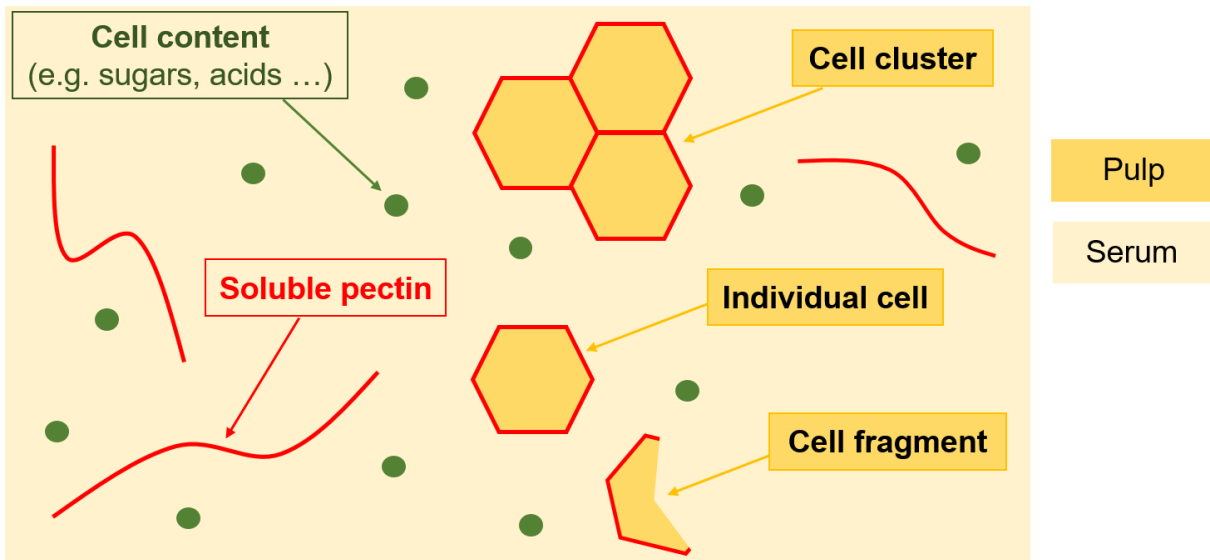
Fig. 28. A schematic representation of the composition of plant-based purees. Based on Moelants, et al. (2014a).

3.3. Apple processing into puree

Processing of plant-based foods aims to prolong shelf life and to increase product edibility and palatability. At the same time, the original sensory and nutritional characteristics of the raw material should be maintained as good as possible (Oey, Lille, van Loey, & Hendrickx, 2008).

The majority of the processed apples is not grown with the objective of being processed but are fruits rejected from the fresh market. The available volume and cultivars thus depend on the demand of the fresh market (Root & Barrett, 2005). Cultivars adapted for processing have high soluble sugars and acids, a pronounced aromatic flavour and bright golden or white flesh. This is why Golden Delicious is one of the most commonly processed apple cultivars.

Apples have often to be stored after harvest and prior to processing. In order to preserve the characteristics of the raw fruits, they are kept at cold temperatures (1–4 °C) and under controlled atmosphere (Root & Barrett, 2005). In the case of controlled atmosphere, the concentrations of carbon dioxide, nitrogen and oxygen can be regulated as well as humidity. Depending on the cultivar, storage temperature and atmosphere have to be adjusted.

Before processing, the apples are washed in a channel filled with water in order to eliminate impurities such as soil particles, pesticide residues and microbiological contaminations. Unripe or rotten apples are also eliminated at this step. Whereas healthy apples show lower density than water and thus float on the surface, rotten apples have higher density and sink. In addition, apples with major visible defects are rejected manually.

Sometimes, the core is removed and the apples are peeled before cooking (Simpson, 2012) but most frequently, apple peel and seeds are removed during refining. Although polyphenols are concentrated in the peel (Oszmianski & Wojdylo, 2008), only few polyphenols migrate from the peel into the puree during processing (Le Bourvellec, et al., 2011).

Apples are mechanically ground before (cold break process, CB) or after heating (hot break process, HB) in order to disrupt the parenchyma tissue into smaller particles (Espinosa-Munoz, Renard, Symoneaux, Biau, & Cuvelier, 2013). At the same time, the cell content is released into the medium. CB process initiates undesired enzymatic browning reactions in the apple flesh due to polyphenol oxidation by the endogenous polyphenoloxidase (PPO) in the presence of oxygen (Simpson, 2012). Although the subsequent heating inactivates PPO with temperatures higher than 50 °C (Martinez & Whitaker, 1995), preservation of an acceptable colour in CB purees usually relies on addition of a substantial amount (0.5–1 g/kg) of ascorbic acid during apple grinding.

Thermal treatment aims to inactivate endogenous enzymes while softening the tissue. The initial loss of firmness is due to membrane disruption and the associated loss of turgor (Greve, et al., 1994). Additional softening occurs as a result of increased cell separation because of solubilisation and depolymerization of pectic polymers that are involved in cell-cell adhesion (Van Buren, 1979; Waldron, Parker, & Smith, 2003). The applied temperatures and cooking durations depend on the manufacturer. Industrial processes can reach temperatures from, for example, 85 °C to 95 °C for 15 or 2 minutes, respectively (Colin-Henrion, Mehinagic, Renard, Richomme, & Jourjon, 2009; Le Bourvellec, et al., 2011).

Apple puree then passes through a refining sieve of a defined diameter (typically between 0.5 and 3 mm) in order to remove skin, seeds and to define smooth (small particles) or grainy textures (big particles). Some supplementary ingredients, such as sugars or ascorbic acid, may be added to improve flavour, colour and shelf life. This step can also be conducted before cooking (notably in CB process).

It is common to fill the hot apple puree immediately after refining into all sorts of containers such as bottles, glass jars or metal cans. Sometimes, immediate bottling is not possible, so that apple puree remains in a heated holding tank (Featherstone, 2016) for up to 30 minutes at 85 °C (Colin-Henrion, et al., 2009). The hot apple puree is then filled into the containers, which have to be closed at 88 °C to ensure a safe product (Root & Barrett, 2005). In order to obtain a vacuum-sealed product, a vapour stream passes over the top of the product just prior to sealing. As the steam condenses, a vacuum is created in the container. Generally, a pasteurization step of 2 or 3 minutes at 90 °C follows to ensure complete sterilization of the product prior to cooling.

The following figure summarizes the steps that might be applied during apple processing into puree (**Fig. 29**).
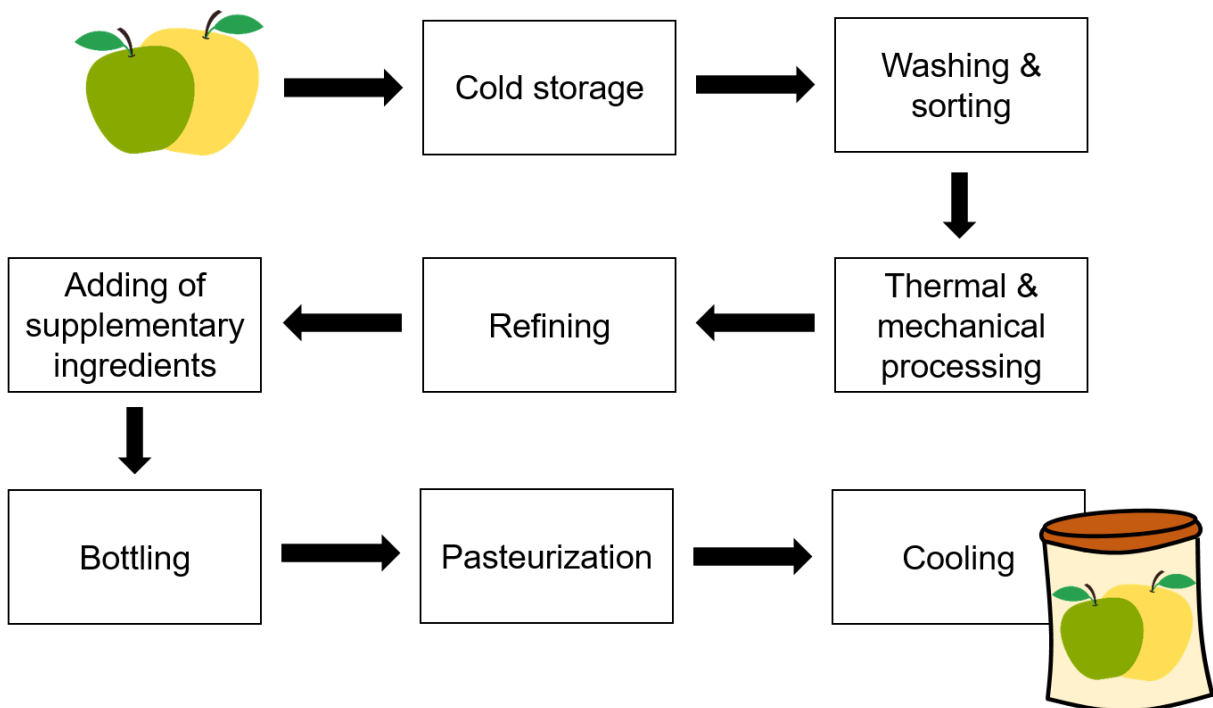
Fig. 29. Typical steps applied during apple processing into puree.

3.4. Introduction to rheology of plant-based suspensions

3.4.1. Rheological properties of fluids and dispersions

Rheology studies the deformation and flow of materials. The behaviour of a material under mechanical stress (**Fig. 30**) can be described by different rheological models (Rao, 2007).
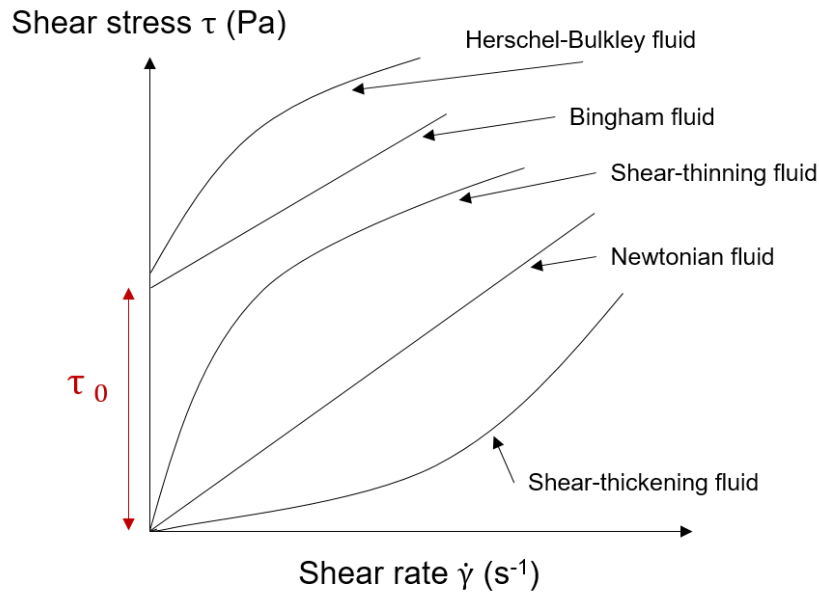
Fig. 30. Presentation of rheological behaviours of different fluids and yield stress dependence (τ_0).

In **Newtonian fluids**, the shear rate is directly proportional to the shear stress, beginning from zero. For these fluids, viscosity η is defined as the shear stress τ divided by the shear rate $\dot{\gamma}$:

$$\eta = \tau/\dot{\gamma} \tag{8}$$

Examples of Newtonian fluids are water, sugar syrups, edible oils, filtered juices and milk. All these fluids contain only dissolved low molecular weight polymers such as sugars but no high concentration of high molecular polymers (pectins, proteins, starches …) or insoluble solids.

In the case that increasing shear stress leads to a more than proportional increase in shear rate, the fluid is **shear-thinning** (pseudoplastic). The plot starts in the origin and is curved upwards. Thus, viscosity decreases with increasing shear stress as

hydrodynamic forces, generated during shear, cause a structural breakdown in the material. This behaviour is common to many fruit and vegetable purees, salad dressings and some concentrated fruit juices.

In **shear-thickening** (dilatant) fluids, an increasing shear stress causes less than proportional increase in shear rate. The resulting plot is curved downwards, but still begins in the origin. Partially gelatinized starch dispersions are an example of this flow type in which viscosity increases with shear.

The **Ostwald-de Waele** (or power law) model makes it possible to model the behaviour of Newtonian and non-Newtonian fluids:

$$\eta = K \cdot \dot{\gamma}^{n-1} \tag{9}$$

This equation gives access to the consistency coefficient K and the flow index n. The flow index n evaluates the shear-thinning character of the purees ($n=1$: Newtonian fluid; $n>1$: shear-thickening; $0<n<1$: shear-thinning).

Some fluids only start to flow when a certain stress, the yield stress (τ_0), is reached. This is associated with the cohesion between the particles packed against each other within the suspension, preventing flow as long as the structure is not damaged. Newtonian fluids exhibiting a yield stress are so called **Bingham fluids**. Viscosity can then be calculated by the Bingham model:

$$\eta = (\tau - \tau_0)/\dot{\gamma} \tag{10}$$

Several food products such as tomato concentrates or ketchup, as well as mustard and mayonnaise are shear-thinning fluids with a yield stress. Shear-thinning and -thickening fluids with a yield stress can be modelled by the Herschel-Bulkley model and are thus so called **Herschel-Bulkley fluids**:

$$\eta = \tau_0 + K \cdot \dot{\gamma}^{n-1} \tag{11}$$

Although several mathematical models exist to describe the flow properties of plant-based suspensions, the Herschel-Bulkley model is the most commonly used (Duran & Costell, 1982; Espinosa Brisset, 2012).

3.4.2. Methods to assess textural properties

3.4.2.1. Bostwick consistometer

One of the simplest methods to determine the consistency of plant-based suspensions is via Bostwick consistometer (**Fig. 31**A). This instrument is cheap and widely used in industry as it is easy to handle and reveals simple values in a short time. The product's consistency (expressed as "Bostwick units") is evaluated by the distance in cm that the product travels in a given time, once it is allowed to flow by gravity. Thicker samples progress less and thus have a lower Bostwick value. However, little information is provided about the rheological behaviour of the product as the result is a combination of yield stress and viscosity coefficient (Cullen, Duffy, & O'Donnell, 2001). Furthermore, this method is highly subjective and depends on the operator. Several simple factors such as the levelling or the dryness of the instrument can influence the result (Barringer, Azam, Heskitt, & Sastry, 1998).
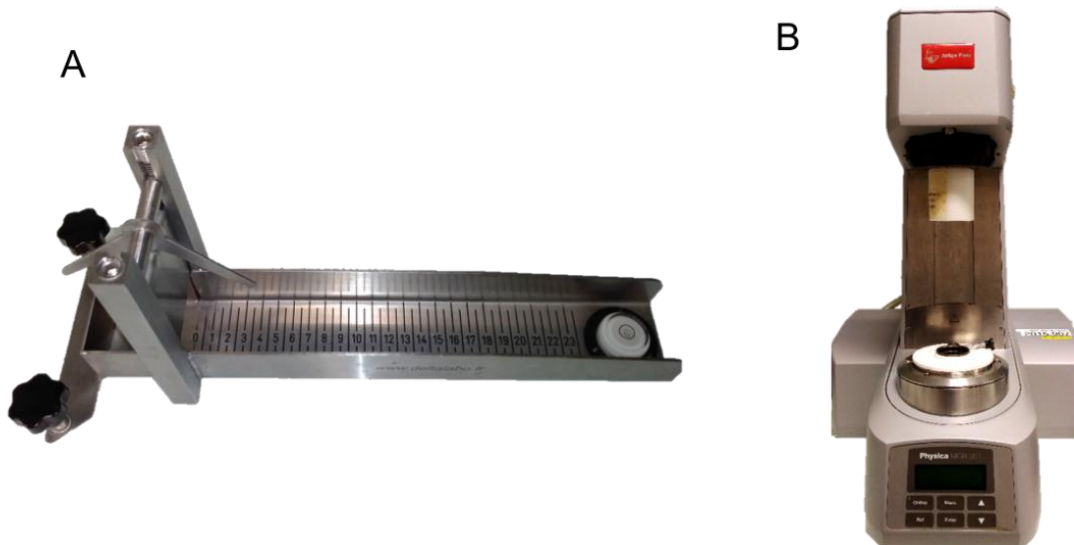
Fig. 31. Bostwick consistometer (A) and stress controlled rheometer (B).

3.4.2.2. Stress controlled rheometer

Stress controlled rheometers (**Fig. 31**B) are important instruments to understand the flow and deformation properties of a material by measuring the stress-strain relationship. In addition, they provide more control during the experiment due to controlled temperature or shear stress/rate. An appropriate measuring system has to be chosen depending on the experiment.

Steady state measurements

Steady state measurements (rotational tests) are used to generate a flow curve. The sample is subjected to increasing or decreasing shear stress τ and the resulting shear rate $\dot{\gamma}$ is measured at each applied stress (**Fig. 30**).

Dynamic rheological measurements

Dynamic rheological measurements (oscillatory tests) provide insight into the microstructural properties of the sample at rest and predict rheological characteristics.

Generally, shear stress τ is applied to the material and the resulting deformation (shear strain γ) is recorded. In order to avoid damage of the sample's structure by the measurement, the test is usually applied in the linear viscoelastic range. This gives access to the shear modulus G, revealing information about the rigidity of the material:

$$G = {}^{\tau}\!/_{\gamma} \qquad\qquad\qquad (12)$$

In oscillatory tests, oscillatory shear strain is plotted versus time and results in a sinusoid with the strain amplitude γ_A. The applied shear strain induces shear stress that can be represented by a second sinusoid with the amplitude τ_A. In the viscoelastic range, these two sine curves oscillate with the same frequency. For ideally elastic, i.e. completely rigid, samples, no time lag between the preset and the response sine curve is recorded (**Fig. 32**A).
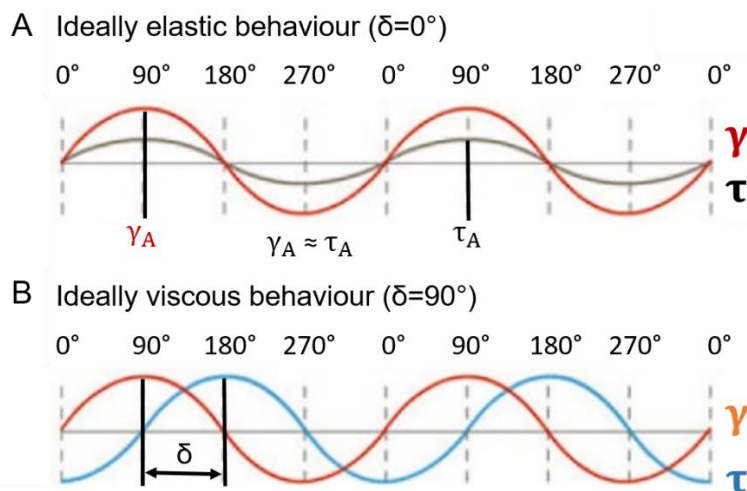
Fig. 32. Comparison of ideally elastic (A) and ideally viscous (B) behaviour by oscillatory test, presented as a sinusoidal function versus time.
Adapted from Anton Paar (2020).

However, most samples are viscoelastic and the response sine curve differs from the preset curve by the phase shift δ (0° > δ > 90°). For ideally viscous samples, the phase shift is 90° (**Fig. 32**B).

The relation between the strain and the stress amplitude gives the complex shear modulus G*, which describes the entire viscoelastic behaviour of a material:

$$G^* = {\tau_A}/{\gamma_A} \tag{13}$$

With the knowledge of the complex shear modulus and the phase shift, the storage modulus (G') and the loss modulus (G'') can be assessed (**Fig. 33**). G' describes the elastic portion of the viscoelastic behaviour. It represents the deformation energy that is stored in the sample during the shear process. G'' is the viscous portion, representing the deformation energy that is used through internal frictions and thus "lost" when flowing.
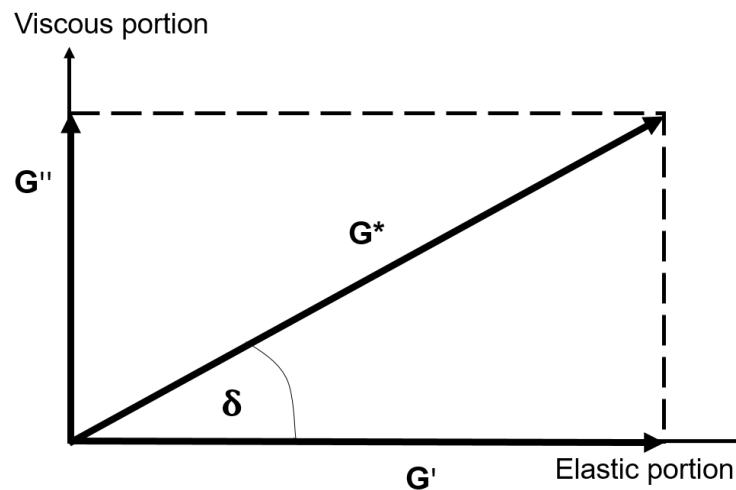
Fig. 33. Relationship between the complex shear modulus G*, the storage modulus G', the loss modulus G'' and the phase-shift angle δ.

At low shear strains in the linear viscoelastic range (LVER), the G' and G'' curve are parallel, mostly on different levels (Mezger, 2014). The viscoelastic behaviour of a sample can be described by analysing the relation between G' and G'' in the LVER:

G' > G'' (tanδ < 1): The elastic behaviour dominates the viscous one, so the material represents rigid character. This is the case for solid materials or stable pastes but also for many dispersions such as pharmaceutical lotions or foodstuffs with gel-like characteristics.

G'' > G' (tanδ > 1): The viscous behaviour dominates the elastic one and materials are liquid. Even at rest, they can flow, although this may occur very slowly. Examples are polymer solutions without stabilizing cross-links.

G' = G'' (tanδ = 1): Materials showing the same G' and G'' in the LVER are at the gel point. This phenomenon is rare and represents a character between the liquid and gel-like state.

Measuring systems

Rotational and oscillatory tests of pureed fruits and vegetables are essentially conducted with the parallel-plate (**Fig. 34**A) (Ahmed & Ramaswamy, 2006; Alvarez, Fernández, & Canet, 2004), the concentric cylinder (**Fig. 34**B) (Espinosa Brisset, 2012; Leverrier, 2016; Schijvens, van Vliet, & van Dijk, 1998; Tarea, 2005) or the vane geometry (**Fig. 34**C) (Lopez-Sanchez, Chapara, Schumm, & Farr, 2012; Moelants, et al., 2014b).
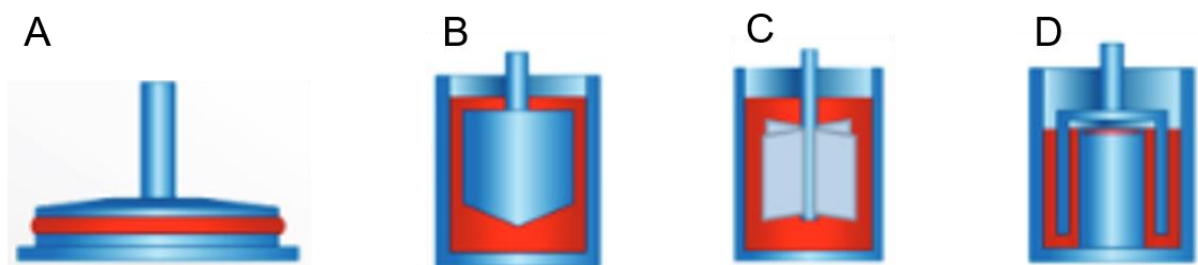
Fig. 34. Parallel-plate (A), concentric cylinder (B), vane (C) and double gap (D) measuring systems.
Taken from Thermo Scientific (2017).

Parallel-plate and concentric cylinder geometries are absolute measuring systems (MeS), following the standards ISO 3219 and DIN 53019-1 or ISO 621-10 and DIN 53019-1, respectively. These systems give absolute values, which do not correlate with the size of the MeS (Mezger, 2014). Parallel-plate MeS are designed to measure dispersions with relatively large particles, but wall slip can occur. This is usually caused by large velocity gradients near the wall, resulting in a local decrease of the dispersed phase. A lubricant layer is then formed at the wall surface, resulting in a potentially large underestimation of the actual viscosity of the sample. This problem can be counteracted by using roughened surfaces. Another disadvantage of parallel-plate MeS is "shear deformation", meaning that shear rate increases from the centre to the edges of the plate. An advantage of concentric cylinder geometries is that high shear rates can be applied without creating "edge failure", summarizing several effects typical for parallel-plate MeS (**Table 3**). This includes inhomogeneous flows at the edges of the plate, as well as migration effects of the sample to the edges due to normal forces or solvent evaporation.

For "non ideal" samples such as plant based foods, absolute MeS are sometimes not advised due to the risks of misestimating rheological properties. Then, relative MeS are used, such as vane geometry MeS. They contain several blades and are used to test pasty materials or products with large particles (Mezger, 2014). When placed in a structured liquid, they cause minimal sample disturbance. In addition, wall slip is prevented since these geometries show roughened surfaces. However, inhomogeneous deformation can occur at high rotational speeds as material in between the vane areas risk to not be sheared.

Flow curves of apple serum are measured with double gap MeS (**Fig. 34**D) (Espinosa, et al., 2011; Leverrier, et al., 2016). These are concentric cylinders, which are adapted for analysis of low-viscous liquids. The cup disposes of an additional inner cylinder and a hollow cylinder turns around it. This increases the available shear area since a large contact area between the sample and the surface of the double gap geometry is provided.

Advantages and disadvantages of different measuring systems are summarized in **Table 3**.

Table 3. Overview of applications, advantages and disadvantages of several measuring systems.

Measuring system	Application	Advantage	Disadvantage
Parallel-plate	• Dispersions with large particles • Samples with 3D structure • Hardening and curing materials • Soft solids	• Absolute measuring system • Roughened surfaces can be used to prevent wall slip • Fast cleaning procedure	• Shear conditions not constant in the gap • Edge failure (inhomogeneous flow, turbulent flow, inertia effects, discharge of the gap, skin formation, surface effects, evaporation of solvents …) • Large temperature gradient in the gap
Concentric cylinder	• Low-viscous samples • Dispersions	• Absolute measuring system • No edge failure, even at high shear rates • Roughened surfaces can be used to prevent wall slip • Good temperature control	• Large gap: Secondary flow effects, time-dependant behaviour, inhomogeneous deformation • Low-viscous samples: Flow instabilities, turbulent flow at high rotational speeds
Vane	• Dispersions with large particles	• Minimal sample disturbance • No wall slip	• Inhomogeneous deformation at high rotational speeds
Double gap	• Low-viscous samples	• Increase of available shear area • Good temperature control	• Time-consuming cleaning procedure

It is extremely important to choose an appropriate gap size in order to allow homogenous flow during analysis and to avoid disorganization of particles. The gap size is set as the height of the parallel-plate, the diameter of the cylinder bob or the cylindrical relative MeS. If the gap is too small, it risks deforming particles. If the gap is too large, the first layers of the product are in contact with the inner cylinder and are thus sheared even at low speed or shear stress, while the outer layers are not. As a general rule of thumb, a gap size between 5 and 10 times the size of the largest particles in the sample is recommended (Mezger, 2014).

3.4.3. Rheological properties of apple purees

Fruit purees are viscoelastic fluids, so they have both the viscous properties of a liquid and the elastic properties of a solid. Apple purees are shear-thinning fluids with a yield stress (Colin-Henrion, Cuvelier, & Renard, 2007; Espinosa, et al., 2011; Rao, 1977, 1992). They are more viscous than serum due to suspended pulp particles. However, serum also shows a shear-thinning behaviour (**Fig. 35**A) due to the presence of soluble pectins (Rao, Cooley, Nogueira, & McLellan, 1986).

The shear-thinning character is typical for concentrated plant-based suspensions. It is a consequence of structural reorganizations within the flowing system since possible particle aggregates disintegrate and the dispersed elements align in the same direction to facilitate the flow (Duran & Costell, 1982). This effect is often reversible almost instantly and the samples recover rapidly their initial viscosity. Thus, the medium does not present marked thixotropy. This has also been observed in apple purees (Qiu & Rao, 1989; Schijvens, et al., 1998; Tarea, 2005).

Studies in both concentrated apple cell wall dispersions (Kunzek, Opel, & Senge, 1997; Müller & Kunzek, 1998; Vetter & Kunzek, 2003) and reconstituted apple purees (Espinosa, et al., 2011) show dominant elastic properties with G' > G" over the entire frequency domain (0.1–40 rad/s) (**Fig. 35**B). This is mainly due to the cell wall particles in the puree as they form an elastic network of weak attractive or repulsive forces. Kunzek, et al. (1997) reported that the viscous portion was only dominant (G" > G') in homogenized suspensions, probably due to smaller and less structured particles.
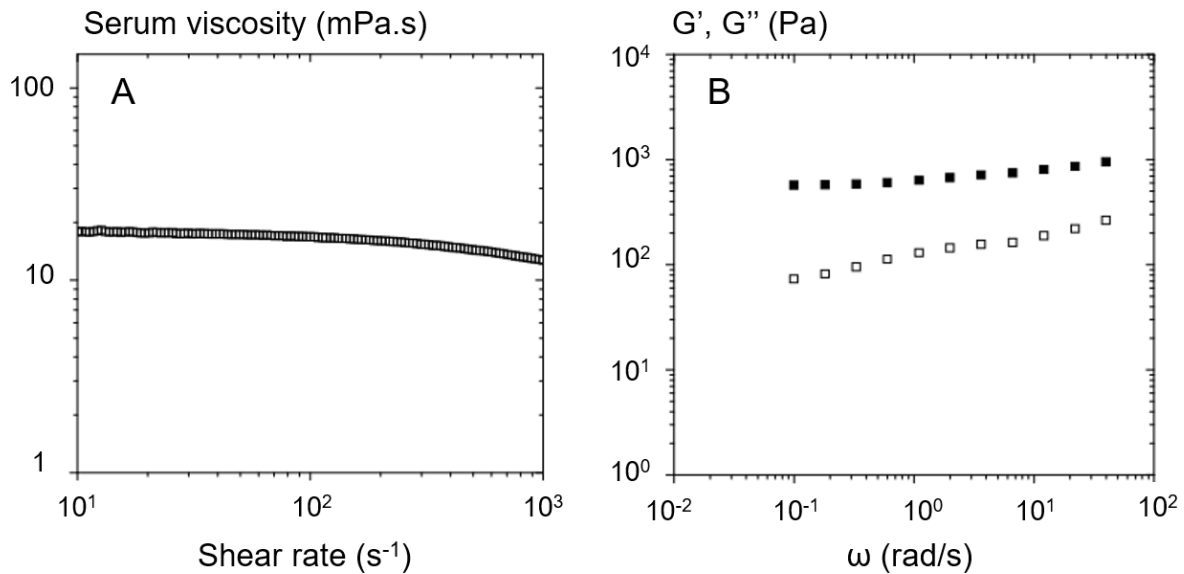
Fig. 35. Serum viscosity showing shear-thinning behaviour (A) and storage (G') and loss modulus (G") of apple puree in the LVER (B).

Adapted from Espinosa Brisset (2012). ■: G'; □:G".

3.5. Determinants of apple puree´s texture

Texture represents a major quality attribute of foods (Waldron, et al., 1997) and food industry is highly interested in predicting and controlling the textural quality of plant-based foods such as soups, smoothies or purees. Stabilizers or texturizing agents can be added to obtain the desired texture, although they may be perceived negatively by consumers and should be avoided in order to produce more natural products. It is known, but not mastered by industry, that the texture of processed fruit and vegetables depends mainly on the original tissue structure (Waldron, et al., 1997). In model systems, three key factors were identified to determine puree's texture (Espinosa-Munoz, et al., 2013; Espinosa, et al., 2011; Kunzek, Kabbert, & Gloyna, 1999; Leverrier, et al., 2016; Rao, 1992; Rao, et al., 1986):

1) Amount of insoluble particles

2) Particle size and shape

3) Viscous properties of the serum

118

The amount of insoluble solids (pulp) impacts the rheological behaviour of plant-based products the most as they determine if the suspension is diluted, semi-diluted or concentrated (Leverrier, et al., 2017b). Apple purees are concentrated suspensions of soft particles and the pulp content can be estimated in several ways.

The total amount of insoluble dry particles can be accessed by extracting the water insoluble solids (WIS) or alcohol insoluble solids (AIS). Both methods express the quantity of cell walls after removing soluble solids by water or alcohol, respectively, and drying. They were both used in apple purees, WIS for example by Schijvens, et al. (1998) and AIS by Colin-Henrion, et al. (2009) and Le Bourvellec, et al. (2011).

To estimate the amount of wet pulp, the puree is centrifuged under given conditions and the percentage of pulp compared to serum is calculated by the wet mass (Espinosa-Munoz, et al., 2013; Rao, 1987; Tarea, 2005). The pulp obtained by this method is compressed by centrifugal forces and contains serum to a differing extent, depending on the parameters used during centrifugation.

The most realistic value is represented by the volume fraction Φ. This is the volume that is effectively occupied by the particles ($V_{particles}$) in the total volume of the suspension (V_{total}):

$$\Phi = V_{particles} \big/ V_{total} \qquad\qquad (14)$$

It depends on the amount of particles, cell packing and deformation characteristics, determined by cell wall rigidity. It is also linked to particle size and shape as cell clusters occupy more effective volume than individual cells and thus hinder flow formation to a higher extent, resulting in increased viscosity (Espinosa-Munoz, et al., 2013).

However, it is difficult to determine the volume fraction as particles are highly deformable and their volume decreases under stress or with increased concentration (Leverrier, et al., 2017b; Lopez-Sanchez, et al., 2012). This is why the pulp wet mass was used in this work.

Leverrier, et al. (2017b) established a protocol to visualize deformation of individual, rehydrated apple cells under confocal microscopy and subsequent 3D image analysis. Different concentrations of AIS in a sodium chloride solution (0.1%, w/w) with identical conductivity as native apple serum allowed to view diluted, semi diluted and concentrated suspensions (**Fig. 36**).
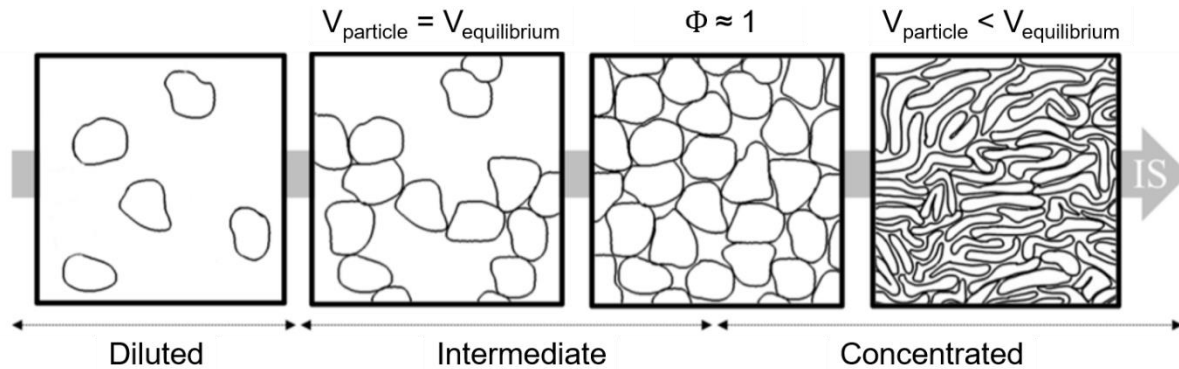
Fig. 36. Evolution of apple cell volume fraction (Φ) with increasing insoluble solids (IS) content.
Taken from Leverrier, et al. (2017b).

In the diluted domain, the cells are free and in equilibrium although they were found to be deflated due to thermal processing. In the intermediate domain, cells occupy more space and begin to build a network. In the concentrated domain, cells adapt to the available volume and are thus forced to compress.

In apple purees, both the apparent viscosity (**Fig. 37**A) and the yield stress (**Fig. 37**B) increase with increasing pulp content and particle size (Espinosa, et al., 2011; Schijvens, et al., 1998). Missaire, Qiu, and Rao (1990) also observed an increase in yield stress with increasing pulp content and particle size. Pulp content and particle size also affect the flow behaviour of apple purees as less shear thinning is observed with low pulp content and small particles (Espinosa, et al., 2011). Both G' and G'' increase with increasing pulp content and larger particles (Espinosa, et al., 2011), although pulp content seems to affect G' more than G'' (Kunzek, et al., 1997).
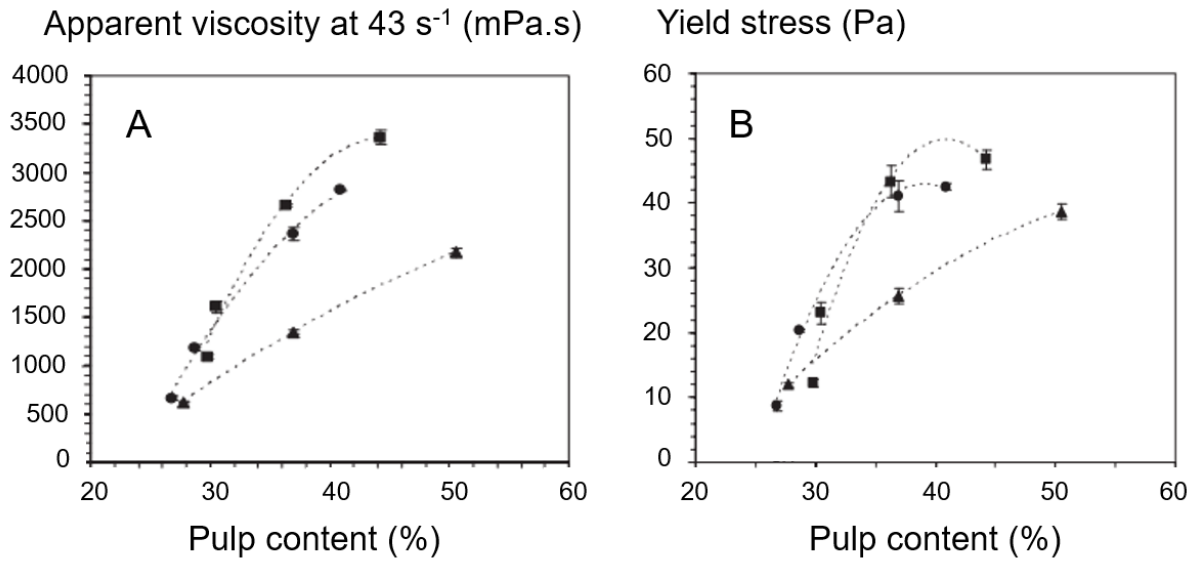
Fig. 37. Impact of pulp content and particle size on apparent viscosity (A) and yield stress (B) of apple purees.

Taken from Espinosa, et al. (2011). ▲: 200 μm; ●: 500 μm; ■: 1100 μm. Yield stress was calculated with Herschel-Bulkley model.

In carrot and broccoli cell wall suspensions, Day, Xu, Oiseth, Lundin, and Hemar (2010) also showed increasing G' and G" values with increasing particle size and concentration. While larger particles could also be linked to increased apparent viscosity in tart cherry purees (Lukhmana, Kong, Kerr, & Singh, 2018) or increased yield stress, G' and G" in carrot and broccoli dispersions, no correlation was found in tomato dispersions (Lopez-Sanchez, et al., 2011). In tomato suspensions, the pulp content seems to be more important than particle size to determine the yield stress and G', which increase with increasing pulp concentration (Belović, Pajić-Lijaković, Torbica, Mastilović, & Pećinar, 2016; Moelants, et al., 2014b). The effect of particle size in tomato purees is controversial since particle shape, deformability and particle surface influence yield stress and G' at the same time (Moelants, et al., 2014b). Particle shape can also be important in apple purees as it seems that more irregular particles increase apparent viscosity, maybe due to their occupied volume (Leverrier, et al., 2016).

121

In apple, tomato, broccoli and carrot dispersions, the viscosity of the continuous phase has a weaker impact on puree´s texture than the properties of the pulp (Lopez-Sanchez, et al., 2011; Rao, et al., 1986). In addition, the impact of serum viscosity on the overall puree's texture decreases with increasing pulp content (Leverrier, Almeida, Menut, & Cuvelier, 2017a). However, it can play a lubricant role between particles and thus improve a "smooth" sensory perception (Espinosa-Munoz, Symoneaux, Renard, Biau, & Cuvelier, 2012). This induces reduced cohesion of the suspension leading to reduced yield stress and elastic properties (G') (Espinosa Brisset, 2012). Serum viscosity might have a more important role in fruits and vegetables with a high starch content. Starch can swell and join the serum when the cells are broken during thermal and mechanical treatment, affecting rheological properties of the serum.

Some studies tried to correlate the rheological behaviour of plant-based suspensions to pulp content and serum viscosity. The impact of pulp content (pulp%) and serum viscosity (η_{serum}) on apparent viscosity (η_{app}) was accessed using two constants a and b and a power law model (Rao, 1987):

$$\eta_{app} = \eta_{serum} + a \cdot (pulp\%)^b \qquad (15)$$

A power law model was also used to model yield stress (τ_0) in reconstituted carrot suspensions (Moelants, et al., 2012). However, other variables such as particle size should be included to better represent the whole system.

$$\tau_0 = a \cdot (pulp\%)^b \qquad (16)$$

Espinosa Brisset (2012) aimed to include the volume fraction (Φ) of the cells in these equations and defined it as the product of the insoluble cell wall content (C) and apparent voluminosity (V). In order to assess this parameter (by pulp wet mass after puree centrifugation) of different particle types present in the puree, a puree essentially made up of individual cells (homogeneous in size and shape) was taken as a reference with the volume V_{ref}. The factor α was defined as $\alpha = V/V_{ref}$, therefore $\alpha = 1$ for the reference puree. After empirical observations, they concluded that a power law could be used to model rheological parameters ($Parameter_{rheo}$) such as apparent viscosity, yield stress and G':

$$Parameter_{rheo} = a \cdot (C \cdot \alpha)^b \qquad (17)$$

Although some attempts were made to model rheological behaviour of cell wall dispersions, particle size was never included in the equations until now. Moelants, et al. (2014b) observed in reconstituted tomato suspensions that the value of the power law exponent changes depending on particle size and shape. Since the effect of particle size on the exponent was not straightforward, the authors supposed that other particle properties, such as particle shape, might be more important. However, more research is needed to integrate particle properties in the mathematical model in order to adapt it to "real" (i.e. not reconstituted) systems.

3.6. Impact of raw material and processing steps on puree´s structure

Since the original tissue structure, particularly the cell wall properties of the raw material, highly determines puree's texture (cf. **II 3.6.**), a targeted application of both the raw material and processing conditions makes it possible to design naturally textured food products.

3.6.1 Raw material

Lopez-Sanchez, et al. (2011) demonstrated that each plant species reacts differently to the applied processing conditions due to their individual microstructure. Thus, rheological properties in the obtained plant-based dispersions strongly differ.

Even in the same fruit species, both the cultivar and the maturity stage modify the chemical and structural properties of the cell wall (cf. **II 2.4.1.**). This as well as different growing conditions, depending on environmental effects and farming practices, could affect rheological properties of the processed food product (Kunzek, et al., 1999; Waldron, et al., 2003).

Indeed, several studies showed that apple cultivars soften to a different extent during heating (Anantheswaran, McLellan, & Bourne, 1985; Bourles, Mehinagic, Courthaudon, & Jourjon, 2009; Kim, Smith, & Lee, 1993). However, the initial apple firmness cannot predict the flesh firmness after heating (Bourles, et al., 2009).

The texture of apple puree is also affected by the cultivar (Rao, et al., 1986), probably due to differences in the pulp content and its chemical composition (Le Bourvellec, et al., 2011) as well as particle size (Schijvens, et al., 1998).

Purees prepared from apples at three maturity stages (unripe, ripe, overripe) showed differences in apparent viscosity and yield stress (Schijvens, et al., 1998). Both values decreased with increased maturity, probably due to particle size and serum viscosity, showing the same trend. The authors hypothesized that particle size may be reduced due to advanced pectin degradation in the middle lamella, leading to enhanced cell separation. Serum viscosity may be reduced due to lower molar mass of soluble pectins. The pulp content, expressed as WIS, did not change.

This demonstrates the potential impact of the raw material on puree's texture. However, it remains little understood as detailed studies that link the cell wall structure of different apples (cultivar, maturity stage …) on the puree's structure (particle content and size, serum viscosity) and thus textural characteristics are still missing. The potential of the raw material to trigger puree's texture is thus not fully exploited.

3.6.2. Mechanical processing

3.6.2.1. Grinding

Mechanical treatment aims to disrupt the tissue structure into smaller cell fragments. It only induces a change in particle size and shape but does not modify the cell wall content (estimated by WIS or AIS) or pectin solubilisation, thus serum viscosity (Espinosa Brisset, 2012; Leverrier, et al., 2016). However, the pulp wet mass, determined after centrifugation of the puree, decreases. The smaller particles occupy less volume as they seem to pack more closely and thus favour compression of the pulp (Espinosa Brisset, 2012). This could be due to the regular shape of individual particles in comparison to irregular shape of cell clusters that hinder dense compression. However, due to microscopic observations, Lopez-Sanchez, et al. (2012) and Leverrier, et al. (2016) support the hypothesis that cell clusters are more rigid as their tissue structure is more preserved. Thus, they occupy more volume in the puree as they deform less and thus increase rheological behaviour.

Auffret, Ralet, Guillon, Barry, and Thibault (1994) described increased water retention capacities in peapods after grinding. This may be due to an increased accessible cell wall surface, capable to retain more water (Guillon & Champ, 2000). This would affect puree's texture as suspensions with cell walls having high water retention capacities show increased viscosity (Kunzek, et al., 1999).

Day, et al. (2010) studied the impact of grinding on blanched and heated carrot and broccoli tissue (**Fig. 38**). Grinding of the samples that were blanched (80 °C, 10 min) resulted in large cell clusters, whereas grinding of cooked samples (100 °C, 30 min) showed smaller particles, mostly individualized cells.
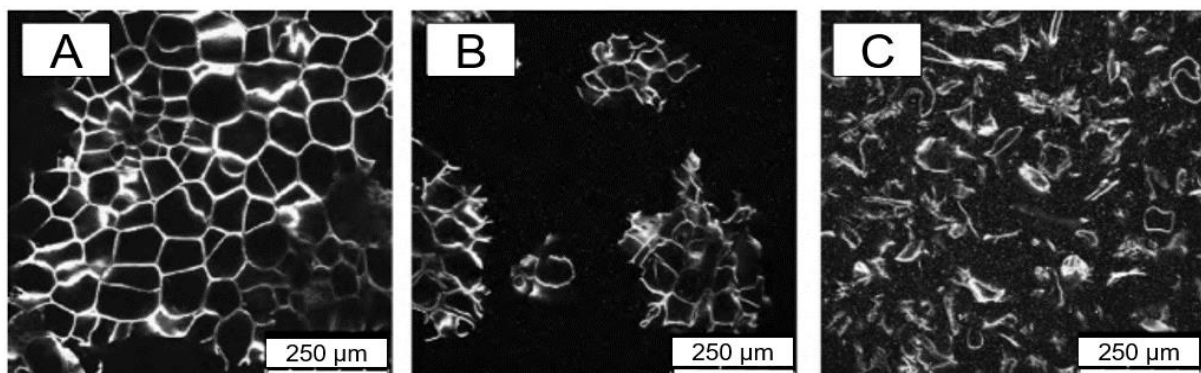
Fig. 38. Confocal micrographs showing the effect of mechanical treatments on raw (A), blanched (80 °C, 10 min) (B) and cooked (100 °C, 30 min) (C) carrot plant cell wall particle morphologies.
Taken from Day, et al. (2010).

Similar results were found by Lopez-Sanchez, et al. (2011). Grinding before heating (90 °C, 40 min) of carrot and broccoli tissue resulted in large cell clusters with broken edges due to cell wall disruption. In contrast, heating before grinding produced smaller particles, even individual cells, with smooth surfaces. This indicates cell separation through the middle lamella that was softened during heating.

These results highlight the complementary effect of heating and grinding in puree processing.

3.6.2.2. Refining

The refining step can also tailor puree's texture. As the puree is forced through sieve openings of a chosen diameter, carpels and peel are retained whereas cell clusters that are larger than the sieve openings tend to be separated into individual cells when they pass through the sieve. As the retained carpels and peel contain a higher proportion of cell wall than apple flesh (Massiot & Renard, 1997), the dry matter content of the puree is reduced (Colin-Henrion, et al., 2009). Depending on the refining device, both the pulp content and the particle size (Schijvens, et al., 1998) or only the pulp content (Rao, et al., 1986) are reduced. It has to be kept in mind that the size of many particles in the refined product can be considerably larger (two to three times) than the diameter of the sieve openings (Den Ouden & Van Vliet, 1997) due to the soft and deformable character of fruit cells (Leverrier, et al., 2017b). Serum viscosity is not affected by refining (Schijvens, et al., 1998).

As a result, the purees are smoother, generally preferred by consumers (Espinosa Brisset, 2012), and less viscous after refining (Rao, et al., 1986; Tarea, 2005).

3.6.3. Thermal processing

Cooking plays a major role in tissue softening and texture loss. While several pectin degrading reactions are described in literature (**Fig. 39**), hemicelluloses and cellulose are rather stable and thus less affected during thermal processing (Renard, 2005a; Van Buren, 1979).

Depending on temperature, different chemical and enzymatic reactions are favoured or inhibited, resulting in degradation and solubilisation of pectic polysaccharides (Massiot & Renard, 1997). This promotes, in turn, texture loss or improvement (Sila, et al., 2009). In general, temperatures higher than 80 °C favour chemical cleavage of pectins due to β-elimination or acid hydrolysis. In contrast, temperatures under 70 °C favour enzymatic cleavage of pectic polymers.
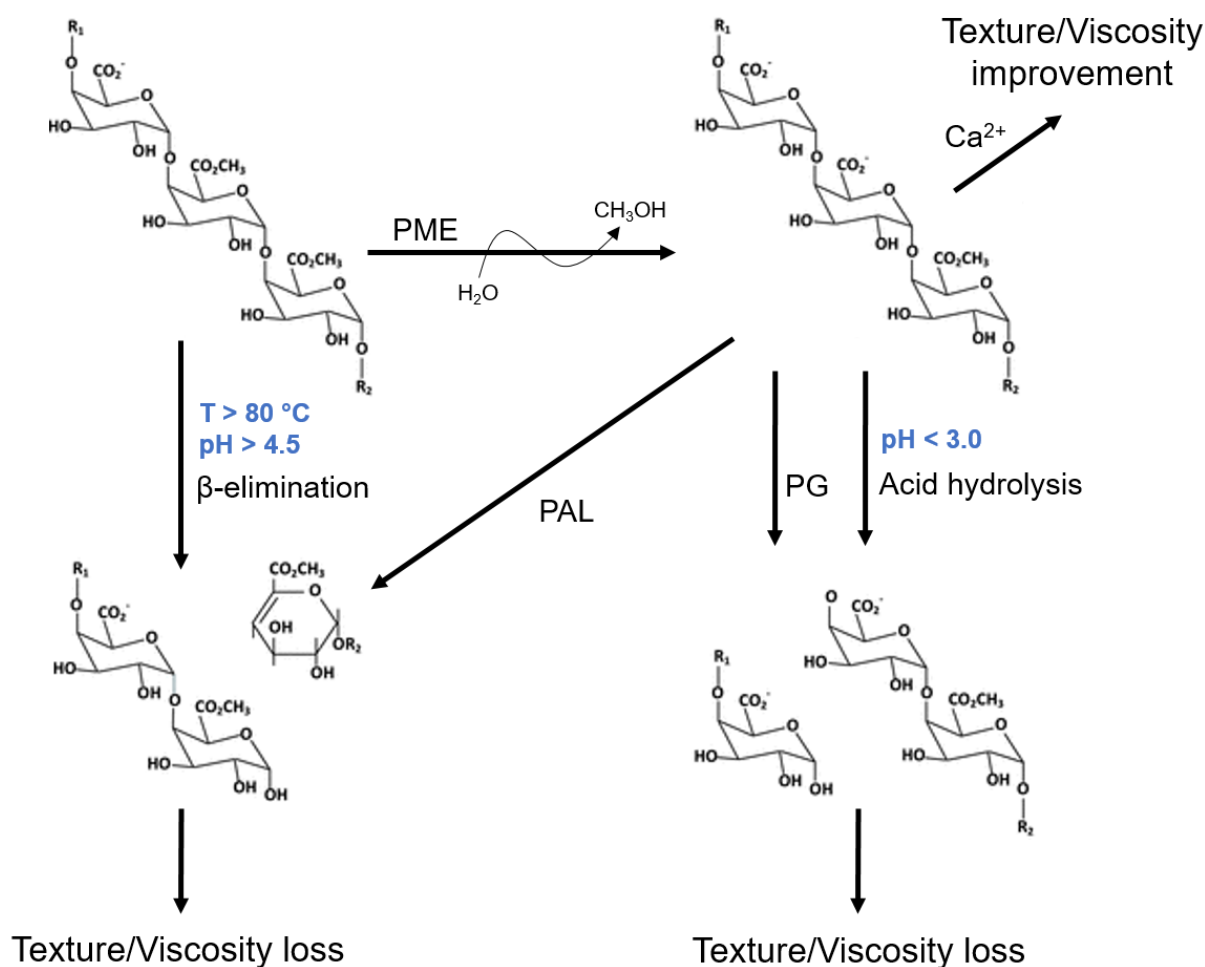
Fig. 39. Schematic representation of possible chemical and enzymatic conversion reactions of homogalacturonan pectins in plant-based foods.
Adapted from Sila, et al. (2009). PME: Pectin methylesterase; PAL: Pectate lyase; PG: Polygalacturonase.

3.6.3.1. Enzymatic reactions

Some endogenous pectinases are not only active during fruit ripening (cf. **II 2.4.2.**) but also during processing. Pectin methylesterase (PME), polygalacturonase (PG) and pectate lyase (PAL) are the most important endogenous enzymes, which may act on HG pectins during processing. In industry, pectinases are also often added as processing aid (Duvetter, et al., 2009). They are employed, for example, to increase the yield of fruit and vegetable juices, control the cloud stability in juices or master the rheological properties of purees and pastes. Knowledge about the catalysed mechanisms and optimum activity conditions of these enzymes are thus important to obtain the desired product characteristics.

PMEs are very sensitive to the ionic environment and can thus be regulated by adjusting the pH value. The pH optima in most plant PMEs lies between pH 6 and 8 and in microbial PMEs between pH 4 and 9 (Bordenave, 1996). PME of the apple variety Golden Delicious (**Fig. 40**) exhibits highest activity at a pH over 7.5 and at a temperature of 63 °C (Denes, et al., 2000).

A

V_{max} (%)

B

V_{max} (%)

pH
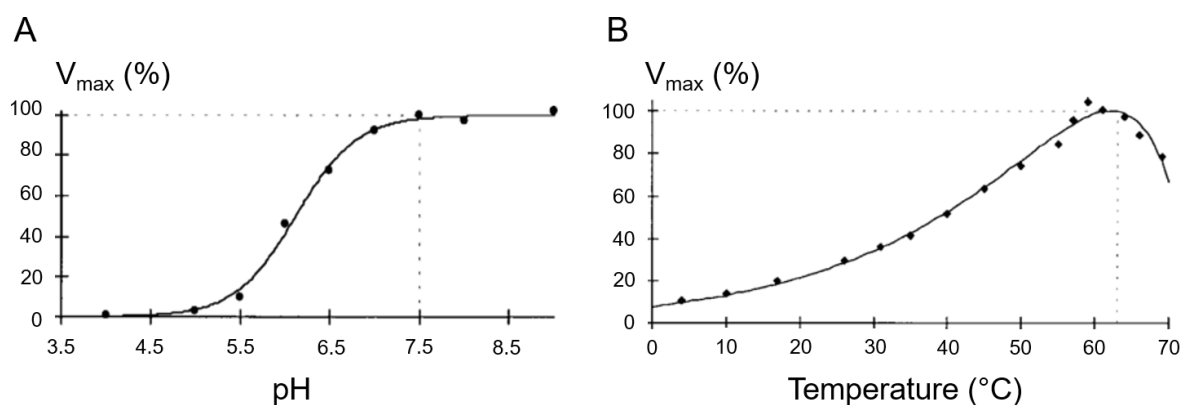
Temperature (°C)

Fig. 40. Effect of pH (A) and temperature (B) on apple PME activity.

Taken from Denes, et al. (2000). Assay conditions: Apple pectin (DM 75) at 2.5 mg/mL in 0.1 M NaCl at 35 °C (A) or pH 7 (B).

The addition of salts allows a shift of the pH optimum (Bordenave, 1996) and the addition of sugars or sugar alcohols increases the thermal stability of PME (Guiavarc'h, Sila, Duvetter, van Loey, & Hendrickx, 2003; Plaza, et al., 2008). Most PMEs are barotolerant and some isoforms are highly thermo-tolerant (Crelier, Robert, Claude, & Juillerat, 2001; Nunes, et al., 2006). Although most PMEs are less vulnerable to thermal inactivation when they are embedded in the original tissue structure compared to the purified form, they can be easily inactivated at temperatures less than 70 °C (Balogh, Smout, Ly Nguyen, van Loey, & Hendrickx, 2004; Sila, et al., 2007). Apple PME is inactivated at 59 °C in less than two minutes (Denes, et al., 2000) and thus hardly relevant during industrial processing of apple puree.

With decreasing DM, PG activity, consisting in cleavage of the HG backbone, increases. PGs are salt- and pH-dependent and show only negligible activity below pH 3.5. Furthermore, they possess a lower pressure but a higher thermal stability than PME. Thus, they can be selectively inactivated with mild high-pressure treatments (500 MPa, 15 min, 25 °C) (Duvetter, et al., 2009).

Although specific activity of apple PG is similar to that of tomato PG, the protein content in apples is between 50- to 100-fold lower than in tomatoes (Wu, et al., 1993). PG activity on a fresh weight basis is thus insignificant. In contrast to tomatoes, no PAL activity nor gene expression were detected in apples.

Cooking can be performed by CB or HB method (cf. **II 3.3.**). Most pectinases are not completely inactivated at 70 °C, which is the temperature commonly used in CB, resulting in pectin solubilisation and depolymerization. During HB, temperatures between 85–95 °C are applied before grinding, resulting in rapid inactivation of both PME and PG. In tomatoes, CB process results in less viscous purees (Cámara Hurtado, Greve, & Labavitch, 2002; Lin, et al., 2005). In contrast, HB process produce more viscous purees since PME and PG are inactivated and can thus not cleave the solubilised pectin molecules (Goodman, Fawcett, & Barringer, 2002). However, this is not necessarily true for other fruit and vegetable purees since Lopez-Sanchez, et al. (2011) demonstrated that carrot and broccoli dispersions showed higher viscoelastic properties after CB treatment. In apples, enzymatic pectin cleavage is also not expected during processing into puree; as apple PMEs are rapidly inactivated by heat, the HG backbone remains highly methylated. This prevents apple pectin from depolymerization by PG. In addition, only low amounts of PG are found in apple tissue (Wu, et al., 1993).

3.6.3.2. Chemical reactions

Softening of heated fruits and vegetables is also due to non-enzymatic pectin degradation (**Fig. 38**). While neutral to alkaline pH favours pectin degradation by a β-elimination mechanism, acidic conditions (pH < 3.0) enhance acid hydrolysis (Albersheim, Neukom, & Deuel, 1960; Fraeye, et al., 2007; Voragen, et al., 1995).

The β-elimination mechanism cleaves the glycosidic bonds between the galacturonic acid residues next to an esterified carboxylic acid (Morris, Foster, & Harding, 2002), forming a C4-C5 double bond at the new non-reducing end. The esterification of the relevant carboxyl group is mandatory for this reaction, as it increases the electron deficit at the C5 position. This explains why the reaction rate is accelerated for pectins with high DM. High temperatures (> 80 °C) and a pH > 4.5 also favour this reaction. However, some β-elimination was also measured at pH values as low as 3.8 (Krall & McFeeters, 1998). Most vegetable-based foods, such as green beans or potatoes have

a pH > 4.5 and are processed at 80 °C or higher for food safety reasons. Thus, they promote optimal conditions for the β-eliminative cleavage (Sila, Smout, Vu Son, Loey, & Hendrickx, 2005).

The β-elimination can be quantified due to the UV absorption at 235 nm of the olefinic bond of the unsaturated ester that is formed during the reaction (Albersheim, et al., 1960; Ceci & Lozano, 1998; Kravtchenko, et al., 1992).

Since high methylated pectins are required for β-elimination, the reaction rate can be controlled by reducing the DM. The kinetics of the β-elimination follow apparent zero order with strong temperature and DM dependence (Albersheim, et al., 1960; Sila, et al., 2006b), whereas the temperature sensitivity of β-elimination can be described using the Arrhenius model.

In fruits, the pH is typically < 4.5 and a milder thermal treatment is sufficient for their microbiological safety. Therefore, β-elimination is less important during the production of fruit-based foods. Another chemical reaction, an acid catalysed hydrolytic splitting of glycosidic bonds (acid hydrolysis), occurs more frequently during the heat treatment of, for example, apple fruits (Waldron, et al., 2003). At a pH around 2.0, this reaction cleaves the glycosidic bonds in the pectin backbone of HG molecules. It is more rapid with increasing temperature and if the pectins are demethylated (Fraeye, et al., 2007; Krall & McFeeters, 1998). The beginning of acid hydrolysis is marked by the protonation of the glycosidic oxygen. The formation of an instable cyclic oxocarbonium ion follows, leading to the rearrangement of the molecule and the subsequent breakage of the disaccharide linkage. Glycosidic bonds between galacturonic acids are the most resistant to acid hydrolysis, followed by linkages between rhamnose and galacturonic acid, while linkages between neutral sugars, especially those involving arabinose, are the most easily split (Thibault, et al., 1993). This is why acid hydrolysis in pectin molecules occurs most likely in neutral sugar side chains or the RG I backbone.

Nevertheless, as pectins are very stable around a pH of 3.5, their pKa value, only minimal effects of both enzymatic and chemical modifications during processing can be expected in apples, exhibiting a pH value around 3.7 (Eisele & Drake, 2005).

3.6.3.3. Examples

In the following, some examples will demonstrate the impact of thermal treatment on the cell wall structure due to enzymatic and chemical pectin degradation.

Müller and Kunzek (1998) showed that rehydrated cell wall material from apple parenchyma separated more easily into individual cells during homogenization when they were heated. The authors hypothesized that this must be due to heat-degraded pectins in the middle lamella. In addition, heat treated cell wall material showed improved water retention and swelling capacities.

Studies on apple puree, conducted by Schijvens, et al. (1998), demonstrated a decrease in particle size with prolonged heating. This was a result of decreased cell adhesion, probably due to acid pectin hydrolysis. In the same study, serum viscosity increases with cooking time due to pectin solubilisation. In contrast, pulp content, expressed as WIS, only increases slightly and the effect is less pronounced than for particle size and serum viscosity. Later studies confirmed pectin solubilisation during heat processing in apple purees (Colin-Henrion, et al., 2009; Le Bourvellec, et al., 2011).

Tissue softening during heat treatment seems to be accompanied by cell separation, an increase in water soluble pectins and a decrease in wall-associated pectins. This could be demonstrated in onions (Lecain, Ng, Parker, Smith, & Waldron, 1999), carrots (De Roeck, et al., 2008; Ng & Waldron, 1997) and tomatoes (Cámara Hurtado, et al., 2002). In onion tissue, softening was accompanied by considerable cell wall swelling (**Fig. 41**).
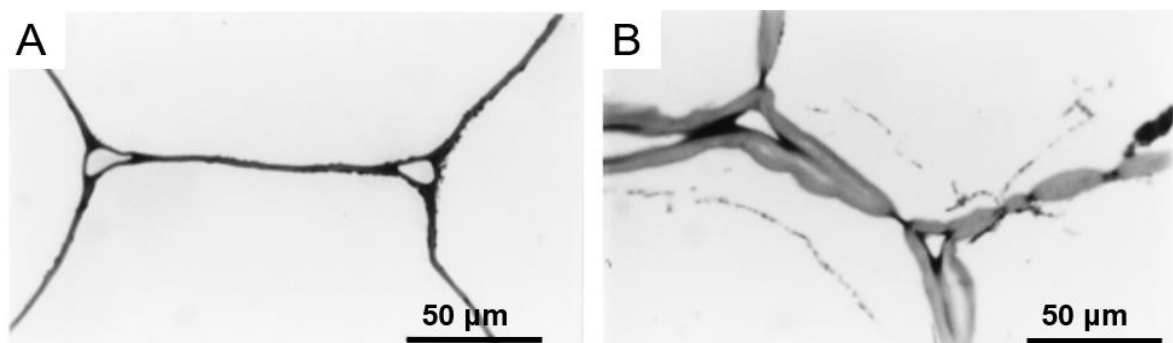
Fig. 41. Transverse light micrographs of fresh (A) and pressure-cooked (B) onion parenchyma cell walls.

Taken from Lecain, et al. (1999).

Pre-treatment of carrot (Ng & Waldron, 1997) or broccoli (Christiaens, et al., 2011) tissue, at low temperature (60 °C or 50 °C, respectively) for 30 min, induces pectin demethylation through PME activity. Hence, β-elimination rate decreases and calcium crosslinks can be established, which results in increased cell adhesion. This causes minimized texture loss and pectin solubilisation during the subsequent heating step as also observed in green beans (Stolle-Smits, Beekhuizen, Recourt, Voragen, & Cees, 2000). Texture of pre-treated carrots could further be improved when carrots were soaked in a calcium chloride solution (Sila, et al., 2006b).

A pre-treatment consisting in high pressure/high temperature processing (600 MPa, 80 °C) also resulted in improved texture preservation in cooked carrots (De Roeck, et al., 2008). This could also be linked to a significant reduction of the DM and lower pectin solubilisation, indicating limited β–elimination. This was mainly due to enhanced demethylation and only to a small extent to PME activity as the enzyme was already inactivated by the pre-treatment.

In carrots (Ng & Waldron, 1997) and broccoli (Christiaens, et al., 2012), thermal treatment mainly induced solubilisation of HG pectins. The authors hypothesized that the highly branched fractions could be more cross-linked and thus better retained in the CW structure. However, De Roeck, et al. (2008) observed an increasing amount of neutral sugars associated to RG I side chains in the water soluble pectins after heat treatment of carrots. It was supposed that fragmentation of RG I side chains could considerably decrease cell wall stability.

In tomato production into puree, a prolonged processing time at elevated temperatures led to depolymerization of soluble pectins (Cámara Hurtado, et al., 2002). This could cause the observed decrease in serum viscosity during prolonged heat treatment. However, conformational changes might be more important in viscosity loss of serum than molar mass due to depolymerization (Diaz, et al., 2009). Pectins were shown to become more compact, although the mechanisms are unknown. DM could not explain conformational changes in serum pectin. Another explanation could be water loss by evaporation, promoting chain-chain interactions (Morris, Gidley, Murray, Powell, & Rees, 1980).

Moelants, et al. (2013) showed pectin solubilisation and depolymerization in both tomato and carrot serum during a strong thermal treatment. Serum viscosity was influenced by a combination of the amount, DM and macromolecular size of soluble pectins. While serum viscosity of tomato products was mainly affected by macromolecular pectin size, the amount of soluble pectins was more important to describe serum viscosity in carrot suspensions.

Interestingly, high-pressure homogenization is able to solubilise pectins mechanically, probably due to enhanced cell wall breakdown. However, this effect was found to be significant in carrots but not in tomatoes (Moelants, et al., 2013).

Beside the impact of pectin degradation on fruit and vegetable softening during cooking, gas expansion is also considered to be an important parameter. Both free gas, which is entrapped in intercellular spaces, and dissolved gas liberate during heating. The gas expands and enhance the breakdown of the cell structure (Dobias, Voldrich, & Curda, 2006).

During thermal processing of fruits and vegetables, both enzymatic and chemical reactions can thus degrade pectins. As a result, pectins are solubilised more easily out of the cell wall and middle lamella (Van Buren, 1979). This promotes tissue softening as cell wall integrity and cellular adhesion are decreased. In plant-based purees, the tissue can be disrupted more easily by mechanical treatment, resulting in smaller particles. In addition, serum viscosity increases due to an increasing amount of soluble pectins. During prolonged heat treatment, however, soluble pectins are depolymerized and serum viscosity decreases as the viscosity of the continuous phase depends not only on the pectin content but also on the pectin structure and size (Moelants, et al., 2014a).

III. Objectives and strategy

1. Objectives

The previous literature review demonstrated that the microstructure of apple tissue is already well studied. The genetic background of apples as well as the cultivation area and growing conditions are known to influence fruit composition and cell development. Pectins are also object of several studies since they contribute to cell wall mechanical strength and cell adhesion. Furthermore, they are the cell wall components that change the most during maturation and processing. Several enzymatic and chemical (only induced by thermal treatments) reactions are thus described for pectins, resulting in fruit softening due to pectin degradation and solubilisation. Besides, the physical structure and rheological behaviour of fruit and vegetable purees are well described. Puree's texture is determined by some structural factors, comprising the proportion and size of particles as well as the viscosity of the continuous phase.

Although the texture of processed fruits and vegetables depends primarily on the original tissue structure and cell wall properties, only little knowledge is available on the link between the textures of the fruit and of the puree. It is also not clear how processing can be used to modulate structural characteristics of the raw material in order to achieve the desired texture (**Fig. 42**).
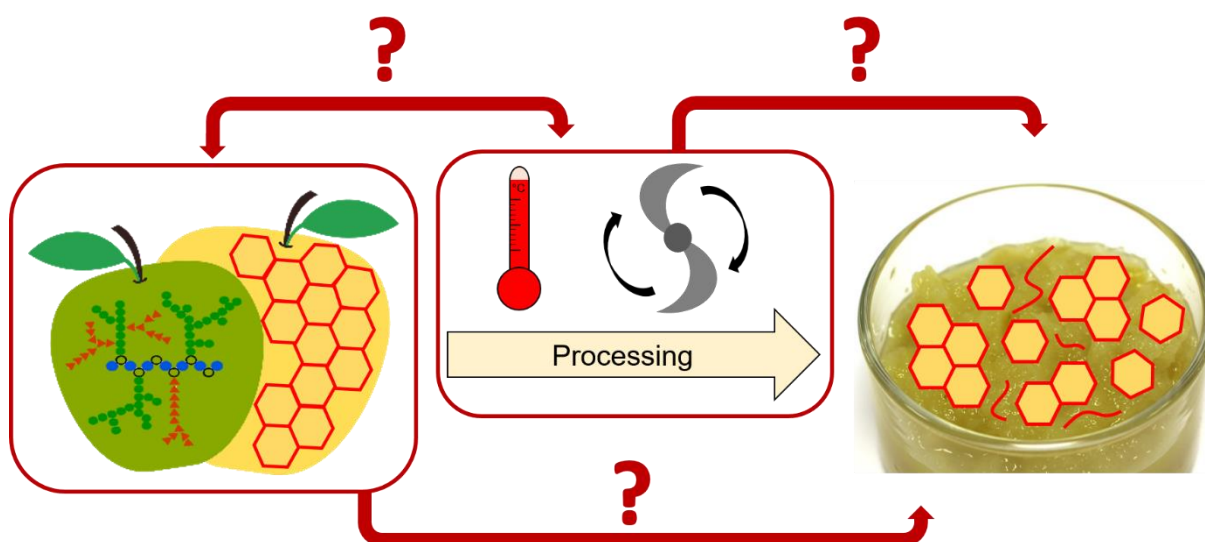
Fig. 42. The impact of the raw material and/or processing conditions on structural characteristics of apple purees remain an unresolved question.

This thesis thus aims to identify:

1) To which extent structural factors of the raw fruit can be linked to structural factors of the purees (and thus texture) after cooking and fragmentation.

2) Mechanisms that determine tissue fragmentation.

It was hypothesized that the **cell size** in the raw fruit could determine particle size of cell clusters and individual cells in purees. **Cell wall microstructure**, especially pectin composition and structure, is responsible for cell adhesion and would thus define particle size. Increased pectin solubilisation affects, in contrast, serum viscosity and the swelling capacity of the cell walls due to increased water retention capacities.

2. Strategy

2.1. General approach

To reach the objectives, raw material and/or process conditions (**Fig. 43**) were modulated in different studies. Generally, one study concerned one harvest year. The structural factors of the puree, comprising proportion and size of particles as well as serum viscosity, were analysed to better understand the link between structural factors of the raw fruit and the puree. Pectin polysaccharides were extracted from raw apples and purees and their chemical composition and structure were determined in order to clarify the contribution of pectins to cell wall microstructure and tissue fragmentation. Finally, the impact of structural factors on puree's texture was described and their importance was ranked.
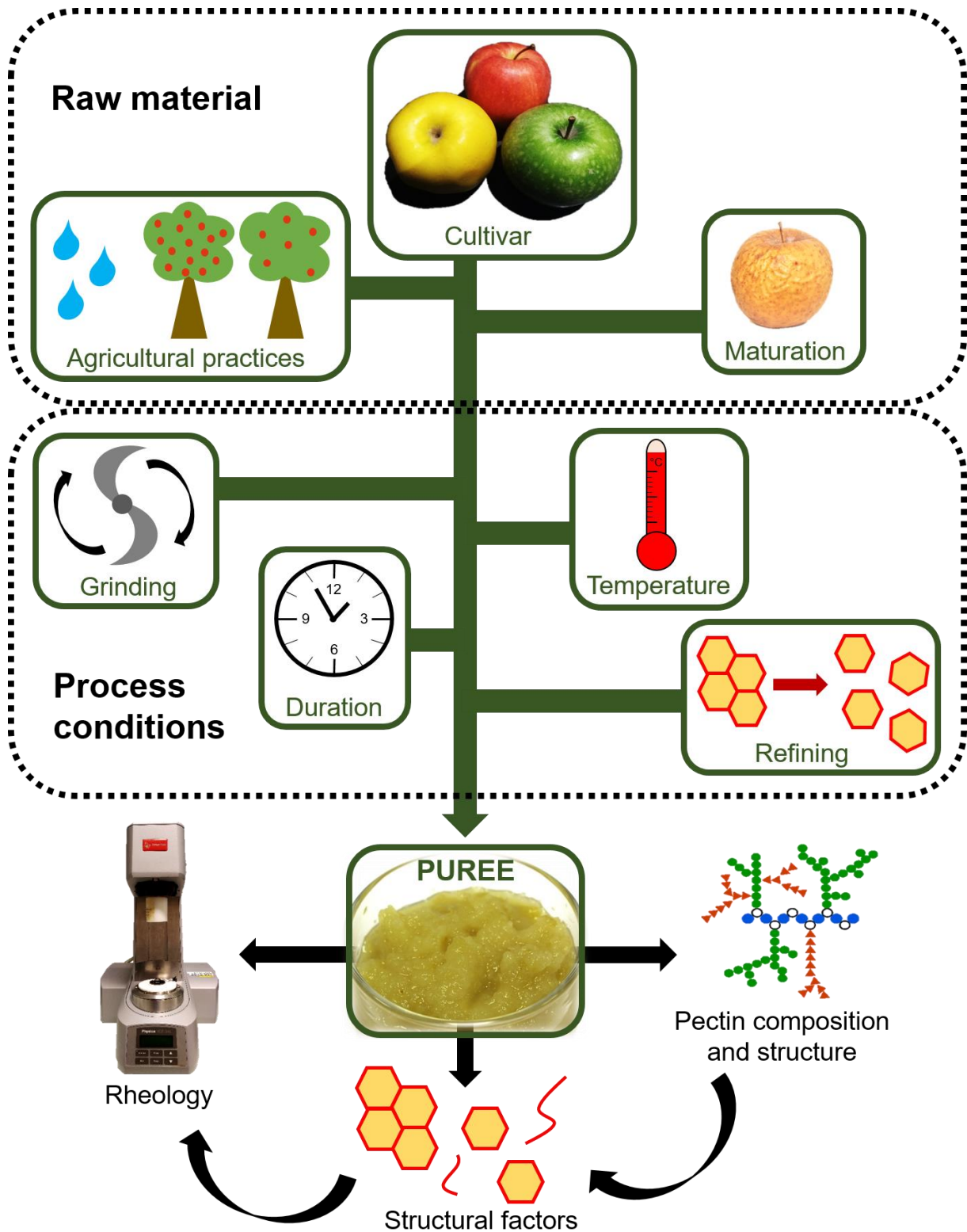
Fig. 43. Experimental strategy of the thesis.

2.2. Raw material

In a first approach, structural factors of the raw fruit, concerning cell size and cell wall microstructure, were modulated directly in the fruit (**Fig. 43**). For this, three input factors related to the fruit were chosen, namely cultivar, agricultural practices and post-harvest storage (maturation). Apple cultivars and agricultural practices modulate cell size. While apple cultivars naturally have different cell sizes, contrasted irrigation levels and thinning practices during fruit development should further increase this effect. Fruit thinning favours the cell division period, leading to larger fruits with more cells, whereas irrigation favours the increase of cell size during the cell expansion period, leading to larger fruits with the same number of cells. Cell wall microstructure is also different between apple cultivars but is especially altered in aged apples. Post-harvest storage was thus also modulated since maturation decreases cell adhesion as a result of pectin solubilisation in the middle lamella due to pectinase activity.

> **The *first chapter* addresses the impact of raw material on puree's structure and texture in order to answer the following questions:**

  ❖ How is puree's texture affected by varietal effects?

  ❖ Do agricultural practices (fruit thinning and irrigation) modify the puree's texture?

  ❖ How is puree's texture modified by storage?

  ❖ Can the puree's texture be related to the texture of raw apples?

  ❖ Can pectin modifications explain the observed differences?

In a first study, structural factors of the raw fruit were modulated by two different cultivars, agricultural practices (irrigation and fruit thinning) and maturation. All apples were processed under the same conditions but different refining levels were applied. The parameters within raw fruits, which affects puree's structure and thus texture the most, were determined. Pectin composition and structure were analysed and linked to structural factors of the puree. The results were published in a research article.

In a second study, four cultivars with contrasted characteristics were compared for puree's structure and texture. Fruit thinning and mealiness (some sort of maturation disorder) were also assessed. All apples were processed by two contrasted processes in order to check if puree's structure can be linked to structural characteristics of the raw apples, no matter the process applied. This study was the object of a second research article.

2.3. Process conditions

During processing, the cell wall microstructure of the fruit is altered and tissue fragmentation is enhanced. To understand how the structural factors of the raw fruit are modified during processing, process conditions were modulated in a second approach (**Fig. 43**). Grinding speed, i.e. shear stress applied during cooking, and temperature history were varied and some purees were refined after processing in order to further enhance tissue fragmentation.

> ➢ **In the *second chapter*, the focus thus lies on how processing could alter structural factors in the raw material in order to elucidate the following questions:**

   ❖ In a thermomechanical process, what is the relative role of thermal and of mechanical treatments on apple puree's texture?

   ❖ What is the relevance of endogenous pectinolytic enzyme activity for apple puree's texture?

   ❖ What are the interactions between apple maturity and processing?

   ❖ Can pectin modifications explain the observed differences?

   ❖ How can the process be used to modulate the perceived texture?

Several pre-studies were conducted, in which grinding speed, temperature and cooking duration were varied. The evolution of puree's structure and texture was followed during processing in order to understand the impact of processing more in detail. This allowed the conceptualization of a large-scale study, combining three temperature regimes and three grinding speeds. Here, only one apple cultivar was

processed. Since post-harvest maturity was shown to be an important factor affecting puree's texture, the processes were repeated on aged apples. This study, in combination with pectin analysis, could identify mechanisms responsible for tissue fragmentation. The results led to a third research article.

In order to assess the impact of processing on the perceived texture of apple purees, the samples obtained from the before-mentioned study were analysed by a sensory panel.

2.4. Combination of the results

➢ **In a *third chapter,* all results are assembled and analysed to identify both the major input factors (raw material and processing) and how they modify the structural determinants that modulate puree's texture as well as the mechanisms that are evidenced in the purees.**

All results concerning structural and textural characteristics of apple purees, acquired by the studies of the previous chapters, were confronted. This allowed to compare the impact of different input factors on puree's structure and to highlight the most important factors. In addition, the complex interactions, synergisms and antagonisms of structural characteristics, which determine the final puree's texture, were assessed. The underlying microstructural mechanisms were related to cell wall modifications, induced by pectic polysaccharides.

IV. Material and methods

1. Plant material per harvest year

Different apple (*Malus x domestica* Borkh.) cultivars were grown and several agricultural practices (fruit thinning, irrigation level) were applied on the orchard to generate apples with contrasted characteristics. In 2016, apples were cultivated within a unit from INRAE, the Unité Expérimentale de Recherches Intégrées (UERI Gotheron, Saint-Marcel-Les-Valence, France), whereas apples in 2017, 2018 and 2019 were cultivated at the experimental station "La Pugère" (Mallemort, France). All apples were harvested according to the optimal commercial harvest dates.

1.1. Harvest year 2016

In 2016, apple cultivar Golden Smoothee (GoS) was produced under organic conditions and manually thinned (**Table 4**). A first batch was processed into puree at harvest (T0). Then, apples were further stored for one (T1) and six (T6) months at 4 °C prior to processing. The fruits were stored in normal atmosphere (i.e. no controlled atmosphere as reduced oxygen) to allow post-harvest storage to have significant impact.

1.2. Harvest year 2017

Two apple cultivars, Granny Smith (GS) and Golden Delicious (GD), were harvested in September 2017. GS and half of the trees of the cultivar GD were thinned chemically (GD1), leading to less but bigger fruits (201 ± 7 g per apple). The other half of GD trees was not thinned (GD2), resulting in more but smaller fruits (176 ± 4 g per apple). The exact thinning parameters are summarized in **Table 4**. Normally, trees were irrigated as soon as the water reserve in the soil reached a limit of 100 mm of available water. For half of GD1 and GD2 apples, the irrigation ramps were closed and no water was supplied during the season. This resulted, theoretically, in smaller cells. A first series of apples was processed at T0. The apples were then stored at 4 °C in normal atmosphere. Further samples were processed into puree at T1, T3 (three months) and T6.

1.3. Harvest year 2018

Four apple cultivars, namely Braeburn (BR), Gala (GA), GD and GS were harvested in August and September 2018. BR, GA, GS and half of the GD trees (GD1) were thinned chemically to reduce fruit load (**Table 4**). The other half of the GD trees were not thinned (GD2). One third of GD1 was stored with the other cultivars for one month at 4 °C in normal atmosphere in order to reduce the starch content prior to processing. Half of the BR apples (BRM) were stored for 11 days at 24 °C and a relative humidity between 90% and 100% (customised phytotron, Froid et Mesures, Beaucouzé, France) in order to accelerate development of mealiness (Barreiro, et al., 1998). For another third of GD1 apples, cold storage at 4 °C was prolonged for processing at T6. The last third of GD1 apples was stored for six months at 2 °C.

1.4. Harvest year 2019

GD apples were chemically thinned (**Table 4**) and harvested in September 2019. They were stored for one month at 4 °C in normal atmosphere.

Table 4. Thinning parameters and date (in brackets) for each apple cultivar of different harvest years.

Harvest year	Cultivar	Thinning treatment 1	Thinning treatment 2	Thinning treatment 3	Thinning treatment 4
2016	GoS	Manual (01–15/06/2016)	-	-	-
2017*	GD1	15 L/ha ATS + 0.15 kg/hL Rhodofix®	3.5 L/ha MaxCel®	-	-
	GD2	-	-	-	-
	GS	600 g/ha Amid-Thin® W	1 kg/hL Rhodofix®	3.5 L/ha MaxCel®	-
2018**	BR	3 L/ha PRM 12® RP (13/04/2018)	5 L/ha MaxCel® + 1.5 kg/ha Rhodofix (30/04/2018)	-	-
	BRM	3 L/ha PRM 12® RP (13/04/2018)	5 L/ha MaxCel® + 1.5 kg/ha Rhodofix® (30/04/2018)	-	-
	GA	3 L/ha PRM 12® RP (13/04/2018)	-	-	-
	GD1	3 L/ha PRM 12® RP (17/04/2018)	2 L/ha PRM 12® RP (24/04/2018)	3.5 L/ha MaxCel® + 1.5 kg/ha Rodofix® (30/04/2018)	3.5 L/ha MaxCel® (04/05/2018)
	GD2	-	-	-	-
	GS	1.5 kg/ha Rhodofix® (27/04/2018)	-	-	-
2019	GD1	18 L/ha ATS (20/04/2019)	0.15 kg/hL Rhodofix® (2704/2019)	5 L/ha MaxCel® (04/05/2019)	-

* Thinning dates not available.

** The given thinning dates were retarded compared to the physiological stages of the apple trees due to phytopathological contingency that concerned another sector of the orchard.

BR: Braeburn; BRM: Braeburn, mealy; GA: Gala; GD1: Golden Delicious, reduced fruit load; GD2: Golden Delicious, high fruit load; GoS: Golden Smoothee; GS: Granny Smith. Amid-Thin® W: 2-(1-naphthyl)acetamide; ATS: Ammonium thiosulphate; MaxCel®: 6-Benzylaminopurine; PRM 12® RP: Ethephon; Rhodofix®: 1-naphthalenacetic acid.

2. Puree preparation per harvest year

A cooker-cutter (RoboQbo Qb8-3, RoboQbo, Bentivoglio, Italy) (**Fig. 44**A) is available within the unit UMR408 SQPOV (INRAE, Avignon, France) and was used for puree processing. With a tank volume of 8 L, RoboQbo makes it possible to process up to 3.7 kg of fruits and vegetables into purees, jams, soups, etc. by applying temperatures up to 120 °C and grinding speeds between 100 and 3000 rpm. Different devices are available to cut (**Fig.44**B) and mix (**Fig. 44**C) the product. In addition, samples can be taken during processing through a valve (**Fig. 44**D), which can be installed to the machine. If needed, vacuum can also be drawn.
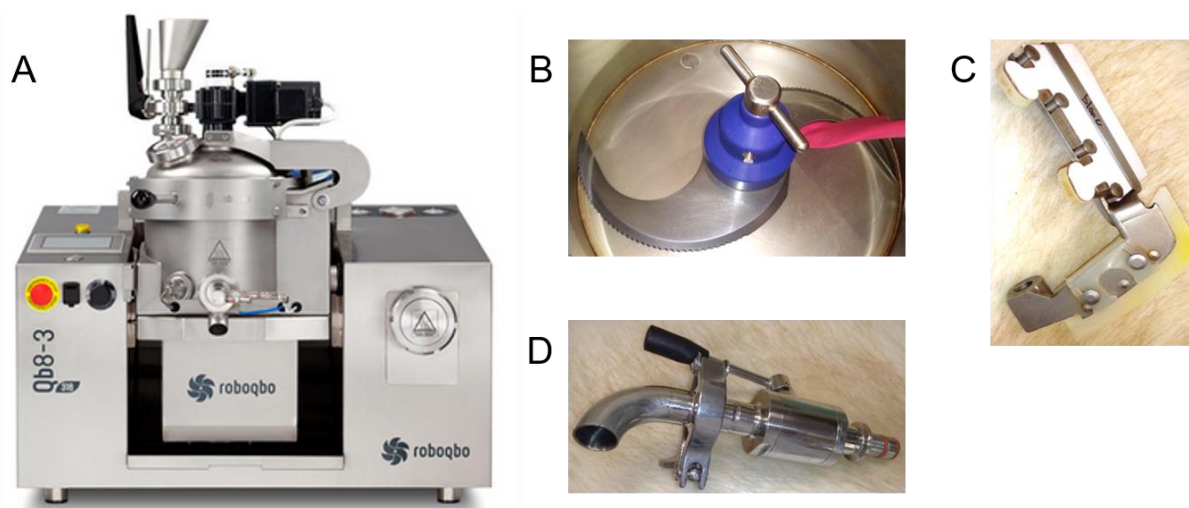
Fig. 44. Cooker-cutter RoboQbo (A) used for puree preparation and accessories to cut (B) and mix (C) and a valve for sampling (D).
Photo of RoboQbo was taken from Foodbay (2020).

Systematically, the day before processing, apples (circa 18 kg) were separated into two equivalent groups (**Fig. 45**), which were representative of the whole apple stock in the distribution of fruit size and colour (**Fig. 46**). The first group was used for raw apple characterization and cell wall extraction, the second group was processed into puree. Generally, processing was conducted in triplicate. Apples (3 kg per triplicate) were cored, sliced into 12 equal portions and processed into puree. Purees were prepared under vacuum and two rotating microserrated knife blades (**Fig. 44**B) were used for grinding, while a rotating blade (**Fig 44**C) mixed the puree. Process conditions varied for each harvest year and are summarized in **Table 5**.
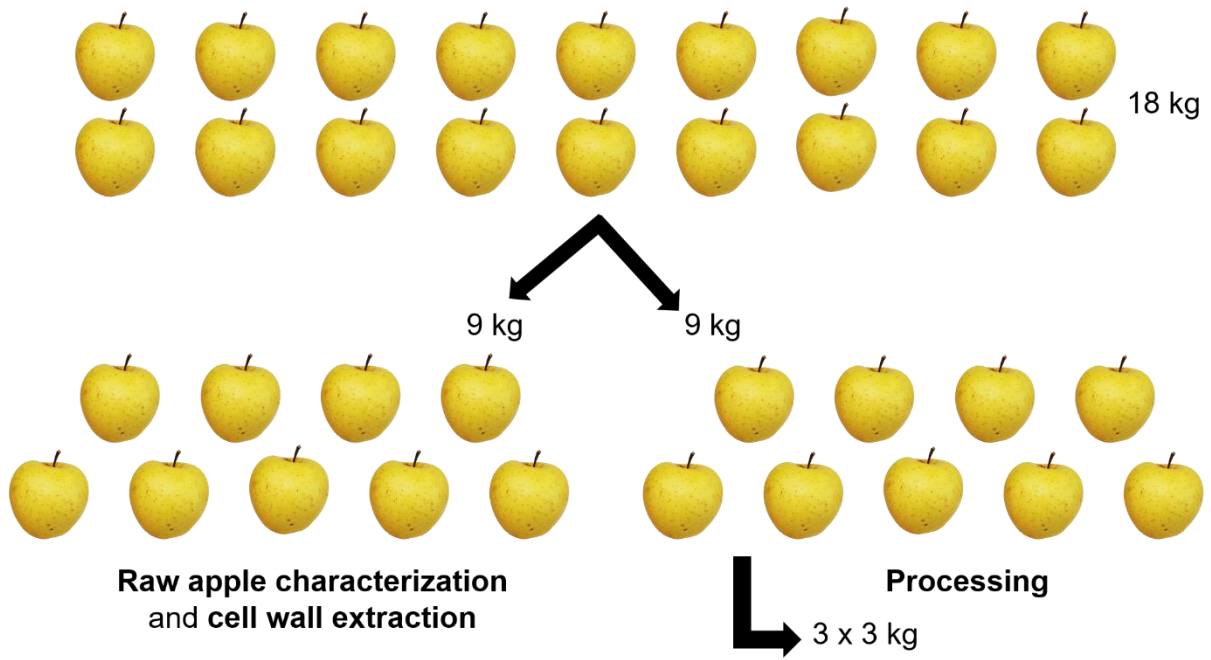
Fig. 45. Preparation of equivalent groups for raw apple characterization and processing.

Fig. 46. Representative Golden Delicious apples of the whole apple stock in the distribution of fruit size and colour.

Once purees reached room temperature, rheology, particle size and pulp wet mass were determined within 48 h after puree preparation.

Table 5. Overview over raw material and processing conditions for main studies in different harvest years.

Harvest year	Cultivar	Storage (months)	Grinding during temperature increase	Process conditions	Pasteurization	Cooling	Refining
2016	GoS	0, 1, 6	1000 rpm	65 °C; 1000 rpm; 5 min	95 °C; 800 rpm; 5 min	55 °C; 1500 rpm; 5 s	NR, RA
			1000 rpm	95 °C; 1000 rpm; 5 min	-	55 °C; 1500 rpm; 5 s	
2017*	GD1, GD2, GS	0, 1,3, 6, 9	1000 rpm	95 °C; 1000 rpm; 5 min	-	55 °C; 1500 rpm; 5 s	NR, RA1, RA2
2018	BR, BRM, GA, GD1, GD2, GS	1	3000 rpm	70 °C; 3000 rpm; 15 min	95 °C; 3000 rpm; 2 min	-	NR, RA2
			3000 rpm	95 °C; 400 rpm; 17 min	-	-	
2018	GD1	6	100 rpm	70 °C | 83 °C | 95 °C; 300 rpm | 1000 rpm | 3000 rpm; 30 min	-	-	NR
2019	GD1	1	100 rpm	70 °C | 83 °C | 95 °C; 300 rpm | 1000 rpm | 3000 rpm; 30 min	-	-	NR

* GD1 and GD2 were produced with and without drought stress but puree's texture and structure was not significantly different. Irrigation level was thus not further assessed.

BR: Braeburn; BRM: Braeburn, mealy; GA: Gala; GD1: Golden Delicious, reduced fruit load; GD2: Golden Delicious, high fruit load; GoS: Golden Smoothee; GS: Granny Smith; NR: Not refined; RA: refined (1.8 mm); RA1: refined (1.0 mm); RA2: refined (0.5 mm).

2.1. Harvest year 2016

Preliminary studies on apple purees were conducted on 2016 harvest to evaluate "real" processing conditions for the Interfaces project in the upcoming seasons. The results are not discussed here since they were part of my Master's Thesis (Buergy, 2017). However, the results were included in the statistical comparison of purees obtained for different apple cultivars and cultural practices by several process conditions (cf. **V 3.**).

Apples were processed under vacuum (-90 kPa) imitating (at the laboratory scale) an industrial cold break (CB) and hot break (HB) process with temperatures of 65 °C and 95 °C, respectively. Apples were heated while being ground at 1000 rpm for 5 min. To stabilize the CB purees, a pasteurization step (95 °C, 800 rpm, 5 min) was applied for these purees. After cooling (55 °C, 1500 rpm, 5 s), one part of the puree was refined (RA, 1.8 mm) by an automatic sieve (Cobot Coupe C80, Robot Coupe SNC, Vincennes, France) to eliminate apple skin and carpels. The other half was not refined (NR). Refined and not-refined purees were filled separately into preserving glasses, closed tightly and autoclaved for 15 min at 100 °C. After cooling, the purees were stored at 4 °C.

2.2. Harvest year 2017

In 2017, only a hot break process at 95 °C was imitated, with stirring at 1000 rpm during 5 min under vacuum. Each batch of apple puree was divided into three portions. Two portions were refined by an automatic sieve of 1 mm (RA1) or 0.5 mm (RA2), removing skin and other larger particles. The third portion was NR. At T0, only NR samples were produced.

2.3. Harvest year 2018

2.3.1. Preliminary study I

In order to establish process conditions, which lead to contrasted puree's texture and structure, several pre-studies were conducted on GD2 apples at T1 (Study I). Only one run was prepared per process and the purees were NR.

2.3.1.1. Variations in grinding speed and cooking duration

In a first study, grinding and cooking duration were analysed. Several grinding speeds (200, 400, 1000, 2000 and 3000 rpm) were tested during a one-hour process at 95 °C. For the low grinding speeds of 200 and 400 rpm, a strong grinding of 1000 rpm had to be applied for the first 3 min of temperature increase in order to obtain analysable purees. For the other grinding speeds, the indicated grinding was maintained during the whole process. The process was done under ambient pressure in order to take samples of the purees (about 100 mL) after each 15 (2000 and 3000 rpm) or 30 min (200, 400 and 1000 rpm). This allowed to follow the evolution of puree's structure and viscosity during processing.

2.3.1.2. Variations in temperature and cooking duration

In a second study, the effect of temperature and cooking duration were evaluated. Three different temperatures were thus chosen. A temperature of 50 °C was selected as it is lower than the temperature required for membrane dissolution (53 °C, Leca, personal communication), 70 °C in order to favour enzymatic reactions and 95 °C to promote chemical hydrolysis. Purees were cooked for 120 (50 °C), 90 (70 °C) and 60 min (95 min). After each process, temperature was increased to 95 °C and maintained during 60 min. The vessel was kept at ambient pressure during processing in order to sample each 30 min. The grinding speed was kept at 1000 rpm during the whole process.

2.3.1.3. Investigation of pasteurization

Two different grinding speeds (400 and 3000 rpm) were applied for 20 min at 50 °C or 15 min at 70 °C. For the process conducted at 400 rpm, a grinding speed of 3000 rpm was applied during the first 3 min to obtain a relatively smooth puree. A pasteurisation

step of 2 min at 95 °C was added after each process. Samples were taken before and after pasteurisation.

2.3.1.4. Variations in grinding and temperature

The joint impact of temperature and grinding speed were determined. Thanks to the knowledge acquired in the above-mentioned studies, contrasted process conditions were chosen. Four process recipes were tested in order to choose only two for the main study. Therefore, two different temperatures (70 °C and 95 °C) and two different grinding speeds (400 rpm and 3000 rpm) were compared. A depression of -90 kPa was drawn. During temperature increase, the apples were ground at 3000 rpm. Once the working temperature was reached, the grinding speed of 3000 rpm was maintained or reduced to 400 rpm during 15 min. After each process, a pasteurisation step (2 min at 95 °C) was applied. All processes were conducted only once.

2.3.2. Main study I

The two most contrasted processes, consisting of a low temperature-high shear (70 °C, 3000 rpm) and a high temperature-low shear process (95 °C, 400 rpm), were chosen and applied on BR, BRM, GA, GD1, GD2 and GS apples. The processes were conducted in triplicate and conditions were as described before (**IV 2.3.1.4**.). Half part of each puree was refined by an automatic sieve of 0.5 mm (RA2), removing skin and particles larger than the sieve opening. The other half was NR.

2.3.3. Preliminary study II

Some more studies were conducted on GD1 apples that were stored for six months at 2 °C (Study II). The aim of these studies was to define several process conditions that will be studied more in detail. Two cooking temperatures (70 °C or 95 °C), grinding speeds (300 rpm or 3000 rpm) and cooking durations (15 or 30 min) were combined in order to obtain 8 processes. During temperature increase to 70 °C or 95 °C, only a slow grinding speed of 100 rpm was applied. Faster grinding speeds of 300 rpm or 3000 rpm were then maintained during 15 or 30 min. All processes were conducted under vacuum (- 90 kPa) and only once.

Exploration of different process variables allowed to design the main study. The conclusions, which led to the choice of process conditions are explained in **V 2.1.2.3.**

2.3.4. Main study II

Finally, a third intermediate temperature (83 °C) and grinding speed (1000 rpm) were added and a process duration of 30 min was retained. This led to 9 different processes since each temperature (70, 83, 95 °C) was combined with each grinding speed (300, 1000, 3000 rpm). Each process was conducted in triplicate and under vacuum on GD1 apples that were stored for 6 months at 4 °C. Since temperature increase was longer for higher temperatures (difference of 140 s between 70 and 95 °C), a slight grinding speed of 100 rpm was applied during this period. This mixed the apples without grinding. Once the working temperature was reached, grinding was raised and maintained for 30 min. All the purees were NR.

2.4. Harvest year 2019

2.4.1. Complement to main study II

GD1 apples of 2019 harvest were stored for 1 month at 4 °C and then processed with the same 9 processes (70, 83, 95 °C combined with 300, 1000, 3000 rpm) as explained in **IV 2.3.4**. This made it possible to compare controlled process conditions between purees that were produced with GD1 apples after cold storage (4 °C) at T1 and T6.

2.4.2. Puree production for sensory analysis

For a sensory analysis, the amount of apple puree produced by RoboQbo was not enough. For this reason, additional puree was produced at CTCPA (Centre technique de la conservation des produits agricoles, Avignon, France) by a similar cooker-cutter (Stephan, CH.European Factory, Saint-Cannat, France) as RoboQbo but with a higher tank volume (44 L). Apples (15 kg, GD1, T1) were processed into puree by applying the same process conditions (combination of 3 grinding regimes and 3 temperatures) as explained in **IV 2.3.4**. Nine purees were produced without repetitions. During temperature increase, a grinding speed of 100 rpm was applied with RoboQbo. However, the minimum grinding speed of the Stephan was 300 rpm, which was thus applied during temperature increase for the purees prepared at CTCPA.

3. Physico-chemical characterization

3.1. Total soluble solids

The amount of total soluble solids in an aqueous solution is estimated by the index of refraction and is referred to as the °Brix. It can be determined using a refractometer (**Fig. 47**) that determines how light is refracted when it passes through a given matrix. By definition, 1 °Brix corresponds to 1 g of sucrose in 100 g of solution. If the sample also contains other dissolved solids such as other sugars, salts, organic acids or solubilised pectins, the measurement only gives an estimation of the total soluble solids content. Since the soluble compounds in apple purees are mainly soluble sugars (cf. **II 3.2.**), the degrees Brix slightly overestimates the total sugar content in the serum. Generally, soluble solids in apples lie between 9.1 and 13.5 °Brix (Tyl & Sadler, 2017).

Fig. 47. Photo of a digital refractometer.

After processing and refining, where applicable, the puree was allowed to cool down to room temperature (20 °C). The digital refractometer (PR-32α ATAGO, Norfolk, VA, USA) was calibrated by distilled water, before approximately 1 g of the puree was placed on its sensing lens. The value that was indicated on the refractometer's display was noted. Systematically, three repeated measurements were conducted of each puree.

3.2. Titratable acidity

Titratable acidity (TA) measures the total concentration of organic acids in a food by titration of intrinsic acids with a standard base. It is a better predictor of food perceived acidity than pH (Tyl & Sadler, 2017). TA was determined in freeze-dried and finely ground purees (3 g). According to the official method of analysis (AOAC 942.15), samples were titrated up to pH 8.1 with NaOH (0.1 M) using an autotitrator (Methrom, Herisau, Switzerland). The amount of TA was then calculated as follows and expressed in mmol H^+/kg of fresh weight (FW).

$$TA = \frac{Volume\ (NaOH) \cdot 0.1M\ (NaOH) \cdot 1000}{Initial\ weight\ (puree)} \tag{18}$$

3.3. Dry matter

The dry matter content of raw apples and purees was determined after freeze-drying. Approximately 300 g of raw apples or puree were placed in a plastic bag that was sealed, weighed and frozen at least one night at -20 °C. The plastic bags were perforated and transferred into a freeze-dryer (Cryonext, Saint Aunes, France), where the pressure was lowered to 500 Pa and the temperature was increased gradually to 20 °C in order to sublime the ice in the sample. Immediately after freeze-drying, the plastic bags were weighed again and the dry matter content was determined as the ratio of the final weight (W_{final}) to the initial weight ($W_{initial}$) and expressed in %. W_{final} was not corrected for the weight of the plastic bag since $W_{initial}$ comprised the weight of the plastic bag.

$$Dry\ matter\ (\%) = \frac{W_{final}}{W_{initial}} \cdot 100 \tag{19}$$

3.4. Colour

Colour is perceived by the human eye after reflection of radiation in the visible region of the electromagnetic spectrum, ranging from 400 to 700 nm (Blum, 1997). It can be evaluated objectively by a reflectance measurement. Reflectance spectra can then be related to colour. A colour space was defined by the International Commission on Illumination (CIE) in 1976 to equalize numerical changes to visually perceived changes. Colour is expressed as three values L*a*b*, representing the axis of a three-dimensional coordinate system (**Fig. 48**). L* represents the axis of the cylinder and shows lightness from black (0%) to white (100%). The radii of the cylinder (a* and b*) represent colour. Neutral grey values are reached at a* = 0 and b* = 0. Green (negative direction) to red (positive direction) components are represented on the a* axis, while blue (negative direction) to yellow (positive direction) components are represented by the b* axis.
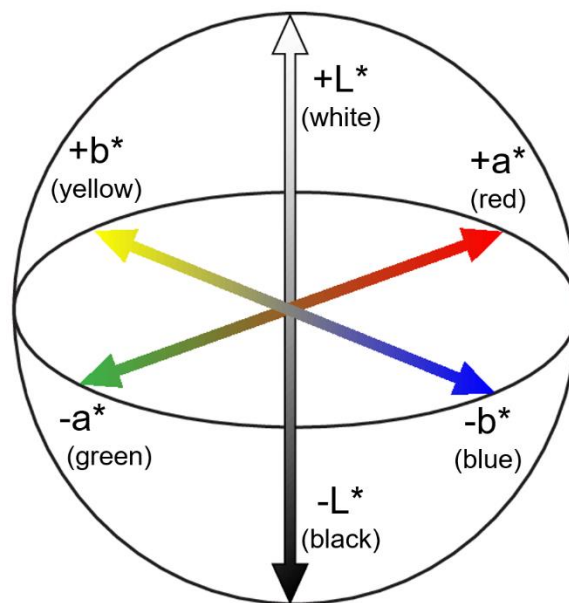
Fig. 48. Model of the CIE 1976 L*a*b* colour space.

Adapted from Bisulca, Nascimbene, Elkin, and Grimaldi (2012).

The colour of apple purees was determined in triplicate through dedicated glass cuvettes using a CR-400 chromameter (Minolta, Osaka, Japan), which was calibrated with a white plate. Results were expressed in the CIE 1976 L*a*b* colour space (illuminant D65, 0° view angle, illumination area diameter 8 mm).

3.5. Texture of raw apples

Texture of raw apples was determined by a puncture test at room temperature (fixed to 23 °C) on three replicates of ten representative apples. A multipurpose texture analyser (TAPlus, Lloyd Instruments, Farenham, UK) was used with a punch probe (diameter 2 mm) that penetrated up to a depth of 17 mm into a peeled section. Firmness of apple flesh was calculated as the ratio of penetration energy to the height of testing, giving the puncture mean load. Crunchiness was estimated by calculating the linear distance between consecutive points from the force-distance curve in a displacement range of 10 mm at the load plateau (Gregson & Lee, 2003).

3.6. Rheology

All rheological tests were performed using a stress-controlled rheometer (Physica MCR301, Anton Paar, Graz, Austria) that was equipped with a Peltier cell (CPTD-200, Anton Paar) and an external cylinder (CC27/S, Anton Paar) containing the sampled product. All rheological measurements were performed at 22.5 °C.

3.6.1. Purees

The concentric cylinder (Espinosa Brisset, 2012; Leverrier, 2016; Schijvens, et al., 1998; Tarea, 2005) and vane geometry (Lopez-Sanchez, et al., 2012; Moelants, et al., 2014b) are the most commonly used measuring systems for the study of fruit purees. Advantages and disadvantages of different measuring systems were compared in **Table 3**. In this study, a six blade vane geometry with a 3.46 mm gap (FL100/6W, Anton Paar) was chosen for both steady state and dynamic rheological measurements of purees since it minimizes the destructuration of the product during insertion of the measuring system and the effects of wall slip, often observed on viscoelastic particle systems (Lopez-Sanchez & Farr, 2012).

3.6.1.1. Steady state measurement

For most studies, the flow curve was recorded by measuring the viscosity over a logarithmically distributed range of shear rate values $\dot{\gamma}$ between 10 and 250 s^{-1}. One point was registered every 15 s. In order to assure homogenous dispersion of the product in the measurement cell, a pre-shear of 50 s^{-1} was applied during 2 min. In order to let the puree return to a rheological equilibrium prior to analysis, a rest time of 5 min followed, as proposed by Lopez-Sanchez, et al. (2011), followed. This is now a common practice in the rheology of fruit and vegetable purees (Leverrier, et al., 2016; Moelants, et al., 2014b). Apparent viscosity of purees was compared using the value at a shear rate of 50 s^{-1} as it represents an approximation of the shear rate to which a soft food product is subjected in the mouth during mastication (Shama & Sherman, 1973; Stokes, 2012).

For some preliminary studies, only a fast measurement of viscosity was conducted. Charging of the measuring cell with the sample was followed by a 30 s rest. A shear rate of 5 s^{-1} was then maintained during 2 min, recording a point every 2 s. Such a low shear rate of 5 s^{-1} was chosen since it allows a good comparison of the viscosities of different purees of the same fruit or vegetable (Maingonnat, personal communication). The results were shown as average values in the constant range between 18 and 120 s.

Since the gap of the measuring cell was approximately 3 mm large, the method used for rheological measurements of the purees was theoretically not adapted for particles larger than 1 mm. The only samples containing particles (skin fragments) larger than 1 mm were NR. However, rheological measurements were confirmed to be repeatable for these samples and the method was thus considered valid.

3.6.1.2. Dynamic measurements

Amplitude sweep

Amplitude sweep tests were performed at deformation values γ between 0.01 and 100% at a fixed angular frequency ω of 10 rad/s. The time required to measure each point (5 points per decade) was set by the software. The values of G' and G" were averaged in the linear viscoelastic range (LVER). The end of the linear domain was estimated as the strain inducing a decrease of G' values exceeding 10% of its value in

the linear domain. The yield stress was obtained at the intersection of G' and G" in the stress-moduli curve. It was used as a characteristic point to estimate the minimum shear stress that must be applied to the puree to initiate flow (Espinosa-Munoz, et al., 2013). This method to determine the yield stress is not the only one but it was chosen as it is the most relevant one for apple purees according to Leverrier (2016).

Frequency sweep

Frequency sweep tests were performed within the LVER, in the range of 0.1–40 rad/s at constant γ. This test was used in harvest years 2016–2018 but provided redundant results with amplitude sweep tests. The results are thus not shown.

3.6.2. Serum

Serum samples were obtained after centrifugation of the puree (cf. **IV 3.7.**). They were not clear and showed high turbidity as indicated by visual inspection and high absorbance at 600 nm, which was measured spectrophotometrically (Zimet & Livney, 2009). Although this might be usual for solutions containing pectins, it could also be due to particles remaining in the liquid phase. Sera were thus centrifuged (7690 x g, 30 min, 4 °C) in order to remove small cell fragments. However, this was not sufficient since the sera were still turbid. Sera were thus analysed by laser granulometry (cf. **IV 3.8.1.**), macroscopy (cf. **IV 3.8.2.**) and light microscopy (cf. **IV 3.8.3.**) in order see what caused turbidity. Very few particles were visible. For laser granulometry, particle sizes in the sera were at the limit of detection. Some cell fragments and even clusters could be detected by macroscopic observation after calcofluor staining but cell concentration seemed to be not enough to cause serum turbidity. Observation of sera under light microscope could not significantly reveal the presence of particles. The sera were thus filtered through 0.7 µm glass microfibres filters (Whatman®, Little Chalfont, United Kingdom) in order to remove particles. This operation was time-consuming (> 1 h to filter 10 mL serum) since a viscous film was retained in the filter, which hindered filtration of the serum. This gel-like film was probably due to soluble pectins. However, it was not the aim to remove them since their effect on serum viscosity as well as their composition and structure were to be analysed in the following experiments.

This is why serum viscosity was analysed directly on serum obtained after a single centrifugation step (7690 x g, 15 min, 15 °C) of the puree to separate serum from pulp.

The viscosity curve of the continuous phase was acquired with a double gap cylinder geometry (DG27, Anton Paar). This geometry was chosen since it allows to observe the shear-thinning behaviour of the serum without causing turbulence in low-viscous samples (Mezger, 2014), explaining its use in existing literature on apple serum analysis (Espinosa Brisset, 2012; Leverrier, 2016). Before each measurement, a resting step of 1 min was applied. Shear rate was then increased from 10 to 1000 s^{-1} (logarithmic ramp) for a total duration of 8 min. Viscosity values (η_{serum}) were presented at a shear rate of 100 s^{-1} from a flow curve, assuming the in-mouth perception of serum requires a higher shear rate than purees.

3.7. Pulp wet mass and water retention capacity

The pulp wet mass (PWM) represents the fraction of humid particles after separation of the puree into pulp and serum by centrifugation (7690 x g, 15 min, 15 °C). One jar of 350 g puree was divided into six polypropylene centrifuge tubes of 50 mL and then separated into serum and pulp (**Fig. 49**)

Fig. 49. Separation of apple puree into serum and pulp by centrifugation.

PWM was calculated as the ratio of the pulp weight (W_{pulp}) to the initial weight of the puree (W_{puree}) and expressed in % as described in literature (Espinosa-Munoz, et al., 2013):

$$\text{PWM (\%)} = \frac{W_{pulp}}{W_{puree}} \cdot 100 \qquad\qquad (20)$$

The residue (pulp) and the supernatant (serum) were frozen separately at -20 °C until further use. Only particle size distribution (cf. **IV 3.8.1.**) and serum viscosity (cf. **IV 3.6.2.**) were analysed on fresh (not frozen) pulp and serum.

The amount of water retained by the mass of the pulp's cell wall polysaccharides (g/g dry weight) was defined as the water retention capacity (WRC) according to Robertson, et al. (2000). It was estimated as the relation between the PWM and the pulp's dry weight (AIS). If the AIS is expressed in the FW (cf. **IV 4.3.1.**), equation (21) can be employed. The mass of the fibre is generally negligible and was thus not considered in this equation.

$$\text{WRC} = \frac{\text{PWM\%}}{\text{AIS\%}} = \frac{\text{PWM\%}}{(\text{AIS\%} \cdot \text{PWM\%})/100} = \frac{100}{\text{AIS\%}} \tag{21}$$

3.8. Particle size distribution

3.8.1 Granulometry

The particle size distribution in the pulp was measured via laser diffraction granulometry (**Fig. 50**). Thereby, a laser beam passes through the dispersed particles of the sample and the angular variation in intensity of the scattered light is detected. It is then analysed by the Mie or Fraunhofer theory of light scattering (Mastersizer 2000, 2007) taking into account that the angle of diffraction in relation to the laser beam increases as particle size decreases. Due to the irregular shape of the particles, the measurement result is expressed as the diameter of a theoretical sphere, i.e. equivalent to that of an ideal sphere. Several values are used to represent particle size since a single value is not sufficient to describe the distribution.

The volume mean diameter $D[4,3]$ describes the mean of a particle size distribution weighted by the total volume of particles. It is expressed by the geometric mean D_i to the fourth power multiplied by the percent in the class v_i and summed over all classes divided by the geometric mean to the third power multiplied by the percent in that class and summed over all classes:

$$D[4,3] = \left.\sum_1^n D_{iv_i}^4 \middle/ \sum_1^n D_{ivi}^3\right. \tag{22}$$

The surface mean diameter $D[3,2]$ represents the mean of a particle size distribution weighted by the total volume of particles:

$$D[3,2] = \frac{\sum_1^n D_{iv_i}^3}{\sum_1^n D_{ivi}^2} \qquad (23)$$

The distribution width can be described by three additional values. The d(0.5) is the median value (in volume), that is to say the diameter where half of the distribution lies below this value. The d(0.1) and d(0.9) represent the diameter where 10% or 90%, respectively, of the volume distribution are below this value.
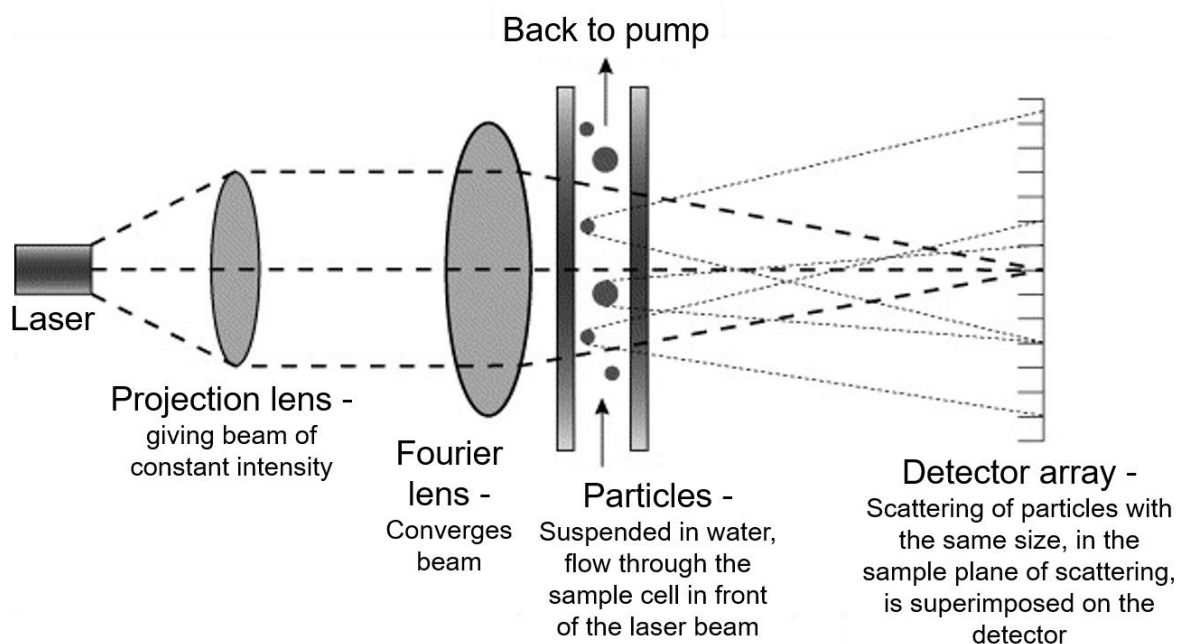
Fig. 50. Schematic representation of a laser diffraction granulometer. Adapted from Pye and Blott (2004).

Approximately 1 g of the pulp was dispersed directly in the tank of the granulometer (Mastersizer 2000, Malvern Instruments, Malvern, UK) in distilled water (refractive index: 1.33). The refractive index of the sample was set at 1.52 (Leverrier, et al., 2016) and the absorptive index was chosen to be 0.00 due to the translucent character of apple cells. As the particle size diameter of apple cells was expected to be not considerably higher than the wavelength of the applied laser beam, the samples were analysed by the Mie theory. The granulometer, supposed to be capable to measure particle sizes between 0.02 and 2000 µm, took three measurements and reported the particle size as a volume equivalent sphere diameter (d). Malvern's software then

averaged the size distribution over three repeated measurements on the same sample. Each sample was analysed in duplicate.

3.8.2. Macroscopy of apple cells

Apple cell walls were stained with fluorescent brightener 28 ("calcofluor"), a fluorescent blue dye, which strongly binds to cellulose and chitin. The size and form of isolated apple cells or particles in apple purees could thus be observed under UV light at 365 nm. A solution of 10 g/L calcofluor in distilled water was prepared and adjusted to pH 10-11 by adding NaOH (1 M). This solution was diluted 1:100 with distilled water (Soukup, 2014). Approximately 0.25 mL of apple cells or particles were then mixed with 7 mL of the prepared calcofluor solution in a Petri dish and incubated for 10 min. Images were then taken by a camera (Baumer VCXU3I) that was linked to a 16 mm macroscopic C-type lens (Pentax, Japan) and an extension tube of a focal length of 20 mm. Gain and exposure time were set at 1 and 300 000 μs, respectively. The "Baumer Camera Explorer" software was used to set capture settings and view images. For observation of possible cell fragments in serum, 0.1 mL serum was mixed with 5 mL calcofluor and exposure time was set at 24 000 μs.

3.8.3. Microscopy of apple cells

The global size and shape of the particles in suspension were observed using a BX50 light microscope (Olympus, Shinjuku, Tokyo, Japan). Apple puree was diluted 1:3 with water before placing 5 μL onto a glass slide that was covered with a cover slip. Samples were observed without coloration with a 10X objective lens. Serum was also observed under light microscopy. Serum (100 μL) was mixed with 100 μL calcofluor (1:100 in water) in order to stain possible cell fragments. This suspension (5 μL) was placed onto a microscope slide and covered with a cover slip. Quartz glass microscope slides and cover slips were used since they guarantee UV transparency. Samples were observed under UV light (365 nm) with a 40X and 100X objective lens.

4. Analytical

4.1. Chemicals and standards

All commercially obtained chemical reagents, solvents and gases are listed in **Table 6**. They were used without further purification.

Table 6. Commercially obtained chemicals, solvents and gases.

Reagent	Producer	CAS number
1-Methylimidazole (99%)	Acros Organics, Geel, Belgium	616-47-7
3-Phenylphenol (≥ 85%)	Sigma-Aldrich, Steinheim, Germany	580-51-8
Acetic acid (glacial)	Fisher Scientific, Loughborough, UK	64-19-7
Acetic anhydride	Acros Organics, Geel, Belgium	108-24-7
Acetone (pure)	Carlo Erba Reagents, Val-de-Reuil, France	67-64-1
Acetonitrile (HPLC LC-MS grade)	VWR Chemicals, Fontenay-sous-Bois, France	75-05-8
Ammonia solution (35%, for analysis)	Fisher Scientific, Loughborough, UK	1336-21-6
Calcium chloride (≥ 99%, dihydrate)	Sigma-Aldrich, Steinheim, Germany	10035-04-8
Compressed air	Linde France, St Priest, France	-
D-(-)-Arabinose (≥ 98%)	Sigma-Aldrich, Steinheim, Germany	10323-20-3
D-(+)-Galactose (≥ 99.5%)	Sigma-Aldrich, Steinheim, Germany	59-23-4
D-(+)-Galacturonic acid (> 97%)	Sigma-Aldrich, Steinheim, Germany	685-73-4
D-(+)-Glucose (≥ 99.5%)	Sigma-Aldrich, Steinheim, Germany	50-99-7
D-(+)-Mannose (≥ 99%)	Sigma-Aldrich, Steinheim, Germany	3458-28-4
D-(+)-Sucrose (≥ 99.5%)	Sigma-Aldrich, Steinheim, Germany	57-50-1
D-(+)-Xylose (≥ 99%)	Sigma-Aldrich, Steinheim, Germany	58-86-6

Reagent	Producer	CAS number
Deuterium oxide (≥ 99.96 atom % D)	Sigma-Aldrich, Steinheim, Germany	7789-20-0
Dextran	Amersham Pharmacia Biotech, Uppsala, Sweden	9004-54-0
Dichloromethane (for HPLC)	VWR Chemicals, Fontenay-sous-Bois, France	75-09-2
Ethanol (96%)	VWR Chemicals, Fontenay-sous-Bois, France	64-17-5
Fluorescent Brightener 28 ("Calcofluor")	Sigma-Aldrich, Steinheim, Germany	4404-43-7
β-Fructosidase (Invertase)	Sigma-Aldrich, Steinheim, Germany	9001-57-4
Helium	Linde France, St Priest, France	7440-59-7
Hydrochloric acid (37%)	VWR Chemicals, Fontenay-sous-Bois, France	7647-01-0
Hydrogen	Linde France, St Priest, France	1333-74-0
L-(-)-Fucose	Sigma-Aldrich, Steinheim, Germany	2438-80-4
L-(+)-Rhamnose (≥ 99%)	Sigma-Aldrich, Steinheim, Germany	3615-41-6
Lugol Solution	Sigma-Aldrich, Steinheim, Germany	12298-68-9
Methanol (LC-MS grade)	Fisher Scientific, Loughborough, UK	67-56-1
Methanol-d_3 (99.5 atom % D)	Acros Organics, Geel, Belgium	1849-29-2
Myo-Inositol	Sigma-Aldrich, Steinheim, Germany	87-89-8
Nitrogen	Linde France, St Priest, France	7727-37-9
Phenol (for synthesis)	Merck KGaA, Darmstadt, Germany	108-95-2
Potassium hydroxide (≥ 85%)	Sigma-Aldrich, Steinheim, Germany	1310-58-3
Potassium iodide	VWR Chemicals, Fontenay-sous-Bois, France	7681-11-0
Pullulan	Showa Denko K.K., Tokyo, Japan	9057-02-7
Sodium acetate (≥ 99%)	Sigma-Aldrich, Steinheim, Germany	127-09-3

Reagent	Producer	CAS number
Sodium borohydride (≥ 98%)	Sigma-Aldrich, Steinheim, Germany	16940-66-2
Sodium hydrogen phosphate (98.5%)	Sigma-Aldrich, Steinheim, Germany	7681-38-1
Sodium hydroxide	VWR International, Leuven, Belgium	1310-73-2
Sodium sulphate (anhydrous)	Fisher Scientific, Loughborough, UK	7757-82-6
Sodium tetraborate (≥ 99.5%, decahydrate)	Sigma-Aldrich, Steinheim, Germany	1330-43-4
Sulphuric acid (≥ 95%, for analysis)	Fisher Scientific, Loughborough, UK	7664-93-9

4.2. Enzymatic determination of glucose, fructose and sucrose

Amounts of common sugars (glucose, fructose and sucrose) in apples were quantified spectrophotometrically by the amount of nicotinamide adenine dinucleotide phosphate (NADPH), which was formed during several enzymatically catalysed transformation reactions of sugars. Absorption measurements were taken at a wavelength of 340 nm, the absorption maximum of NADPH.

D-glucose (**Fig. 51**A) and D-fructose (**Fig. 51**B) were analysed enzymatically according to EN 1140:1994 and sucrose according to EN 12146:1996. Monosaccharides D-glucose and D-fructose are phosphorylated by hexokinase and adenosine-5-triphosphate (ATP). Phosphorylated fructose is transformed into phosphorylated glucose by action of glucose-6-phosphate isomerase. Phosphorylated glucose is then oxidized by glucose-6-phosphate dehydrogenase and nicotinamide adenine dinucleotide phosphate (NADPH). Sucrose (**Fig. 51**C) is hydrolysed into D-glucose and D-fructose by the action of β-fructosidase (invertase) and then follows the reaction scheme of D-glucose.

The amount of NADPH is proportional to the amount of D-glucose, which is, in the case of sucrose analysis, also proportional to the amount of sucrose.

A

1) D-glucose + ATP $\xrightarrow{\text{Hexokinase}}$ Glucose-6-phosphate + ADP

2) Glucose-6-phosphate + NADP⁺ $\xrightarrow{\text{Glucose-6-phosphate dehydrogenase}}$ D-gluconate-6-phosphate + NADPH + H⁺

B

1) D-fructose + ATP $\xrightarrow{\text{Hexokinase}}$ Fructose-6-phosphate + ADP

2) Fructose-6-phosphate $\xrightarrow{\text{Glucose-6-phosphate isomerase}}$ Glucose-6-phosphate

3) Glucose-6-phosphate + NADP⁺ $\xrightarrow{\text{Glucose-6-phosphate dehydrogenase}}$ D-gluconate-6-phosphate + NADPH + H⁺

C

1) Sucrose + H_2O $\xrightarrow{\beta\text{-fructosidase}}$ D-glucose + D-fructose

2) D-glucose + ATP $\xrightarrow{\text{Hexokinase}}$ Glucose-6-phosphate + ADP

3) Glucose-6-phosphate + NADP⁺ $\xrightarrow{\text{Glucose-6-phosphate dehydrogenase}}$ D-gluconate-6-phosphate + NADPH + H⁺

Fig. 51. Scheme of enzymatic reactions during quantification of glucose (A), fructose (B) and sucrose (C).

ATP: adenosine-5-triphosphate, ADP: adenosine-5-diphosphate, NADPH: nicotinamide adenine dinucleotide phosphate.

Fresh pulp (5 g) was mixed with distilled water (20 mL) in a centrifuge tube, homogenised with Ultra-Turrax-appliances (Ika, Staufen, Germany) for 1 min and centrifuged (7690 x g, 10 min, 4 °C). The supernatant was filtered through a nylon matrix filter and can be stored at -20 °C. Before analysis, the extracts for glucose and sucrose analyses were diluted 1:5 and the extract for glucose-fructose analysis 1:10. Enzymes and reagents were supplied in the enzymatic kits for food analysis (Sigma-Aldrich, Deisenhofen, Germany) and prepared according to the instructions. Standard solutions were prepared for glucose and glucose-fructose (0.25–2 g/L in water) and sucrose (0.5–4 g/L in water). To prepare glucose-fructose standards, D-sucrose was dissolved in 0.7 M HCl and heated for 1 h at 100 °C.

For sugar analysis, microplates were filled with 5 µL of samples or standards. The reaction was followed at 37 °C and absorbance was read at 340 nm by a microplate reader (SAFAS flx-Xenius XM spectrofluorimeter, SAFAS, Monaco).

For glucose and glucose-fructose analysis, an aliquot (250 µL) of a solution containing NADP, ATP, hexokinase and glucose-6-phosphate dehydrogenase was added before the microplates were transferred to the microplate reader. For glucose-fructose analysis, the solution contained also glucose-6-phosphate isomerase. The absorbance was read after 10 min (glucose) or 16 min (glucose-fructose).

A solution of β-fructosidase (2 g/L, 25 µL) was added to samples and standards for sucrose quantification. Microplates were then transferred to the microplate reader and an aliquot (250 µL) of a solution containing NADP, ATP, hexokinase and glucose-6-phosphate dehydrogenase was added. The absorbance was read after 10 min.

The concentrations (c) of glucose, glucose-fructose and sucrose were calculated from the absorbance (A) using an external calibration obtained from standard solutions of known concentrations and the Beer-Lambert law according to:

$$A = \varepsilon \cdot l \cdot c \qquad\qquad\qquad (24)$$

With the molar extinction coefficient (ε) and the optical length (l). Subtraction of the glucose content from glucose-fructose present in the samples gave the amount of fructose. Since free glucose was co-determined in sucrose analysis, it was subtracted from total glucose to give the concentration of sucrose. The results were expressed in g/kg FW.

4.3. Cell wall isolation

Cell wall polysaccharides were isolated as alcohol insoluble solids (AIS), as described by Renard (2005b). They are insoluble in ethanol but other components as free sugars, amino acids, organic acids and salts are washed away by this treatment.

4.3.1. Raw apples

Three replicates of ten representative apples were chosen, cored and cut in 12 equal portions. The pieces were separated equally into three groups and cut vertically (**Fig. 52**). Only four pieces per apple, systematically spread over sides and height, were retained in order to obtain a batch of 40 apple pieces (Renard, 2005b). They were immediately frozen in liquid nitrogen and then stored at -20 °C before freeze-drying.
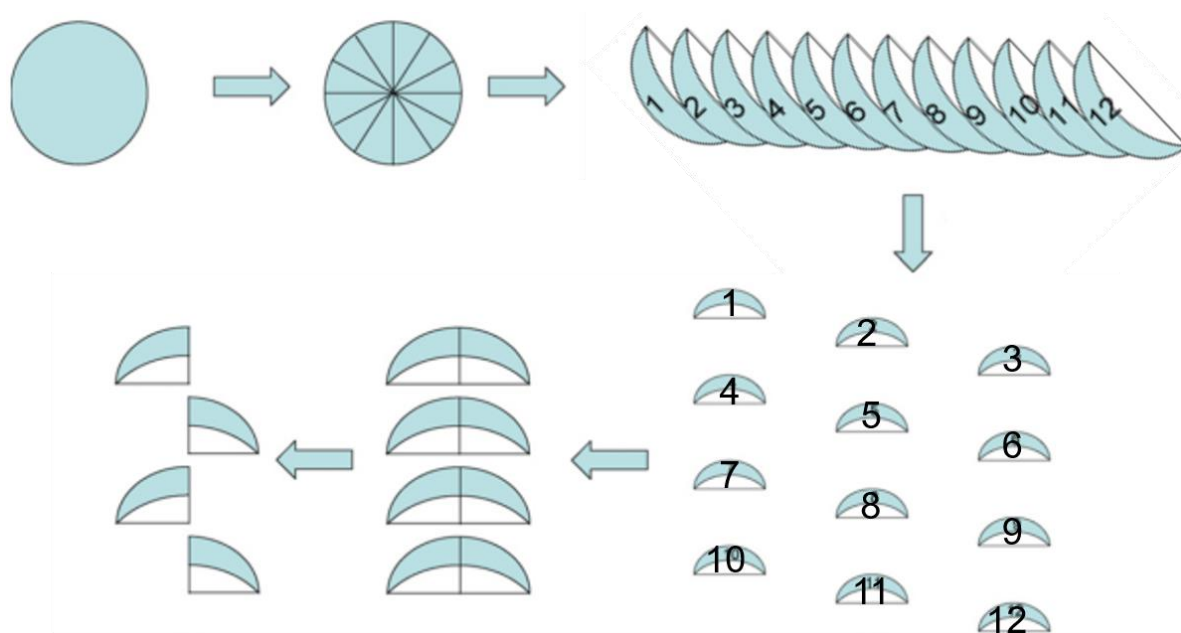
Fig. 52. Scheme of systematic apple fractionation for AIS analysis.
Adapted from Le Bourvellec, et al., 2011.

Approximately 2 g ($W_{initial}$) of finely ground material were suspended in 30 mL boiling ethanol (70% v/v, 30 min) in order to inactivate endogenous enzymes. The suspension was then filtered by a 75 mL Sep-pack column (Interchim, Montluçon, France), equipped with a 20 µm filter. The extraction was repeated several times with ethanol (70% v/v) until absence of free sugars. This was tested by the phenol-sulfuric acid reaction (Dubois, Gilles, Hamilton, Rebers, & Smith, 1956). In a test tube, 0.5 mL of

the filtrate were mixed with 0.5 mL of a solution of phenol in water (50 g/L) and 2.5 mL sulfuric acid (96%). The solution should show a pale yellow colour (less than 10 µg glucose/mL). Subsequently, the samples were washed twice with acetone (60% v/v), once with acetone (80% v/v) and three times with acetone (100% v/v). The residue was dried at 40 °C during 48 h in a drying oven (Memmert, Schwabach, Germany) and weighed (W_{final}). The cell wall content of the freeze-dried apples was estimated as follows:

$$AIS_{dry} \left({g}/{100 \text{ g DW}} \right) = \frac{W_{final}}{W_{initial}} \cdot 100 \quad\quad\quad (25)$$

To calculate the AIS content of the apples before freeze-drying (fresh weight, FW), AIS_{dry} has to be multiplied with the dry matter content:

$$AIS_{fresh} \left({g}/{100 \text{ g FW}} \right) = \frac{AIS_{dry}(\%) \cdot Dry \text{ matter } (\%)}{100} \qu\quad (26)$$

If starch was present in the fruits, it remains in the AIS during extraction. Equation (25) and (26) express thus the amount of cell wall polysaccharides and potentially starch.

4.3.2. Puree

In contrast to AIS extraction of raw apples, purees were not freeze-dried. They were thus humid and more concentrated ethanol was added to balance the water content in the puree. Furthermore, the boiling step could be omitted since endogenous enzymes have already been inactivated during puree processing. Fresh puree (20 g) was mixed with 80 mL ethanol (96% v/v) and stirred during one night (100 rpm, 4 °C). The supernatant was removed by filtration and a portion of 70% ethanol was added. The same washing and drying procedures were used as for apples. AIS of the puree were calculated as the relation between the dry weight and the initial weight of fresh puree and expressed in g/100 g FW.

4.3.3. Pulp

Pulp was water-washed to eliminate the remaining serum before AIS extraction. Some pulp (25 g) was stirred (100 rpm, 4 °C) one night in water (130 mL), before the water was removed by centrifugation (7690 x g, 10 min, 15 °C). The residue was rinsed once again with fresh water. Afterwards, the pulp (10 g) was stirred (100 rpm, 4 °C) one night in ethanol (96% v/v, 50 mL). The same washing and drying steps were then applied as described before for raw apples. AIS of the pulp were determined as the relation between the dry pulp weight and the initial weight of fresh pulp after water-washing and expressed in g/100 g FW.

4.4. Serum precipitation

The soluble polysaccharides in the serum were also alcohol-precipitated. However, the method had to be adapted because the polysaccharides present in the serum are primarily pectins (cf. **II 3.2**). They clog the filter and agglomerate during the drying process in the drying oven. For this reason, the serum (100 mL) was stirred (300 rpm, 4 °C) overnight in ethanol (96% v/v, 250 mL) and then centrifuged (7690 x g, 10 min, 15 °C) to eliminate the residual ethanol. The insoluble contents were washed with ethanol (70% v/v) until all free sugars were removed. The residue was then stirred (300 rpm, 4 °C) one night in water (50 mL) to redissolve the pectins for the subsequent freeze-drying. The freeze-dried serum was ground with an *A11 basic* batch mill (IKA, Staufen, Germany). The pectin content in the serum was roughly estimated by calculating the ratio between the weight of the sample after freeze-drying (W_{final}) and the initial weight of 100 mL serum ($W_{initial}$), expressed in g/100 g FW:

$$\text{AIS}_{\text{serum}} \left({}^{g}\!/_{100 \text{ g FW}} \right) = \frac{W_{\text{final}}}{W_{\text{initial}}} \cdot 100 \qquad\qquad (27)$$

When starch is present in the sample, equation (27) overestimates the soluble fibre content in the serum.

4.5. Cell wall polysaccharide analysis

Raw apples, puree, pulp and serum were all characterized in the same way for their cell wall polysaccharide composition. In the following paragraphs, they are thus summarized by the simple designation "sample".

4.5.1. Neutral sugars

Pectins' side chains and hemicelluloses are degraded into their individual neutral sugars by a simple acid hydrolysis. Therefore, AIS (10 mg) were mixed with myo-inositol (1 g/L in water, 1 mL), used as an internal standard and sulfuric acid (2 M, 1 mL).

In contrast, cellulose has to be solubilised under harsher conditions. For this reason, a double hydrolysis (Saeman, Moore, Mitchell, & Millett, 1954) was performed. AIS (10 mg) were subjected to a first hydrolysis in sulfuric acid (72% v/v, 0.25 mL) for 1 h at room temperature. Afterwards, the samples were mixed with the standard myo-inositol (1 g/L in water, 1 mL) and water (1.7 mL).

Additionally, a standard solution (1 g/L per sugar) was prepared with arabinose, fucose, galactose, glucose, mannose, rhamnose, xylose and myo-inositol in water. Three repetitions, each containing an aliquot of standard solution (1 mL) and sulfuric acid (2 M, 1 mL) were prepared.

Hereinafter, all the prepared samples and standards were treated the same way. After incubation for 3 h at 100 °C to liberate the monosaccharides by acidic hydrolysis, 0.35 mL ammonia solution (35%) was added gradually to an aliquot (1 mL) of each sample until the pH of the solution was > 9. Afterwards, the free sugars were derivatized to volatile alditol acetates according to the method described by Englyst, Wiggins, and Cummings (1982). Therefore, the sugars in the solution were reduced to the equivalent alditols by adding sodium borohydride (100 g/mL in 3 M ammonia solution, 0.1 mL) followed by incubation (1 h) at room temperature. Acetic acid (glacial, 0.1 mL) was then added to the samples for neutralization and degradation of residual borohydride. An aliquot (0.3 mL) of this solution was mixed with the catalyst 1-methylimidazole (0.2 mL) and acetic anhydride (3 mL) in order to obtain the volatile alditol acetates via acetylation after incubation (30 min) at room temperature.

Cold water (5 mL) and dichloromethane (3 mL) were added and the solution was stirred vigorously in order to transfer the sugar derivatives to the organic phase. This phase was washed three times with a sodium hydrogen carbonate solution (0.2 M, 5 mL), then dried with anhydrous sodium sulphate and concentrated to 0.5 mL under nitrogen flow.

The main chemical reactions of this method are summarized in **Fig. 53**.
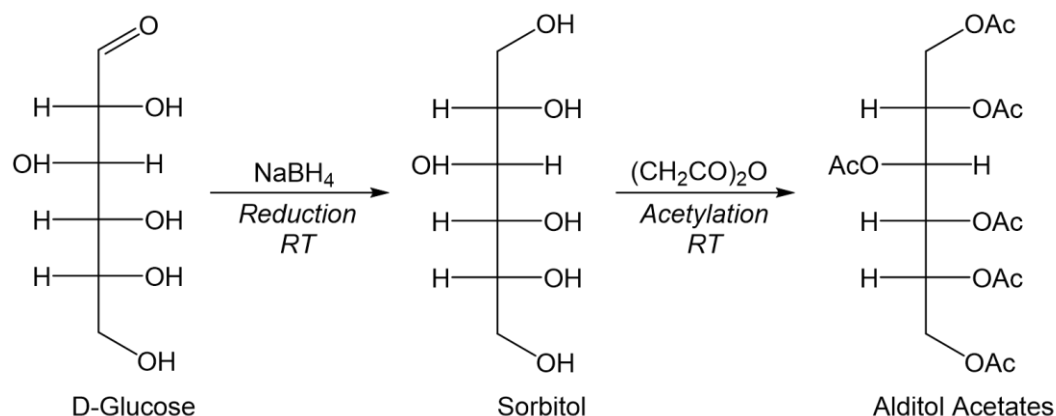
Fig. 53. Main reactions during neutral sugar determination by GC-FID.

The measurement of the volatile alditol acetates was performed with a *Clarus 500* gas chromatograph (PerkinElmer, Waltham, USA), equipped with a flame ionization detector (FID). The parameters that were applied are listed in **Table 7**.

Table 7. Instrumental parameters of the GC-FID used for neutral sugar analysis.

Parameter	GC-FID
Instrument type	PE Autosystem GC with built-in autosampler
Injection technique	Split (Ratio 8:1)
Injection volume	1.5 µL
Carrier gas	H_2 (1.5 mL/min)
Capillary column	Optima, 30 m × 0.25 mm ID, 0.25 µm film (Macherey-Nagel, Düren, Germany)
Temperature program	230 °C (20 min)
Detector	FID (250 °C, H_2 and compressed air)

The quantification was realized in comparison to the internal standard myo-inositol. The response factors of each sugar derivative in comparison to inositol were calculated by means of the standard solution. The results are expressed as anhydrosugars to account for loss of water during the formation of the glycosidic bonds.

4.5.2. Galacturonic acid

AIS (10 mg) of samples containing cell wall (raw fruits, purees, pulp) were analysed after double hydrolysis as described in **IV 4.5.1.** (Saeman, et al., 1954). AIS containing only pectins (serum) should be analysed after saponification (cf. **IV 4.5.3.**). However, all samples were treated the same way and uronic acids were quantified after double hydrolysis. This underestimates the amount of individual galacturonic acid molecules in pectins as not all linkages between them were broken. Only soluble serum pectins that were analysed by HPSEC were saponified before galacturonic acid analysis.

Samples were then measured by the 3-phenylphenol assay described by Blumenkrantz and Asboe-Hansen (1973). Three test tubes were prepared for each sample (2 tests, 1 blank). The samples (0.5 mL) were placed in the test tubes, mixed with a solution of sodium tetraborate (0.0125 M in concentrated sulfuric acid, 3 mL) and heated (80 °C). Thereby, the pectin molecules are depolymerized and the uronic acids are converted into 5-formyl-2-furoic acids (**Fig. 54**).
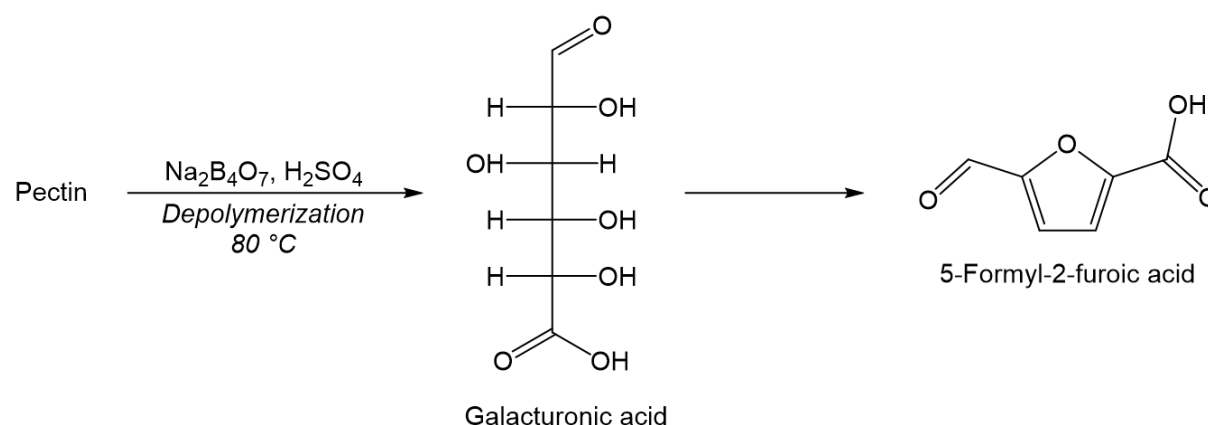
Fig. 54. Reaction scheme of the 3-phenylphenol assay.

After incubation (10 min), the test tubes were placed in an ice bath to stop the reaction. Once the samples reached room temperature, 3-phenylphenol (0.15% in 1M NaOH, 0.05 mL) was added to the samples in order to form violet colorants. NaOH (1 M, 0.05 mL) was added to the blank. After 10 min of incubation, the solutions were transferred into disposable plastic cuvettes and the absorbance was read at a wavelength of 520 nm by a spectrophotometer (Jasco, Gross-Umstadt, Germany). The absorbance of blanks was deducted from the absorbance of the corresponding sample. The amount of the uronic acids was determined using an external calibration varying from 25 to 100 µg/L (galacturonic acid in water). As galacturonic acid is the main uronic acid in apples, forming the backbone of pectic polysaccharides, the detected amount of uronic acids is expressed as anhydrous galacturonic acids.

4.5.3. Methanol

The methyl esters linked to the galacturonic acid backbone in pectins were saponified by KOH (**Fig. 55**). The released methanol was then quantified by gas chromatography-mass spectrometry (GC-MS) using the headspace technique (Renard & Ginies, 2009).
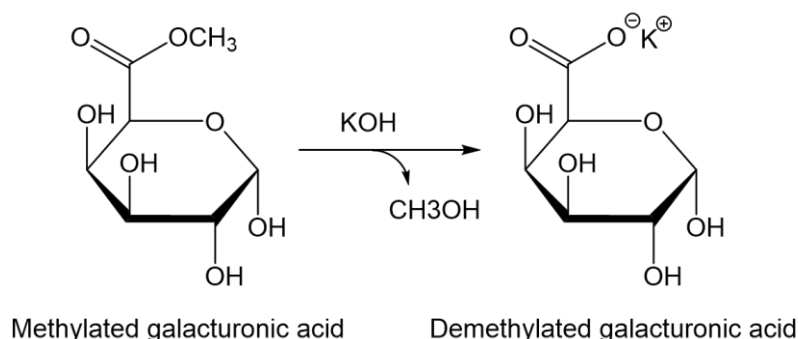
Fig. 55. Saponification reaction of galacturonic acid.

AIS (10 mg) was directly weighed into a 20 mL vial and mixed with KOH (1 M) and water. Deuterated methanol was added as an internal standard and quantification was carried out with an external calibration containing both deuterated and non-deuterated methanol (**Table 8**).

Table 8. Pipetting scheme (mL) for methanol analysis by Headspace GC-MS.

	KOH (1M)	CD$_3$OH[a]	CH$_3$OH[b]	H$_2$O
Standard 1	0.8 mL	0.4 mL	0.1 mL	3.7 mL
Standard 2	0.8 mL	0.4 mL	0.2 mL	3.6 mL
Standard 3	0.8 mL	0.4 mL	0.4 mL	3.4 mL
Standard 4	0.8 mL	0.4 mL	0.8 mL	3.0 mL
Standard 5	0.8 mL	0.4 mL	1.0 mL	2.8 mL
Samples	0.8 mL	0.4 mL	–	3.8 mL

[a] 30 mg/50 mL H$_2$O

[b] 250 mg/50 mL H$_2$O, then diluted (1:5 v:v)

Before the vials were transferred to the injector, they were stirred 15 min at 50 °C in the *TRIPLUS RSH* autosampler (Thermo Scientific, Waltham, USA) to ensure complete saponification. The subsequent measurement of the vials´ headspace was carried out with a *Trace 1300* gas chromatograph (Thermo Scientific, Waltham, USA) and a coupled *ISQ LT* single quadrupole mass spectrometer (Thermo Scientific, Waltham, USA) using the parameters described in **Table 9**.

Table 9. Instrumental parameters of the GC-MS (Headspace).

Parameter	GC-FID
Syringe temperature	60 °C
Injection technique	Split (Ratio 15:1)
Injection volume	500 µL
Injection temperature	220 °C
Carrier gas	Helium (70 kPa)
Capillary column	TG-WaxMS, 30 m × 0.25 mm ID, 0.5 µm film (Thermo Scientific, Waltham, USA)
Temperature program	40 °C (7 min)
Interface temperature	230 °C
Ion source	Electron Ionization (EI, 250 °C, 70 eV)

Parameter	GC-FID
Analyser	Single quadrupole mass spectrometer (Thermo Scientific, Waltham, USA)
Detector	Secondary electron multiplier with conversion diode
Scans	5 scans/s (29 m/z, 31 m/z, 32 m/z, 35 m/z)

The amount of methanol in the sample's headspace was calculated by plotting the peak area ratio for ion pairs (m/z 31/35), referring to the normal and deuterated form of methanol, over the range of the concentration ratios. Therefore, the ion at 31 m/z corresponds to methanol (CH_3O^+) and 35 m/z refers to the parent ion for deuterated methanol ($CD_3OH^{+\cdot}$).

The degree of methylation (DM) was calculated as molar ratio of methanol (MeOH) to galacturonic acid (GalA) and expressed in %:

$$DM\ (\%) = \frac{MeOH}{GalA} \cdot 100 \qquad\qquad (28)$$

4.5.4. Starch determination

The starch content in fresh apples was determined qualitatively by the iodine test with lugol solution (iodine/potassium iodide). Triiodide anions (I_3^-), deriving from the lugol solution, form a dark blue coloured complex with starch amylose, allowing visual starch detection (**Fig. 56**).
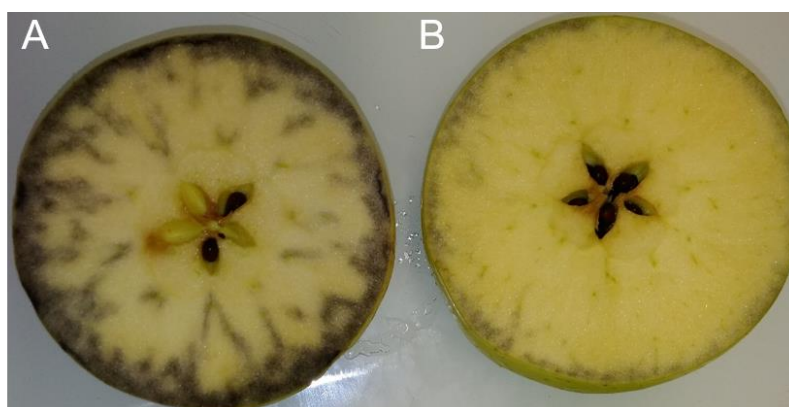
Fig. 56. Apple halves after qualitative iodine test showing medium (A) and no starch (B) content.

The apples were halved horizontally and held 1 min into the lugol solution before rinsing with water. The dark blue coloured pattern was then compared to a rating chart proposed by the Ontario Ministry of Agriculture, Food and Rural Affairs (OMAFRA) (Chu & Wilson, 2000).

The quantitative starch content in fresh apples, purees, pulp and serum was determined in the AIS by using the total starch assay kit *K-TSTA* (Megazyme, Wicklow, Ireland). The principle of this assay is based on enzymatic degradation reactions from starch to glucose and a following colorimetric reaction. Thereby, α-amylase converts starch into maltodextrins and amyloglucosidase degrades them to glucose. D-Glucose is oxidized by glucose oxidase to D-gluconate with the release of one mole of hydrogen peroxide. The latter is quantitatively measured as a quinoneimine dye in a colorimetric reaction employing *p*-hydroxybenzoic acid, 4-aminoantipyrine and peroxidase as a catalyst. The following figure (**Fig. 57**) illustrates the different reactions that take place during starch quantification.

1) $Starch + H_2O \xrightarrow{\text{α-amylase, 100 °C}} Maltodextrins$

2) $Maltodextrins \xrightarrow{\text{Amyloglucosidase}} \text{D-glucose}$

3) $\text{D-glucose} + O_2 + H_2O \xrightarrow{\text{Glucose oxidase}} \text{D-gluconate} + H_2O_2$

4) $H_2O_2 + \textit{p}\text{-hydroxybenzoic acid} + \text{4-aminoantipyrine} \xrightarrow{\text{Peroxidase}} \text{Quinoneimine dye} + 4\,H_2O$
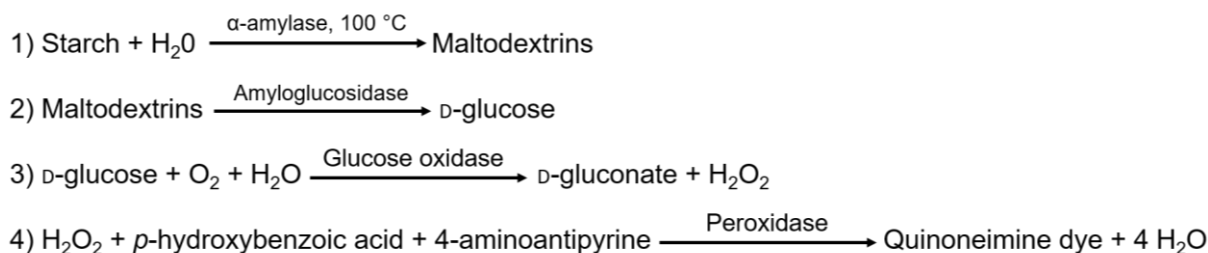
Fig. 57. Reaction scheme of starch quantification by total starch assay kit K-TSTA.

The same method was applied as described in the Megazyme test kit but the protocol was adapted to 50 mg AIS due to limited sample material. Furthermore, the amount of enzymes was doubled taking into account that remaining polyphenols in the AIS could interact with the enzymes leading to a reduced activity. The enzymes and GOPOD reagent buffer for the colour formation were supplied in the kit. Only a sodium acetate buffer (100 mM, pH 5, CaCl₂ 5 mM) and glucose standard solutions (0.25–1 g/L glucose in water) were prepared and α-amylase was diluted at a ratio of 1:30 in the sodium acetate buffer.

Samples were analysed in duplicate and a blank was prepared according to the same protocol but without enzymes. Buffer was added instead. A mixture of AIS (50 mg) and α-amylase solution (3 mL, buffer for blanks) was incubated in 15 mL plastic centrifuge tubes for 24 min in a boiling water bath (Julabo, Seelbach, Germany) and vortexed every 4 min. The tubes were cooled to 50 °C before the supplied amyloglucosidase (0.1 mL, buffer for blanks) was added. The mixture was further incubated at 50 °C for 30 min. The suspension was centrifuged (7690 x g, 10 min, 25 °C) twice in order to obtain a clear solution. Afterwards, it was diluted depending on the expected starch content. An aliquot (0.05 mL) of the sample and standard glucose solutions were then mixed with the supplied GOPOD reagent buffer (1.5 mL) containing glucose oxidase, peroxidase, p-hydroxybenzoic acid and 4-aminoantipyrine. The solution was heated for 20 min at 50 °C in order to develop the coloration. The absorbance was then read against the GOPOD blank (0.05 mL water in 1.5 mL GOPOD reagent buffer) at 510 nm. The absorbance of blanks was deducted from the corresponding sample's absorbance. All values for AIS, neutral sugars, galacturonic acid and methanol were corrected by the respective starch content in the sample.

4.6. High performance size-exclusion chromatography coupled to multi-angle laser light scattering (HPSEC-MALLS) and online viscometry

Molar mass and size distributions of soluble pectins were analysed by HPSEC-MALLS (cf. **II 2.5.3.1.**) coupled to online viscometry. An Ultra Fast Liquid Chromatography Prominence system (Shimadzu, Kyoto, Japan) including a LC-2OAD pump, a DGU-20A5 degasser, a SIL-20ACHT autosampler, a CTO-20 AC column oven, a SPD-M20A diode array detector and a RID-10A refractive index detector from Shimadzu (Tokyo, Japan) was employed together with a multi-angle laser light scattering detector (DAWN HELEOS 8+ fitted with a K5 flow cell and a GaAs laser, λ = 660 nm) and a ViscostarIII viscometer from Wyatt Technology Corporation (Santa Barbara, CA). To visualize β–elimination products, the 235 nm wavelength in the prominence diode array detector (DAD) signal was particularly analysed.

Pectins were separated by three HPSEC columns (PolySep-GFC-P3000, P5000 and P6000, 300 × 7.8 mm) and a guard column from Phenomenex (Le Pecq, France). The whole HPSEC-MALLS system was maintained at 40 °C. The eluent, an acetate buffer (0.2 M) at pH 3.6, was composed of acetic acid (0.2 M, 926 mL) and sodium acetate (0.2 M, 74 mL). It was filtered through a 0.1 µm omnipore™ membrane from Millipore (Milford, USA) and degassed. Some crucial parameters are summarized in **Table 10**.

Table 10. Instrumental parameters of the HPSEC-MALLS system.

Parameter	HPSEC
Injection technique	Direct
Injection volume	100 µL
Eluent	Acetate buffer (0.2 M) at pH 3.6
Eluent flow	0.6 mL/min
Temperature program	40 °C (130 min)
1st capillary column	PolySep-GFC-P3000, 300 × 7.8 mm (Phenomenex, Le Peq, France)
2nd capillary column	PolySep-GFC-P5000, 300 × 7.8 mm (Phenomenex, Le Peq, France)
3rd capillary column	PolySep-GFC-P6000, 300 x 7.8 mm (Phenomenex, Le Peq, France)
Guard column	PolySep-GFC-P, 35 x 7.8 mm (Phenomenex, Le Peq, France)
Prominence diode array detector (DAD)	SPD-M20A (Shimadzu, Tokyo, Japan)
Multi-angle laser light scattering detector (MALLS)	DAWN HELEOS 8+, λ = 660 nm (Wyatt Technology Corporation; Santa Barbara, CA)
Viscometric detector	ViscostarIII (Wyatt Technology Corporation, Santa Barbara, CA)
Refractive Index Detector (RID)	RID-10A (Shimadzu, Tokyo, Japan)

M_i and R_{gi}, the molar mass and the radius of gyration at the ith slice of the chromatogram were determined by ASTRA® software from Wyatt Technology Corporation (version 7.1.4 for PC). The light scattering signal from six angles (20.4°–110°) and the Zimm formalism with a one order polynomial fit were used to extrapolate the data to zero angle (Rolland-Sabaté, Colonna, Potocki-Véronèse, Monsan, & Planchot, 2004). The viscometric hydrodynamic radius was also calculated by ASTRA® software. It was obtained by combining viscosity and molar mass measurements using the following equation deduced from the Einstein and Simha relation (Einstein, 1906, 1911; Simha, 1940):

$$[\eta]_i M_i = \gamma N_A V_{hi} = \frac{10\pi}{3} N_A R_{hi}^3 \qquad\qquad (29)$$

Here, $[\eta]_i$, R_{hi} and V_{hi} are the intrinsic viscosity, the hydrodynamic radius and the hydrodynamic volume at the ith slice of the chromatogram, $\gamma = 2.5$ for spheres and N_A is the Avogadro number. The weight-average molar mass $\overline{M}_w$, the z-average radius of gyration $\overline{R}_{gz}$, the z-average intrinsic viscosity $\overline{[\eta]}_z$ and the z-average viscometric hydrodynamic radius $\overline{R}_{hz}(v)$ were either indicated as the value at the apex of the main peak or by taking the summations over the whole peaks. The values at the apex of the main peak are representative of the main pectic fraction and are more suitable to compare samples when the molar mass calculations are not very accurate at the minor peak because of low signal to noise ratio or abnormal elution. The refractive index increment (dn/dc) for glycans was fixed at 0.146 mL/g and the photodiodes were normalised using a low molar mass pullulan standard (P20) from Showa Denko K.K. (Tokyo, Japan).

Soluble pectins from raw apple (100 mg) or serum (25 mg) AIS were solubilised directly in the filtered eluent (10 mL) by stirring the solution overnight at 4 °C. The samples were centrifuged (7690 x g, 10 min, 4 °C) and the supernatant was filtered through 0.45 µm hydrophilic PTFE syringe filter (Macherey-Nagel, Düren, Germany) before injection (100 µL) and elution at a flow rate of 0.6 mL/min for 130 min. To estimate the pectin content that was lost during centrifugation and filtration, the amount of galacturonic acid was quantified. The sample (1 mL) was frozen at -80 °C after both the centrifugation and filtration step. The samples were freeze-dried and the galacturonic content was analysed as described in **IV 4.5.2**.

Before the system was put into operation, pullulan (P20, P800) and dextran standards (D500) of varying size were systematically injected in order to control the cleanness of the system and the response of the detectors.

4.7. Nuclear magnetic resonance (NMR) spectroscopy

NMR analyses were performed by the Biopolymers and Structural Biology (BIBS) platform in Nantes (France).

4.7.1. Porosity evaluation of the cell wall

Water mobility in fresh and ethanol-extracted (AIS) pulp was assessed by T_2 relaxation times. As the T_2 relaxation time increases, water mobility in the system also increases. This can be roughly linked to the porosity of the material since an increase in T_2 relaxation times involve, among others, an increase in average pore size (Meng & Ragauskas, 2014).

Fresh pulp (50 g) was washed twice with distilled water and then stabilized for storage and transport by adding NaN_3 (0.05% in water) and stored at 4 °C. Freezing was avoided since cell wall structure should remain intact. Samples were placed in 10 mm NMR tubes and allowed to reach 4 °C before the spectrum was acquired at the same temperature. Transverse relaxation times (T_2) were measured on a Minispec mq20 (20 MHz, 0.47 T) from Bruker (Billerica, USA), which was equipped with a thermostated ^{1}H probe using the Carr-Purcell-Meiboom-Gill (CPMG) pulse sequence. Echo Time (ET) was 0.04 ms, 300 points were collected and 128 scans were acquired with a recycle delay of 10 s.

Since soluble substances in the pulp such as sugars, acids and salts impact water mobility and thus hinder interpretation of the results, extracted cell wall material was analysed (AIS). In addition, a positive (PoC) and a negative control (NeC) were prepared. For PoC, AIS (115 mg) were heated in 4.5 mL water for 1 h in a boiling water-bath to increase cell wall porosity. Since heat might have liberated free sugars, PoC was extracted by ethanol (70%) and dried by solvent exchange, followed by 48 h at 40 °C, as described in **IV 4.3**.

Cell wall porosity was reduced by freeze-drying pulp AIS (115 mg), which was suspended in 4.5 mL water prior to freeze-drying. This sample was designated as NeC. However, differences between PoC and NeC were not enormous (**Fig. 58**) and interpretation was difficult, maybe due to irreversible modifications of polysaccharides in freeze-dried samples.
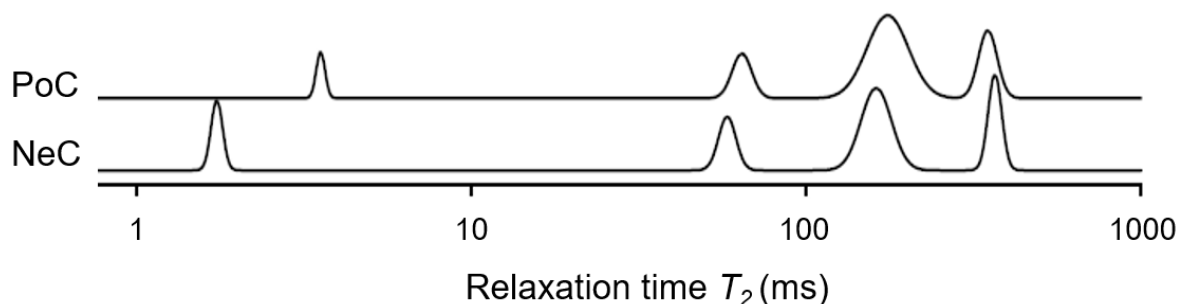
Fig. 58. Relaxation times T_2 for positive (PoC) and negative control (NeC).

Since the low hydration of AIS samples hindered interpretation of the results, pulp AIS (100 mg) were rehydrated in distilled water. Excess water was gently removed before samples were placed in NMR tubes and T_2 was measured at 4 °C, using the following acquisition parameters: ET 0.5 ms, 2000 points, 128 scans, recycle delay 7 s.

T_2 relaxation curves were treated by a multi-exponential analysis using a continuous approach. The inverse Laplace transformation (ILT) of the relaxation signal $S_2(t)$ acquired with the CPMG pulse sequence was used. $S_2(t)$ corresponds to

$$S_2(t) = \sum_{j=1}^{n} P_{2j} e^{-t/T_{2j}} + C \qquad (30)$$

with the normalized amplitude/population $\sum_{j=1}^{n}(P_{2j} = 1)$ of the jth component (P_{2j}), the T_2 associated to the jth component (T_{2j}) and a constant associated to the relaxation curve offset (C) and to

$$S_2(t) = \int_0^{\infty} e^{-t/T_2} f(T_2)\, dT_2 + E(t) \qquad (31)$$

with the probability density (f(T_2)) and the measurements error (E(t)).

To calculate quantitative information such as the relative peak area, peak width/dispersion and T_2 mean values of each peak, T_2 distributions were modelled by a sum of peaks with asymmetrical normal shape using Matlab® sofware.

4.7.2. Determination of β–elimination products

In order to quantify β-elimination products in soluble pectins (2.5 mg/mL acetate buffer, 0.2 M, pH 3.6), the 235 nm wavelength in the DAD signal was analysed after sample separation by HPSEC (cf. **IV 4.6.**) but there was not enough β-elimination to be detected. The absorbance of these samples was further measured at 235 nm using a spectrophotometer (Jasco, Gross-Umstadt, Germany) (Shpigelman, Kyomugasho, Christiaens, Van Loey, & Hendrickx, 2014) but turbidity of the samples seemed to bias the measurement.

^{1}H-NMR was thus employed to visualize β-elimination products of soluble pectins according to Tjan, et al. (1974). Serum AIS (5 g/L) were solubilised at 4 °C for 1 h in distilled water before adjusting to pH 6 with NaOH (0.01 M). The samples were centrifuged (4272 x g, 15 min, 4 °C) to eliminate possible cell wall remnants and the supernatant was freeze-dried. Samples were then suspended in D_2O (0.75 mL) for one night at 4 °C, before they were freeze-dried again. This (suspension in D_2O and freeze-drying) was repeated once again. A positive control was prepared by dissolving 10 mg serum AIS (95 °C, 3000 rpm) in 2 mL distilled water, adjusting to pH 6 and heating for 30 min at 100 °C. Afterwards, the control was readjusted to pH 6 and treated in the same way as the samples. Samples and controls were analysed in D_2O. The NMR spectra were recorded on an Avance III 400 MHz spectrometer (Bruker, Billerica, USA), equipped with a BBO 5 mm probe. The experiments were recorded at 70 °C to shift the hydrogen deuterium oxide residual peak from 4.8 ppm to 4.3 ppm using as chemical shift calibration. A quantitative 1D ^{1}H spectrum was recorded. A [1]H 90° pulse of 10.2 μs and an accumulation of 128 scans with a recycling delay of 10 s were the most significant acquisition parameters for the 1D sequence including a water signal presaturation and were applied to decrease the HDO signal in the same order of magnitude than the others peaks.

5. Sensory analysis

A Flash Profile analysis (Dairou & Sieffermann, 2002) was employed by Terra'Senso (Avignon, France) to describe the visual aspect, as well as flavour, odour and textural properties of nine contrasted apple purees (**Fig. 59**) by a sensory panel of 10 trained assessors. Purees were produced by a combination of three temperature (70, 83, 95 °C) and three grinding (300, 1000, 3000 rpm) regimes as explained in **IV 2.3.4.**

Fig. 59. Nine contrasted apple purees for Flash Profile analysis.

Flash Profile analysis emerged from the free-choice profiling (FCP) method (Williams & Langron, 1984). This is a quick and inexpensive method, in which each participant defines its own attributes to describe the sample. A product rating follows, in which participants are asked to rank the products according to the individually perceived intensity of each defined attribute. An advantage of this method is that individual product sensitivities are preserved due to the use of personalised vocabulary (Quarmby & Ratkowsky, 1988). The results are statistically interpreted by a Generalized Procrustes Analysis (GPA) (Gower, 1975), searching for the existence of a consensus between the different product descriptors that were attributed by each participant.

In contrast to FCP, Flash Profile analysis does not require training sessions since the products are not rated by their intensities but freely classified for each of the descriptors. That is why this method can be performed in a single half-day session. However, the sensory panel has to be experienced in sensory analysis. As a conclusion, Flash profile analysis makes it possible to compare various opinions on the same product and check if there is a consensus. The relative position of the products as obtained by GPA then provides adequate vocabulary to explain the products and the differences between them.

6. Statistical treatment

Data, comprising textural and structural characteristics of purees but also composition and structure of pectins, was treated by several statistical methods. Standard deviations were calculated as pooled standard deviations (PSD), representing the weighted average of standard deviations. Kruskal-Wallis non-parametric test was used to determine significant differences on a given variable between samples. Exploratory data analysis by principal component analysis (PCA) or linear discriminant analysis (LDA) and a modelling method (linear regression), estimating the relationship between two variables, were also used.

6.1. Pooled standard deviation (PSD)

PSD combines standard deviations from several series of replicated measurements under the condition that the series have in principal equal standard deviations. It is recommended for series of measurements each with few replicates, and was used since each series of textural and structural analyses of purees as well as analyses of pectin composition included maximal 3 replicated measurements. PSD was calculated using the sum of individual variances for each series of replicated measurement weighted by the individual degrees of freedom (Box, Hunter, & Hunter, 1978):

$$\text{PSD} = \sqrt{\frac{1}{N-K}\sum_{i=1}^{N}(n_i - 1)\cdot s_i^2} \qquad\qquad (32)$$

Here, s is the standard deviation of each series, n_i is the number of measurements in each series, N the total number of measurements and K the number of series.

Since PSD is a weighted average of the standard deviation of each series, larger series of measurements have a proportionally greater effect on the overall standard deviation.

6.2. Kruskal-Wallis non-parametric test

The Kruskal-Wallis test (Kruskal & Wallis, 1952) is a non-parametric alternative to one-way analysis of variance (ANOVA) and is robust to not-normally distributed data. It compares n objects (n≥2) according to a quantitative variable and determines whether two or more independent samples of equal or different sample sizes originate from the same distribution. Kruskal-Wallis test replaces the original values by their ranks: the smallest value in rank 1, the next smallest in rank 2, etc. Information is thus lost during this test so that it is less powerful than one-way ANOVA.

The null hypothesis H_0 of the Kruskal-Wallis test is that the mean ranks of the groups are the same. To decline H_0 and determine whether at least one of the differences between the ranks is statistically significant, the P-value has to be compared to the significance level α. When the P-value is ≤ α, H_0 is declined and differences between ranks are statistically significant. Typically, α = 0.05 is used and indicates a risk of 5% that an existing difference will be affirmed while there is none.

Kruskal-Wallis test does not indicate which samples are different from others. A non-parametric post-hoc analysis, for example Dunn's multiple comparison test (Dunn, 1964), has to be performed to obtain this information.

Since the Shapiro-Wilk test indicated that not all results were normally distributed, the samples were compared by Kruskal-Wallis non-parametric test at the 95% level (α = 0.05) of significance. The XLSTAT package (Addinsoft, 2020) for Microsoft Excel was used.

6.3. Principal component analysis (PCA)

PCA is one of the multidimensional methods, which allows to reduce the dimensions of a dataset into its principal components (PC) with minimal loss of information. PCs are not correlated and the first few retain most of the variation of all the original dataset (Jolliffe, 2002), indicating the directions where there is the most variance. Although some accuracy is lost, data analysis is facilitated since the number of variables is reduced and can be visualized graphically.

Variables have to be standardized before analysis, especially when they are measured in different units. Otherwise, certain variables would be favoured or artificially disadvantaged. Standardization is achieved by:

$$\text{Value}_{\text{standardized}} = \frac{x_i - \text{mean}(x)}{\text{sd}(x)} \qquad (33)$$

With the value of each variable (x_i), the mean value ($\text{mean}(x)$) and the corresponding standard deviation ($\text{sd}(x)$).

After calculation of the covariance matrix, summarizing the correlations between all the possible pairs of variables, the principal components can be identified. The results can then be presented graphically in the form of two-dimensional graphs. The correlation between a variable and a PC and other variables is represented in a correlation circle. Here, positively correlated variables are grouped together, whereas negatively correlated variables are positioned on opposite sides and uncorrelated variables are perpendicular to each other. Variables which are positioned close to the origin are less well represented than variables which are away from the origin. Individual samples can be represented in the sample map relative to the PCs. Their positions give an indication of the intensity of the value of the individual on this variable compared to other individuals. In addition, sample separation into classes can be visualised.
PCA was performed using the package "FactoMineR" (Lê, Josse, & Husson, 2008) for R statistical software (R Core Team, 2018).

6.4. Linear discriminant analysis (LDA)

Like PCA, LDA is a statistical technique for dimensionality reduction. Whereas PCA establishes the directions of maximal variance, LDA aims to enhance separability of known classes by creating a new linear axis and projecting data on that axis (Raschka, 2014).

In order to maximize the distance between classes, the variance between classes is calculated and defined as the distance between the mean of different classes. The variance within classes also has to be calculated and is defined as the distance between the mean and the sample of every class. Then, the Fisher's criterion tries to

find the lower-dimensional space that maximizes the variance between classes and minimizes the variance within classes.

While PCA aims to find axes that maximize the variance and LDA aims to maximize separation of classes (**Fig. 60**).
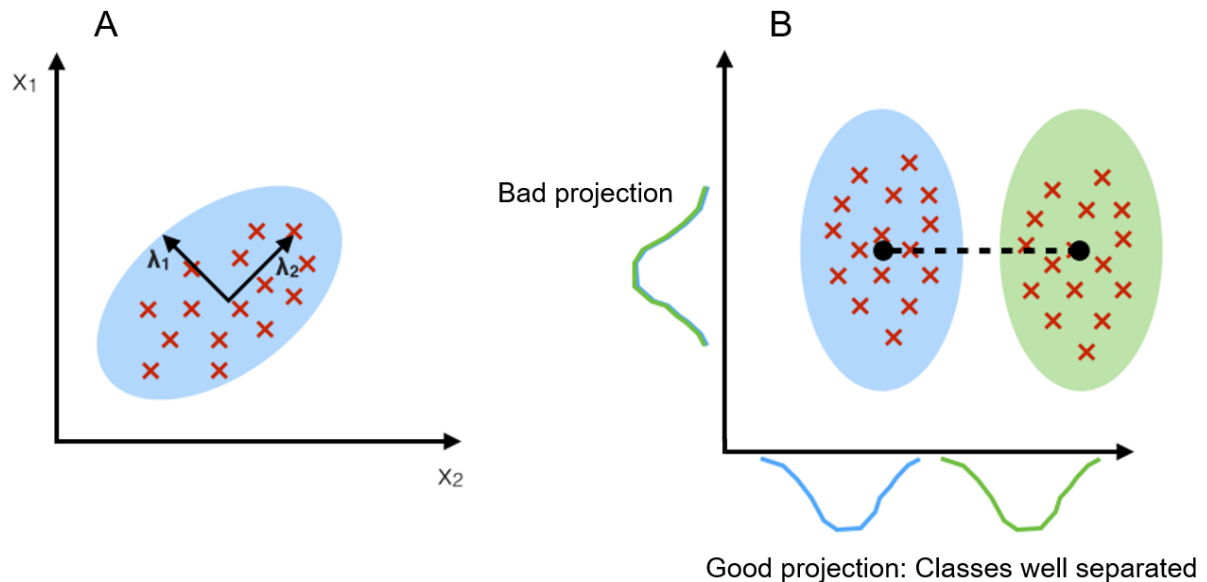
Fig. 60. Comparison between principal component analysis (PCA, A) and linear discriminant analysis (LDA, B).
Adapted from Raschka (2014).

The XLSTAT package (Addinsoft, 2020) for Microsoft Excel was used to assess LDA. Confusion matrix of the classification vectors were used to evaluate the classification of the samples.

6.5. Linear regression

Linear regression is a linear approach to establish an empirical model in order to describe the relationship between a set of dependent (response) variables Y and a set of independent (explanatory) variables X (Lane, 2015). It consists in calculating the coefficients b_i of the linear function linking the variable Y to a single variable X (simple regression) or several X_i (multiple regression). Here, the principle of least squares is applied to estimate the unknown coefficients b_i by minimizing the sum of the squares

of the differences between the observed variable Y in the given dataset and those predicted by the linear function.

The multiple linear regression model is written as follows:

$$Y = a + \sum b_i X_i + e \qquad\qquad (34)$$

With the y-intercept a and the error term e.

The correlation coefficient (r) describes the strength of the linear relationship between two variables X and Y and ranges between 1 (for a perfect positive correlation) and -1 (for a perfect negative correlation). When r = 0, there is no linear relationship between X and Y. The method of calculation differs slightly depending on the type of correlation coefficient. Pearson and Spearman correlation coefficients are the most commonly used. While Pearson correlation implies a parametric test and thus normality of both variables, Spearman correlation is a non-parametric alternative and is based on the rank of the values. Spearman correlation is also more robust to non-linear (but monotonous) correlations. Both values should be calculated and be in the same order of magnitude since Pearson correlation is more sensible to outliers.

Linear regression was conducted using the "stats" package, included in the base of R statistical software (R Core Team, 2018).

V. Results and discussion

1. Texture modulation of apple purees by means of the raw material

The first chapter deals with the question of how structural characteristics of the raw material can be used to modulate the structural factors, and thus texture, of apple purees. In a first study, the focus lies on apple maturity, while the second study highlights the effect of different cultivars and mealiness.

1.1. Storage duration

In this study, two cultivars of 2017 harvest, Golden Delicious (GD) and Granny Smith (GS), were processed into puree directly after harvest and after 1, 3 and 6 months of cold storage. Fruit thinning and drought stress (only for GD) were also evaluated. However, there were experimental difficulties to establish drought stress in the orchard, with the result that no differences in the rheological behaviour or particle size of apple purees were obtained between more or less irrigated fruits. This was probably due to the fact that the roots of the apple trees reached the phreatic zone. Thus, the effect of drought stress was less pronounced as the trees received a sufficient amount of water. Consequently, the impact of drought stress was not further assessed and discussed. Pectins were extracted from raw apples, puree, pulp and serum. Their characteristics were then compared between the different fractions and linked to structural characteristics of the puree.

This allowed to answer the following questions:

- ❖ How is puree's texture modified by storage?
- ❖ Do agricultural practices (fruit thinning and irrigation) modify the puree's texture?
- ❖ Can pectin modification explain the observed differences?

The following results are presented as a research article, which was published in *Food Hydrocolloids*.

Pectin modifications in raw fruits alter texture of plant cell dispersions

Alexandra Buergy[a], Agnès Rolland-Sabaté[a], Alexandre Leca[a], Catherine M. G. C. Renard[b]

[a] *INRAE, Avignon Université, UMR SQPOV, 84914 Avignon, France*
[b] *INRAE, CEPIA, 44316 Nantes, France*

Abstract

The texture of pureed fruits and vegetables depends primarily on the original tissue structure and cell wall (CW) properties. However, how variations in the raw fruits' cellular and molecular structure determine the rheological behaviour of the purees is little understood, though pectin degradation appears to play a key role. Cultivars, fruit load and post-harvest storage were used to obtain raw apples with different tissue structures, which were processed into purees under simulation of an industrial process. The rheological behaviour of the purees was then compared to particle size, pulp wet mass and serum viscosity. The polysaccharide composition of soluble and insoluble CW material were determined after preparation of alcohol insoluble residue. Macromolecular size and molar mass distributions of soluble pectins were analysed using high performance size-exclusion chromatography coupled to multi-angle laser light scattering and online viscometry. Variations in the raw material, especially induced by post-harvest storage, generated a wide range of different puree's textures. Rheological behaviour of apple purees was driven by particle size, which decreased during prolonged post-harvest storage due to reduced cell adhesion. This was correlated with pectic side chain hydrolysis and modifications in pectin molar mass and structure. Similar trends during storage were observed with different apple cultivars and agricultural practices.

Fruit processing, Apple, Puree, Rheology, Particle size, Polysaccharide

1.1.1. Introduction

Purees are manufactured from the edible parts of fruits and vegetables, which are mainly composed of parenchyma cells. They are dispersions of soft and deformable insoluble particles (pulp) in an aqueous medium (serum) composed of sugars, organic acids and pectic polysaccharides (Rao, 1992). The pulp is primarily composed of cell wall clusters, individual cells whose content was emptied during puree processing or cell fragments from the parenchyma of the original fruit, ranging between some mm and some hundred µm in size (Espinosa, et al., 2011; Leverrier, et al., 2016). In apple fruits, parenchyma cells are polyhedral in shape and between 50 and 300 µm in diameter (Khan & Vincent, 1990).

In reconstituted model systems, the amount, size and shape of individual cells or cell clusters as well as the viscosity of the serum are reported to be key factors in determining the puree's texture (Espinosa-Munoz, et al., 2013; Espinosa, et al., 2011; Leverrier, et al., 2016; Rao, 1992), and are all closely linked to the quality of pectic polysaccharides. However, to the best of our knowledge, no extensive study investigated the relationship between quality variations of raw apples, linked to pectins, and texture of corresponding purees. In contrast, the evolution of pectic substances in raw apples is well documented. For example, fruit cultivar as well as maturity stage modify the chemical and structural properties of the cell wall (Billy, et al., 2008; Fischer & Amado, 1994; Le Bourvellec, et al., 2011).

The main compartment of parenchyma cells is the large central vacuole, surrounded by the gel-like cytoplasm. The thin (0.1 to 10 µm) and semi-rigid cell wall, containing cellulose, hemicellulose and pectins, is located around this complex and plays an important role as it assures structural support to the plant cell (Darvill, et al., 1980). The colloidal middle lamella is situated between the primary cell walls of adjacent cells, holding them together and thus, forming the tissue (Thakur, et al., 1997). The middle lamella is almost only composed of pectic polysaccharides, accompanied by proteins (Carpita & Gibeaut, 1993) but without cellulose (Guillemin, et al., 2005).

Pectin molecules are a group of different complex polysaccharides rich in covalently linked D-galacturonic acid that form a negatively charged backbone (Albersheim, et al., 1996). The homogalacturonans (HG) are composed of a long, linear chain of α-D-($1\rightarrow4$)-galacturonic acids. These regions do not carry any neutral sugars as side

chains but the galacturonic acid residues can be methyl esterified to a varying degree at C6 positions, defining the degree of methylation (DM) (Thakur, et al., 1997). Depending on the DM, HG chains may self-associate; an unmethylated C-6 position of the HG backbone is negatively charged and may ionically interact with calcium-ions to form a stable gel with other HG molecules if more than 10 consecutive unmethyl-esterified galacturonic acid residues are coordinated (Kohn & Luknár, 1977). In the rhamnogalacturonan I (RG I) backbone, α-D-(1 → 4)-galacturonic acid and α-L-(1 → 2)-linked rhamnose molecules residues alternate, whereas the rhamnosyl residues can be substituted with neutral sugar chains. These lateral chains can be linear or branched and are mainly composed of α-L-arabinofuranosyl and/or β-D-galactopyranosyl forming arabinans, galactans and arabinogalactans (Ridley, et al., 2001). Rhamnogalacturonan II (RG II) molecules consist of a galacturonic acid backbone, carrying four complex oligosaccharide chains consisting of 12 different glycosyl residues in over 20 different linkages (Mohnen, 2008). *In muro*, RG II exists predominantly as a dimer that is cross-linked by a borate-diol ester (O'Neill, et al., 1996).

During processing into puree, rising temperatures destabilize cellular membranes and favour both enzymatic and chemical reactions, resulting in degradation and solubilisation of pectic polysaccharides that are involved in cell-to-cell adhesion (Massiot & Renard, 1997). The tissue is then softened due to increased cell separation. In addition, mechanical treatment partly disrupts the parenchyma cells that release their cell content.

Due to the increasing number of consumers and purchased quantities of fruit purees, food companies are highly interested in predicting and controlling the puree's texture since this is a major quality attribute and thus a key for the liking and, in turn, repeated purchase of the products (Waldron, et al., 1997). However, fruit purees may need to be rectified by concentration, addition of sugar or hydrocolloids, which may be perceived negatively by consumers. Thus, there is a global trend towards the production of healthier and more natural fruit products and the reduction of artificial stabilizers or texturizing agents (Market Resarch Future, 2019). This could be reached by playing on the structural factors of the raw fruit, as it is known, but not mastered by industry, that texture of plant-based products highly depends on the cell wall structure of the raw material (Waldron, et al., 1997).

The objective of this study was thus to identify the impact of pectin structure in raw apples on texture variations of the corresponding purees. To reach this aim, two apple cultivars, four post-harvest storage durations and two growing conditions were chosen to generate contrasted raw apples. Their impact on the structural factors as well as the cell wall composition of the apple purees was studied in order to relate microstructure to the puree's texture.

1.1.2. Material and Methods

1.1.2.1. Plant material

Apple (*Malus x domestica* Borkh.) cultivars, namely 'Granny Smith' and 'Golden Delicious' were cultivated in Mallemort, France and harvested in September 2017 according to the optimal harvest dates. 'Granny Smith' (GS) and half of the trees of the cultivar 'Golden Delicious' (GD) were thinned chemically (GD1), leading to less but bigger fruits (201 ± 7 g per apple). GS trees showed regular fruit growth and were thus thinned with 600 g/ha Amid-Thin®W (2-(1-naphthyl)acetamide) and 1 kg/hL Rhodofix® (1-naphthalenacetic acid). GD1 trees exhibited low fruit charge and were thus treated with 15 L/ha ammonium thiosulfate and 0.15 kg/hL Rhodofix®. Additionally, 3.5 L/ha MaxCel® (6-Benzylaminopurine) were applied on small fruits of both varieties. The other half of GD trees was not thinned (GD2), resulting in more but smaller fruits (176 ± 4 g per apple). The raw apples used in this article were characterized in detail (e.g. fruits' texture) in another study (Lan, Jaillais, Leca, Renard, & Bureau, 2020).

A first series of samples were processed directly after harvest (T0). The apples were then stored for one (T1), three (T3) and six (T6) months at 4 °C prior to processing. The atmosphere was not controlled to allow post-harvest storage to have significant impact.

1.1.2.2. Puree preparation

For each cultivar, growth condition and storage time, processing was conducted in triplicate. Approximately 3 kg of apple fruits per batch were cored, sliced into 12 equal portions and processed into puree. A cooker-cutter (RoboQbo Qb8-3, RoboQbo, Bentivoglio, Italy) was used for apple processing, imitating a hot break process at 95 °C, with stirring at 105 rad/s during 5 min under vacuum. Each batch of apple puree was divided into two portions: one was refined by an automatic sieve (Cobot Coupe

C80, Robot Coupe SNC, Vincennes, France) of 0.5 mm (RA2), removing skin and other larger particles, and the other one was not refined (NR). At T0, only NR samples were produced. Rheological measurements, particle size analysis and determination of pulp wet mass were conducted in the same week as puree preparation. Pulp and serum were then frozen separately (-20 °C) until cell wall extraction and analysis.

1.1.2.3. Rheological measurements

All tests were performed using a stress-controlled rheometer (Physica MCR301, Anton Paar, Graz, Austria) equipped with a Peltier cell (CPTD-200, Anton Paar) and an external cylinder (CC27/S, Anton Paar). All rheological measurements were performed at 22.5 °C and samples were changed for each test.

Puree

A vane measuring system with a 3.46 mm gap (CC27/S + FL100/6W, Anton Paar) was used to analyse the rheological behaviour of the purees. The flow curve was recorded by measuring the viscosity over a logarithmically distributed range of shear rate values $\dot{\gamma}$ between 10 and 250 s^{-1}. One point was recorded every 15 s. Homogenous dispersion of the product in the measurement cell was ensured by application of a pre-shear of 50 s^{-1} during 2 min, followed by a 5 min rest to let the puree return to a rheological equilibrium prior to analysis. The texture of the purees was compared by means of the apparent viscosity (η_{app}) at a shear rate of 50 s^{-1} as this value represents an approximation of the shear rate to which a soft food product is subjected in the mouth during mastication (Stokes, 2012).

Amplitude sweep tests were performed at deformation values γ between 0.01 and 100% at a fixed angular frequency ω of 10 rad/s. Five points were measured per decade and the time required to measure each point was set by the software. The yield stress obtained at the intersection of G' and G'' was used as a characteristic point to estimate the minimum shear stress that must be applied to the puree to initiate flow (Espinosa-Munoz, et al., 2013). The values of G' and G'' were averaged in the linear viscoelastic range. The end of the linear domain was estimated as the strain inducing a decrease of G' values exceeding 10% of its value in the linear domain.

The method used for rheological measurements of the purees was theoretically not adapted for particles larger than 1 mm as the gap of the measuring cell was

approximately 3 mm large. The only samples containing particles (skin fragments) larger than 1 mm were not refined purees. However, rheological measurements were repeatable for these samples and the method was thus considered valid.

Serum

The viscosity of the continuous phase obtained by centrifugation of the puree was measured using a double gap cylinder geometry (DG27, Anton Paar). Before each measurement, a resting step of 1 min was applied. Viscosity values (η_{serum}) were taken at a shear rate of 100 s^{-1} from a flow curve, assuming the in-mouth perception of serum requires a higher shear rate than purees.

1.1.2.4. Pulp wet mass

The pulp wet mass represented the fraction of humid particles after separation of the puree into pulp and serum by centrifugation at 7690 x g for 15 min at 15 °C. It was calculated as the ratio of the pulp weight to the initial weight of the puree and expressed in % as described in literature (Espinosa-Munoz, et al., 2013).

1.1.2.5. Particle size distribution

The particle size distribution of the pulp was measured by laser granulometry (Mastersizer 2000, Malvern Instruments, Malvern, UK). The samples were dispersed in distilled water (refractive index: 1.33) and analysed by the Mie theory. The refractive index of the sample was set at 1.52 (Leverrier, et al., 2016) and the absorptive index was chosen to be 0.00 due to the translucent character of apple cells. Each sample was analysed in duplicate and the Malvern's software averaged the size distribution over three repeated measurements on the same sample.

1.1.2.6. Alcohol insoluble solids (AIS)

AIS of raw apples and purees were extracted as described by Le Bourvellec, et al. (2011). AIS of serum and pulp were prepared based on Renard (2005b) and Le Bourvellec, et al. (2011).

Prior to cell wall extraction, pulp was water-washed to remove soluble pectins. Approximately 25 g of fresh pulp were suspended in ultrapure water (130 mL), then stirred one night (10 rad/s, 4 °C) and centrifuged (7690 x g, 10 min, 15 °C). The residue was rinsed once again with water before 10 g of the sediment were stirred (10 rad/s, 4 °C) one night in ethanol (96% v/v, 50 mL). The suspension was filtered on a 75 mL Sep-pack column (Interchim, Montluçon, France) equipped with a 20 µm filter. The extraction was continued with ethanol (70% v/v) till absence of sugars as shown by negative reaction in the phenol sulphuric test (Dubois, et al., 1956). Subsequently, the samples were washed twice with acetone (60% v/v), once with acetone (80% v/v) and three times with acetone (100% v/v). The residue was dried at 40 °C during 48 h in a drying oven and weighed. The cell wall content of the pulp was estimated as the relation between the dry pulp weight and the initial pulp weight after water-washing, expressed in %.

For serum, 100 mL were stirred (31 rad/s, 4 °C) overnight in 250 mL ethanol (96% v/v), then centrifuged (7690 x g, 15 °C, 10 min). The residue was washed several times with ethanol (70% v/v) until all free sugars were removed. Afterwards, samples were dissolved in water (50 mL) overnight (31 rad/s, 4 °C) to redissolve the pectins, then freeze-dried and ground with an *A11 basic* batch mill (IKA, Staufen, Germany). A rough estimation of the soluble pectin content can be calculated by the relation between the samples' weight after freeze-drying and the initial weight of 100 mL serum, expressed in %.

1.1.2.7. Water retention capacity

The water retention capacity of the pulp was calculated as the amount of water retained by the mass of the pulp's AIS (g/g dry weight) according to Robertson, et al. (2000). In this study, it was estimated as the relation between the pulp wet mass and the mass of the pulp's AIS. The mass of the fibre is generally negligible and was thus not considered in this equation.

1.1.2.8. Sugar composition of AIS

Cell wall analysis

AIS (10 mg) were subjected to prehydrolysis with sulphuric acid (72% v/v) for 1 h at room temperature. Afterwards, the samples were diluted to 1 M sulphuric acid by addition of water and internal standard (inositol) and heated at 100 °C for 3 h (Saeman, et al., 1954). For neutral sugars analysis, the free sugars were derivatized to volatile alditol acetates according to the method described by Englyst, et al. (1982). They were injected on a Clarus 500 gas chromatograph (PerkinElmer, Waltham, USA) equipped with a flame ionization detector (FID) and a OPTIMA® capillary column of 30 m × 0.25 mm i.d. and 0.25 µm film thickness (Macherey-Nagel, Düren, Germany). Helium was used as carrier gas at 1.5 mL/min and the injector temperature was set at 250 °C in split mode (ratio 1:8). The oven temperature was maintained at 230 °C.

Galacturonic acid was measured spectrophotometrically by the *m*-hydroxydiphenyl assay (Blumenkrantz & Asboe-Hansen, 1973) in the acid hydrolysates.

Methanol was quantified via stable isotope dilution assay after saponification (Renard & Ginies, 2009) on a *Trace 1300* gas chromatograph (Thermo Scientific, Waltham, USA) and a coupled *ISQ LT* single quadrupole mass spectrometer (Thermo Scientific, Waltham, USA). Capillary column was a TG-WaxMS of 30 m × 0.25 mm i.d. and 0.5 µm film thickness. Samples' headspace was injected in split injector (ratio 15:1) at 220 °C. Helium (70 kPa) was used as carrier gas. The oven temperature was set at 40 °C. Electron ionization (70 eV) was used at 250 °C.

The degree of methylation (DM) was calculated as molar ratio of methanol to galacturonic acid and expressed in %.

Starch determination

Starch was quantified in the AIS of the pulp, serum and raw apples using the total starch assay kit K-TSTA (Megazyme, Wicklow, Ireland) according to the manufacturer's instructions except that the amount of enzymes was doubled to counteract enzyme inhibition by the interaction of remaining polyphenols in the AIS with the enzymes. The test was performed in duplicate. All values for AIS, neutral sugars, galacturonic acid and methanol were corrected by the respective starch content in the sample.

1.1.2.9. High performance size-exclusion chromatography coupled to multi-angle laser light scattering (HPSEC-MALLS) and online viscometry

Molar mass and size distributions of soluble pectins was obtained by HPSEC-MALLS coupled to viscometric detection. An Ultra Fast Liquid Chromatography Prominence system (Shimadzu, Kyoto, Japan) including a LC-2OAD pump, a DGU-20A5 degasser, a SIL-20ACHT autosampler, a CTO-20 AC column oven, a SPD-M20A diode array detector and a RID-10A refractive index detector from Shimadzu (Tokyo, Japan) was employed together with a multi-angle laser light scattering detector (DAWN HELEOS 8+ fitted with a K5 flow cell and a GaAs laser, $\lambda = 660$ nm) and a ViscostarIII viscometer from Wyatt Technology Corporation (Santa Barbara, CA). Three HPSEC columns (PolySep-GFC-P3000, P5000 and P6000 300 × 7.8 mm) and a guard column from Phenomenex (Le Pecq, France) were used for the separation and all the HPSEC-MALLS system was maintained at 40 °C. The eluent, an acetate buffer (0.2 M) at pH 3.6, was carefully filtered through a 0.1 µm omnipore^{TM} membrane from Millipore (Milford, USA) and degassed before elution at a flow rate of 0.6 mL/min for 130 min. Pectins were solubilised overnight under magnetic stirring directly in the filtered eluent at 4 °C to a theoretical concentration of 10 mg AIS/mL (raw apples) and 2.5 mg AIS/mL (serum). The samples were centrifuged (7690 x g, 4 °C, 10 min) and the supernatant was filtered through 0.45 µm hydrophilic PTFE syringe filter (Macherey-Nagel, Düren, Germany) before injection (100 µL). ASTRA® software from Wyatt Technology Corporation (version 7.1.4 for PC) was used to establish M_i and R_{gi}, the molar mass and the radius of gyration at the ith slice of the chromatogram using the light scattering signal from six angles (20.4°-110°) and the Zimm formalism with a one order polynomial fit to extrapolate the data to zero angle (Rolland-Sabaté, et al., 2004). ASTRA® software was also used to calculate the viscometric hydrodynamic radius for the equivalent sphere by combining viscosity and molar mass measurements using the following equation derived from the Einstein and Simha relation (Einstein, 1906, 1911; Simha, 1940):

$$[\eta]_i M_i = \gamma N_A V_{hi} = \frac{10\pi}{3} N_A R_{hi}^3 \qquad (35)$$

where $[\eta]_i$, R_{hi} and V_{hi} are the intrinsic viscosity, the hydrodynamic radius and the hydrodynamic volume at the ith slice of the chromatogram, $\gamma = 2.5$ for spheres and N_A is the Avogadro number. The weight-average molar mass $\overline{M}_w$, the z-average radius of

gyration $\overline{R}_{gz}$, the z-average intrinsic viscosity $\overline{[\eta]}_z$ and the z-average viscometric hydrodynamic radius $\overline{R}_{hz}(v)$ were obtained by taking the summations over the whole peaks. The refractive index increment (dn/dc) for glycans was fixed at 0.146 mL/g and the normalization of photodiodes was achieved using a low molar mass pullulan standard (P20) from Showa Denko K.K. (Tokyo, Japan).

1.1.2.10. Statistical analysis

The Shapiro-Wilk test showed that not all data were normally distributed. Therefore, they were assessed by Kruskal-Wallis non-parametric test (Kruskal & Wallis, 1952) using R statistical software (R Core Team, 2018). Here, the H value is the test statistic that is used to calculate the P values. Differences were considered to be significant at P < 0.05. Standard deviations were calculated for each series of replicated measurement using the sum of individual variances weighted by the individual degrees of freedom (Box, et al., 1978). Principal Component Analysis (PCA) was performed using the package "FactoMineR" (Lê, et al., 2008) for R statistical software.

1.1.3. Results and discussion

1.1.3.1. Rheological parameters of apple purees

All apple purees showed a shear-thinning behaviour (data not shown) as already described (Espinosa, et al., 2011; Rao, et al., 1986). Apple cultivar and tree thinning practice (summarized as "raw material", **Table 11**) led to significantly different puree's viscosities. The highest values were obtained for GD1 and the lowest for GD2 (**Fig. 61**A). The apparent viscosity of the purees (η_{app}) also changed significantly with post-harvest storage (**Table 11**). However, this change did not follow a monotonous tendency, as for GD (GD1 and GD2) the viscosity decreased during the first months of post-harvest storage before increasing again between three and six months. For GS, however, η_{app} decreased monotonously for not refined samples during storage whereas viscosity of refined samples increased (**Fig. 61**A). The refined purees showed significantly lower viscosity values than not refined samples which might be explained by particle size.

Table 11. Kruskal-Wallis *H*-values and *P*-values performed on apparent viscosity at 50 s^{-1} (η_{app}), yield stress, serum viscosity at 100 s^{-1} (η_{serum}) and pulp wet mass (% Pulp).

	η_{app} 50 s^{-1} (mPa.s)	Yield stress (Pa)	η_{serum} 100 s^{-1} (mPa.s)	% Pulp (%)
Raw material *H*	16	34	45	7
Raw material *P*	**< 0.05**	**< 0.05**	**< 0.05**	**< 0.05**
Storage *H*	16	12	3	20
Storage *P*	**< 0.05**	**< 0.05**	0.41	**< 0.05**
Refining *H*	34	2	1	0
Refining *P*	**< 0.05**	0.17	0.31	0.93

Different apple cultivars and fruit loads also generated significantly different yield stress values (**Table 11**), the highest for GD2 and the lowest for GS (**Fig. 61**B). For GD apples, yield stress decreased abruptly between purees prepared from directly harvested apples and purees made from apples stored for one month. Interestingly, yield stress values from purees obtained from GD at the two fruit loads converged between three and six months. During post-harvest storage, the yield stress showed similar tendencies as apparent viscosity as a minimum was observed after three months for GD1, GD2 and not refined GS samples. Refined GS purees showed continuously increasing yield stress values. Unlike apparent viscosity, yield stress was not significantly affected by refining (**Table 11**).

1.1.3.2. Structural parameters of apple purees

Serum viscosity

Highest values of serum viscosity (**Fig. 61**C) were obtained with GS and the lowest with GD2, except at T6. Even if serum viscosity of GS decreased markedly between T0 and T1, no significant variations were detected over post-harvest storage (**Table 11**). Interestingly, the purees showing the highest serum viscosities revealed the lowest yield stress values. This might be due to the lubricant effect of the serum as stated by Espinosa-Munoz, et al. (2013), even if this trend was only observed for purees prepared with freshly harvested apples. It was hypothesized that pectins' characteristics, such as chemical structure and molar mass, were modified over

storage so that the lubricant effect of the serum became less important. Refining did not influence the viscosity of the soluble phase.
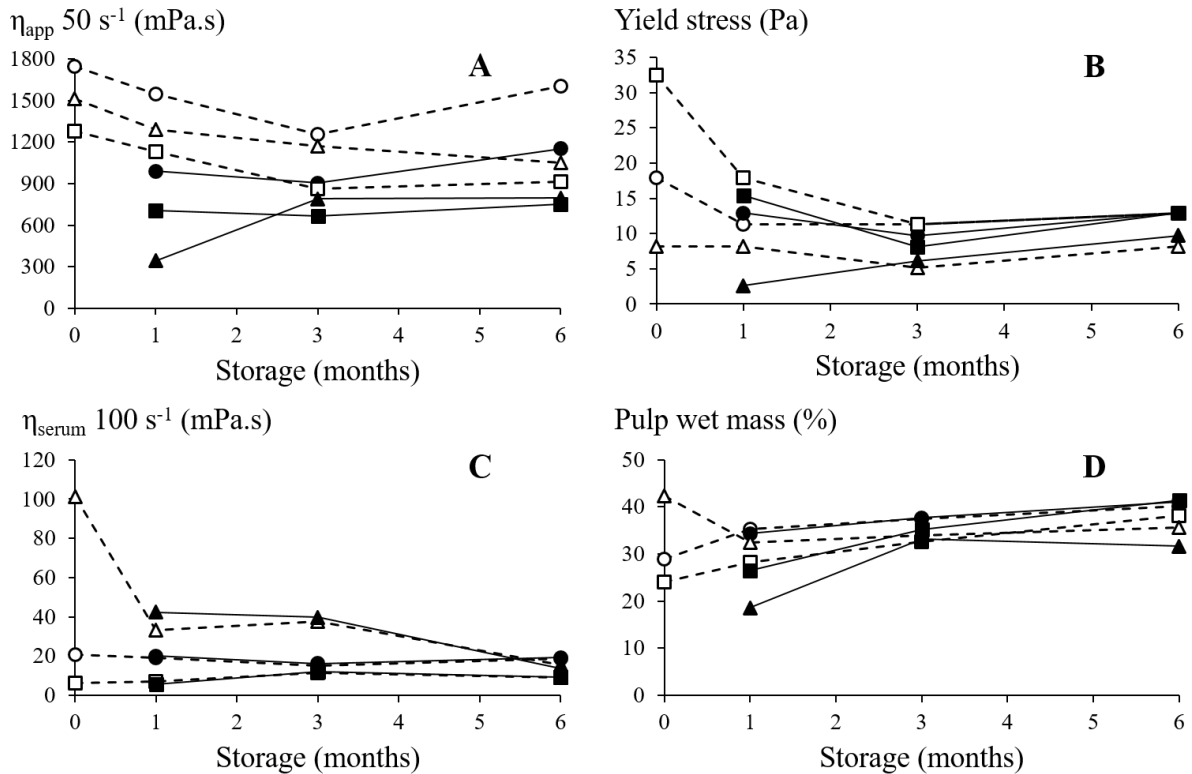
Fig. 61. Rheological and structural parameters of apple purees in function of post-harvest storage duration.

Apparent viscosity at 50 s^{-1} (A), yield stress (B), serum viscosity at 100 s^{-1} (C), pulp wet mass (D). Round symbols represent GD1, rectangular symbols GD2 and triangular symbols GS. Empty symbols display not refined and filled symbols refined (0.5 mm) samples.

Pulp wet mass

For GD apples, pulp wet mass (**Fig. 61**D) increased significantly over post-harvest storage. However, for GS, the pulp wet mass decreased strongly during the first month of post-harvest storage, then increased again. The contrasted trends between the two cultivars could be due to differences in the cell wall structure, leading to different water retention capacities. Generally, refining did not induce differences in pulp wet mass, though the not refined samples contained skin particles.

Particle size distribution

As a representative example, **Fig. 62** shows the evolution of particle size distribution during post-harvest storage for GD2. Directly after harvest (T0), purees showed a single peak around 1000 µm representing cell clusters (Espinosa-Munoz, et al., 2013; Leverrier, et al., 2016). Refining eliminated some large particles and the peak shifted to particle sizes close to 800 µm. Although a screen opening of 0.5 mm was used for refining, particles bigger than 0.5 mm were detected, probably because these flexible and deformable particles (Leverrier, et al., 2017b) could be pressed through the openings.

After one month of post-harvest storage, a second peak around 200 µm appeared for not refined samples. Espinosa-Munoz, et al. (2013) and Leverrier, et al. (2016) attributed this peak to individual cells by confocal and light microscopy, respectively. Refined samples still showed a monomodal size distribution with a broader peak compared to T0, near 500 µm. Smaller particles in refined purees were in line with lower viscosity values (**Fig. 61**A) as described in literature (Espinosa, et al., 2011; Schijvens, et al., 1998).

At three and six months of post-harvest storage, the particle size remained stable and both the refined and not refined purees showed a similar size distribution with a main peak around 200 µm. The size and amount of cell clusters in apple purees thus decreased over post-harvest storage to individual cells. This could be explained by reduced cell adhesion due to pectin solubilisation in the middle lamella by pectinase activity (Koziol, Cybulska, Pieczywek, & Zdunek, 2017). Thus, a prolonged storage period led to softer tissues, which could be fragmented more easily during processing.

A remarkable result was the convergence of the particle size of not refined and refined purees over storage time. Consequently, refining of apple purees had limited effect after three months of post-harvest storage as the particles were already very small after processing. The same results were obtained with GD1 and GS (data not shown). The texture of refined and not refined purees was, however, still different after three or six months of post-harvest storage (**Fig. 61**A). Fragments of apple skin remained in not refined samples, and thus increased the apparent viscosity of these samples, but were too big to be detected by laser granulometry.
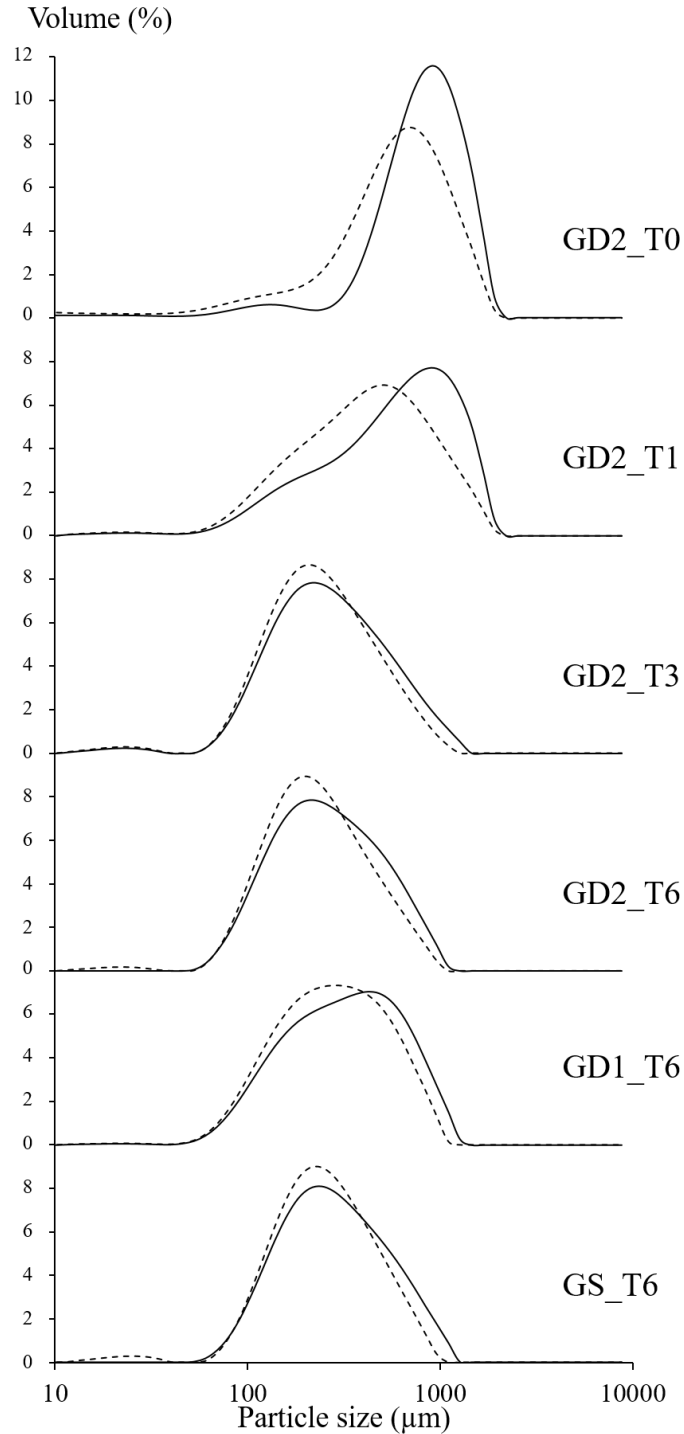
Fig. 62. Particle size distribution of the purees issued from different apple cultivars and at different post-harvest maturity stages.

GD1: Golden Delicious, reduced fruit load; GD2: Golden Delicious, high fruit load; GS: Granny Smith; T0: Directly after harvest; T1: After 1 month of post-harvest storage; T3: After 3 months of post-harvest storage; T6: After 6 months of post-harvest storage; Continuous lines represent not refined purees and dashed lines refined (0.5 mm) purees.

Particle size analysis also revealed differences depending on the apple cultivar and fruit load (**Fig. 62**). Between three and six months of post-harvest storage, particle size was stable for GD purees but still decreased slightly for GS samples (data not shown). Therefore, a plateau seemed to be reached after six months of post-harvest storage, which was used to compare the particle size of different apple cultivars and fruit loads. Fruit thinning enhances cell division (Goffinet, et al., 1995) and, depending on apple cultivar and thinning treatment, cell expansion (Milić, et al., 2017; Wismer, et al., 1995). Purees of thinned GD1 apples revealed bigger particles than GD2, being in accordance with literature (Milić, et al., 2017). GS apples were also thinned but showed a similar particle size distribution as GD2. This could be due to varietal effects, which do not respond in the same way to fruit thinning. It is also pointed out that GS and GD1 apples were not thinned with the same chemicals and the same dose as the trees of these varieties initially possessed different fruit loads.

Interestingly, GD1 purees, revealing the biggest particles, also showed the highest viscosity value after six months of post-harvest storage (**Fig. 61**A). For GD1 and GD2, apparent viscosity of the purees decreased until three months of post-harvest storage, which was in line with a decreasing particle size. Apparent viscosity then increased from three to six months of post-harvest storage, while particle size remained unchanged. In this case, the puree's texture was determined by pulp wet mass as it was the only structural factor that increased during post-harvest storage (**Fig. 61**D). The apparent viscosity of not refined GS samples decreased monotonously during post-harvest storage, which was in line with continuously decreasing particle sizes. Consequently, particle size was the most important factor determining puree's texture in this experiment. Pulp wet mass appeared to be the second most important factor as it affected texture only when particle size between two or more purees were the same.

The key factors determining puree's texture are particle size, insoluble cell wall content and serum viscosity and are all strongly linked to the cell wall (CW) composition and tissular structure. Hence, the composition of CW polysaccharides as well as pectins' macromolecular characteristics in raw fruits and purees were examined in the following sections.

1.1.3.3. Composition of cell wall polysaccharides

Table 12 summarizes the yields and compositions of the AIS of raw apples (FR), pulp (PL) and serum (SE). Puree results are not shown given that Le Bourvellec, et al. (2011) described only minor modifications in CW polysaccharides from raw apples into puree during processing. Post-harvest storage was identified as the factor inducing the most significant changes in CW polysaccharides compared to raw material or refining. Consequently, for legibility, **Table 12** only shows the evolution of cell wall polysaccharides and starch during post-harvest storage for not refined samples, averaged for GS, GD1 and GD2. The whole dataset can be found in **Table 13**.

AIS composition of raw apples (**Table 12**) is consistent with previous studies (Fischer & Amado, 1994; Le Bourvellec, et al., 2011; Massiot & Renard, 1997; Renard, 2005b), i.e. presence of cellulose, highly methylated pectins rich in xylogalacturonans and hemicelluloses fucogalactoxyloglucans and mannans. The AIS content of raw apples decreased over post-harvest storage. The same trend was observed by Fischer and Amado (1994) and the values were similar to those found in literature (15-27 mg/g FW) (Colin-Henrion, et al., 2009; Le Bourvellec, et al., 2011; Massiot & Renard, 1997; Renard, 2005b). The main sugars found in the AIS of raw apples were glucose and galacturonic acid, corresponding to cellulose and pectins, respectively. The glucose content (corrected for starch) was not altered by storage duration, whereas galacturonic acid slightly increased and arabinose and galactose decreased. Arabinose and galactose are part of the side chains of RG I and showed the highest values after glucose and galacturonic acid. A decrease of pectin side chains is a common feature in stored fruits, observed for apples and many other fruits such as tomatoes, pears and strawberries (Fischer & Amado, 1994; Gross & Sams, 1984; Gwanpua, et al., 2014). Rhamnose did not evolve during post-harvest storage. Xylose showed a slight but significant increase that has already been observed by Fischer and Amado (1994) and that might be attributed to the decrease of the neutral sugars arabinose and galactose, resulting in a relatively higher amount of xylose. Together with fucose and some galactose and glucose, xylose forms fucogalactoxyloglucan, which is the main hemicellulose of apple CWs (Aspinall & Fanous, 1984; Renard, Voragen, Thibault, & Pilnik, 1991). Mannose, the main element of the hemicellulose mannan (Voragen, et al., 1986b), increased slightly during apple fruit storage. Pectins in the AIS of raw apples were highly methylated (> 50%), in accordance with previously

published values (65-80%) (Billy, et al., 2008; De Vries, et al., 1981; Le Bourvellec, et al., 2011). The DM remained unchanged during storage. Billy, et al. (2008), De Vries, et al. (1981) and Gwanpua, et al. (2014) also observe no change in the DM of raw apple CW during post-harvest storage.

The AIS content of the pulp (**Table 12**) was between three to four times higher than AIS of raw apples. This reflected the concentration of insoluble fibres, namely cellulose, hemicellulose and insoluble pectins, in the pulp. Major trends of CW composition found in FR were maintained during apple processing and could be detected in the pulps' polysaccharides. The main sugar was glucose, coming primarily from cellulose, followed by galacturonic acid. The starch content was lower than in raw fruit, decreasing to not detectable values at T6. The DM of pectins occurring in the pulp remained stable over post-harvest storage and was slightly higher than the DM of raw apple pectins. The sugars constituting the side chains of RG I, arabinose and galactose, decreased significantly during storage. Sugars associated with hemicelluloses (xylose, mannose and fucose) showed similar or slightly higher values, all increasing (by balance) during post-harvest storage. Interestingly, AIS of the pulp decreased significantly over post-harvest storage. However, the pulp wet mass (**Fig. 61**D) generally increased. This demonstrated improved water retention capacities of aged cells as calculated in **Table 12**, resulting in an alleged higher pulp wet mass. The water retention capacity of plant cells is thought to be affected by the porosity of the CW induced by structural changes of CW polysaccharides and their association (Bidhendi & Geitmann, 2016). Lopez-Sanchez, et al. (2020) showed that calcium cross-linking of HG pectins impedes interaction of pectin chains with cellulose and thus reduces densification of the CW. As a result, water retention increases. However, this effect can be excluded in this study: the CW charge, necessary to initiate calcium cross-linking, did not change over post-harvest storage as the DM of the pectins in the pulp remained constant. Another study reported an interaction between RG I side chains and the cellulose-xyloglucan network in the CW (Zykwinska, et al., 2005). The decreasing amounts of arabinose and galactose during storage (**Table 12**) might thus be responsible for CW loosening. Hence, CW porosity could increase and would be able to retain a higher amount of water.

212

Table 12. Yields AIS from fresh weight (mg/g fresh weight), water retention capacity of the pulp (g/g dry weight) and compositions (mg/g AIS) of the AIS of raw apples (FR), pulp (PL) and serum (SE).

Storage (months)	Type	Yields AIS	Water retention	Rha	Fuc	Ara	Xyl	Man	Gal	Glc	GalA	MeOH (DM%)	Starch
0	FR	29		13	12	138	52	22	127	344	259	34 (70)	220
	PL	103	10	13	11	130	63	24	135	339	249	36 (80)	72
	SE	3		23	9	96	28	0	122	222	426	73 (92)	554
1	FR	26		12	15	125	61	22	93	313	319	40 (70)	54
	PL	89	11	16	13	130	69	27	101	361	248	36 (81)	27
	SE	2		13	6	71	16	0	79	38	670	107 (86)	176
3	FR	25		13	19	106	68	23	74	325	329	44 (74)	5
	PL	87	12	16	14	106	79	28	84	379	258	35 (76)	4
	SE	1		12	7	55	19	0	55	32	709	111 (89)	12
6	FR	23		15	15	95	69	26	74	347	319	41 (73)	2
	PL	76	13	16	15	101	82	29	84	406	232	36 (86)	0
	SE	2		18	14	69	27	0	64	39	649	120 (100)	9
	FR	*4*		*3*	*5*	*14*	*6*	*4*	*18*	*31*	*34*	*7 (14)*	*39*
SD	*PL*	*11*	*1*	*2*	*1*	*13*	*5*	*2*	*20*	*24*	*22*	*3 (10)*	*25*
	SE	*1*		*3*	*4*	*18*	*10*	*0*	*26*	*135*	*100*	*19 (10)*	*71*

Storage (months)	Type	Yields AIS	Water retention	Rha	Fuc	Ara	Xyl	Man	Gal	Glc	GalA	MeOH (DM%)	Starch
	FR *H*	7		4	6	23	21	11	21	8	15	7 (0.8)	33
	FR *P*	0.07		0.25	0.10	*< 0.05*	*< 0.05*	*< 0.05*	*< 0.05*	0.05	*< 0.05*	0.08 (0.84)	*< 0.05*
Kruskal-Wallis	PL *H*	16	16	14	23	18	27	12	18	20	8	0.4 (5)	29
	PL *P*	*< 0.05*	*< 0.05*	*< 0.05*	*< 0.05*	*< 0.05*	*< 0.05*	*< 0.05*	*< 0.05*	*< 0.05*	0.05	0.94 (0.21)	*< 0.05*
	SE *H*	10		25	15	18	9	-	27	3	23	14 (9)	30
	SE *P*	*< 0.05*		*< 0.05*	*< 0.05*	*< 0.05*	*< 0.05*	-	*< 0.05*	0.34	*< 0.05*	*< 0.05 (<0.05)*	*< 0.05*

Rha: Rhamnose; Fuc: Fucose; Ara: Arabinose; Xyl: Xylose; Man: Mannose; Gal: Galactose; Glc: Glucose without starch; GalA: Galacturonic acid; MeOH: Methanol; DM%: Degree of methylation; SD: Standard deviation of the mean (degrees of freedom: 32). All values were corrected for the starch content. Yields of AIS in serum and pulp are expressed relative to the weight of serum and pulp, respectively, collected after centrifugation. Data are averaged from compositions of GS, GD1 and GD2 at a given storage time and puree results are those of not refined (NR) samples. For detailed dataset, see **Table 13**.

Table 13. Yields AIS from fresh weight (mg/g fresh weight) and compositions (mg/g AIS) of the AIS of raw apples (FR), pulp (PL) and serum (SE).

Raw material	Storage (months)	Refining	Type	Yields	Rha	Fuc	Ara	Xyl	Man	Gal	Glc	GalA	MeOH (DM%)	**Starch**
GD1	0	NR	FR	35 *2.1*	14 *0.7*	11 *0.8*	144 *13*	56 *5.4*	20 *1.8*	152 *16*	358 *32*	214 *19*	32 *8.7* (70 *6.1*)	299 *28*
GD1	0	NR	PL	105 *0.8*	13 *0.9*	11 *0.3*	139 *0.9*	63 *0.8*	23 *0.5*	137 *4.9*	327 *7.0*	251 *7.5*	37 *1.2* (81 *4.4*)	57 *2.6*
GD1	0	NR	SE	3.0 *0.6*	20 *2.9*	9 *1.3*	66 *12*	23 *5.1*	0 *0.0*	88 *13*	575 *61*	183 *31*	34 *5.1* (100 *20*)	633 *25*
GD1	1	NR	FR	30 *1.6*	15 *0.8*	12 *0.8*	124 *11*	65 *4.9*	22 *1.4*	106 *8.3*	320 *14*	300 *22*	36 *1.8* (67 *6.5*)	83 *13*
GD1	1	NR	PL	87 *5.1*	17 *0.3*	14 *1.3*	132 *4.7*	73 *1.8*	26 *0.9*	118 *1.5*	357 *13*	227 *8.1*	35 *1.0* (86 *1.7*)	56 *3.0*
GD1	1	NR	SE	2.4 *0.2*	14 *2.0*	8 *1.4*	64 *9.5*	19 *2.4*	0 *0.0*	76 *8.4*	40 *4.9*	632 *54*	102 *17* (89 *15*)	321 *13*
GD1	1	R	PL	74 *2.6*	14 *0.7*	15 *0.3*	125 *3.2*	83 *3.9*	26 *1.4*	123 *1.7*	354 *12*	232 *19*	30 *1.7* (72 *2.3*)	74 *8.6*
GD1	1	R	SE	2.2 *0.1*	15 *0.3*	9 *1.6*	69 *7.2*	21 *2.7*	0 *0.0*	81 *6.2*	64 *34*	633 *37*	108 *8.3* (94 *4.0*)	321 *11*
GD1	3	NR	FR	28 *0.8*	14 *3.3*	12 *2.0*	104 *9.4*	68 *2.9*	19 *5.3*	81 *15*	314 *15*	350 *53*	37 *5.4* (60 *16*)	9 *3.0*
GD1	3	NR	PL	86 *8.3*	14 *0.4*	14 *0.6*	116 *3.1*	77 *4.2*	25 *0.7*	106 *0.4*	350 *12*	266 *14*	32 *3.1* (66 *8.9*)	11 *2.0*
GD1	3	NR	SE	1.7 *0.2*	11 *1.8*	10 *0.9*	55 *7.5*	28 *2.3*	0 *0.0*	62 *8.5*	48 *3.6*	682 *28*	104 *6.1* (84 *8.2*)	28 *0.7*
GD1	3	R	PL	65 *4.9*	15 *1.1*	15 *0.2*	107 *3.4*	83 *4.1*	25 *1.2*	111 *2.1*	378 *8.1*	236 *3.7*	30 *0.4* (71 *1.4*)	15 *3.5*
GD1	3	R	SE	1.6 *0.1*	12 *0.5*	9 *1.2*	57 *1.4*	28 *1.9*	0 *0.0*	64 *2.6*	42 *3.2*	680 *13*	107 *8.0* (87 *8.0*)	32 *1.3*

Raw material	Storage (months)	Refining	Type	Yields	Rha	Fuc	Ara	Xyl	Man	Gal	Glc	GalA	MeOH (DM%)	**Starch**
GD1	6	NR	FR	27 *1.3*	17 *1.4*	13 *1.2*	107 *4.7*	67 *4.1*	25 *0.6*	99 *2.6*	329 *9.5*	302 *21*	40 *2.5* (73 *1.8*)	2 *0.4*
GD1	6	NR	PL	76 *4.2*	16 *0.1*	14 *1.2*	128 *5.2*	77 *5.5*	27 *0.5*	116 *2.3*	364 *12*	222 *10*	35 *2.4* (86 *5.1*)	0 *0.0*
GD1	6	NR	SE	2.8 *0.1*	16 *4.2*	17 *4.5*	65 *9.5*	40 *6.8*	0 *0.0*	77 *9.1*	63 *10.7*	616 *48*	106 *5.4* (95 *12*)	10 *3.5*
GD1	6	R	PL	64 *4.8*	16 *0.4*	14 *0.2*	109 *3.5*	78 *1.0*	28 *0.7*	118 *1.5*	390 *6.7*	214 *10*	31 *0.9* (80 *1.6*)	0 *0.0*
GD1	6	R	SE	2.8 *0.2*	14 *0.7*	16 *0.8*	60 *2.5*	36 *1.7*	0 *0.0*	70 *2.8*	54 *5.5*	658 *12*	93 *2.1* (78 *1.1*)	12 *3.9*
GD2	0	NR	FR	23 *1.8*	15 *1.1*	17 *1.0*	153 *14*	59 *1.2*	25 *3.3*	107 *2.5*	300 *32*	282 *10*	42 *10* (82 *19*)	136 *29*
GD2	0	NR	PL	121 *12*	14 *2.2*	12 *0.6*	125 *3.2*	66 *3.9*	24 *2.2*	109 *3.1*	344 *4.0*	271 *12*	36 *4.6* (73 *9.1*)	30 *3.0*
GD2	0	NR	SE	0.7 *0.1*	26 *2.5*	16 *0.4*	139 *2.9*	37 *2.6*	0 *0.0*	188 *4.3*	25 *16*	493 *13*	77 *14* (86 *18*)	452 *61*
GD2	1	NR	FR	22 *0.7*	12 *4.7*	19 *3.7*	120 *3.1*	66 *1.5*	20 *6.3*	91 *2.1*	325 *23*	304 *24*	43 *1.6* (78 *8.8*)	55 *9.5*
GD2	1	NR	PL	99 *3.7*	15 *1.3*	12 *1.2*	120 *5.6*	68 *5.3*	26 *0.7*	90 *6.9*	360 *28*	273 *41*	36 *0.9* (73 *14*)	13 *1.2*
GD2	1	NR	SE	0.9 *0.3*	14 *1.5*	7 *0.6*	69 *3.3*	19 *1.5*	0 *0.0*	82 *2.1*	37 *13*	665 *30*	107 *9.5* (89 *12*)	110 *14*
GD2	1	R	PL	66 *6.3*	14 *1.1*	14 *1.1*	116 *6.2*	84 *4.8*	29 *0.7*	102 *3.9*	367 *5.8*	239 *12*	34 *2.3* (78 *9.2*)	18 *1.8*
GD2	1	R	SE	0.8 *0.2*	14 *1.1*	8 *0.6*	69 *2.7*	19 *1.2*	0 *0.0*	90 *2.6*	35 *11*	650 *12*	115 *8.1* (97 *7.6*)	108 *3.2*
GD2	3	NR	FR	24 *0.7*	12 *6.1*	27 *5.0*	103 *8.6*	71 *5.1*	20 *8.9*	77 *4.2*	309 *4.8*	336 *37*	46 *5.6* (76 *19*)	4 *3.1*
GD2	3	NR	PL	86 *6.7*	19 *1.7*	15 *0.8*	92 *4.7*	81 *2.1*	28 *0.8*	81 *4.1*	393 *6.1*	256 *9.8*	35 *1.4* (74 *5.8*)	0 *0.0*
GD2	3	NR	SE	0.5 *0.1*	13 *0.3*	8 *0.7*	48 *2.5*	21 *2.0*	0 *0.0*	53 *3.0*	40 *4.0*	702 *20*	115 *9.1* (90 *9.8*)	4 *1.0*

Raw material	Storage (months)	Refining	Type	Yields	Rha	Fuc	Ara	Xyl	Man	Gal	Glc	GalA	MeOH (DM%)	Starch
GD2	3	R	PL	56 *3.3*	18 *1.6*	16 *1.4*	85 *0.8*	91 *1.7*	30 *1.7*	80 *0.7*	426 *5.3*	222 *8.2*	32 *0.6* (79 *3.7*)	0 *0.0*
GD2	3	R	SE	1.2 *0.1*	14 *1.1*	8 *0.6*	51 *1.3*	20 *0.6*	0 *0.0*	53 *1.8*	35 *1.4*	701 *20*	117 *14* (92 *13*)	4 *0.5*
GD2	6	NR	FR	20 *1.8*	16 *0.8*	16 *1.6*	82 *2.0*	70 *2.5*	26 *0.6*	65 *3.9*	356 *20*	333 *28*	36 *3.1* (61 *6.8*)	2 *0.0*
GD2	6	NR	PL	73 *7.5*	17 *1.7*	15 *0.9*	90 *4.6*	84 *5.4*	29 *1.0*	75 *4.7*	415 *19*	241 *31*	34 *1.6* (78 *6.9*)	0 *0.0*
GD2	6	NR	SE	1.9 *0.2*	17 *1.5*	92 *136*	58 *5.1*	28 *1.0*	0 *0.0*	53 *7.2*	37 *2.2*	610 *112*	109 *12* (99 *11*)	8 *1.0*
GD2	6	R	PL	56 *3.1*	17 *0.6*	17 *0.5*	81 *5.2*	91 *2.3*	30 *0.8*	76 *4.1*	442 *5.9*	212 *7.9*	35 *1.7* (90 *2.5*)	0 *0.0*
GD2	6	R	SE	1.8 *0.2*	22 *1.0*	17 *1.7*	80 *1.8*	34 *2.8*	0 *0.0*	76 *2.0*	53 *7.7*	615 *9.4*	104 *5.9* (93 *5.8*)	5 *1.7*
GS	0	NR	FR	30 *1.4*	10 *1.4*	10 *2.2*	116 *23*	42 *10*	20 *3.5*	123 *26*	373 *61*	280 *33*	27 *8.3* (58 *21*)	226 *4.5*
GS	0	NR	PL	83 *6.7*	11 *0.8*	11 *0.7*	127 *6.4*	59 *2.0*	27 *1.6*	160 *3.5*	345 *13*	224 *24*	35 *2.3* (87 *14*)	129 *23*
GS	0	NR	SE	5.1 *0.4*	19 *3.7*	3 *1.5*	75 *16*	22 *2.5*	0 *0.0*	79 *16*	66 *40*	538 *118*	95 *11* (100 *6.5*)	576 *17*
GS	1	NR	FR	26 *1.3*	9 *3.3*	13 *1.6*	130 *6.3*	54 *2.1*	24 *0.6*	83 *1.9*	294 *4.4*	353 *8.1*	41 *1.0* (65 *2.6*)	23 *4.5*
GS	1	NR	PL	82 *2.2*	14 *0.5*	12 *0.3*	137 *5.5*	66 *2.2*	30 *0.4*	95 *1.8*	366 *16*	244 *15*	37 *2.8* (83 *5.5*)	13 *1.9*
GS	1	NR	SE	1.4 *0.2*	10 *1.1*	3 *0.2*	77 *5.6*	8 *1.3*	0 *0.0*	77 *4.3*	38 *17*	681 *21*	107 *6.6* (94 *7.3*)	96 *17*
GS	1	R	PL	73 *1.9*	12 *1.1*	13 *0.7*	136 *7.2*	71 *3.4*	30 *0.8*	97 *1.7*	363 *12.5*	239 *16*	39 *1.4* (91 *6.7*)	45 *1.2*
GS	1	R	SE	0.9 *0.0*	10 *1.0*	4 *0.9*	77 *0.2*	10 *0.5*	0 *0.0*	78 *2.7*	36 *6.3*	681 *4.3*	102 *6.8* (90 *3.7*)	56 *7.5*

Raw material	Storage (months)	Refining	Type	Yields	Rha	Fuc	Ara	Xyl	Man	Gal	Glc	GalA	MeOH (DM%)	Starch
GS	3	NR	FR	24 *0.3*	14 *2.2*	16 *1.9*	110 *6.1*	66 *1.0*	28 *1.7*	65 *1.5*	352 *7.3*	300 *16*	49 *3.1* (84 *1.9*)	3 *0.3*
GS	3	NR	PL	89 *12*	16 *0.7*	14 *0.8*	110 *6.7*	78 *6.1*	32 *2.3*	66 *1.3*	395 *15*	251 *11*	40 *3.1* (87 *2.8*)	0 *0.0*
GS	3	NR	SE	0.9 *0.2*	11 *0.8*	3 0.3	63 *2.3*	7 *0.3*	0 *0.0*	49 *1.8*	10 *2.5*	743 *15*	114 *10* (92 *4.9*)	8 *2.7*
GS	3	R	PL	61 *3.8*	15 *0.9*	15 *0.6*	105 *3.0*	81 *1.6*	31 *0.6*	66 *1.8*	419 *2.1*	232 *9.9*	37 *1.7* (87 *7.5*)	0 *0.0*
GS	3	R	SE	1.0 *0.2*	11 *0.7*	3 0.2	60 *3.6*	7 *0.5*	0 *0.0*	48 *2.7*	10 *0.6*	750 *14*	112 *9.4* (89 *3.3*)	8 *2.3*
GS	6	NR	FR	23 *0.1*	11 *3.3*	16 *1.6*	95 *8.7*	69 *3.8*	28 *1.7*	57 *4.0*	356 *18*	321 *27*	47 *4.3* (83 *10*)	1 *0.1*
GS	6	NR	PL	80 *2.9*	15 *0.5*	15 *0.4*	84 *2.8*	84 *5.4*	30 *1.3*	61 *1.3*	437 *2.9*	234 *9.2*	40 *0.4* (95 *2.8*)	0 *0.0*
GS	6	NR	SE	1.5 *0.4*	20 *0.5*	12 *3.2*	77 *2.8*	11 *0.2*	0 *0.0*	59 *1.8*	15 *1.7*	672 *14*	135 *8.5* (100 *9.0*)	4 *1.1*
GS	6	R	PL	58 *6.9*	15 *0.5*	15 *0.3*	81 *3.0*	82 *1.1*	31 *0.5*	61 *2.2*	459 *4.6*	220 *9.5*	36 *1.2* (90 *1.0*)	0 *0.0*
GS	6	R	SE	1.5 *0.3*	17 *2.1*	9 0.7	65 *6.4*	9 *0.8*	0 *0.0*	50 *5.1*	14 *0.8*	710 *26*	124 *12* (91 *12*)	4 *0.0*

GD1: Golden Delicious, reduced fruit load; GD2: Golden Delicious, high fruit load; GS: Granny Smith; NR: Not refined purees; R: Refined purees (0.5 mm); Rha: Rhamnose; Fuc: Fucose; Ara: Arabinose; Xyl: Xylose; Man: Mannose; Gal: Galactose; Glc: Glucose; GalA: Galacturonic acid; MeOH: Methanol; DM%: Degree of methylation; Values in italic correspond to the standard deviation of the mean n = 3.

Serum samples contained low concentrations of soluble polysaccharides, in accordance with the values (1-5 mg/g FW) found by Le Bourvellec, et al. (2011). At T0, the serum AIS contained high values of glucose and relatively low galacturonic acid. The abnormal values at T0 could be explained by presence of gelatinized starch in the serum at T0, accounting for more than half of the AIS. From T1, glucose content was more than five times less and galacturonic acid became the main sugar. This confirmed that pectins were the main constituent in serum, as expected (Le Bourvellec, et al., 2011). Soluble pectins were highly methylated and contained arabinose and galactose, probably from RG I side chains, which decreased significantly until T3. Interestingly, values for arabinose and galactose increased again between three and six months of post-harvest storage. Xylose and fucose, both neutral sugars deriving from hemicelluloses, showed lower values compared to FR or pulp AIS and no obvious trend during storage could be observed. No mannose was detected in the serum AIS. Colin-Henrion, et al. (2009) and Le Bourvellec, et al. (2011) found similar trends regarding the amount and composition of the AIS in the pulp and the serum.

The CW composition showed a clear decrease of RG I side chains during post-harvest storage. This might be related to decreasing particle sizes in the puree (cf. **Fig. 62**) as a reduction of cell adhesion in apples through RG I debranching has already been described in literature (Pena & Carpita, 2004). Another study correlated apple fruit softening to a decreasing number of HG-calcium complexes in the middle lamella (Ng, et al., 2013). The DM of firmer apples should then be less important to initiate cross-linking with calcium ions. Nevertheless, the latter study showed an increase of firmness without demethylation, leading to the conclusion that calcium cross-linking does not always induce firmer fruits. As the calcium content in the fruit is determined at harvest and will not alter significantly during post-harvest storage (slight changes may only occur due to altered dry matter) and as the pectins analysed in this study were highly methylated (**Table 12**), and thus unlikely to form calcium bridges, these complexes were not considered in this study.

1.1.3.4. Relationship between pectin composition and the purees' texture

In order to visualize the relation between the puree's viscosity, its determining factors (CW content, particle size, serum viscosity) and pectin composition of the puree, a principal component analysis (PCA) was performed (**Fig. 63**). The first two principal components (PC1 and PC2) explained together nearly 65% of the total variance. A group of correlated variables (**Fig. 63**A) was that comprising puree's viscosity (napp), starch content in the puree (Starch, deduced from starch analysis of raw apples), particle size (Particle_Size) and the pectic sugars arabinose (Ara) and galactose (Gal). All these parameters decreased during post-harvest storage and allowed differentiation of the purees by post-harvest storage duration (**Fig. 63**B). Although the studied apple cultivars and agricultural practices showed differences for both textural characteristics and pectin composition (**Table 13**), their CW structure failed to explain puree´s texture. It was thus decided to not further consider these parameters and to group the samples by post-harvest storage. "Starch" was most modified between T0 and T1, which could be linked with individuation of the T0 samples on the sample map. Mannose (Man) contributed highly to PC1, which was probably linked to the higher mannose content in GS apples (**Table 13**), as all GS samples were shifted to the negative side of PC1 relative to GD. Serum viscosity (nserum) was highly accounted for on PC2 (**Fig. 63**A). A second group of correlated variables was that of xylose (Xyl), fucose (Fuc) (both key components of fucogalactoxyloglucans), rhamnose (Rha) and to a lesser extent yield stress (Yield_Stress). Puree's AIS (AIS), methanol (MeOH), galacturonic acid content (GalA) and pulp wet mass (Yield_Pulp) were all poorly represented on plane 1x2. Interestingly, purees at T0 showed a high dispersion, whereas the other purees were less dispersed. According to these results, puree's viscosity was mainly affected by starch content and particle size, both parameters that decreased during post-harvest storage of apples.
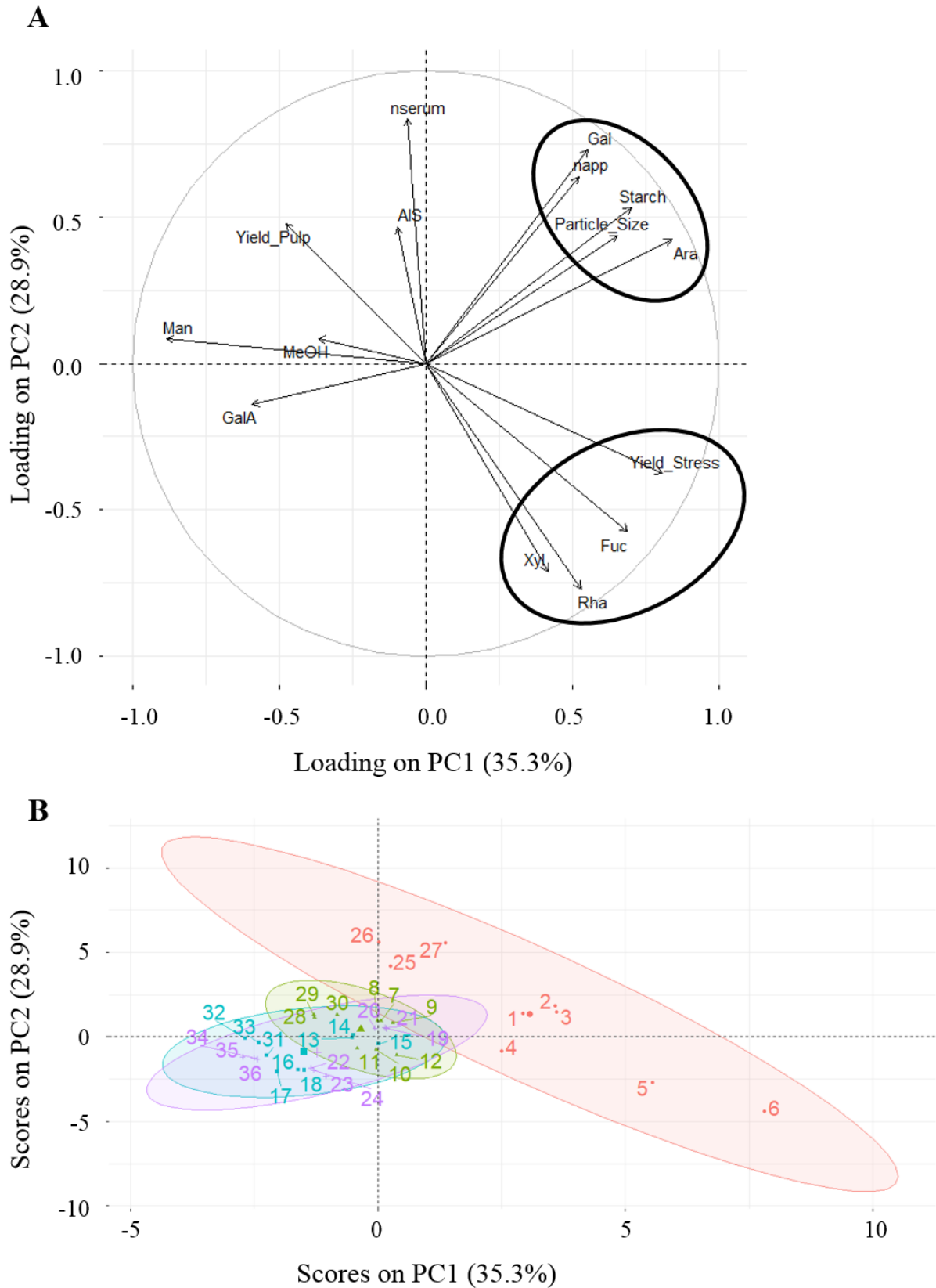
Fig. 63. Principal component analysis (PCA) of neutral sugars, rheological and structural characteristics of apple purees over post-harvest storage.

Correlation circle of variables loadings on PC1 (33.8%) and PC2 (27.4%)

Fig. 63 (Continuation). (A). Sample map of scores on PC1 (33.8%) and PC2 (27.4%) as function of post-harvest storage (B). The red ellipse represents samples at T0, the green ellipse samples at T1, the blue ellipse samples at T3 and the violet ellipse samples at T6. All correlation ellipses correspond to the 95% confidence interval around the barycentre. Only not refined (NR) samples were considered and the values of AIS and neutral sugars were corrected for the starch content (deduced from starch analysis of raw apples). napp: Apparent viscosity of the puree at 50 s^{-1}; Yield_Stress: Yield stress of the puree; nserum: Serum viscosity at 100 s^{-1}; Yield_Pulp: Pulp wet mass; Particle_Size: Particle size in the puree (d 0.9); AIS: Alcohol Insoluble Solids; Rha: Rhamnose; Fuc: Fucose; Ara: Arabinose; Xyl: Xylose; Man: Mannose; Gal: Galactose; GalA: Galacturonic acid; MeOH: Methanol; Starch: Starch in the puree (deduced from starch analysis of raw apples). 1-3: T0_GD1; 4-6: T0_GD2; 7-9: T1_GD1; 10-12: T1_GD2; 13-15: T3_GD1; 16-18: T3_GD2; 19-21: T6_GD1; 22-24: T6_GD2; 25-27: T0_GS; 28-30: T1_GS; 31-33: T3_GS; 34-36: T6_GS (GD1: Golden Delicious, reduced fruit load; GD2: Golden Delicious, high fruit load; GS: Granny Smith; T0: Directly after harvest; T1: After 1 month of post-harvest storage; T3: After 3 months of post-harvest storage; T6: After 6 months of post-harvest storage).

In model systems, the apple puree´s texture was shown to be determined by the volume occupied by the particles, that is to say their quantity and size (Espinosa-Munoz, et al., 2013; Leverrier, et al., 2016). In these reconstituted systems, the amount of insoluble cell walls (AIS) and the size of the particles could be varied independently, so that the insoluble solids content has a first-order effect on the rheological behaviour of apple purees. In real systems, however, particle size seemed to be the most important factor determining the puree´s texture, given the fact that the amount of AIS did not change sufficiently to have an impact on texture.

1.1.3.5. Macromolecular characteristics of soluble pectins

The decrease of particle size over post-harvest storage could be further explained by analysis of the macromolecular characteristics of soluble pectins. As they followed common trends over post-harvest storage and processing, they were averaged from the samples of GD1, GD2 and GS (**Table 14**). Although the structural features of soluble pectins varied according to different cultivars and agricultural practices (**Table 15**), no clear trend could be detected.

Table 14. Evolution of macromolecular features of soluble pectins in raw apples (FR) and corresponding sera (SE) during post-harvest storage measured by HPSEC-MALLS coupled to online viscometry.

Storage (months)	Type	$\overline{M}_w$ x 10^3 (g/mol)	$\overline{R}_{hz}(v)$ (nm)	$\overline{[\eta]}_z$ (mL/g)	$\rho = \overline{R}_{gz}/\overline{R}_{hz}(v)$
0	FR	1374	66	1162	0.9
	SE	924	68	1619	1.0
1	FR	430	50	1496	1.3
	SE	361	51	1721	1.5
6	FR	181	40	1396	1.6
	SE	410	52	1502	1.4
SD	*FR*	*215*	*5*	*210*	0.1
	SE	*157*	*8*	*212*	0.2
Kruskal-Wallis	FR *H*	23	16	11	21
	FR *P*	*<0.05*	*<0.05*	*<0.05*	*<0.05*
	SE *H*	17	8	4	14
	SE *P*	*<0.05*	*<0.05*	*0.17*	*<0.05*

FR: Raw fruit; SE: Serum; $\overline{M}_w$: weight-average molar mass; $\overline{R}_{hz}(v)$: z-average viscometric hydrodynamic radius; $\overline{[\eta]}_z$: z-average intrinsic viscosity; $\overline{R}_{gz}$: z-average radius of gyration; SD: Standard deviation of the mean (degrees of freedom: 22). Data are averaged from compositions of GS, GD1 and GD2 at a given storage time and serum results are those of not refined samples. For detailed dataset, see **Table 15**.

Table 15. Evolution of structural features of soluble pectins in raw apples (FR) and corresponding sera (SE) during post-harvest storage for different apple cultivars, measured by HPSEC-MALLS coupled to online viscometry.

Raw material	Storage (months)	Type	$\overline{M}_w \times 10^3$ (g/mol)	$\overline{R}_{hz}(v)$ (nm)	$\overline{[\eta]}_z$ (mL/g)	$\rho = \overline{R}_{gz}/\overline{R}_{hz}(v)$
GD1	0	FR	912	58	1123	1.0
GD1	0	SE	1060	68	967	0.8
GD1	1	FR	334	44	1253	1.3
GD1	1	SE	297	42	1210	1.6
GD1	6	FR	172	37	1167	1.6
GD1	6	SE	301	43	1209	1.5
GD2	0	FR	1725	69	1030	0.8
GD2	0	SE	1000	73	1792	0.9
GD2	1	FR	368	44	1097	1.4
GD2	1	SE	278	45	1363	1.4
GD2	6	FR	154	34	978	1.8
GD2	6	SE	291	43	1167	1.5
GS	0	FR	1485	71	1333	0.9
GS	0	SE	713	63	2097	1.3
GS	1	FR	589	63	2139	1.3
GS	1	SE	508	66	2589	1.6
GS	6	FR	219	50	2041	1.5
GS	6	SE	638	70	2129	1.2
	SD	*FR*	*215*	*5*	*210*	*0.1*
		SE	*157*	*8*	*212*	*0.2*

GD1: Golden Delicious, reduced fruit load; GD2: Golden Delicious, high fruit load; GS: Granny Smith; $\overline{M}_w$: weight-average molar mass; $\overline{R}_{hz}(v)$: z-average viscometric hydrodynamic radius; $\overline{[\eta]}_z$: z-average intrinsic viscosity; $\overline{R}_{gz}$: z-average radius of gyration; SD: Standard deviation of the mean (degrees of freedom: 22). Results are those of not refined (NR) samples.

GD2 was chosen as a representative example to illustrate the molar mass distribution of soluble pectins in raw apples (**Fig. 64**A) and sera (**Fig. 64**B). Both showed a shift of the main peak to higher elution volumes, i.e. polysaccharides of smaller macromolecular sizes, during storage. This shift was the most drastic during the first month of post-harvest storage. A second, narrower peak was detected at high elution volumes. Interestingly, its concentration diminished from T0 to T6. However, starch could be excluded to contribute to this peak as the determined molar mass was too small compared to values reported in literature (1.0×10^8–4.8×10^8 g/mol) (Rolland-Sabate, Guilois, Jaillais, & Colonna, 2011). Hence, this peak was assigned to some oligosaccharides remaining in the AIS. Molar mass of soluble pectins (**Table 14**) in raw apples decreased significantly during post-harvest storage. The viscometric hydrodynamic radius also decreased for raw apple pectins, further confirming a decrease in pectin size during apple storage. Gwanpua, et al. (2014) also showed a decrease in molar mass of water soluble pectins during post-harvest storage of apples and ascribed this change to either pectin depolymerisation, an extensive loss of RG I side chains or both. Molar mass of serum pectins only decreased during the first month of post-harvest storage, before a slight increase was observed at T6. The same trend was observed for the hydrodynamic radius. Apparently, high molar mass pectins could be extracted during puree processing at T6.

During the first month of post-harvest storage, $\overline{[\eta]}_z$ of both raw apple and serum pectins increased even if molar mass decreased (**Table 14**). This was due to structural changes in soluble pectins, showing more extended and less dense conformations during storage. However, $\overline{[\eta]}_z$ decreased for raw apples and sera at T6 while molar mass values kept decreasing (raw fruit pectins) or remained similar (serum pectins). This indicated presence of pectins with less extended and denser conformations. The shape and structure of polysaccharides can also be assessed by calculating the ρ-parameter ($\rho = \overline{R}_{gz}/\overline{R}_{hz}$) which has theoretical values of ~1.0 for soft spheres, values higher than 1.5 for linear polymers and increasing values with the linearity and the stiffness of the system (Burchard, 1983). This ratio increased for soluble pectins of raw apples over post-harvest storage, indicating a process of shape extension of soluble raw apple pectins that corresponds well to the linearization of the pectins. In contrast, the ρ-parameter increased for serum pectins until T1, then decreased slightly. Thus, serum pectins seemed to be the most linear at T1.
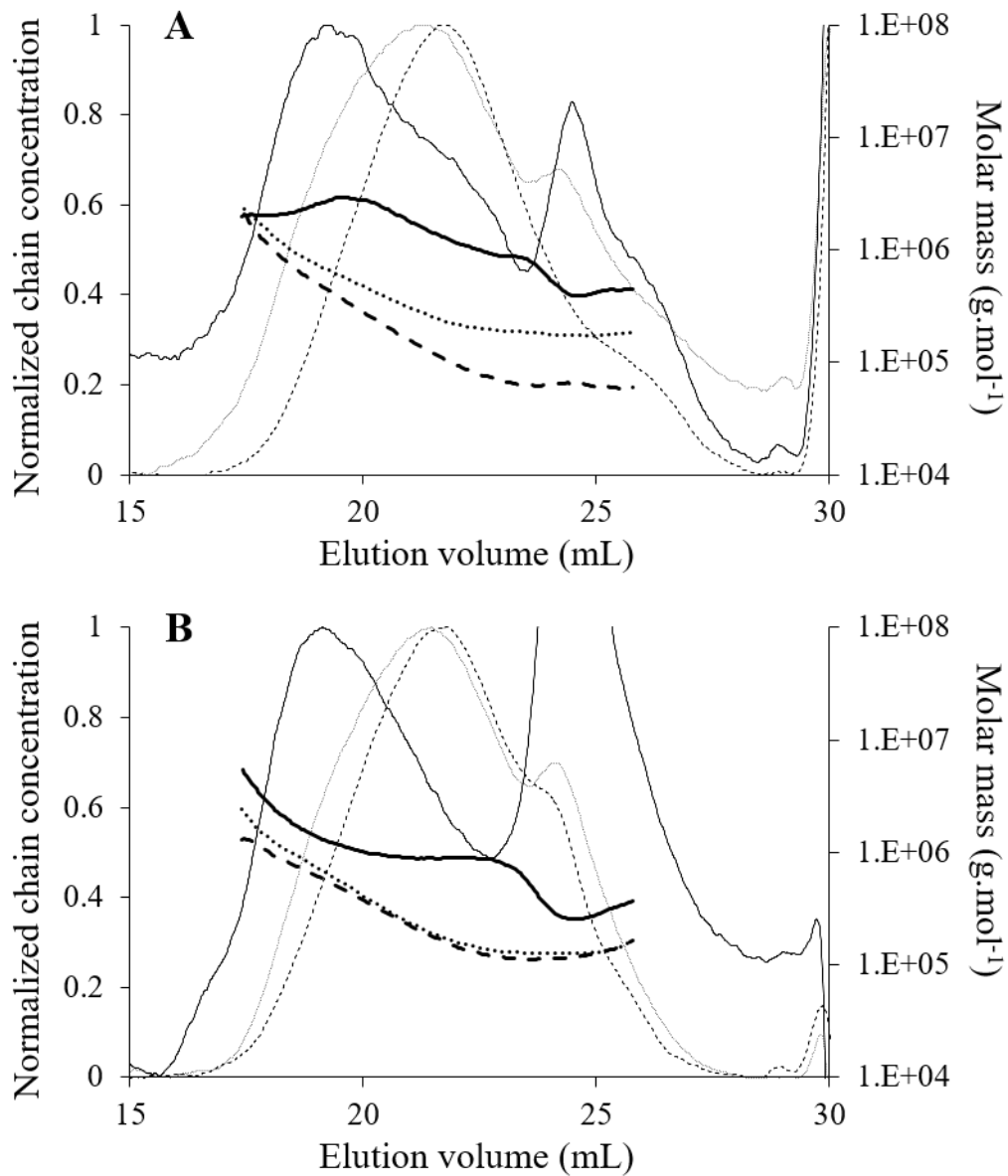
Fig. 64. Representative chromatograms for the cultivar GD2 in the function of storage. Normalized chain concentration and molar mass versus elution volume of soluble pectins in raw apples (A) and sera (B).

Continuous lines represent samples at T0, dotted lines samples at T1 and dashed lines samples at T6. The signal (mV) obtained by the RID detector was normalised through dividing all data points by the peak signal.

In summary, macromolecular sizes and molar masses of raw apple pectins decreased during prolonged post-harvest storage. In addition, they became more linear, probably due to RG I side chain hydrolysis. The decrease of neutral sugars arabinose and galactose during storage, as detected in section **V 1.1.3.3.**, supported this hypothesis. Serum pectins revealed the same trend during the first month of post-harvest storage. At T6, in contrast, high molar mass pectins could be extracted during puree processing. They also showed less linear characteristics, in line with increased arabinose and galactose contents of serum pectins at T6 (cf. **V 1.1.3.3.**).

RG I side chains were found to interact with the cellulose-xyloglucan network in the CW (Zykwinska, et al., 2005). We thus think that RG I side chain hydrolysis as well as a decrease in macromolecular size and molar mass of raw apple pectins during storage reduced pectin entanglement in the CW structure. This might enhance extractability of high molar mass pectins from RG I regions during processing.

Interestingly, soluble pectins in raw apples and sera showed the same macromolecular size but different molar masses both at T0 (**Fig. 65**A) and T6 (**Fig. 65**B). At T0 and T1, soluble pectins in raw fruits showed higher molar masses than serum pectins (**Table 14**). Processing at T0 and T1 did thus not lead to degradation of the pectic main chain (same macromolecular size) but to loss of RG I side chains (decreased molar mass). In addition, serum pectins exhibited similar $\overline{R}_{hz}(v)$ but higher $\overline{[\eta]}_z$ and ρ values at T0 and T1, further confirming existence of more linear and thus less branched pectins in the serum. However, at T6, serum pectins showed higher molar masses, higher $\overline{R}_{hz}(v)$ and $\overline{[\eta]}_z$ but lower ρ values at same macromolecular sizes compared to raw fruit pectins. It thus seemed that, after prolonged post-harvest storage, less linear and more branched pectins could be solubilised in the serum, probably because they were less attached to the CW. However, no simple links were found between serum viscosity and the molar mass of soluble pectins.
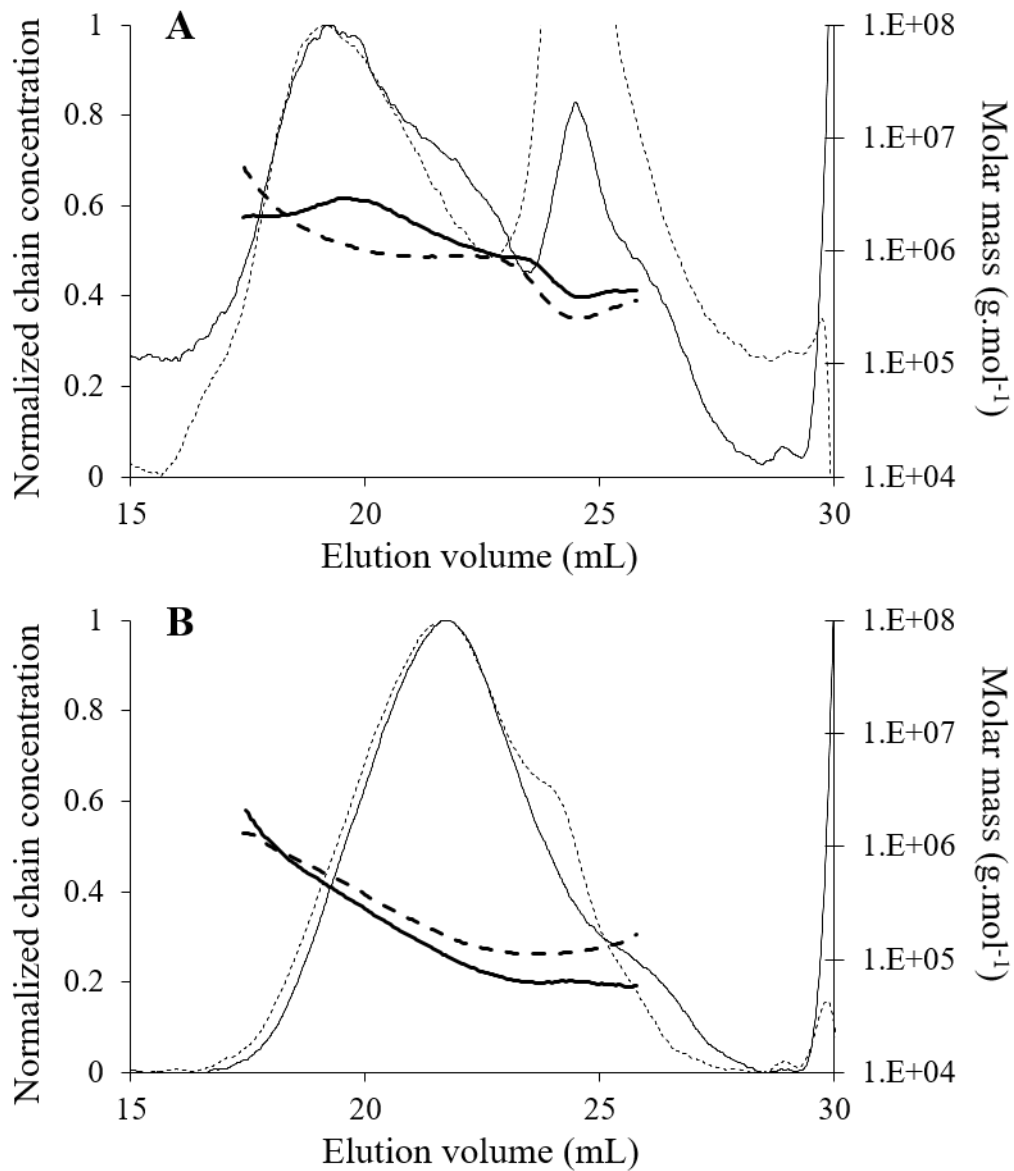
Fig. 65. Representative chromatograms for the cultivar GD2 in the function of the type (raw apple versus serum pectins). Normalized chain concentration and molar mass versus elution volume of soluble pectins at T0 (A) and T6 (B).

Continuous lines represent raw apple and dashed lines serum pectins. The signal (mV) obtained by the RID detector was normalised through dividing all data points by the peak signal.

1.1.4. Conclusions

Post-harvest storage duration influenced puree's viscosity the most, whereas the CW composition of apple cultivars and agricultural practices failed to explain the puree´s texture. However, they all showed similar trends during storage. Particle size decreased during prolonged post-harvest storage and seemed to be the most important factor determining puree's texture as smaller particles generated less viscous purees. When two purees showed similar particle sizes, pulp wet mass determined texture. In raw apples, prolonged storage led to pectin RG I side chain hydrolysis as well as to a reduction of soluble pectins' macromolecular size and molar mass. This promoted softening of apple tissue due to reduced cell adhesion, leading to facilitated fragmentation during processing. In addition, water retention capacities of the cells increased when aged, probably due to elevated porosity as the pectins were less entangled in the CW structure. During puree processing, prolonged post-harvest storage facilitated extractability of high molar mass pectins that were less linear and more branched. However, the pectic main chain was not degraded during processing.

Acknowledgements

Highlights

- Post-harvest storage was the main factor affecting puree's texture and pectins.

- Pectic side chain hydrolysis was correlated with tissue fragmentation over storage.

- Water retention capacities of apple cell wall polysaccharides increased when aged.

- Post-harvest storage enhanced extractability of high molar mass pectins.

- Pectic main chain was not degraded during puree processing.

1.2. Cultivar and mealiness

In this study, four different cultivars (2018 harvest) with contrasted fruit firmness were selected. Fruit firmness was additionally altered by development of mealiness in one cultivar. The effect of fruit thinning was evaluated once more since the first study did not allow conclusions on how this parameter might alter puree's texture. In addition to texture evaluation of purees, fruit firmness was also considered in this study in order to investigate if fruit firmness can be linked to puree's texture.

Two contrasted processes were chosen in order to check if the structural characteristics of raw apples can be linked to puree's structure no matter the process. Process conditions, which led to contrasted puree's texture were established in chapter **V 2.1.1.5**.

Pectin composition and structure of raw apples was analysed and linked to fruit texture and structural characteristics.

This study allowed to answer the following questions:

❖ How is puree's texture affected by varietal effects?

❖ What is the impact of mealiness on puree's texture?

❖ Does fruit thinning modify the puree's texture?

❖ Can the texture of the puree be related to the texture of raw apples?

❖ Can pectin modification explain the observed differences?

The results are presented in form of a research article, which was submitted to *LWT – Food Science and Technology*.

Apple puree's texture is independent from fruit firmness

Alexandra Buergy[a], Agnès Rolland-Sabaté[a], Alexandre Leca[a], Catherine M. G. C. Renard[b]

[a] *INRAE, Avignon Université, UMR SQPOV, 84000 Avignon, France*
[b] *INRAE, TRANSFORM, 44000 Nantes, France*

Abstract

How cellular and molecular structure of raw fruits impact puree's texture is still an unresolved question. Texture variations of purees obtained from four apple cultivars of contrasted texture (Braeburn, Gala, Golden Delicious, Granny Smith) and two modalities (mealiness, fruit load) after two contrasted processes were investigated. Although puree's viscosity strongly varied between cultivars (562 mPa.s–1368 mPa.s), it did not correlate with apple firmness, except for Granny Smith. This cultivar had the firmest fruits (3.2 N) and the most viscous purees (1368 mPa.s), in accordance with large particles (around 650 μm), high pulp wet mass and serum viscosity. Mealy Braeburn apples showed lower puree's viscosity (562 mPa.s) than their not-mealy homologues (779 mPa.s). This was due to reduced cell adhesion, maybe because of lower (arabinose+galactose)/rhamnose ratio, leading to smaller particles during processing. Process also impacted puree's viscosity (692 mPa.s–939 mPa.s), with more viscous purees obtained with the high temperature-low shear process.

Malus x domestica Borkh., Processing, Cell adhesion, Pectin, Mealiness

1.2.1. Introduction

Plant-based purees are concentrated suspensions of soft particles, composed of individual parenchyma cells and cell clusters (pulp) of the original fruit. These are dispersed in the aqueous content (serum) of the cells' vacuoles, which are emptied during processing (Rao, 1992). In plant-based purees, texture is an important quality characteristic (Szczesniak & Kahn, 1971). It is determined by particle size distribution, pulp content and serum viscosity (Espinosa, et al., 2011; Leverrier, et al., 2016; Rao, 1992) and depends on the original cell wall structure (Waldron, et al., 1997).

Pectins are known to be the polysaccharides in the plant cell wall, which are the most affected by enzymatic and chemical degradation during processing (Van Buren, 1979). In raw fruits, pectins contribute to the mechanical strength of the tissue, among others because they associate individual cells through the middle lamella (Carpita & Gibeaut, 1993; Jarvis, 1984). Pectin solubilisation during heat treatment leads to softening of the apple tissue, which can consequently be disrupted by mechanical treatment. The magnitude of cell disruption and pectin solubilisation thus defines the puree's texture.

However to this day, cell wall properties defining the firmness of raw apples were never correlated to the puree's texture. Bourles, et al. (2009) found no strict correlation between the firmness of raw apples and the texture of cooked apple slices. However, they did not analyse cell wall polysaccharides although pectins seem to play a key role in understanding texture deterioration during cooking (Ella Missang, Maingonnat, Renard, & Audergon, 2012).

Pectins' homogalacturonan (HG) consists of α-1,4-linked galacturonic acids that can be methyl-esterified at the C6 positions. Depending on the degree of methylation (DM) and the distribution of ester groups, HG molecules can form cross-links with calcium ions (Kohn & Luknár, 1977), contributing to intercellular adhesion in the middle lamella. Although degradation of pectic HGs are the most studied, other pectin domains may also affect fruit texture, especially rhamnogalacturonan I (RG I). RG I possesses a backbone with alternating rhamnose molecules in addition to galacturonic acid. Neutral sugar side chains, composed of galactose and/or arabinose are attached to the rhamnosyl residues (Ridley, et al., 2001), and are associated with firm texture in apple fruits (Nara, et al., 2001; Pena & Carpita, 2004). Recently, a loss of RG I side chains during post-harvest storage of raw apples was correlated to less viscous purees:

233

because of RG I loss, cell adhesion in the raw fruits decreased and fragmentation during processing was facilitated (Buergy, Rolland-Sabaté, Leca, & Renard, 2020).

In this study, the impact of fruit firmness on puree's texture was investigated using four apple cultivars and two modalities (mealiness, fruit load). The cultivars (Braeburn, Gala, Golden Delicious, Granny Smith) were selected as they were expected to show contrasted fruit firmness and might respond differently to heat treatment (Kim, et al., 1993; Rao, et al., 1986). Two different processes (high temperature-low shear process and low temperature-high shear process), chosen to generate contrasted puree's textures, were applied. Cell wall composition and firmness of raw fruits were compared to the puree's texture and macromolecular characteristics of soluble pectins.

1.2.2. Material and Methods

1.2.2.1. Plant material

Raw apples

Four apple (*Malus x domestica* Borkh.) cultivars, namely Braeburn (BR), Gala (GA), Golden Delicious (GD) and Granny Smith (GS) were grown in Mallemort, France and harvested in August and September 2018 corresponding to the commercial harvest dates. BR, GA, GS and half of the GD trees (GD1) were thinned chemically to reduce fruit load (**Table 4**). The other half of the GD trees were not thinned (GD2), resulting in more but smaller fruits.

Apples were stored for one month at 4 °C in normal atmosphere in order to reduce the starch content. Half of the BR apples (BRM) were stored for 11 days at 24 °C and a relative humidity between 90% and 100% (customised phytotron, Froid et Mesures, Beaucouzé, France) prior to processing in order to accelerate development of mealiness (Barreiro, et al., 1998).

The day before processing, apples were separated into two equivalent groups, one determined for puree processing, one for raw apple characterization. For analysis of raw fruits, three replicates of ten representative apples were chosen per cultivar. After determination of fruit texture at 23 °C, apples were cored and cut in 12 equal portions. The pieces were separated equally into three groups and cut vertically. Only four pieces per apple, systematically spread over sides and height, were retained in order

to obtain a batch of 40 apple pieces that were immediately frozen in liquid nitrogen and then stored at -20 °C to isolate the alcohol insoluble solids (AIS) (Renard, 2005b).

Puree preparation

For all cultivars, each process was conducted in triplicate. Apples (3 kg) were cored, sliced into 12 equal pieces and processed under vacuum into puree by a cooker-cutter (RoboQbo Qb8-3, RoboQbo, Bentivoglio, Italy). To inactivate apple pectin methylesterase and only consider chemical pectin degradation, temperatures higher than 59 °C (Denes, et al., 2000) were applied in both processes (**Supplementary Fig. S2 and S3**). Process I consisted in grinding at 3000 rpm during temperature increase (202 s) and the following 15 min at 70 °C. The purees were then pasteurized (95 °C, 2 min). Process II comprised grinding at 3000 rpm during temperature increase (360 s), followed by 400 rpm for 17 min at 95 °C. Half part of each puree was refined by an automatic sieve (Robot Coupe C80, Robot Coupe SNC, Vincennes, France) of 0.5 mm, removing skin and particles larger than the sieve opening. Once purees reached room temperature, rheology, particle size and pulp wet mass were analysed. Pulp and serum were separated by centrifugation of the puree (7690 x g, 15 min, 15 °C) and then frozen separately (-20 °C) until AIS extraction.

1.2.2.2. Physico-chemical characterization

Texture of raw apples

Texture of raw apples was determined by a puncture test via a multipurpose texture analyser (TAPlus, Lloyd Instruments, Farenham, UK), using a punch probe (diameter 2 mm), penetrating up to a depth of 17 mm into a peeled apple section. Firmness of apple flesh was calculated as the ratio of penetration energy to the height of testing, giving the puncture mean load. Crunchiness was estimated by calculating the linear distance between consecutive points from the force-distance curve in a range of 10 mm at the load plateau (Gregson & Lee, 2003).

Rheology of the purees and sera

Samples were analysed at 22.5 °C using a stress-controlled rheometer (Physica MCR301), equipped with a Peltier cell (CPTD-200) and a measuring cylinder (CC27/S), all from Anton Paar (Graz, Austria).

A vane measuring system (FL100/6W) with a 3.46 mm gap was used for purees. For flow curves, viscosity was followed over a logarithmically distributed range (shear rate values between 10 and 250 s^{-1}), recording one point every 15 s. Apparent viscosity at 50 s^{-1} was chosen to compare the puree's textures as it represents the approximate shear rate in mouth (Shama & Sherman, 1973).

Amplitude sweep tests were measured from 0.01 to 100% at a constant angular frequency (10 rad/s), recording five points per decade. The time required to measure each point was defined by the software. The values of G' and G'' were averaged in the linear viscoelastic range.

Considering the gap of the measuring system, rheological analysis was theoretically not adapted for purees containing particles larger than 1 mm. However, NR purees, the only samples containing particles (skin fragments) larger than 1 mm, showed high repeatability. The method was thus considered valid for internal comparison.

Serum viscosity was analysed by a flow curve (10 to 1000 s^{-1}, 8 min) using a double gap cylinder geometry set (DG27). The value at a shear rate of 100 s^{-1} was retained, as it was expected that oral perception of serum would require a higher shear rate than purees.

Particle size distribution

The particle size distribution was analysed by laser granulometry (Mastersizer 2000, Malvern Instruments, Malvern, UK) as described previously (Buergy, et al., 2020). Each sample was analysed twice and the Malvern's software averaged the size distribution over three repeated measurements on the same sample.

Pulp wet mass (PWM) and water retention capacity (WRC)

The PWM was calculated as the ratio of the pulp weight after centrifugation to the initial weight of the puree and expressed in % (Espinosa, et al., 2011). The amount of water retained by the mass of the pulp's cell wall polysaccharides (g/g dry weight) was defined as the WRC (Robertson, et al., 2000). It was estimated as the relation between the PWM and the pulp's dry weight. The fibres' mass in the wet mass is generally negligible and was thus not considered.

1.2.2.3. Analytical

Chemicals

Acetic anhydride, methanol-d_3 (99.5 atom % D) and o-methylimidazole (99%) were from Acros Organics (Geel, Belgium). Acetone (pure) was from Carlo Erba Reagents (Val-de-Reuil, France). Acetic acid (glacial), ammonia solution (35%), methanol (LC-MS grade), sodium sulphate (anhydrous) and sulphuric acid ($\geq$ 95%) were from Fisher Scientific (Loughborough, UK). Sodium hydroxide and phenol were from Merck KGaA (Darmstadt, Germany). Calcium chloride ($\geq$ 99%, dihydrate), galacturonic acid (> 97%), myo-inositol, m-hydroxydiphenyl ($\geq$ 85%), potassium hydroxide ($\geq$ 85%), sodium acetate ($\geq$ 99%), sodium borohydride ($\geq$ 98%), sodium hydrogen phosphate (98.5%), sodium tetraborate ($\geq$ 99.5%, decahydrate) and sugars (arabinose, fucose, galactose, glucose, mannose, rhamnose, xylose) were from Sigma-Aldrich (Steinheim, Germany). Dichloromethane and ethanol (96%) were from VWR Chemicals (Fontenay-sous-Bois, France). All reagents were used without further purification.

Cell wall isolation

Cell wall polysaccharides were isolated as alcohol insoluble solids (AIS).

The frozen apple pieces were freeze-dried and finely ground before AIS were extracted with ethanol (700 mL/L) as described by Le Bourvellec, et al. (2011). AIS were expressed in mg/g fresh weight (FW). Pulp was water-washed and AIS were prepared according to Buergy, et al. (2020). Once free sugars were absent (Dubois, et al., 1956), samples were dried by solvent exchange, followed by 48 h in a drying oven at 40 °C. The AIS of the pulp was determined as the relation between the dry pulp weight and the initial pulp weight after water-washing and expressed in mg/g FW.

Serum precipitation

AIS of the serum was alcohol-precipitated as described by Buergy, et al. (2020). The pectin content in the serum was roughly estimated by calculating the ratio between the weight of the sample after freeze-drying and the initial weight of serum (100 mL), expressed in mg/g FW.

Cell wall polysaccharide analysis

Neutral sugars and myo-inositol (internal standard) were analysed after acid hydrolysis (Saeman, et al., 1954). The free sugars were derivatised to volatile alditol acetates (Englyst, et al., 1982) and analysed using a Clarus 500 gas chromatograph (PerkinElmer, Waltham, USA), equipped with a flame ionization detector (FID) and a OPTIMA® capillary column (30 m × 0.25 mm i.d., 0.25 µm film thickness, Macherey-Nagel, Düren, Germany) at 230 °C, using helium as carrier gas.

The acid hydrolysates were tested spectrophotometrically for galacturonic acid (GalA) using the *m*-hydroxydiphenyl assay (Blumenkrantz & Asboe-Hansen, 1973).

Methanol content was determined by stable isotope dilution assay after saponification (Renard & Ginies, 2009). It was analysed on a Trace 1300 gas chromatograph (Thermo Scientific, Waltham, USA) with a TG-WaxMS capillary column (30 m × 0.25 mm i.d., 0.5 µm film thickness, Thermo Scientific, Waltham, USA), coupled to an ISQ LT single quadrupole mass spectrometer (Thermo Scientific, Waltham, USA).

The degree of methylation (DM) was calculated as molar ratio of methanol to GalA and expressed in %.

Starch determination

Starch was quantified in the AIS of raw apples using the total starch assay kit K-TSTA (Megazyme, Wicklow, Ireland). As residual polyphenols in the AIS might inactivate the enzymes, the enzyme concentrations were doubled compared to the manufacturer's instructions. Each sample was analysed twice. All values for AIS, neutral sugars, GalA and methanol were corrected by the respective starch content in each sample.

High performance size-exclusion chromatography coupled to multi-angle laser light scattering (HPSEC-MALLS)

Molar mass and size distribution of soluble pectins were determined by HPSEC-MALLS, coupled to a differential refractive index detector (Shimadzu, Tokyo, Japan). The equipment, detectors and sample preparation were the same as reported previously (Buergy, et al., 2020). Serum pectins (2.5 mg AIS/mL eluent, 100 μL) were eluted at 40 °C with an acetate buffer (0.2 mol/L, pH 3.6) at a flow rate of 0.6 mL/min and separated by three PolySep-GFC columns (P3000, P5000 and P6000, 300 × 7.8 mm) and a guard column, all from Phenomenex (Le Pecq, France). Data were treated by ASTRA® software (Wyatt Technology Corporation, version 7.3.2.19 for PC) as described before (Buergy, et al., 2020).

1.2.2.4. Statistical analysis

Fruit texture was determined on thirty apples. All other measurements were conducted once for each of the three replications, except starch determination and particle size distribution that were analysed twice for each of the three replications. At least two of three serum pectins were injected on the HPSEC-MALLS system. As the Shapiro-Wilk test indicated that not all results were normally distributed, they were compared with Kruskal-Wallis non-parametric test (Kruskal & Wallis, 1952) at the 95% level of significance. The XLSTAT package (Addinsoft, 2020) for Microsoft Excel was used. Pooled standard deviations were calculated for each series of replicated measurement using the sum of individual variances weighted by the individual degrees of freedom (Box, et al., 1978). Principal component analysis (PCA) was performed using the package "FactoMineR" (Lê, et al., 2008), linear regression using the package "ggplot2" (Wickham, 2016), both for R statistical software (R Core Team, 2018).

1.2.3. Results

1.2.3.1. Apple texture

Determination of apple firmness and crunchiness (**Table 16**) confirmed significant differences in apple texture, depending on the cultivar. GS showed the highest firmness and crunchiness values, whereas GD1 and GD2 showed the lowest values. Here, fruit thinning of GD apples did not lead to different fruit textures. BR was firm and crunchy, while BRM was firm but not crunchy, confirming acquisition of the mealy texture of BRM apples (Barreiro, et al., 1998). GA revealed intermediate firmness and crunchiness values.

1.2.3.2. Cell wall composition of raw apples

Apple fruit texture might be influenced by the cell wall structure and composition (**Table 16**). AIS of raw apples were in a usual range of 15-27 mg/g FW (Le Bourvellec, et al., 2011; Massiot & Renard, 1997; Renard, 2005b), with GS showing the highest values. Except BR, with noticeably high starch contents, all cultivars were nearly starch-free. Amounts of GalA in the AIS varied between cultivars. DM were also significantly different between cultivars but all pectins were highly methylated (> 50%). The pectic RG I branching was estimated as the ratio of neutral sugars (arabinose+galactose)/rhamnose. It was highest in GS and lowest in GA pectins. Pectins of BRM apples were slightly less branched than BR apples.

Table 16. Textural characteristics and cell wall composition of raw apples depending on the cultivar and modalities (mealiness, fruit load), followed by Kruskal-Wallis *H* and *P* values.

Cultivar	Firmness (N)	Crunchiness (dimensionless)	AIS (mg/g FW)	Starch	GalA	Rha	Fuc	Ara (mg/g AIS)	Xyl	Man	Gal	Glc	DM (%)	$\dfrac{Ara + Gal}{Rha}$
BR	2.5	14	22	52	377	10	11	102	57	24	90	282	67	19
BRM	2.7	11	21	5	383	10	10	80	67	25	73	308	59	15
GA	2.4	12	20	4	328	11	11	91	75	18	50	369	76	12
GD1	1.9	11	23	3	318	11	13	120	70	24	88	309	82	18
GD2	2.1	11	26	3	268	11	11	124	67	21	89	370	82	19
GS	3.2	14	27	3	363	8	9	137	52	25	95	266	67	28
PSD	*0.4*	*0.9*	*0.5*	*2*	*19*	*1*	*2*	*3*	*3*	*0.6*	*3*	*11*	*5*	*2*
H value	*102*	*109*	*16*	*10*	*15*	*11*	*10*	*17*	*15*	*15*	*14*	*15*	*14*	*15*
P value	***< 0.001***	***< 0.001***	***0.007***	*0.066*	***0.012***	*0.054*	*0.080*	***0.005***	***0.011***	***0.009***	***0.015***	***0.011***	***0.013***	***0.011***

BR: Braeburn; BRM: Braeburn, mealy; GA: Gala; GD1: Golden Delicious, reduced fruit load; GD2: Golden Delicious, high fruit load; GS: Granny Smith; AIS: Alcohol insoluble solids; GalA: Galacturonic acid; Rha: Rhamnose; Fuc: Fucose; Ara: Arabinose; Xyl: Xylose; Man: Mannose; Gal: Galactose; Glc: Glucose without starch; DM: Degree of methylation; FW: Fresh weight; PSD: Pooled standard deviation (degrees of freedom: 174 for firmness and crunchiness (n for each cultivar = 30), 30 for starch (n for each cultivar = 6) and 12 for other analyses (n for each cultivar = 3)). The ratio (Ara+Gal)/Rha estimated RG I branching. All values were corrected for the starch content.

1.2.3.3. Rheological characterization of apple purees

Although the refining step generated less viscous purees, refined (**Table 17**) and not refined (**Table 18**) purees showed the same trends between cultivars and the two processes. Therefore, only not refined purees are detailed in the results section.

The chosen cultivars and processes generated a wide range of textures (**Table 18**), with "cultivar" being the major parameter. The highest viscosities were obtained with GS and the lowest with GA and BRM. Purees prepared with BR apples were more viscous than purees of their mealy homologue. Purees of GD2 showed slightly higher viscosity values than GD1. Process II produced systematically slightly more viscous purees and higher G' and G''. All samples showed higher G' than G'' values, corresponding to a structured viscoelastic product with soft solid-like behaviour, in accordance with another study on apple purees (Espinosa, et al., 2011).

1.2.3.4. Analysis of texture determinants in purees

Particle size distribution

Particle size was demonstrated to be the most important factor influencing puree's texture in "real" systems (Buergy, et al., 2020), i.e. without dilution or concentration of the purees. Here, particle size showed a monomodal distribution for all cultivars and both process conditions (**Fig. 66**).

Generally, Process I generated smaller particles. An exception was BRM. While BR showed cell clusters around 400 µm (Process I) and 650 µm (Process II), apple flesh of BRM was ground to individual cells around 200 µm with both processes. Among all cultivars, GS showed the largest particles (500–800 µm). GD2 showed slightly larger particles than GD1.

Pulp wet mass and water retention capacity

In "real" systems, PWM (**Table 18**) is considered to have a second order impact on puree's texture (Buergy, et al., 2020). It differed significantly between cultivars but not between the two processes. However, purees prepared by Process II showed slightly higher PWM for all cultivars, except BRM. WRC (**Table 18**) was also not significantly influenced by the process. GS had notably high PWM and WRC.

Table 17. Rheological characteristics and texture determinants of refined apple purees depending on the cultivar, modalities (mealiness, fruit load) and the process (Process I: 70 °C, 3000 rpm; Process II: 95 °C, 400 rpm), followed by Kruskal-Wallis *H* and *P* values.

Cultivar	Process	η_{app} 50 s^{-1} (mPa.s)	G' (Pa)	G'' (Pa)	PWM (%)	WRC (g/g DW)	η_{serum} 100 s^{-1} (mPa.s)	Serum AIS (mg/g FW)
BR	I	578	988	193	23	19	7	0.2
	II	820	1055	210	25	19	17	1.1
BRM	I	455	958	196	26	14	5	0.1
	II	659	1288	279	28	18	9	0.6
GA	I	465	676	126	22	16	7	0.3
	II	620	810	161	24	18	10	0.1
GD1	I	580	922	172	26	16	11	2.3
	II	842	1200	242	30	16	14	2.3
GD2	I	729	1159	222	28	12	12	1.2
	II	921	1351	274	28	13	14	3.0
GS	I	1051	1132	228	31	20	46	1.7
	II	1015	944	280	46	17	180	4.6
PSD		*52*	*129*	*31*	*2*	*2*	*6*	*0.3*
Cultivar	*H value*	*23*	*18*	*19*	*29*	*21*	*24*	*26*
	P value	***<0.001***	***0.003***	***0.002***	***<0.001***	***0.001***	***<0.001***	***<0.001***
Process	*H value*	*9*	*3*	*8*	*3*	*0.5*	*7*	*3*
	P value	***0.003***	*0.071*	***0.005***	*0.114*	*0. 486*	***0.010***	*0.082*

BR: Braeburn; BRM: Braeburn, mealy; GA: Gala; GD1: Golden Delicious, reduced fruit load; GD2: Golden Delicious, high fruit load; GS: Granny Smith; η_{app}: Apparent viscosity at 50 s^{-1}; G', G'': Storage and loss modulus, respectively, at an angular frequency of 10 rad/s; PWM: Pulp wet mass; WRC: Water retention capacity of the pulp; η_{serum}: Serum viscosity at 100 s^{-1}; AIS: Alcohol insoluble solids; DW: Dry weight; FW: Fresh weight; PSD: Pooled standard deviation (degrees of freedom: 12 (n for each cultivar = 3)).

Table 18. Rheological characteristics and texture determinants of not refined apple purees depending on the cultivar, modalities (mealiness, fruit load) and the process (Process I: 70 °C, 3000 rpm; Process II: 95 °C, 400 rpm), followed by Kruskal-Wallis H and P values.

Cultivar	Process	η_{app} 50 s⁻¹ (mPa.s)	G' (Pa)	G'' (Pa)	PWM (%)	WRC (g/g DW)	η_{serum} 100 s⁻¹ (mPa.s)	Serum AIS (mg/g FW)
BR	I	630	1080	216	26	14	8	0.5
	II	1088	1509	323	28	12	17	0.7
BRM	I	456	965	200	29	13	5	0.3
	II	680	1373	310	28	16	9	0.8
GA	I	480	720	138	24	14	7	0.2
	II	681	934	194	27	14	10	0.1
GD1	I	632	984	191	28	15	11	0.5
	II	943	1391	291	32	12	14	2.6
GD2	I	776	1246	247	29	12	12	0.9
	II	1060	1601	342	30	11	14	1.0
GS	I	1467	1836	386	37	23	52	1.4
	II	1937	1794	543	44	17	155	3.9
PSD		*55*	*121*	*31*	*1*	*1*	*3*	*0.2*
Cultivar	*H value*	*23*	*24*	*24*	*28*	*22*	*24*	*24*
	P value	*< 0.001*	*< 0.001*	*< 0.001*	*< 0.001*	*< 0.001*	*< 0.001*	*< 0.001*
Process	*H value*	*10*	*7*	*8*	*2*	*2*	*6*	*4*
	P value	*0.002*	*0.010*	*0.004*	*0.137*	*0.206*	*0.012*	*0.049*

BR: Braeburn; BRM: Braeburn, mealy; GA: Gala; GD1: Golden Delicious, reduced fruit load; GD2: Golden Delicious, high fruit load; GS: Granny Smith; η_{app}: Apparent viscosity at 50 s⁻¹; G', G'': Storage and loss modulus, respectively, at an angular frequency of 10 rad/s; PWM: Pulp wet mass; WRC: Water retention capacity of the pulp; η_{serum}: Serum viscosity at 100 s⁻¹; AIS: Alcohol insoluble solids; DW: Dry weight; FW: Fresh weight; PSD: Pooled standard deviation (degrees of freedom: 12 (n for each cultivar = 3)).
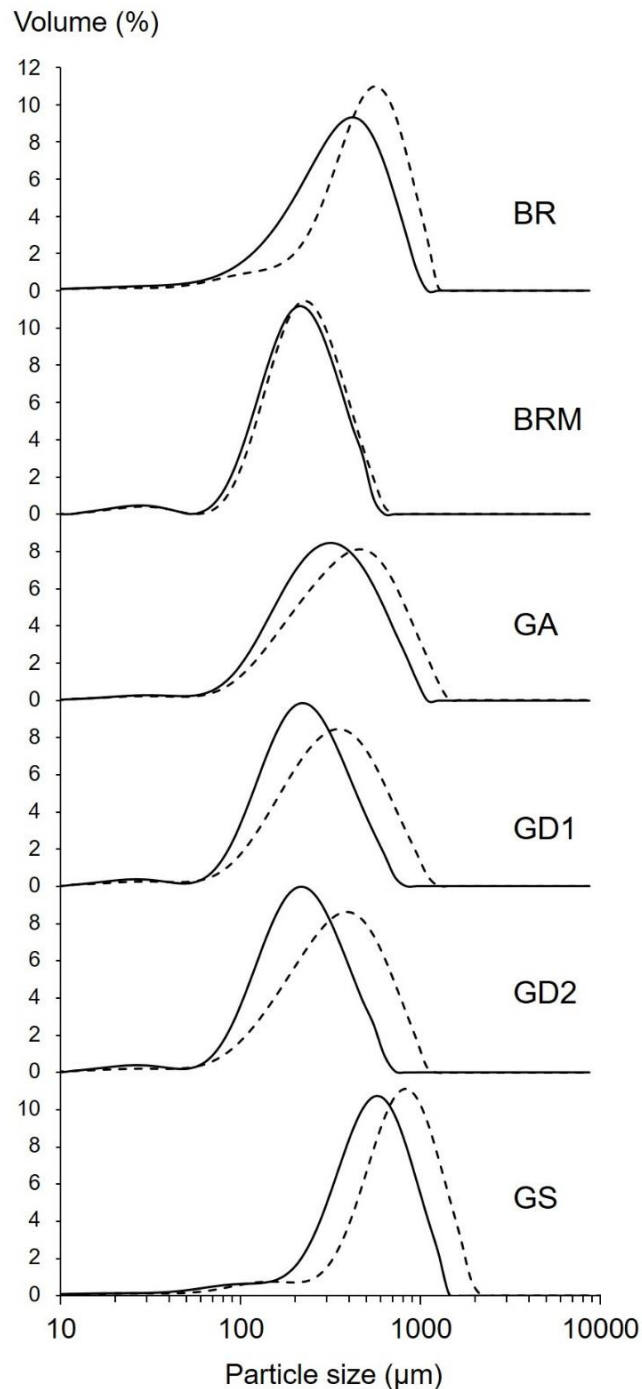
Fig. 66. Particle size distribution of purees issued from different apple cultivars and modalities.

Continuous lines represent purees obtained by Process I (70 °C, 3000 rpm) and dashed lines purees obtained by Process II (95 °C, 400 rpm). BR: Braeburn; BRM: Braeburn, mealy; GA: Gala; GD1: Golden Delicious, reduced fruit load; GD2: Golden Delicious, high fruit load; GS: Granny Smith. One representative sample was chosen out of six replications to illustrate particle size distribution.

Serum viscosity, soluble pectin content and molar mass

Process II increased serum viscosity and soluble pectin content in the sera of BR, BRM, GD1 and GS but not of GA and GD2 (**Table 18**). GS purees had remarkably high serum viscosities. Serum viscosity of BR was similar to BRM for Process I but higher for Process II.

Molar mass and molecular size were determined for soluble pectins of Process II. GS pectins exhibited the highest molecular size (lowest elution volume) and BRM a smaller size than BR, which eluted before (**Fig. 67**). All other cultivars had medium sizes between BR and BRM (not shown). GS had the highest molar mass at the main peak (459x10^3 g/mol), whereas molar masses of BR (277x10^3 g/mol) and BRM (230x10^3 g/mol) were not significantly different.
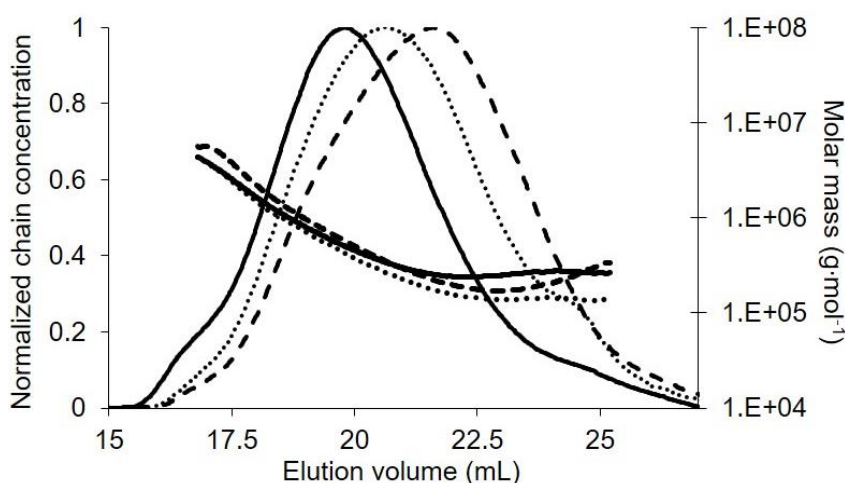
Fig. 67. Normalized chain concentration and molar mass versus elution volume of soluble pectins for GS (continuous lines), BR (dotted lines) and BRM (dashed lines) for Process II (95 °C, 400 rpm).

The signal (mV) obtained by the differential refractive index detector was normalised through dividing all data points by the signal at the summit of the peak.

1.2.4. Discussion

A PCA was conducted on raw apples' and purees' characteristics. The first two principal components (PC1 and PC2) explained together more than 70% of the total variance. Variables related to apple texture (firmness and crunchiness) were grouped in the correlation circle (**Fig. 68**A). Neither starch nor GalA contents could be

correlated to fruit texture, whereas the DM showed a slight negative correlation. Calcium cross-links can be formed between HG pectins in the middle lamella of parenchyma cells if pectin molecules exhibit more than 10 consecutive unmethyl-esterified GalA residues (Kohn & Luknár, 1977). They are associated with improved cell adhesion (Jarvis, et al., 2003) but cannot always be linked to firmer fruits (Ng, et al., 2013). In apple, decreased RG I branching correlates with a loss of fruit texture due to decreased cell adhesion (Pena & Carpita, 2004). RG I branching was the highest in pectins from GS (**Table 16**), which also had the highest apple firmness and crunchiness. Pectins of BRM apples were slightly less branched than BR apples due to a loss of arabinose and galactose side chains in BRM, also associated with mealiness in apples (Nara, et al., 2001). Nevertheless, no simple relation linking RG I branching to apple texture was found, so that no correlation was detected in the PCA. Cell shape and packing might better explain apple firmness (Lapsley, Escher, & Hoehn, 1992; McAtee, Hallett, Johnston, & Schaffer, 2009) but were not analysed here.

Both apple firmness and crunchiness were orthogonal to rheological properties of the puree (apparent viscosity, G' and G") in **Fig. 68**A and thus varied independently, as confirmed in **Fig. 68**D. Bourles, et al. (2009) reached the same conclusion for the texture of cooked apple slices. As an exception, GS had the firmest and crunchiest apples (**Table 16**) and showed the highest puree's texture (**Table 18**). Fruit thinning did not induce different fruit textures. GD2 purees were, however, slightly more viscous than GD1, linked to particle size, while Buergy, et al. (2020) described higher viscosity and bigger particles for GD1 purees. The harvest year or, most probably, the late fruit thinning in this study might explain this difference.

Rheological properties of the puree formed a group in the PCA's correlation circle (**Fig. 68**A) with several factors (particle size, PWM and serum viscosity) that are known to alter puree's texture (Espinosa, et al., 2011; Leverrier, et al., 2016; Rao, 1992). Interestingly, RG I branching and AIS of raw apples were also part of this group, whereas WRC of the pulp was not. Correlation of particle size, PWM and serum viscosity to apparent viscosity of the purees could be confirmed with **Fig. 68**E-G. However, several slopes were visible, indicating that cultivars responded differently to processing. Especially GS showed particularly high particle sizes, PWM and serum viscosities, resulting in highly viscous purees.

Cultivars could be clearly distinguished on the sample map (**Fig. 68**B) and thus strongly affected puree's viscosity. Process I and II could not be differentiated on the sample map (**Fig. 68**C), indicating limited impact of process. However, all purees prepared with Process II were slightly shifted to positive values on PC1. This was in accordance with higher viscosity, G' and G'', linked to increased particle size, PWM and serum viscosity.

Process II generally induced larger particles (**Fig. 66**) because of lower grinding speed, leading to more viscous purees. An exception was BRM. While BR purees showed cell clusters, apple flesh of BRM was ground to individual cells with both processes. Cell adhesion appeared reduced in mealy apples, as even a low grinding speed was sufficient to induce tissue fragmentation during processing. Reduced cell adhesion in BRM apples might be correlated to decreased RG I branching (**Table 16**) as had been hypothesized before (Nara, et al., 2001; Pena & Carpita, 2004). Due to smaller particles, BRM purees were less viscous than BR purees.

Among all cultivars, GS showed the largest particles (**Fig. 66**), in accordance with the highest puree's texture. Cell adhesion in GS apples seemed particularly high, maybe due to higher RG I branching (**Table 16**). Initially larger cells in GS could be excluded as Buergy, et al. (2020) showed similar particle sizes for individualised cells in GS and GD apples.

In several cultivars, pectin solubilisation was favoured by high temperatures of Process II (**Table 18**), as already reported in tomato and carrot purees (Lin, et al., 2005; Moelants, et al., 2013). This increased serum viscosity. However, soluble pectin content alone could not explain the remarkably high serum viscosities of GS. The high macromolecular size and molar mass of soluble GS pectins also contributed to viscosity increase.

BR showed higher serum viscosities than BRM for Process II, although the AIS content of both modalities was similar (**Table 18**). Molar mass was also similar but BRM pectins were smaller (**Fig. 67**) and thus contributed less to serum viscosity.

BRM purees showed similar particle sizes and similar PWM for both processes but different puree's textures. Serum viscosity, higher for Process II, coincided with the higher puree's texture for this process. Serum viscosity could thus have a significant impact on puree's texture when particle size and PWM were identical.
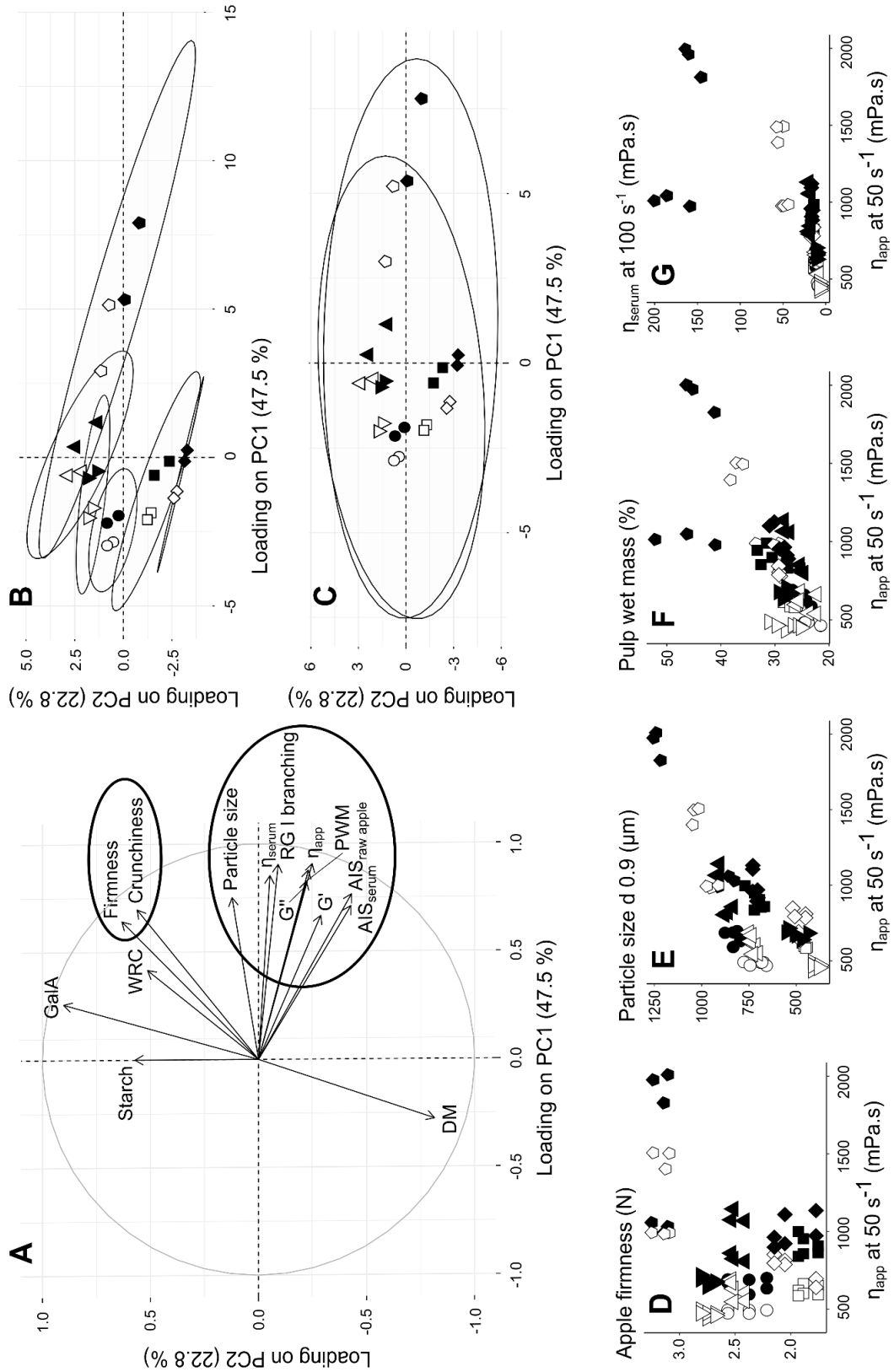
Fig. 68. Principal component analysis (PCA) (A-C) and scatterplots (D-G) of textural characteristics and cell wall composition of raw apples and rheological characteristics and texture determinants of 0.5 mm refined and not refined apple purees.

Fig. 68 (Continuation). Correlation circle of variables loadings on PC1 and PC2 (A). Sample maps of scores on PC1 and PC2 as a function of the cultivar (B) and the process (C). For more legibility, PCA was conducted on the mean value of three replications as the same sample patterns were obtained as for PCA with all values. All correlation ellipses correspond to the 95% confidence interval around the barycentre. Scatterplots of apple firmness (D), particle size (d 0.9) in the puree (E), pulp wet mass (F) and serum viscosity at 100 s^{-1} (G) as a function of apparent puree viscosity at 50 s^{-1}. The values of AIS and cell wall composition of raw apples were corrected for the starch content. Raw apple's characteristics in the PCA: Firmness, Crunchiness, AIS$_{raw apple}$ (alcohol insoluble solids of the raw apples) Starch, GalA (galacturonic acid), DM (degree of methylation), RG I branching (ratio of neutral sugars (arabinose+galactose)/rhamnose). Puree's characteristics in the PCA: η$_{app}$ (apparent viscosity of the puree at 50 s^{-1}), G', G'' (puree's storage and loss modulus, respectively, at an angular frequency of 10 rad/s), Particle size (particle size d 0.9), PWM (pulp wet mass), WRC (water retention capacity of the pulp), η$_{serum}$ (serum viscosity at 100 s^{-1}), AIS$_{serum}$ (alcohol insoluble solids of the serum). Braeburn (triangle); Braeburn, mealy (inverted triangle); Gala (circle); Golden Delicious, reduced fruit load (square); Golden Delicious, high fruit load (lozenge); Granny Smith (pentagon). Empty symbols represent Process I (70 °C, 3000 rpm) and filled symbols represent Process II (95 °C, 400 rpm).

1.2.5. Conclusions

Apple texture could not predict rheological properties of purees, although the cultivars strongly affected puree's viscosity. Remarkably high puree's texture obtained for GS was in accordance with the biggest particles, highest PWM and serum viscosity. Mealy apples showed reduced cell adhesion and were thus more susceptible to cell fragmentation during puree processing, resulting in less viscous purees. The process had a limited effect, although the high temperature-low shear process (Process II) produced more viscous purees. The lower grinding speed generated bigger particles and the higher temperature increased both the PWM and the serum viscosity because of facilitated pectin solubilisation. Combined effects of temperature regime and shear intensities could modulate puree's texture and thus mitigate poor performance of some cultivars.

Acknowledgements

Highlights

- Fruit firmness could not predict puree's viscosity.

- Cultivars highly affected puree's viscosity.

- Granny Smith revealed particularly high fruit and puree's textures.

- Mealy apples generated less viscous purees because of reduced cell adhesion.

- High temperature-low shear process produced more viscous purees.

2. Texture modulation of apple purees by means of the process conditions

Not only the raw material but also the processing conditions are important tools to design innovative plant-based products. They define the extent of tissue fragmentation and pectin solubilisation, both important factors that determine particle size, pulp wet mass and serum viscosity. These parameters, in turn, determine the puree's texture.

This chapter thus aimed to elucidate the impact of different process variables such as mechanical treatment and thermal history on the viscosity of apple purees. Since increased temperatures during puree processing impact pectin structure and composition, the role of pectins was also evaluated.

First, process variables were explored. This allowed to establish the main study, in which the impact of process variables on pectins, puree's structure and texture were analysed more in detail. Last, a sensory analysis was conducted on contrasted purees prepared during the main study to investigate the impact of puree's structure on perceived texture.

2.1. Process variables exploration

Several preliminary studies were conducted in order to better know the system that is apple puree and to assess the impact of endogenous pectinolytic enzyme activity and processing on apple puree's texture. This allowed to define the processing parameters for the products that will be studied in the detailed main study (**V 2.2.**). For this purpose, several combinations of different temperatures and grinding speeds were applied on apples from the 2018 harvest. Apples were stored for one month at 4 °C (Study I) or for six months at 2 °C (Study II). The cultivar Golden Delicious was processed in both studies. Apple trees were not thinned (GD2) in Study I and thinned (GD1) in Study II. Purees were not refined. Puree was sampled several times during processing in order to follow its viscosity. The impact of processing on the three main factors that determine puree's viscosity (particle size, pulp wet mass and serum viscosity) was also analysed.

2.1.1. Study I (GD2 apples stored for one month at 4 °C)

The aim of this study was to investigate how several combinations of different process variables could be used to modulate the tissue structure of raw fruits. To this end, the impacts of mechanical and thermal treatment, both applied for different durations, were evaluated on puree´s structure and viscosity.

2.1.1.1. Impact of grinding speed and cooking duration

Evolution of puree´s viscosity was monitored during 60 min for five different grinding speeds (200, 400, 1000, 2000 and 3000 rpm) at 95 °C (**Fig. 69**). A pre-grinding of 1000 rpm during 3 min was applied for the two lowest grinding speeds (200 and 400 rpm). This was necessary to produce purees with sufficiently small particles, which could be analysed by the same rheological methods as other purees. For the other processes (1000, 2000 and 3000 rpm), the stated speed was maintained all over cooking.
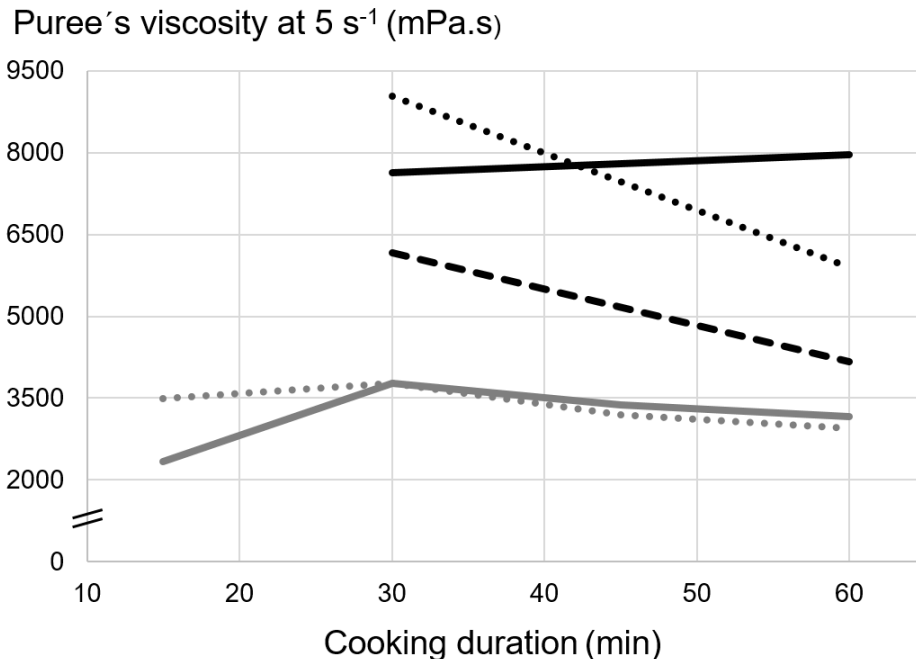
Fig. 69. Temporal evolution of viscosity for purees prepared at 95 °C with different grinding speeds.
Continuous black line: 200 rpm; Dotted black line: 400 rpm; Dashed black line: 1000 rpm; Continuous grey line: 2000 rpm; Dotted grey line: 3000 rpm.

Puree´s viscosity globally decreased with increased grinding speed and cooking duration. After 60 min, a grinding speed of 200 rpm led to a viscosity of 8000 mPa.s, whereas 3000 rpm produced puree's viscosity of around 3000 mPa.s.

<u>Structural characteristics could be explained by grinding speed and cooking duration</u>

Fig. 70 shows the viscosity of the continuous phase. A powerful mechanical treatment (2000 and 3000 rpm) led to a strong increase in serum viscosity during the first 30 min. Serum viscosity then kept increasing during the next 15 min but the curve flattened. After 45 min of continuous cooking and grinding, serum viscosity decreased. When comparing the grinding speeds after 30 min, it can be clearly seen that the stronger the mechanical treatment, the higher serum viscosity. However, between 30 and 60 min, serum viscosity strongly increased in the purees ground at 200 and 400 rpm but less in the puree ground at 1000 rpm. Similar serum viscosities were thus observed after 60 min, whatever the grinding speed.

Serum viscosity at 100 s^{-1} (mPa.s)
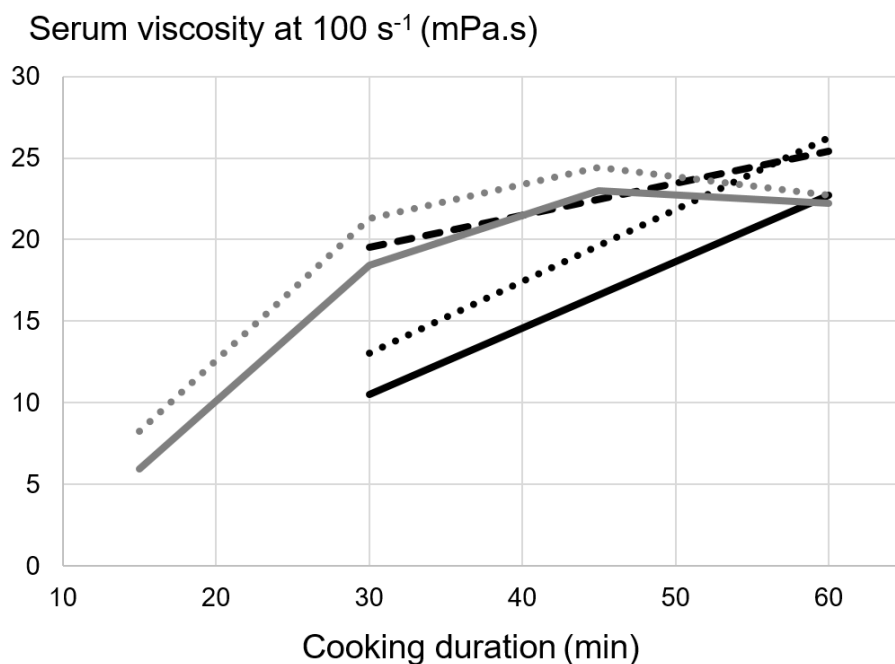
Fig. 70. Temporal evolution of serum viscosity for purees prepared at 95 °C with different grinding speeds.

Continuous black line: 200 rpm; Dotted black line: 400 rpm; Dashed black line: 1000 rpm; Continuous grey line: 2000 rpm; Dotted grey line: 3000 rpm.

After 30 min of processing, increased grinding speed led to higher serum viscosity. Serum viscosity can be supposed to result from two phenomena, namely pectin solubilisation and pectin degradation, influenced differently by grinding and heating. The more powerful the grinding, the more damaged the cell wall, leading to enhanced pectin extraction and thus increased serum viscosity. After a certain time, serum viscosity decreased in the purees ground at high speeds, probably due to pectin degradation. This effect might be delayed or disappear when lower grinding speeds were applied. This would explain why serum viscosity still increased after 1 h at 200 and 400 rpm, but already decreased in purees ground at 2000 and 3000 rpm. Castro, Bergenståhl, and Tornberg (2013) showed pectin solubilisation by homogenization after heat treatment of parsnip suspensions. However, they declared that this was dependent on the applied heat treatment: Pectins were additionally solubilised by mechanical treatment only when they had been exposed to conditions leading to pectin depolymerisation. This might explain why Espinosa Brisset (2012) and Leverrier (2016) did not observe differences in serum viscosity by increased grinding speed. They applied powerful grinding at room temperature (except for the internal heating effects in the grinder) after initial puree processing.

The higher the grinding speed, the smaller the particles in the puree (**Fig. 71**).
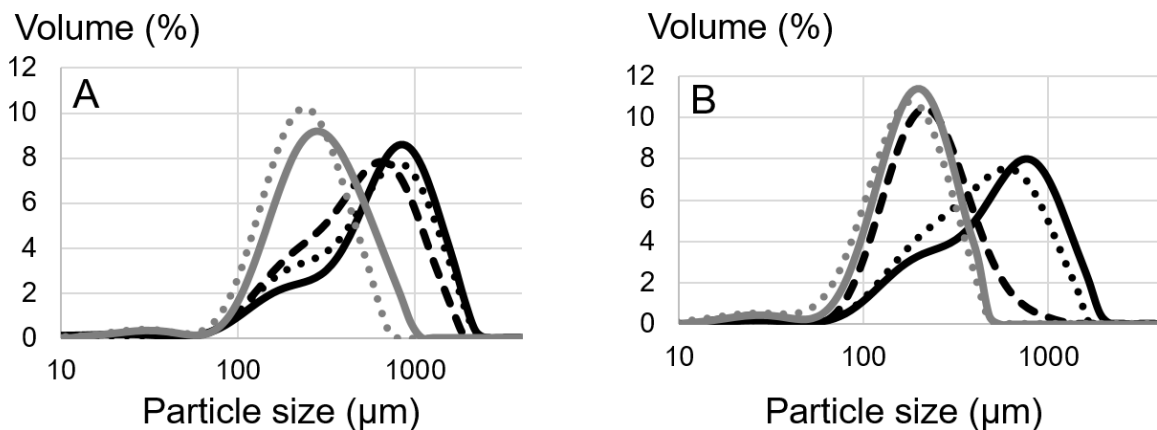
Fig. 71. Particle size distribution for purees prepared at 95 °C with different grinding speeds during 30 min (A) or 60 min (B).

Continuous black line: 200 rpm; Dotted black line: 400 rpm; Dashed black line: 1000 rpm; Continuous grey line: 2000 rpm; Dotted grey line: 3000 rpm.

After 30 min at 95 °C, purees ground by a speed of 200, 400 and 1000 rpm showed mostly cell clusters and only few individualized cells. When grinding speeds of 2000 or 3000 rpm were applied during cooking, the puree contained mostly individualized cells. After 60 min, the puree ground at 1000 rpm also displayed individual cells. Although prolonged grinding resulted in smaller particles, grinding speeds of 200 and 400 rpm were not sufficient to separate cell clusters, even after 60 min at 95 °C.

Particles in the puree were further observed by light microscopy (**Fig. 72**A) and visual inspection (**Fig. 72**B).
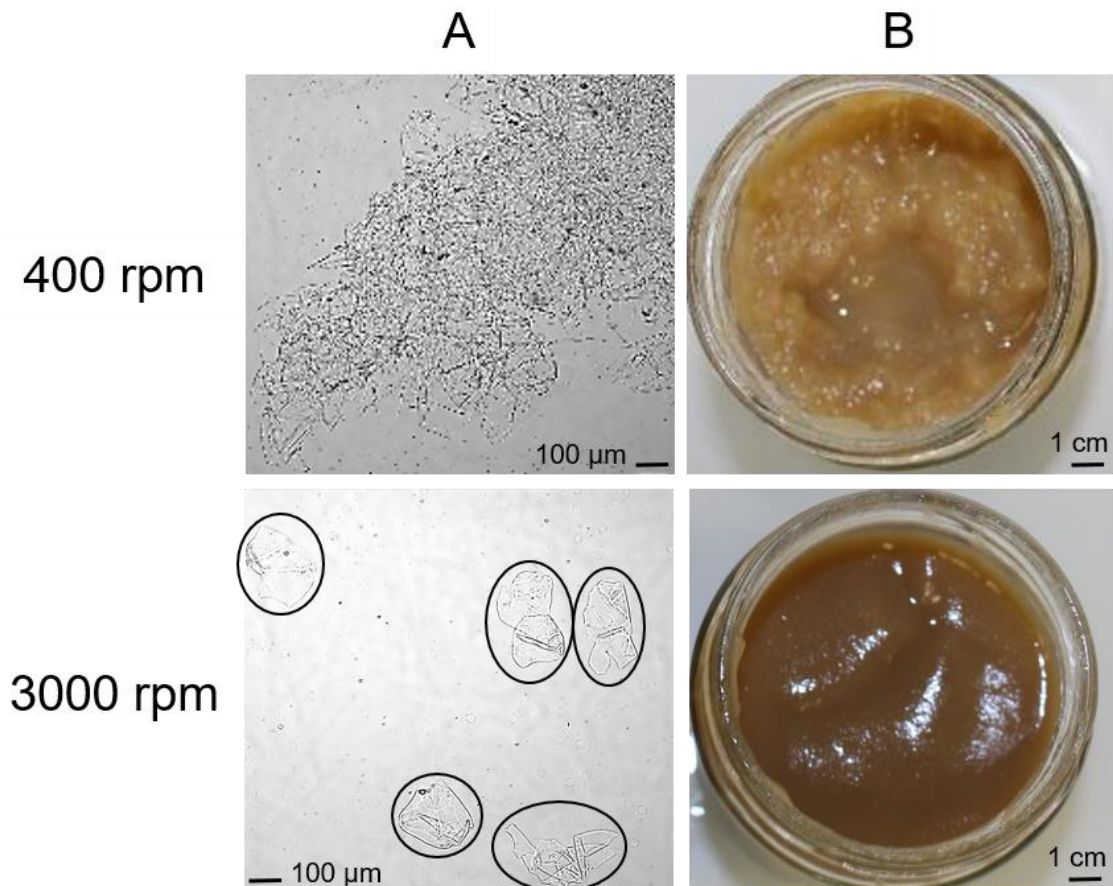
Fig. 72. Light microscopy images at a magnification x10 (A) and photos (B) of purees ground at 400 rpm or 3000 rpm (95 °C, 30 min).

The puree ground at 400 rpm (30 min) showed large cell clusters under the light microscope. Even with the naked eye, big particles could be seen, leading to inhomogeneous aspect. Compared to this, the puree ground at 3000 rpm (30 min) looked homogenous and smooth, due to presence of individual cells or small cell clusters as could be seen under the light microscope.

This confirmed that increased grinding, i.e. increased shear stress, led to smaller particles, as already shown for apple purees (Espinosa Brisset, 2012; Leverrier, et al., 2016; Tarea, 2005). Cooking duration also reduced particle size, although Schijvens, et al. (1998) associated this with increased acid hydrolysis during thermal treatment and thus weakened cell adhesion as proposed by Anantheswaran, et al. (1985) and not to persisting grinding intensity. It would be interesting to clarify this point in further studies.

Pulp wet mass (PWM, **Table 19**) represents the humid particle fraction of the puree after centrifugation. It did not change with grinding speed. After 30 min of cooking, PWM of all the purees accounted for around 26–27% of initial puree. With prolonged heating, PWM slightly increased to 29–30%.

Table 19. Temporal evolution of pulp wet mass (PWM) during cooking at 95 °C and different grinding speeds.

Temperature (°C)	Time (min)	Grinding (rpm)	PWM (%)
95	30	200	26.2
95	60	200	29.8
95	30	400	25.6
95	60	400	29.6
95	15	2000	22.9
95	30	2000	27.1
95	45	2000	29.2
95	60	2000	29.5
95	15	3000	22.7
95	30	3000	26.8
95	45	3000	30.2
95	60	3000	29.4

Former studies observed a decrease of PWM with increased grinding due to enhanced packing of smaller cells (Espinosa Brisset, 2012; Leverrier, et al., 2016). However, purees were ground without concomitant cooking. As heating probably increased water retention capacity (Guillon, Barry, & Thibault, 1992), this could balance the effect observed in literature.

Puree's viscosity was mainly explained by alteration of particle size

Puree´s viscosity decreased with increased grinding. Generally, serum viscosity increased along with the grinding speed and could thus not explain the viscosity loss in highly ground purees. PWM remained stable with increased grinding, so that this parameter also failed to explain puree's viscosity. Particle size seemed to be the predominant factor in explaining puree's viscosity in this experiment, since it was the only parameter that decreased with increased grinding.

Smaller particles have been already linked to less viscous apple purees (Espinosa Brisset, 2012; Leverrier, et al., 2016; Tarea, 2005). Besides mechanical disruption of the fruit tissue, high-pressure homogenisation (HPH) is applied in industry to reduce particle size. In tart cherry purees, smaller particles also led to less viscous purees (Lukhmana, et al., 2018). In tomato suspensions, however, HPH decreased particle size but viscosity increased (Moelants, et al., 2014b). The authors linked this phenomenon to more irregular particles in highly homogenised samples. They concluded that particle surface and shape might be more important on viscosity than particle size. In the present study, particle size between samples was rather different and explained thus well puree's viscosity. However, particle shape might be important when it is far from a sphere or when particle sizes are similar.

2.1.1.2. Impact of temperature and cooking duration

The evolution of structure and viscosity of purees prepared at different temperatures (50, 70, 95 °C) was followed over time. Grinding speed was kept constant at 1000 rpm. A first series of purees was prepared at 50 °C for 120 min, before temperature was raised to 95 °C for an additional 60 min. A second series consisted of purees prepared at 70 °C for 90 min and 95 °C for an additional 60 min. A third series of purees was processed at 95 °C for 120 min. The processes were conducted under normal atmosphere in order to take samples every 30 min.
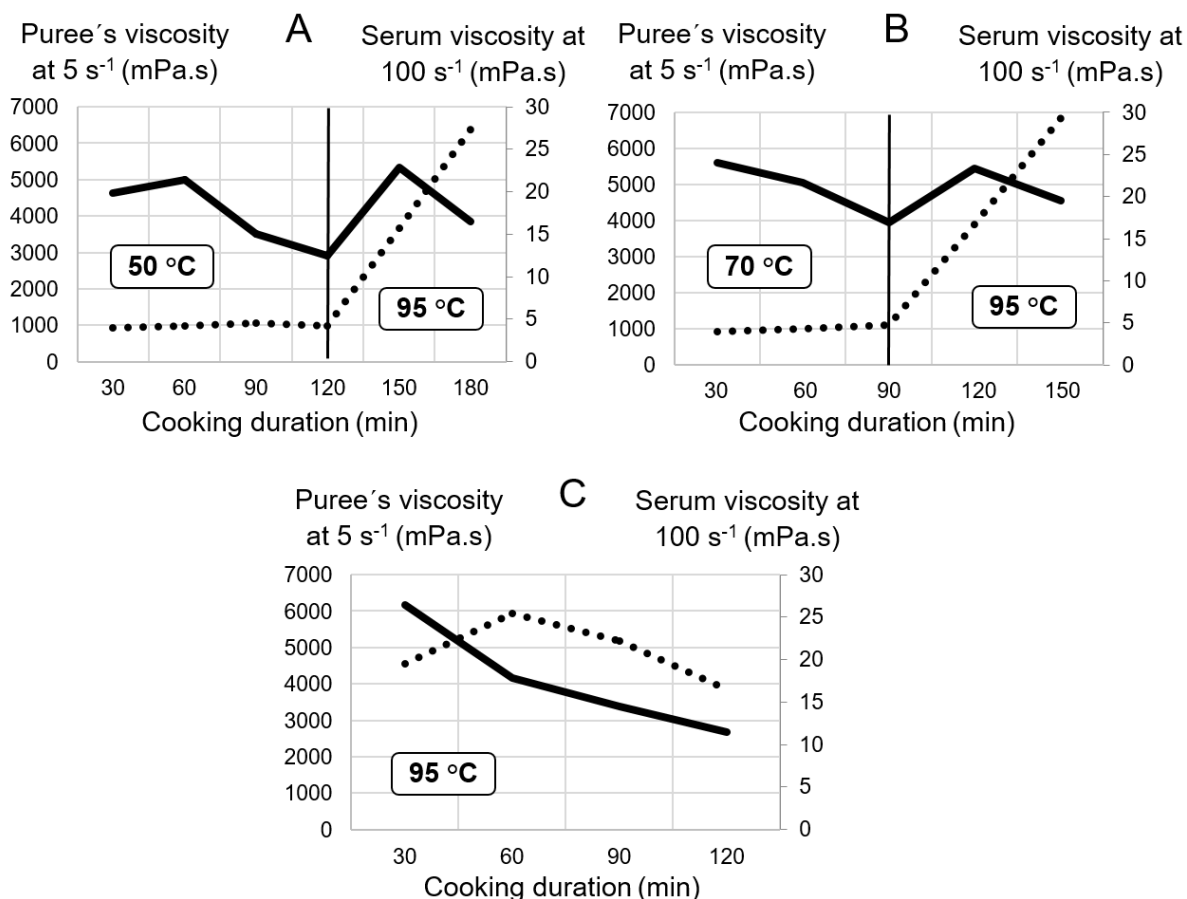
Fig. 73. Temporal evolution of puree and serum viscosity during 120 min at 50 °C, followed by 60 min at 95 °C (A), during 90 min at 70 °C, followed by 60 min at 95 °C (B) and during 120 min at 95 °C (C) at constant grinding speed (1000 rpm).
Continuous line represents puree viscosity and dotted line represents serum viscosity.

For purees prepared at 50 °C (**Fig. 73**A), viscosity showed a slight increase between 30 and 60 min before it decreased constantly from 60 to 120 min from 5000 to 2900 mPa.s. After application of 95 °C, viscosity increased during the first 30 min before decreasing again after prolonged heating at 95 °C. The viscosity of the continuous phase remained constant during heat treatment at 50 °C. Serum viscosity increased strongly, after the temperature was raised to 95 °C, from around 5 mPa.s to 27 mPa.s. Similar trends were observed in purees prepared at 70 °C (**Fig. 73**B). Puree's viscosity decreased monotonously within 90 min at 70 °C. When temperature rose to 95 °C, viscosity increased from 4000 mPa.s to 5500 mPa.s during the first 30 min, then decreased to 4500 mPa.s during the next 30 min. Serum viscosity remained stable during cooking at 70 °C but increased from 5 mPa.s to 30 mPa.s when 95 °C were applied. Purees heated at 95 °C (**Fig. 73**C) behaved differently. Puree's

viscosity decreased all over the process, whereas serum viscosity increased during the first 60 min from 20 to 25 mPa.s before decreasing to 16 mPa.s. After 30 min of cooking, the puree prepared at 95 °C was more viscous than purees prepared at lower temperatures. As the viscosity of this puree decreased rapidly between 30 and 60 min, it was then lower than viscosity of purees prepared at 50 or 70 °C at both 60 and 90 min.
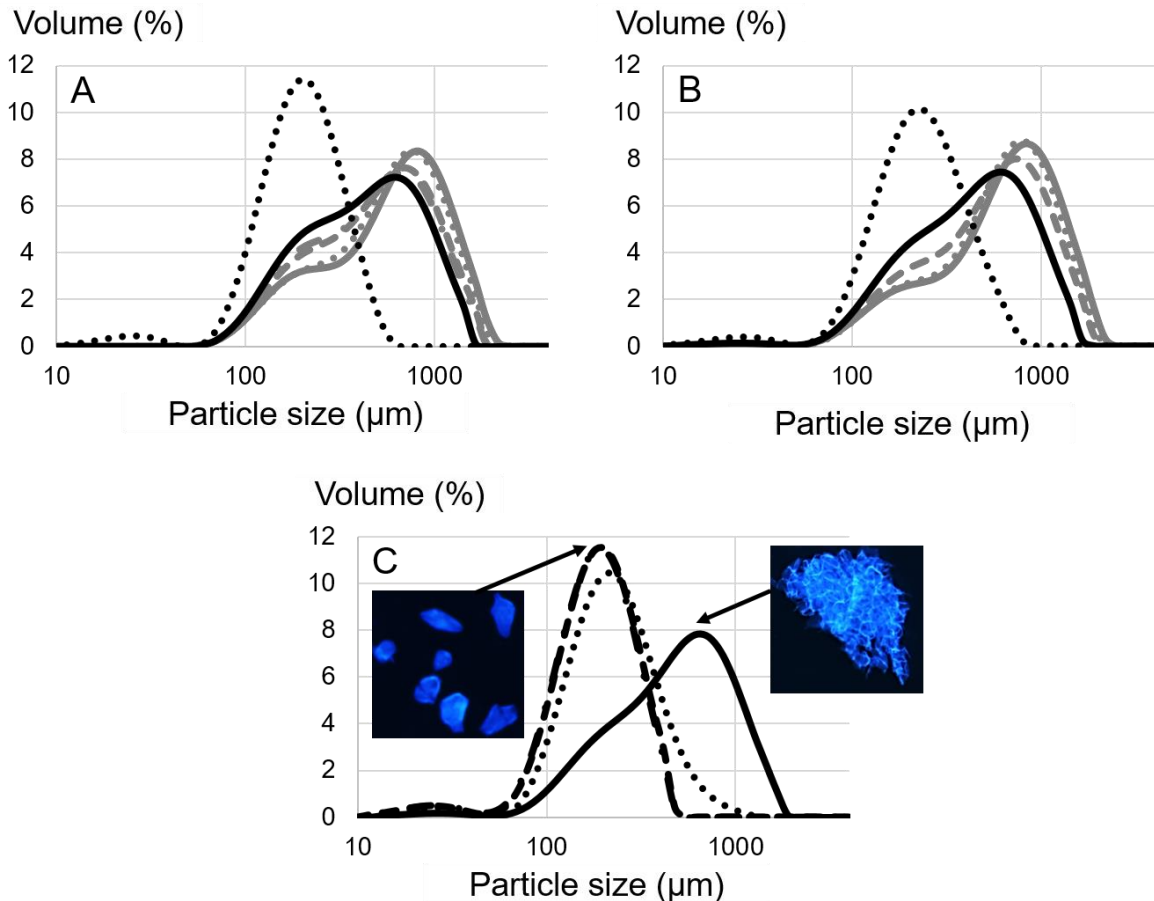
Fig. 74. Temporal evolution of particle size distribution during 120 min at 50 °C, followed by 60 min at 95 °C (A), during 90 min at 70 °C, followed by 60 min at 95 °C (B) and during 120 min at 95 °C (C) at constant grinding speed (1000 rpm).

Continuous line: 30 min; Dotted line: 60 min; Dashed line: 90 min; Dashed and dotted line: 120 min. Grey lines represents 50 °C or 70 °C and black lines represent 95 °C.

Particle size distribution changed little within 120 min at 50 °C (**Fig. 74**A) or 90 min at 70 °C (**Fig. 74**B). The initial bimodal distribution showed a main peak around 830 µm and a second, smaller peak around 210 µm. The first peak showed cell clusters, whereas the second one was attributed to individual cells (Espinosa-Munoz, et al.,

2013). The main peak shifted slightly to smaller sizes (725 µm) within 120 min at 50 °C or 90 min at 70°C and the volume of the second peak increased. This trend continued when temperature was raised to 95 °C. Particle size clearly decreased only after 60 min at 95 °C and a single peak around 210 µm was visible. For purees prepared at 95 °C, particle size (**Fig. 74**C) showed a bimodal distribution after 30 min. The presence of cell clusters could be visualized by staining the cell walls with calcofluor. The main peak was situated around 630 µm and the second peak around 210 µm. With prolonged cooking duration, particle size converged into a single peak. After 60 min of cooking, this peak was situated around 240 µm and after 90 min at 210 µm. Particle size did not change between 90 and 120 min at 95 °C. This was due the fact that the size of individual cells was reached, as demonstrated by calcofluor staining.

Pulp wet mass (PWM, **Table 19**) did not change during heating at 50 °C or 70 °C. PWM increased only when temperature rose to 95 °C. It further increased with prolonged cooking at 95 °C. In purees heated at 95 °C from the beginning, PWM showed a slight increase between 30 and 60 min and a slight decrease during 90 and 120 min, so that the initial value was reached. As this study was conducted without duplicates, it could not be concluded if these changes were significant or if PWM remained stable.

Table 20. Temporal evolution of pulp wet mass (PWM) for purees prepared at 50 °C, 70 °C and 95 °C at constant grinding speed (1000 rpm).

Time (min)	PWM 50 °C (%)	PWM 70 °C (%)	PWM 95 °C (%)
30	25.3	23.0	28.9
60	24.9	23.0	30.8
90	25.1	24.4	30.7
120	23.0	27.5*	28.6
150	28.3*	30.4*	-
180	32.1*	-	-

*Temperature increase to 95 °C.

Puree's structure evolved differently in purees heated at 95 °C compared to purees prepared at lower temperatures (50 °C and 70 °C). Particle size, PWM and serum viscosity all changed little when temperatures of 50 or 70 °C were applied. Hence, apple tissue seemed to be not affected by these temperatures. Only higher temperatures (95 °C) modified apple tissue and thus the structure of the purees.

<u>Structural characteristics could be explained by temperature and cooking duration</u>

Serum viscosity increased by a factor 5 when purees, prepared at low temperatures, were heated to 95 °C. Several studies linked increase in serum viscosity to pectin solubilisation during prolonged thermal treatment of apple puree (Colin-Henrion, et al., 2009; Schijvens, et al., 1998), tomato puree (Diaz, et al., 2009; Hurtado, Greve, & Labavitch, 2002) and carrots (Greve, et al., 1994). It was thus confirmed that high temperatures enhanced pectin solubilisation. This was in line with the fact that increased temperatures generally favour chemical pectin degradation (cf. **II 3.6.3.2.**). In apples, mainly acid hydrolysis of the pectin RG I backbone and side chains is expected during processing due to their acid pH of 3.7 (Eisele & Drake, 2005). This might result in pectin solubilisation as RG I side chains are necessary to retain pectins in the cell wall complex (Zykwinska, et al., 2005). However, serum viscosity decreased with prolonged heating at 95 °C. This was probably due to pectin depolymerisation and has been already observed during prolonged processing of tomatoes and carrots at elevated temperatures (Cámara Hurtado, et al., 2002; Moelants, et al., 2013). However, conformational changes might be more important in viscosity loss of serum than decrease of molar mass due to depolymerisation (Diaz, et al., 2009). To evaluate the impact of pectin depolymerisation on serum viscosity, the amount and chemical structure of soluble pectins will be analysed in further studies.

Tissue fragmentation also seemed to be favoured by pectin solubilisation. While particle size was hardly altered at low temperatures, it was reduced when high temperatures were applied. As a result of pectin solubilisation at 95 °C, cell adhesion decreased, leading to smaller particles, even individual cells.

PWM showed higher values in purees heated at 95 °C. This might also be explained by pectin solubilisation. The cell wall structure might be more damaged, so water was better retained by the cell wall. This was observed previously for heat-treated dietary fibres (Guillon, et al., 1992) and cell wall material (Müller & Kunzek, 1998). Another

reason could be that smaller particles show improved water retention capacities as Auffret, et al. (1994) described for peapods.

Puree's viscosity was explained by structural characteristics

Viscosity of purees prepared at 50 °C slightly increased between 30 and 60 min. This could not be explained and might be due to viscosity measuring system, which was disturbed by large particles. The decrease of viscosity between 60 and 120 min at 50 °C or 30 and 90 min at 70 °C was probably linked to particle size, which decreased not a lot but monotonously. Both PWM and serum viscosity were not modified by thermal treatment at 50 °C or 70 °C and did thus not contribute to the modifications observed in puree's viscosity at low temperatures. When these purees were heated to 95 °C, viscosity increased strongly during the first 30 min. This was not linked to particle size as it was still decreasing. Possible factors could thus be water loss, increased PWM or serum viscosity. After 30 min of constant heating at 95 °C, puree's viscosity decreased again, although PWM and serum viscosity still increased. This was probably linked to a clear decrease in particle size as mainly individual cells were present in the puree. Interestingly, viscosity of these purees did not decrease as low as viscosity before heating to 95 °C in spite of much smaller particles. This may be explained by the interplay of increased PWM and serum viscosity.

Viscosity of purees prepared at 95 °C decreased over time. Particle size seemed to be the key driver. It was the only parameter which decreased monotonously, while serum viscosity and PWM increased during the first 60 min of cooking. The abrupt decrease in viscosity from 6200 to 4200 mPa.s between 30 and 60 min was reflected by a radical change in particle size distribution. Then, viscosity decreased more slowly. This was in line with the fact that particle size had reached a plateau, as almost only individual cells were present in the puree. However, puree's viscosity kept decreasing during 90 and 120 min, while particles showed constant sizes. In this case, decreasing serum viscosity and maybe PWM seemed to be responsible for puree's viscosity. The fact that, after 30 min, the puree was more viscous than purees prepared at lower temperatures may be explained by the higher serum viscosity and maybe by the slightly higher pulp wet mass. Interestingly, only temperatures of 95 °C were able to separate cell clusters into individual cells and only after one hour of cooking (at 1000 rpm). Temperatures of 50 and 70 °C were not sufficient to obtain this effect,

even after 120 min (50 °C) or 90 min (70 °C). This was in line with the results published by Day, et al. (2010) and Lopez-Sanchez, et al. (2011) who observed enhanced cell separation for cooked broccoli and carrot tissue compared to uncooked or slightly cooked tissue.

2.1.1.3. Impact of low temperature pre-treatments

The impact of low-temperature pre-treatments on structural and textural characteristics was studied by means of purees prepared in **V 2.1.1.2.** Puree and serum viscosity are presented for purees cooked for 30 min (**Fig. 75**A) or 60 min (**Fig. 75**B) at 95 °C (1000 rpm) with pre-treatment at 50 °C (120 min, 1000 rpm) or 70 °C (90 min, 1000 rpm) and without pre-treatment.
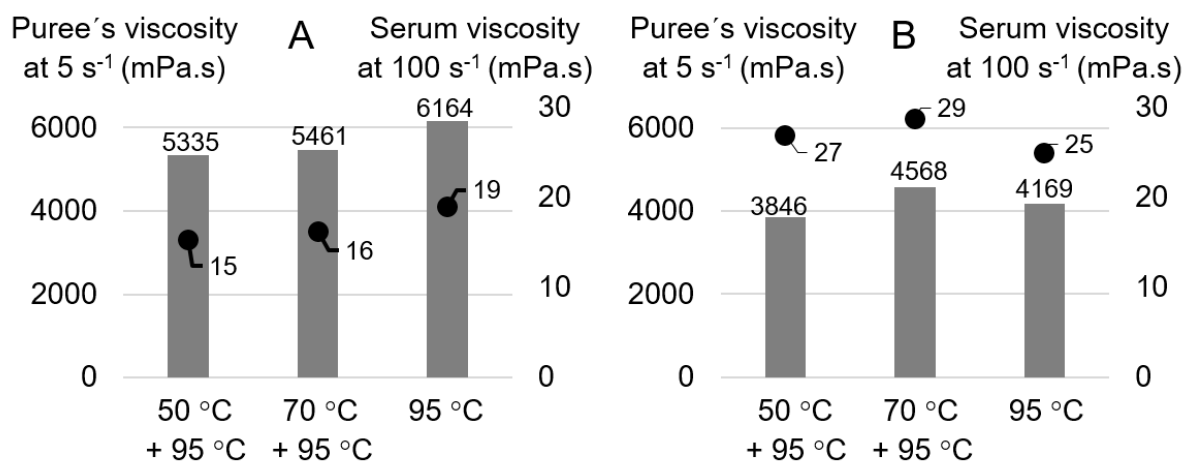
Fig. 75. Puree viscosity (grey bar) and serum viscosity (black dot) of purees cooked for 30 min (A) or 60 min (B) at 95 °C (1000 rpm) with or without pre-treatment. Pre-treatments were 50 °C for 120 min (50 °C + 95 °C) and 70 °C for 90 min (70 °C + 95 °C).

Puree's viscosity (**Fig. 75**A) was higher for the puree prepared without pre-treatment after 30 min. This could be explained by slightly bigger particles (**Fig. 76**A). After 60 min at 95 °C, puree's viscosity (**Fig. 75**B) was similar with and without pre-treatment, due to similar particle size distributions (**Fig. 76**B).

Interestingly, serum viscosity (**Fig. 75**) was not higher in purees that underwent a pre-treatment at 50 °C or 70 °C. Hence, a pre-treatment at these temperatures did not influence pectin solubilisation. Only the temperature of 95 °C was thus able to do so, no matter which pre-treatment was applied.

Particle size (**Fig. 76**) was also highly influenced by temperature. Individual cells (peak around 200 µm) were obtained after one hour at 95 °C, irrespective of the temperature or even the existence of a pre-treatment. Low temperatures (50 and 70 °C), although applied for already 120 min (50 °C) or 90 min (70 °C) before heating to 95 °C, were not sufficient to lead to cell separation. This might be related to pectin solubilisation. As more pectins were solubilised from the middle lamella and cell walls only at 95 °C (cf. **V 2.1.1.2.**), cell fragmentation was enhanced.
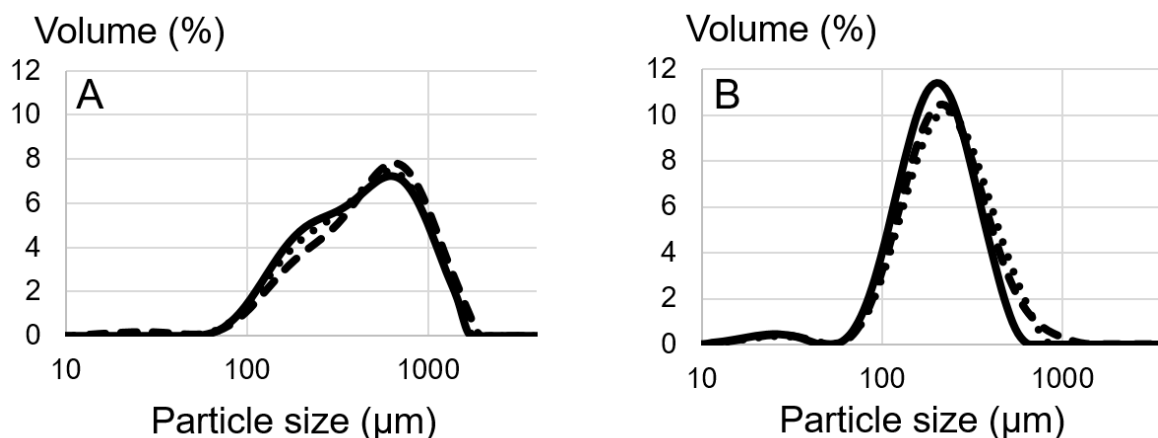
Fig. 76. Particle size distribution of purees cooked for 30 min (A) or 60 min (B) at 95 °C (1000) rpm with or without pre-treatment.
Continuous line: 50 °C, 120 min + 95 °C; Dotted line: 70 °C, 90 min + 95 °C; Dashed line: 95 °C.

PWM (**Table 19**) showed very similar values between purees cooked for 30 min (28–29%) or 60 min (30–32%) at 95 °C with or without pre-treatment. Since apples were heated over a much longer time during pre-treatments, increased PWM was expected due to increased water retention capacities. However, temperatures of 50 or 70 °C, as applied during pre-treatments, were not able to modify apple cell wall structure. Only higher temperatures (95 °C) led to pectin solubilisation (increased serum viscosity) and cell separation (decreased particle size).

Purees prepared with pre-treatment could be considered as cold break (CB) samples. In tomato purees, CB purees are more liquid due to enzymatic pectin degradation in the serum (Goodman, et al., 2002). It is not the case in apple purees, since Athiphunamphai, Bar, Cooley, and Padilla-Zakour (2014) find more consistent purees for CB with larger particles and no impact on content and degree of methylation (DM) of soluble pectins. In the current study, the effect of particle size was also predominant over possible enzymatic pectin degradation. Apple pieces were already ground to smaller particles during pre-treatment of 120 min (50 °C) or 90 min (70 °C).

For many vegetables, such as carrots (Sila, et al., 2006a), broccoli (Christiaens, et al., 2012) or green beans (Stolle-Smits, et al., 2000), low-temperature pre-treatment (50–70 °C) leads to increased tissue firmness. This phenomenon is associated with increased PME activity, enhancing demethylation of pectin polysaccharides. Pectins showing a low DM are less susceptible to β-elimination and thus less degraded during processing. In addition, low methylated pectins can form calcium crosslinks with other pectins. Both mechanisms result in preserved texture. This was not confirmed in apples since tissue fragmentation was nearly identical between purees with or without pre-treatment. Particle size was not altered. This might be due to the acid pH in apples. Although PME might demethylate pectin backbones, pectins are very stable at mild acid pH (around pH 3.5) and chemical reactions are limited (Liu, Renard, Rolland-Sabaté, Bureau, & Le Bourvellec, 2021).

2.1.1.4. Impact of pasteurization

Apples were processed at 50 °C for 20 min with two different grinding speeds (400 and 3000 rpm), followed by a pasteurisation for 2 min at 95 °C. Puree's viscosity was analysed before and after pasteurisation. A more powerful grinding led to less viscous purees (**Fig. 77**). Puree's viscosity was also slightly lower after the pasteurisation step.

In contrast to purees heated at 95 °C (cf. **V 2.1.1.1.**), serum viscosity (**Fig. 77**) was not affected by different grinding speeds at 50 °C. This confirmed the results obtained by Espinosa Brisset (2012) and Leverrier, et al. (2016), who do not observe any change in serum viscosity by grinding at room temperature. The viscosity of the continuous phase only increased when 95 °C were applied. As seen in **V 2.1.1.2.**, prolonged cooking duration did not alter serum viscosity at temperatures as low as 50 or 70 °C. The rise in serum viscosity was thus linked to temperature increase. Apparently, 2 min

at 95 °C were sufficient to initialize pectin solubilisation. At 95 °C (but not at 50 °C), a faster grinding (i.e. more shear) slightly increased serum viscosity, maybe due to better pectin solubilisation.
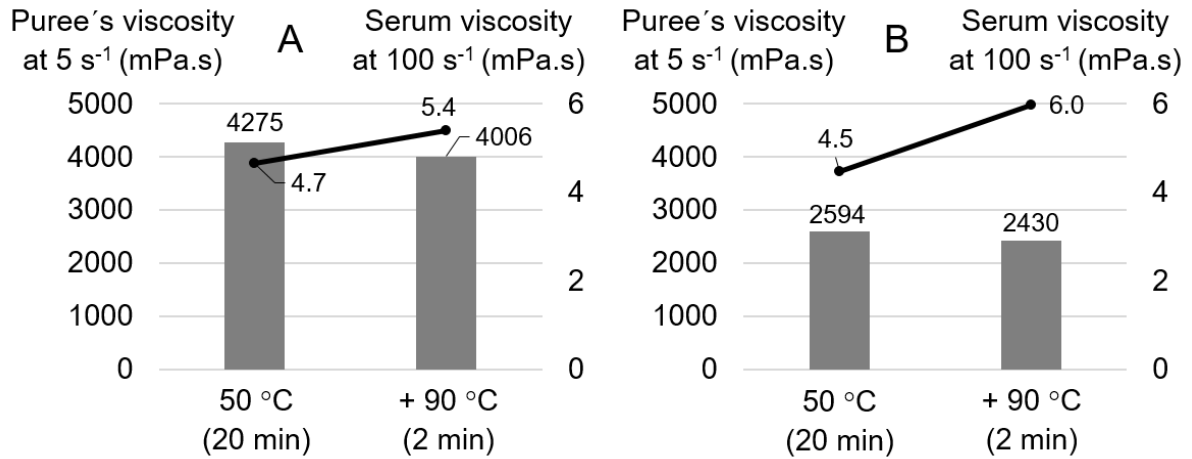
Fig. 77. Puree viscosity (grey bar) and serum viscosity (black line) of purees heated to 50 °C (20 min) and ground at 400 rpm (A) or 3000 rpm (B) before and after pasteurization (95 °C, 2 min).
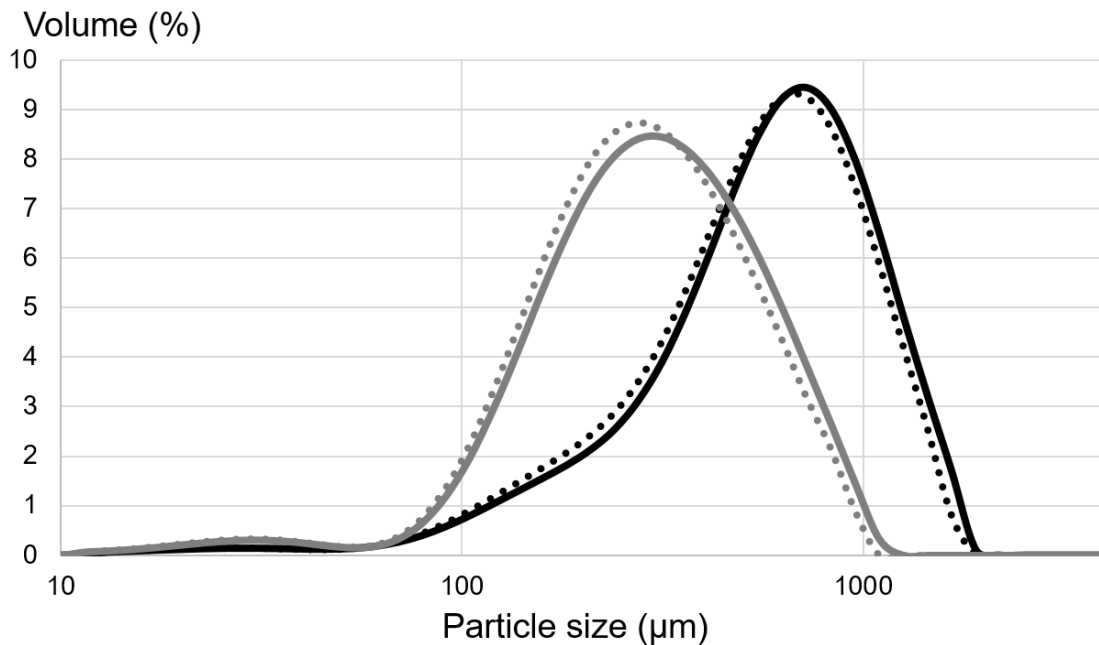
Fig. 78. Particle size distribution of purees heated to 50 °C (20 min) and ground at 400 or 3000 rpm before and after pasteurization (95 °C, 2 min).

Black lines: 400 rpm; Grey lines: 3000 rpm; Continuous lines: Before pasteurization; Dotted lines: After pasteurization.

Particle size (**Fig. 78**) decreased with increased grinding, as already observed. After pasteurization, particles were also slightly smaller. This might be due to prolonged grinding or enhanced cell separation at 95 °C, or maybe both.

As already observed in **V 2.1.1.1.**, PWM (**Table 21**) did not change with increased grinding speed. However, it increased slightly after 2 min at 95 °C.

Table 21. Pulp wet mass of purees heated to 50 °C (20 min) and ground at 400 or 3000 rpm before and after pasteurization (95 °C, 2 min).

Temperature (°C)	Time (min)	Grinding (rpm)	Pulp wet mass (%)
50	20	400	24.3
+ 95	+ 2	400	25.7
50	20	3000	24.6
+ 95	+ 2	3000	25.7

Increased grinding speed led to less viscous purees due to decreased particle size, as already observed. Serum viscosity and PWM remained constant. Temperature increase to 95 °C during pasteurization for 2 min was sufficient to induce cell wall degradation. Both serum viscosity and PWM increased, probably due to pectin solubilisation. Particle size was slightly decreased, leading to somewhat less viscous purees after pasteurization.

Apple purees that were cooked at 70 °C showed the same trends before and after pasteurisation as purees cooked at 50 °C. These results were thus not presented.

2.1.1.5. Impact of temperature and grinding

Mechanical and thermal treatments seemed to interact during processing. Both temperature (Christiaens, et al., 2012) and grinding (Leverrier, et al., 2016) were shown to affect structural characteristics in plant cell wall dispersions but studies investigating combinations of thermal and mechanical treatments are scarce. Knowledge about how combined effects of thermal and mechanical treatments could be used to modulate texture, would be helpful to overcome the variability of raw material.

For this purpose, mechanical treatments were combined with thermal treatments and their impact on puree's structure and viscosity was compared. Two contrasted grinding speeds and temperatures were chosen in order to generate a wide range of different purees. Four combinations of thermomechanical processes were thus designed: low temperature-low shear (70 °C, 400 rpm), high temperature-low shear (95 °C, 400 rpm), low temperature-high shear (70 °C, 3000 rpm) and high temperature-high shear (95 °C, 3000 rpm). The four processes were applied to Golden Delicious apples that had been stored for 1 month at 4°C. Cooking time was 15 min, before pasteurisation for 2 min at 95 °C. The time that RoboQbo needed to reach the working temperature was recorded and can be examined in **Supplementary Fig. S1–S4**.

The following figure illustrates puree's viscosity at 70 °C (**Fig. 79**A) and 95 °C (**Fig. 79**B). Purees were less viscous when high shear processes were applied, irrespective of temperature, and more viscous when high temperatures were used, whichever the grinding speed.
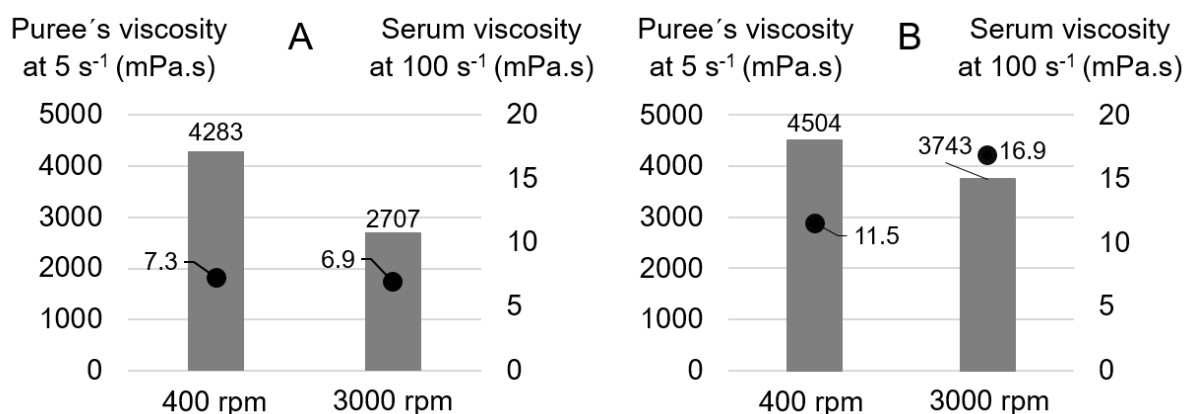
Fig. 79. Puree viscosity (grey bar) and serum viscosity (black dot) of purees ground at two contrasted grinding speeds (400 and 3000 rpm) and heated at 70 °C (15 min) + 95 °C (2 min) (A) or 95 °C (17 min) (B).

As already exposed before, serum viscosity (**Fig. 79**) did not change with grinding speed in the purees prepared at low temperatures, but increased with faster grinding at 95 °C. In addition, sera of high temperature processes were more viscous.

As expected, particles (**Fig. 80**) were smaller after high shear processes. At 400 rpm, particle sizes were slightly lower when the higher temperature was used, while this effect was absent at 3000 rpm. High temperature thus enhanced cell separation during grinding, especially during the low shear process. This was probably due to increased pectin solubilisation (cf. increased serum viscosity) at 95 °C. However, pectin degradation alone was not sufficient to ensure cell separation. Individual cells could be generated with increased grinding speed. Since both high and low temperature processes showed similar particle sizes at 3000 rpm, high mechanical force seemed to cause tissue rupture without pectin solubilisation.
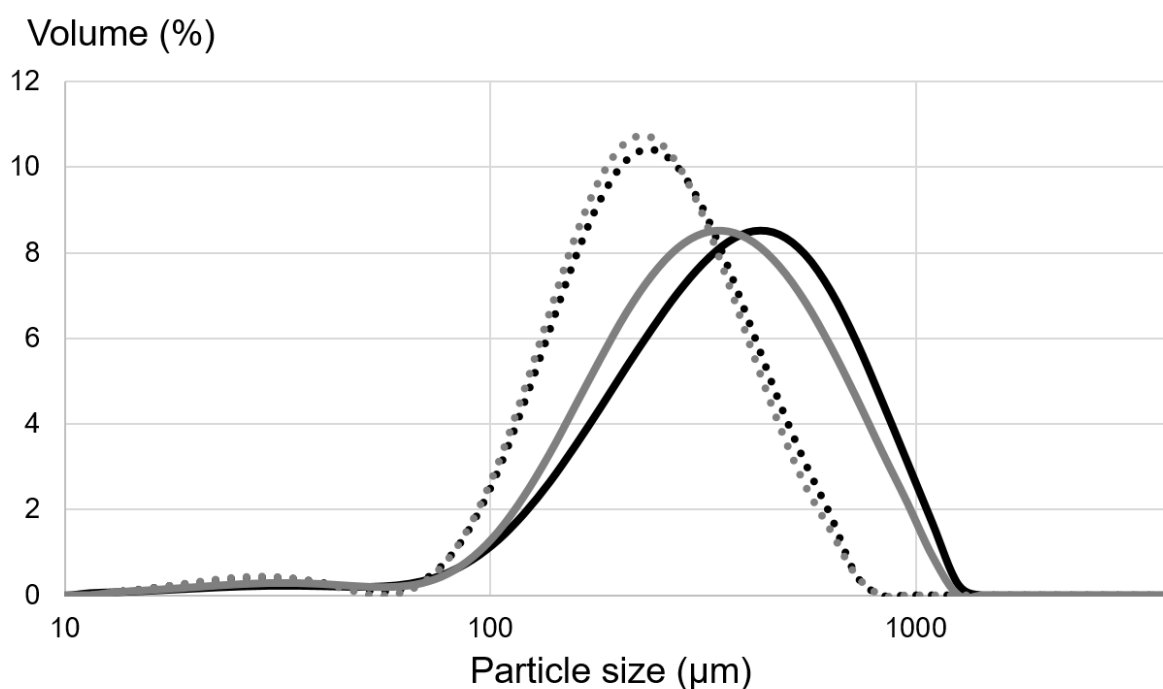
Fig. 80. Particle size distribution of purees ground at two contrasted grinding speeds (400 and 3000 rpm) and heated at 70 °C or 95 °C.
Black lines: 70 °C (15 min) + 95 °C (2 min); Grey lines: 95 °C (17 min); Continuous lines: 400 rpm; Dotted lines: 3000 rpm.

A more powerful mechanical treatment increased PWM (**Table 22**) slightly at 70 °C but decreased PWM at 95 °C. High temperature increased PWM at 400 rpm but decreased PWM at 3000 rpm. However, these variations were negligible since all values were in a similar range of 27–29%.

Table 22. Pulp wet mass (PWM) of purees ground at two contrasted grinding speeds (400 and 3000 rpm) and heated at 70 °C or 95 °C, followed by a pasteurization step (95 °C, 2 min).

Temperature (°C)	Time (min)	Grinding (rpm)	PWM (%)
70 (+ 95)	15 (+ 2)	400	26.8
70 (+ 95)	15 (+ 2)	3000	27.8
95 (+ 95)	15 (+ 2)	400	29.3
95 (+ 95)	15 (+ 2)	3000	26.6

Viscosity decrease in high shear processes was due to decreased particle size, as already observed (**V 2.1.1.1.**). However, high viscosity values after high temperature processes could not be explained by particle size, as particles were smaller than in low temperature processes. PWM was similar for all samples and could thus not be the explanatory variable. Serum viscosity was higher in high temperature processes and might increase puree's viscosity. More viscous purees for high temperature processes were already observed in **V 2.1.1.2.** This was also due to higher serum viscosity and probably PWM. Both values were affected by high temperatures as a result of thermal pectin degradation. However, prolonged cooking enhanced cell separation at 95 °C, leading to smaller particles. Hence, puree's viscosity was reduced. There was clearly a synergism between temperature and shear for cell separation. For low temperature processes, gentle grinding (1000 rpm) did not result in complete cell separation, probably due to absence of pectin solubilisation that would reduce cell adhesion. Gentle mechanical treatment as applied in **V 2.1.1.2.** (1000 rpm) and here (400 rpm) could not separate the cells without pectin solubilisation induced by high temperatures (95 °C). In contrast, intense mechanical treatment (3000 rpm) could decrease particle size by tissue disruption without pectin solubilisation.

The process variables that gave a maximal contrast in puree's viscosity were low temperature-high shear process (70 °C, 3000 rpm, low viscosity) and high temperature-low shear process (95 °C, 400 rpm, high viscosity), both processes followed by 2 min at 95 °C. These processes were thus selected for **V 1.2.**

2.1.2. Study II (GD1 apples stored for six months at 2 °C)

The aim of this second study was to validate process parameters that were comparable but resulted in contrasted puree's viscosity. The results were used to construct a study for further in-depth analysis, comprising textural, structural and pectin analysis of the obtained purees. For this purpose, two contrasted temperatures (70 °C or 95 °C), grinding speeds (300 rpm or 3000 rpm) and cooking durations (15 or 30 min) were tested.

2.1.2.1. Determination of pre-grinding

It was suspected that a pre-grinding step at high grinding speeds such as 3000 rpm, as applied in **V 2.1.1.4.**, might bias the results; If the impact of the mechanical treatment needs to be analysed, it should be maintained all over apple processing. This is why the minimal grinding speed that led to smooth purees was evaluated first in this study. Homogenous texture was important to analyse puree's viscosity correctly by the rheological tests used.

As can be seen in **Fig. 81**A, a grinding speed of 100 rpm during 30 min at 70 °C was not enough to obtain a smooth puree. Big cell clusters as well as skin particles were visible and would disturb texture analyses. A puree ground at 300 rpm during 30 min at 70 °C led to a more homogenous puree (**Fig. 81**B). This texture was considered acceptable for analysis by rheology.

Piece of apple skin
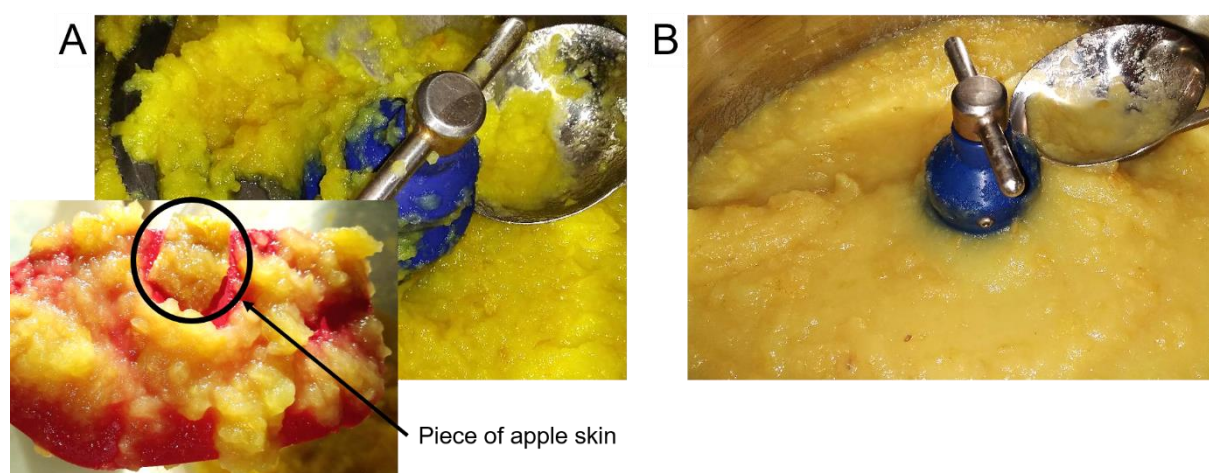
Fig. 81. Visual aspect of purees (70 °C, 30 min) ground at 100 rpm (A) or 300 rpm (B).

The process variables used in this study were thus 70 °C versus 95 °C, 300 rpm versus 3000 rpm and 15 versus 30 min.

It took more time (140 s) to reach the working temperature at 95 °C compared to 70 °C (cf. **Supplementary Fig. S1–S4**). Only a moderate grinding speed of 100 rpm was thus applied during temperature increase. This mixed the apples but minimized tissue separation. Once the working temperature was reached, grinding speed was raised to 300 or 3000 rpm and kept constant for 15 or 30 min.

The visual aspects of the purees are shown in **Fig. 82**. Grinding at 300 rpm led to more granular purees, especially after 15 min. Pieces of apple skin were also visible. When the apples were ground at 3000 rpm, texture was more homogenous and apple skin was not perceptible any more. Apple purees were not oxidised, as they were prepared under depression.
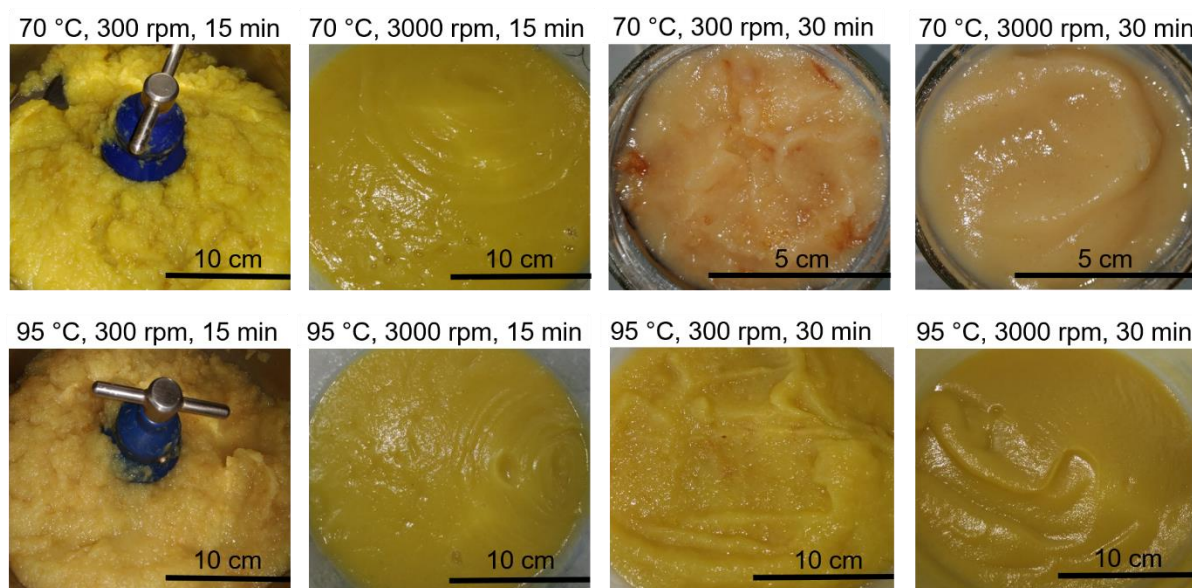
Fig. 82. Visual aspect of differently prepared apple purees.

2.1.2.2. Comparison of process variables

Puree's viscosity (**Fig. 83**) did not decrease much with prolonged cooking duration, i.e. during 15 and 30 min, at 95 °C. Viscosity decrease was more obvious during low temperature processes. Puree's viscosity decreased strongly with increased grinding speed. High temperature led to more viscous purees, except at 300 rpm and 15 min. Globally, the trends were similar to former studies, although viscosity was not measured at the same shear rate.
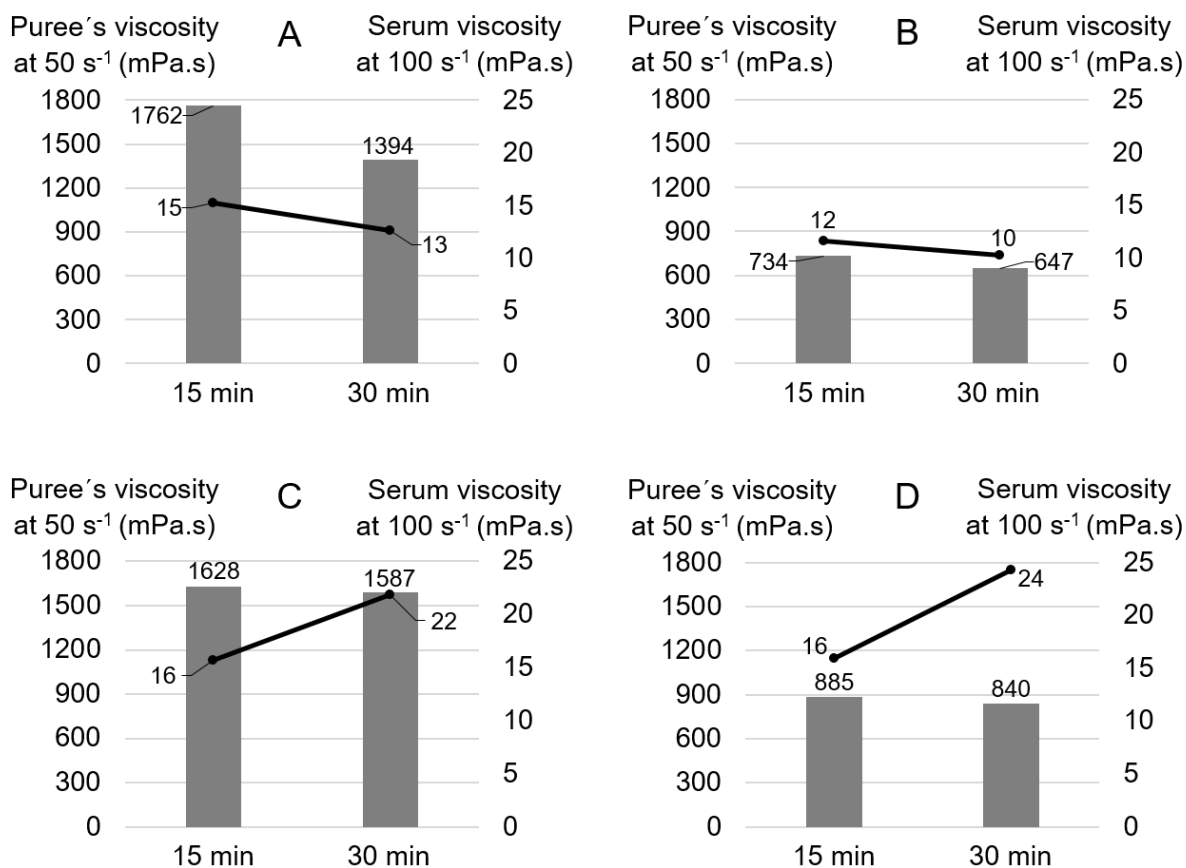
Fig. 83. Puree viscosity (grey bar) and serum viscosity (black line) of purees produced at 70 °C (A and B) or 95 °C (C and D) and ground at 300 rpm (A and C) or 3000 rpm (B and D) during 15 or 30 min.

Serum viscosity (**Fig. 83**) was two to three times higher in the purees heated at 70 °C compared to the results of study **V 2.1.1.**, in which fresh apples (stored for 1 month) were processed into puree. Consequently, serum viscosity was similar between purees prepared at 70 or 95 °C for 15 min. After 30 min, viscosity was higher in purees prepared at 95 °C, since prolonged cooking at higher temperature led to increased

viscosity of the continuous phase. Prolonged treatment had no impact on serum viscosity at 70 °C. Grinding speed did not alter serum viscosity.
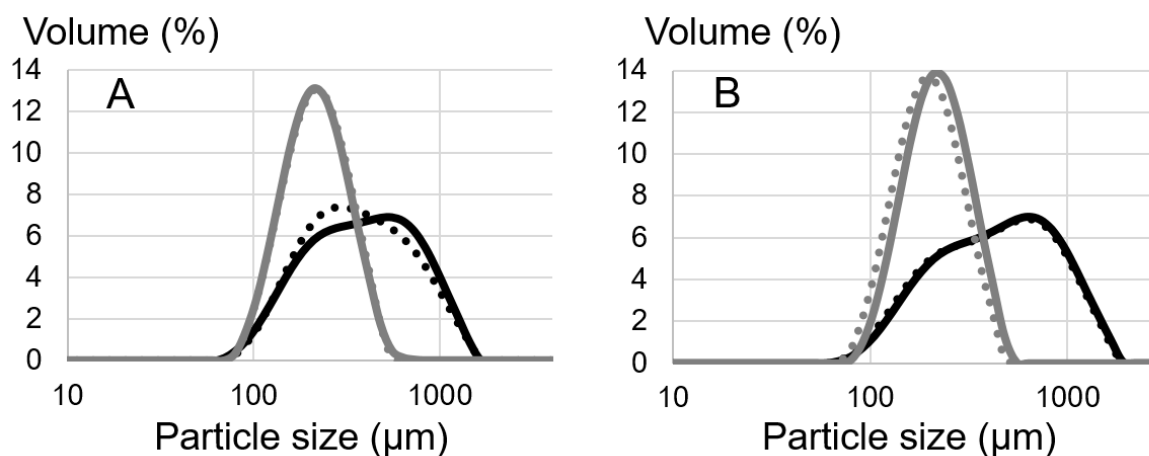
Fig. 84. Particle size distribution of purees produced with two contrasted grinding speeds (300 and 3000 rpm) and cooking durations (15 and 30 min) at 70 °C (A) or 95 °C (B).

Black lines: 300 rpm; Grey lines: 3000 rpm; Continuous lines: 15 min; Dotted lines: 30 min.

Particle size (**Fig. 84**) decreased sharply with increased grinding but only slightly with prolonged cooking duration. Differences between both temperatures were minor. Compared to Study I (cf. **Fig. 71**), particles were smaller in mature apples. Grinding at 3000 rpm led to a narrower particle size distribution, showing more individual cells. Bimodal distribution after grinding at 300 rpm (as compared to 400 rpm) showed less cell clusters and more individual cells. Cell separation was thus enhanced in mature apples. This was probably due to RG I side chain loss, leading to reduced cell adhesion as stated in **V 1.1.**

PWM (**Table 23**) showed higher values than observed in **V 2.1.1.**, in which apples were stored for only one month compared to six months in this study. Since the cell wall structure was certainly more damaged in aged apples due to pectin depolymerization and solubilisation, as well as the loss of RG I side chains (Brummell & Harpster, 2001; Thakur, et al., 1997; Voragen, et al., 1995), this might increase water retention capacities, resulting in higher PWM.

Soluble solids, as estimated by the degree Brix (**Table 23**), generally overestimate slightly the total sugar content in the serum. 12–14 ° Brix were measured in the apple purees of this study, with no clear trend depending on the process variables. Hence, concentration effects through water evaporation at higher temperature seemed to be negligible.

Table 23. Pulp wet mass (PWM) and °Brix of purees prepared with two different temperatures (70 or 95 °C), grinding speeds (300 or 3000 rpm) and cooking durations (15 or 30 min).

Temperature (°C)	Time (min)	Grinding (rpm)	PWM (%)	°Brix
70	15	300	48.8	13.7
70	30	300	42.9	13.1
70	15	3000	38.1	12.3
70	30	3000	35.1	13.0
95	15	300	43.5	13.3
95	30	300	43.2	13.7
95	15	3000	39.6	13.1
95	30	3000	41.6	12.1

Impact of cooking duration

Puree's viscosity remained nearly constant during processing for up to 30 min at 95 °C. This was in accordance with similar particle sizes, although serum viscosity increased. In purees heated at 70 °C, puree's viscosity decreased during processing but particle size and serum viscosity remained nearly constant. PWM decreased with increased cooking duration, maybe due to an increased water release out of the cells when they were broken. This could explain different viscosities between purees cooked for 15 or 30 min at 70 °C.

Since only minor differences were observed in aged apples during prolonged cooking, a 15 min process was sufficient to obtain contrasted purees.

Impact of grinding speed

Intense grinding led to a sharp decrease of viscosity, which was linked to particle size distribution. A powerful mechanical treatment thus led to individualized cells, no matter which temperature was applied during grinding. Increased grinding speed did not increase serum viscosity in this study. This might be linked to the raw material. The apples that were processed in this study were quite more mature than the apples used in Study I. Cell wall of these apples might be less intact and pectins attached less strongly to the cell wall. Consequently, even moderate grinding would be able to solubilise pectins. This might also explain the fact that serum viscosity was two to three times higher in the purees heated at 70 °C compared to the results of Study I, in which "fresh" apples (1 month of post-harvest storage) were processed into puree.

The colour of the continuous phase (**Fig. 85**) varied with the strength of mechanical treatment. High grinding speed led to more yellow and more opaque samples. This might be due to the presence of small particles that remain in the serum after separation or pectin solubilisation. This is an important question as both factors can affect serum viscosity. Although no small particles were detected in the serum (cf. **IV 3.6.2.**), presence of particles cannot be completely ruled out.

Fig. 85. Visual comparison of the continuous phase of apple purees prepared at 70 °C for 15 min at either 300 rpm (A) or 3000 rpm (B).

<u>Impact of temperature</u>

Only slight differences could be observed in puree's viscosity and particle size between the purees cooked at 70 and 95 °C. Interestingly, serum viscosity showed similar values for the purees cooked for 15 min at 70 and 95 °C. However, serum viscosity was about twice as high when the apples were cooked for 30 min at 95 °C. This highlighted the previous observation that hot temperatures better solubilised pectic polymers of the cell wall, even in aged apples.

2.1.2.3. Choice of process variables for main study

These preliminary studies were necessary to identify the process parameters that seemed the most suitable for the following main study. Since the modification of one process parameter involved the modification of another one, the parameters have to be chosen with caution. For example, a comparison of two different temperatures was not simple as the time needed to reach 95 °C was longer than for lower temperatures. Consequently, cooking duration and grinding were prolonged. It was thus proposed to grind at the lowest possible speed (100 rpm in this case) during temperature increase. This mixed the apple pieces for thermal homogenisation but damage to tissue structure was minimal.

Purees prepared by a grinding speed of 300 rpm for 15 min at 70 °C were considered smooth enough to be analysed unambiguously by rheology. In the following main study, three temperatures (70, 83, 95 °C) and three grinding speeds (300, 1000, 3000 rpm) will thus be applied. As no difference could be detected between purees prepared at 50 or 70 °C, only 70 °C was retained. Nevertheless, a temperature lying in between the extremes was chosen in order to have three points. Although purees with contrasted structure and texture were obtained after 15 min, the 30 min process was chosen in order to force cell wall modifications. Prolonged cooking might enhance pectin hydrolysis, since the pH in apples (circa 3.5) is close to optimal preservation of pectins (Liu, et al., 2021).

Pasteurization will be avoided since a treatment of 2 min at 95 °C was shown to enhance pectin solubilisation (cf. **V 2.1.1.4.**), which would also affect the results. Since some interesting differences were observed concerning apple maturity, the impact of the chosen process parameters will be studied on "fresh" (1 month of post-harvest storage) and stored (6 months of post-harvest storage) apples.

2.1.3. Conclusions

The presented processes were clearly exaggerated and not applicable in food industry as purees were cooked for up to several hours. However, they helped to better understand the mechanisms that determine the final viscosity of apple purees.

Increased grinding speed decreased particle size. Cell separation was enhanced by cooking at 95 °C and apple maturity due to pectin solubilisation, which reduced cell adhesion. However, pectin degradation was not sufficient to ensure on its own cell separation. Intense grinding led to tissue disruption, irrespective of pectin solubilisation. Smaller particles decreased viscosity of apple purees and seemed to be the dominant factor in explaining puree's viscosity.

PWM, determined by centrifugation of the puree, was not affected by grinding but increased when the puree was heated to 95 °C and in mature apples. This could be due to increased water retention capacities of the cell wall when damaged due to temperature increase or longer maturation period. When particle size was constant, increased PWM determined puree's viscosity.

Intense grinding seemed to facilitate pectin extraction, maybe due to a better extractability of pectins from more disrupted cell walls. However, this seemed to be only true for elevated temperatures (95 °C) and only for "fresh" apples. When apples that were stored for six months at 2 °C were processed into puree, no effect of grinding on serum viscosity was observed, but initial serum viscosities were noticeably higher. Serum viscosity increased fivefold when a temperature of 95 °C was applied during processing, whereas low temperatures (50–70 °C) had no effect. It thus seemed that only high temperatures induced pectin degradation and thus solubilisation during processing. This explained enhanced cell separation and PWM at high temperatures. Prolonged heating (more than one hour) at 95 °C decreased serum viscosity, probably due to pectin depolymerisation. Literature attributes serum viscosity a less important role. However, in apple purees showing the same particle size distribution and similar PWM, the viscosity of the continuous phase determined puree´s viscosity.

Low temperature treatments did not alter cell wall microstructure. Hence, enzymatic activity in apples seemed to be not sufficient to cause pectin degradation during processing. A pasteurization step of only 2 min at 95 °C altered cell wall structure. Possible alterations of puree's viscosity have thus to be kept in mind when pasteurization is necessary.

Highlights

- Intense grinding disrupted apple tissue irrespective of pectin solubilisation.

- Pectin degradation alone was not sufficient to ensure cell separation.

- Pulp wet mass was not altered by grinding in combination with heat.

- In some cases, intense grinding facilitated pectin extraction.

- Enzymatic activity in apples was not sufficient to cause pectin degradation during processing.

- Low temperature pre-treatments did not alter cell wall structure.

- Pasteurization step of 2 min at 95 °C altered puree's structure and viscosity.

2.2. Combination of thermomechanical processes

The process conditions established in **V 2.1.** were used in this study to investigate their impact on puree's texture and structure more in detail. A combination of three thermal (70, 83, 95 °C) and three mechanical (300, 1000, 3000 rpm) treatments were thus applied on one apple cultivar, namely Golden Delicious (thinned). Since post-harvest storage was shown to highly affect puree's structure, apples were processed after one (2019 harvest) and six (2018 harvest) months of cold storage. Special attention was paid to soluble pectins as they might explain differences in structural factors, which determine puree's texture. Pectin composition and structure were thus analysed in order to elucidate the chemical processes that occur during apple processing and post-harvest storage.

This study thus considered the following questions:

❖ In a thermomechanical process, what is the relative role of thermal and of mechanical treatments on apple puree's texture?

❖ What are the interactions between apple maturity and processing?

❖ Can pectin modifications explain the observed differences?

> The results are presented in form of a research article, which is in preparation for submission to *Food Hydrocolloids*.

Pectin degradation explains tissue fragmentation of fruits during thermomechanical processes for puree production

Alexandra Buergy[a], Agnès Rolland-Sabaté[a, *], Alexandre Leca[a], Xavier Falourd[b], Loïc Foucat[b], Catherine M. G. C. Renard[c]

[a] *INRAE, Avignon Université, UMR SQPOV, 84000 Avignon, France*
[b] *INRAE, UR 1268 Biopolymères Interactions Assemblages, 44316 Nantes, France*
[c] *INRAE, TRANSFORM, 44000 Nantes, France*

Abstract

The relationship between fruit and puree's characteristics is still poorly understood. In particular, it is not understood how pectin solubilisation and degradation alter the texture of plant-cell dispersions and how a targeted application of processing conditions can be used to design naturally textured food products. Systematic combinations of thermal and mechanical treatments with three different temperatures (70, 83, 95 °C) and grinding speeds (300, 1000, 3000 rpm), applied on one-month (T1) and six-months stored (T6) apples, were used to generate apple purees with contrasted structural and textural characteristics. At T1, serum viscosity increased with increased temperature (8–104 mPa.s), in parallel with marked increase in pectin solubilisation (1–6 mg/g serum), and changes in its composition and structure. At T6, pectin showed decreased galactose, leading to facile cell separation, low serum viscosities (~16 mPa.s) and limited impact of process conditions. Grinding had limited impact on pectin solubilisation at T1 and T6, but strongly impacted particle size (498–1096 µm) and puree's texture (116–1475 mPa.s) at T1. Tissue fragmentation was favoured by temperature increase and grinding at T1 and by maturation of raw apples. Apples responded differently to process parameters depending on their maturation level, which was linked to pectin degradation and notably loss of side chains.

Apple, Texture, Rheology, Particle size, Cell separation, Polysaccharide

2.2.1. Introduction

Plant-based purees are suspensions of individual cells and cell clusters (pulp) that are dispersed in an aqueous phase (serum) (Rao, 1992). Texture is an important quality characteristic of plant-based dispersions (Szczesniak & Kahn, 1971) and is determined by particle size distribution, pulp content and serum viscosity (Espinosa, et al., 2011; Leverrier, et al., 2016; Rao, 1992). These factors can be modulated by the application of particular thermal and mechanical treatments on raw material in order to optimize the textural characteristics of pureed food without the addition of texture-controlling agents such as starches, gums and stabilizers. Many studies focused either on the effect of thermal (Anthon, Diaz, & Barrett, 2008; Christiaens, et al., 2012) or mechanical (Espinosa, et al., 2011; Moelants, et al., 2012; Moelants, et al., 2014b) treatments and only few studies analysed systematically the combined effect of thermal and mechanical processes on puree's texture (Day, et al., 2010; Lopez-Sanchez, et al., 2011). However, both heating and grinding are complementary during processing since both treatments alter puree's structure.

The structural characteristics are linked to modifications in pectin structure and composition (Sila, et al., 2009) as they are the polysaccharides in the plant cell wall that are the most vulnerable to enzymatic and chemical degradation and thus solubilisation during processing (Van Buren, 1979). Pectins contribute to intercellular adhesion as well as cell wall porosity and strength (Carpita & Gibeaut, 1993; Jarvis, 1984) and their degradation and solubilisation during processing induce tissue softening. Tissue can then be partly disrupted through mechanical treatment.

Pectins are a complex group of polysaccharides, comprising homogalacturonan (HG), rhamnogalacturonan I (RG I) and II (RG II). HG is composed of a linear chain of α-1,4-linked galacturonic acids, which can be methyl-esterified at the C6 positions. The degree of methylation (DM) but also the distribution of ester groups over the HG backbone are crucial since sequences of several consecutive non-esterified galacturonic acids can induce cross-links with calcium ions (Kohn & Luknár, 1977). This mechanism may contribute to cell-cell adhesion in the middle lamella. During processing, endogenous pectin methylesterase (PME) can demethoxylate the HG backbone, which can consequently either be cross-linked by calcium ions and thus increase cell adhesion and texture (Waldron, et al., 1997) or be further degraded by

polygalacturonase (PG) (Sila, et al., 2009) and thus result in texture loss. While enzyme activity is rapidly inactivated by heat, chemical reactions are generally promoted. Due to an acid pH in apples and other fruits, pectins are mainly susceptible to acid hydrolysis, while β-elimination is less important during the production of fruit-based foods (Waldron, et al., 2003). Although the most studied changes are reported for HG pectins, RG I domains are also susceptible to heat treatment. RG I consists of a backbone with alternating rhamnose and galacturonic acid molecules. Rhamnose residues can be decorated by neutral sugar side chains, composed of galactose and/or arabinose (Ridley, et al., 2001). Arabinans are known to be particularly susceptible to acid hydrolysis, followed by galactans (Green, 1967; Thibault, et al., 1993), and "debranching" (i.e. loss of arabinans and galactans) was associated with decreased cell adhesion in apple fruits (Nara, et al., 2001; Pena & Carpita, 2004). RG II, accounting for less than 10% of pectins, has a backbone of galacturonic acids, which carry several complex oligosaccharide side chains (Mohnen, 2008; Ndeh, et al., 2017).

Although modifications in pectin composition and structure are crucial in understanding the impact of processing on the structure and thus texture of plant-based food, no extensive study analysed the combined effect of thermal and mechanical treatment on pectins. This study thus aimed to elucidate the process-structure-function relationship of pectins and their impact on apple puree's texture mediated by particle size, pulp wet mass and serum viscosity, by applying combinations of three temperature and grinding regimes. As pectin modifications in the raw material linked to post-harvest storage alters puree's texture (Buergy, et al., 2020), the impact of processing conditions was compared between apples stored for one and six months.

2.2.2. Material and Methods

2.2.2.1. Plant material

Apple (*Malus x domestica* Borkh.) cultivar Golden Delicious was grown in Mallemort, France and harvested in September 2018 and 2019 corresponding to the commercial harvest dates. In 2018, apples were thinned chemically by 3 L/ha PRM 12® RP (ethephon, 17 April 2018), 2 L/ha PRM 12® RP (24 April 2018), 3.5 L/ha MaxCel® (6-Benzylaminopurine) and 1.5 kg/ha Rhodofix® (1-naphthalenacetic acid, 30 April 2018) and 3.5 L/ha MaxCel® (4 May 2018). In 2019, apples were thinned by application of 18 L/ha ATS (ammonium thiosulphate, 20 April 2019), 0.15 kg/hL Rhodofix® (27 April 2019) and 5 L/ha MaxCel® (4 May 2019). Apples harvested in 2018 were stored for six months (T6) and apples harvested in 2019 for one month (T1) at 4 °C in normal atmosphere. One day before processing, apples were divided into two equal groups. The first batch was used to isolate the alcohol insoluble solids (AIS) as described later, the second batch was processed into puree.

2.2.2.2. Puree preparation

Approximately 3 kg of apples were cored, cut into 12 pieces and processed under vacuum using a cooker-cutter (RoboQbo Qb8-3, RoboQbo, Bentivoglio, Italy), equipped with two microserrated cutting blades and a mixing blade. Apples at T1 and T6 were processed under equal conditions (**Fig. 86**). Each temperature (70, 83, 95 °C) was combined with each blade rotation speed (300, 1000, 3000 rpm), leading to nine different processes. Each process was conducted in triplicate.

Since temperature increase was longer for higher temperatures (difference of 140 s between 70 and 95 °C), a low blade rotation speed of 100 rpm was applied during this period. This mixed the apples without grinding. Once the working temperature was reached, blade rotation speed was raised and maintained for 30 min.

Purees were not refined. Rheology, particle size and pulp wet mass were determined once purees reached room temperature. Analytical measurements were conducted on frozen samples.
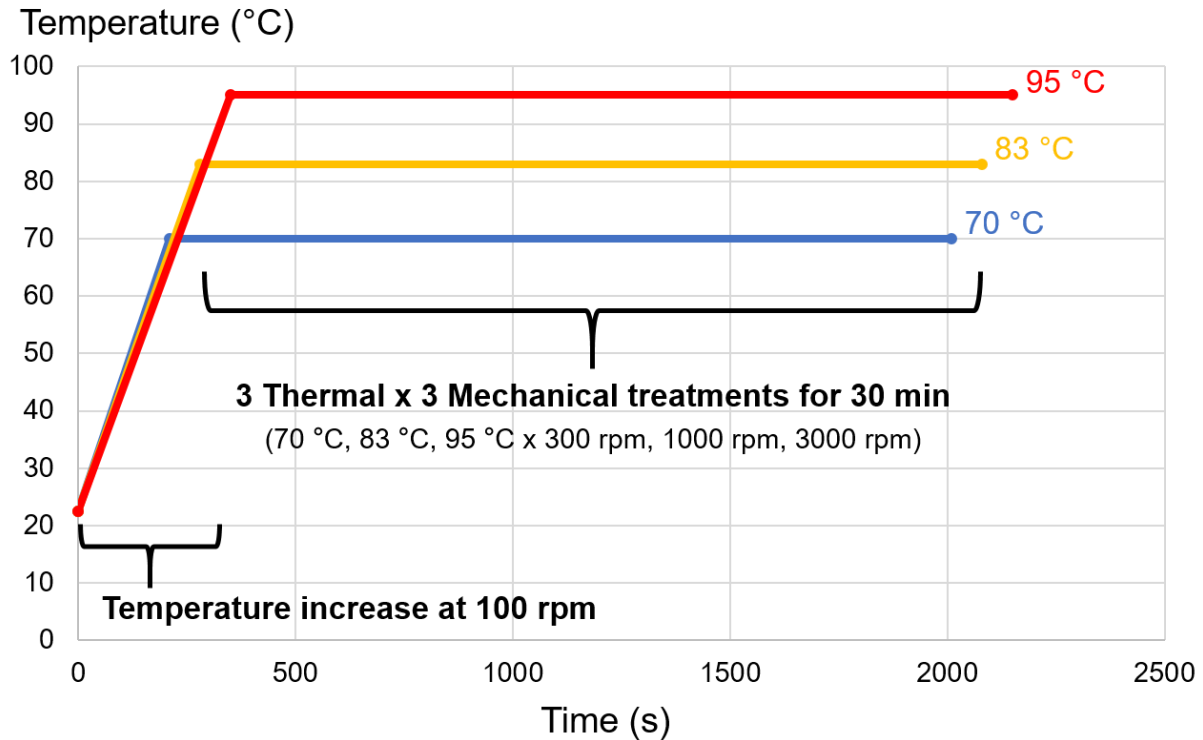
Fig. 86. Simplified scheme of applied thermomechanical conditions during apple processing into puree.

2.2.2.3. Physico-chemical characterization

Rheology of purees and sera

Rheological analyses of both purees and sera were conducted at 22.5 °C as reported previously (Buergy, et al., 2020). A stress-controlled rheometer (Physica MCR301), equipped with a Peltier cell (CPTD-200) and a measuring cylinder (CC27/S) from Anton Paar (Graz, Austria) was used. For purees, flow curve and amplitude sweep were measured using a vane measuring system (FL100/6W). Rheological analyses were theoretically not adapted for purees with particles larger than 1 mm since the gap of the measuring system was 3.46 mm large. Rheological values obtained for purees prepared at 70 and 83 °C and 300 rpm should thus be treated with caution.

Serum viscosity was measured by a flow curve using a double gap cylinder geometry set (DG27).

Particle size distribution

Laser granulometry (Mastersizer 2000, Malvern Instruments, Malvern, UK) was employed to measure the particle size distribution in the puree as described before (Buergy, et al., 2020). The Malvern's software averaged the size distribution over three repeated measurements on the same sample. Each puree was analysed twice.

Pulp wet mass (PWM) and water retention capacity (WRC)

The puree was centrifuged (7690 x g, 15 min, 15 °C) into pulp and serum. The ratio of the pulp weight to the initial weight of the puree was defined as the PWM and expressed in % (Espinosa, et al., 2011). The WRC of the pulp was calculated as the amount of water retained by the mass of the pulp's cell wall polysaccharides (g/g dry weight) (Robertson, et al., 2000). It was estimated as the ratio of the PWM and the pulp's dry weight. The WRC was only analysed for samples at 3000 rpm since these purees represented individual cells. One sample of each temperature was measured, both at T1 and T6.

2.2.2.4. Analytical

Cell wall isolation and serum precipitation

Cell wall polysaccharides were extracted as alcohol insoluble solids (AIS). The protocol established by Le Bourvellec, et al. (2011) was applied for preparation and AIS extraction (ethanol, 700 mL/L) of raw apples. AIS were expressed in mg/g fresh weight (FW).

Pulp was water-washed and AIS were isolated as described previously (Buergy, et al., 2020). The AIS of the pulp was calculated as the ratio of the dry pulp weight and the initial pulp weight after water-washing and expressed in mg/g FW.

Serum AIS were isolated by alcohol precipitation according to Buergy, et al. (2020). The ratio of the weight of the dry sample and the initial weight of serum roughly estimated the soluble pectin content in the continuous phase. Serum AIS were expressed in mg/g serum FW. AIS extraction was conducted for all three replicates at T1 but only for one at T6 since the main study focused on apples stored for one month.

Cell wall polysaccharide analysis

After acid hydrolysis of neutral sugars and the internal standard myo-inositol (Saeman, et al., 1954), the free sugars were derivatized to volatile alditol acetates (Englyst, et al., 1982). They were analysed at 230 °C using a Clarus 500 gas chromatograph (PerkinElmer, Waltham, USA), which was equipped with a flame ionization detector (FID) and a OPTIMA® capillary column (30 m × 0.25 mm i.d., 0.25 µm film thickness, Macherey-Nagel, Düren, Germany). Helium was used as carrier gas.

The content of galacturonic acid (GalA) in the acid hydrolysates was determined spectrophotometrically by the *m*-hydroxydiphenyl assay (Blumenkrantz & Asboe-Hansen, 1973).

Methanol was quantified by stable isotope dilution assay after saponification (Renard & Ginies, 2009). It was analysed on a Trace 1300 gas chromatograph (Thermo Scientific, Waltham, USA), equipped with a TG-WaxMS capillary column (30 m × 0.25 mm i.d., 0.5 µm film thickness, Thermo Scientific, Waltham, USA) and coupled to an ISQ LT single quadrupole mass spectrometer (Thermo Scientific, Waltham, USA).

The molar ratio of methanol to GalA gave the degree of methylation (DM) that was expressed in %.

Starch determination

The total starch assay kit K-TSTA (Megazyme, Wicklow, Ireland) was used to quantify the starch content in the AIS of serum and raw apples. The specified enzyme concentrations were doubled since residual polyphenols in the AIS might reduce enzyme activity. Each sample was analysed in duplicate. All values for AIS, neutral sugars, GalA and methanol were adjusted by the respective starch content.

High performance size-exclusion chromatography coupled to multi-angle laser light scattering (HPSEC-MALLS) and online viscometry

Molar mass and size distribution of soluble pectins were determined by HPSEC, coupled to a multi-angle laser light scattering detector (DAWN HELEOS 8+ (Wyatt Technology, Santa Barbara, USA) fitted with a K5 flow cell and a GaAs laser, λ = 660 nm), a differential refractive index detector (Shimadzu, Tokyo, Japan) and an online viscometer (Viscostar III, Wyatt Technology). The same equipment and sample preparation were used as described by Buergy, et al. (2020). Pectins were solubilised directly in the eluent (acetate buffer, 0.2 M, pH 3.6) to a concentration of 2.5 mg AIS/mL (serum) or 10 mg AIS/mL (raw apples) and eluted at a flow rate of 0.6 mL/min at 40 °C. Samples were separated by three PolySep-GFC columns (P3000, P5000 and P6000, 300 × 7.8 mm) and a guard column, all from Phenomenex (Le Pecq, France). ASTRA® software (Wyatt Technology, version 7.3.2.19 for PC) was used for data treatment as detailed before (Buergy, et al., 2020). The weight-average molar mass $\overline{M}_w$, the z-average intrinsic viscosity $\overline{[\eta]}_z$ and the z-average viscometric hydrodynamic radius $\overline{R}_{hz}(v)$ were obtained at the summit of the main peak. Each sample was injected once. At T1, samples of the first repetition were not considered since molar mass distribution was significantly different from the other repetitions.

Nuclear magnetic resonance spectroscopy (NMR)

^{1}H-NMR was employed to visualize β-elimination products in the serum AIS according to Tjan, et al. (1974). At 4 °C, AIS (5 mg/mL) were solubilised for 1 h in distilled water before adjusting to pH 6 with NaOH. The samples were centrifuged (4272 x g, 15 min, 4 °C) to eliminate possible cell wall remnants. The supernatant was freeze-dried before the sample was suspended in D_2O (0.75 mL) for one night at 4 °C. The sample was freeze-dried again and the operation was repeated. Samples obtained at all temperatures (3000 rpm, T1) were analysed. A positive control was also prepared by heating serum AIS (95 °C, 3000 rpm) (5 mg/mL in distilled water) at pH 6 for 30 min at 100 °C. Afterwards, the control was readjusted to pH 6 and treated in the same way as the samples. Samples and the control were analysed in D_2O on a NMR spectrometer (AvanceIII 400 NB, Bruker, Billerica, USA), equipped with a BBO 5 mm probe. A quantitative 1D ^{1}H spectrum was recorded at 70 °C. A [1]H 90° pulse of 10.2 µs and an accumulation of 128 scans with a recycling delay of 10 s were the most

significant acquisition parameters for the 1D sequence including a water signal presaturation and were applied to decrease the HDO signal in the same order of magnitude than the others peaks.

NMR relaxation was used to estimate cell wall porosity in samples ground at 3000 rpm for all temperatures and both T1 and T6, since they all presented individual cells. Pulp AIS (100 mg) were rehydrated in distilled water, excess water was gently removed and transverse relaxation (T_2) was measured at 4 °C on a Bruker Minispec mq20 (20 MHz, 0.47 T), which was equipped with a thermostated ^{1}H probe using the Carr-Purcell-Meiboom-Gill pulse sequence. Echo time was 0.5 ms, 2000 points were collected and 128 scans were acquired with a recycle delay of 7 s. T_2 relaxation curves were analysed by a continuous approach as described by Lahaye, et al. (2018).

2.2.2.5. Statistical analysis

Analyses were generally conducted once for each of the three repetitions. Exceptions are stated in the text. The Shapiro-Wilk test indicated that not all results were normally distributed. Hence, Kruskal-Wallis non-parametric test (Kruskal & Wallis, 1952) was employed to access differences between the samples at the 95% level of significance, using the XLSTAT package (Addinsoft, 2020) for Microsoft Excel. Pooled standard deviations (PSD) were calculated for each series of repeated measurement using the sum of individual variances weighted by the individual degrees of freedom (Box, et al., 1978). R statistical software (R Core Team, 2018) was used to perform principal component analysis (PCA) and linear regression using the packages "FactoMineR" (Lê, et al., 2008) and the "stats" package, included in the base of R statistical software, respectively.

2.2.3. Results

Given the fact that purees prepared at 50 and 70 °C in a preliminary test resulted in equal puree's texture, it was concluded that enzymatic activity in apples was not sufficient to cause pectin degradation during processing and 70 °C was retained as the lowest temperature.

2.2.3.1. Textural characteristics of apple purees

Contrasted textures were obtained with the various temperatures and grinding speeds (**Fig. 87**). However, puree's viscosity (**Fig. 88**A) obtained at 70 °C and 300 rpm showed a high standard deviation. This was caused by heterogeneous puree's texture due to large cell clusters of former apple tissue that was not separated sufficiently by slow grinding (**Fig. 87**). Therefore, the values obtained for these purees have limited reliability. When they were not considered, increased grinding speed decreased significantly puree's viscosity (**Table 24**).
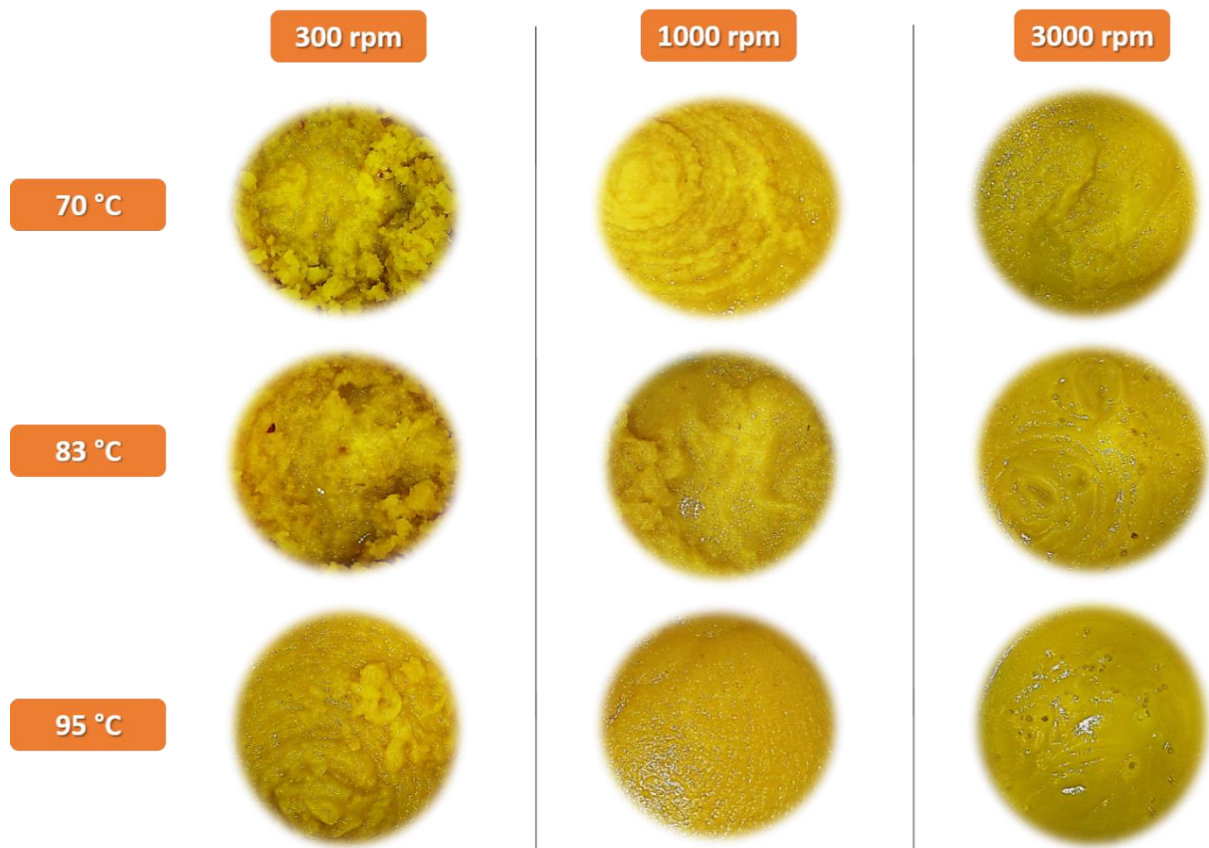
Fig. 87. Visual aspects of purees prepared by different thermomechanical conditions (70, 83 or 95 °C and 300, 1000 or 3000 rpm) with apples stored for one month.
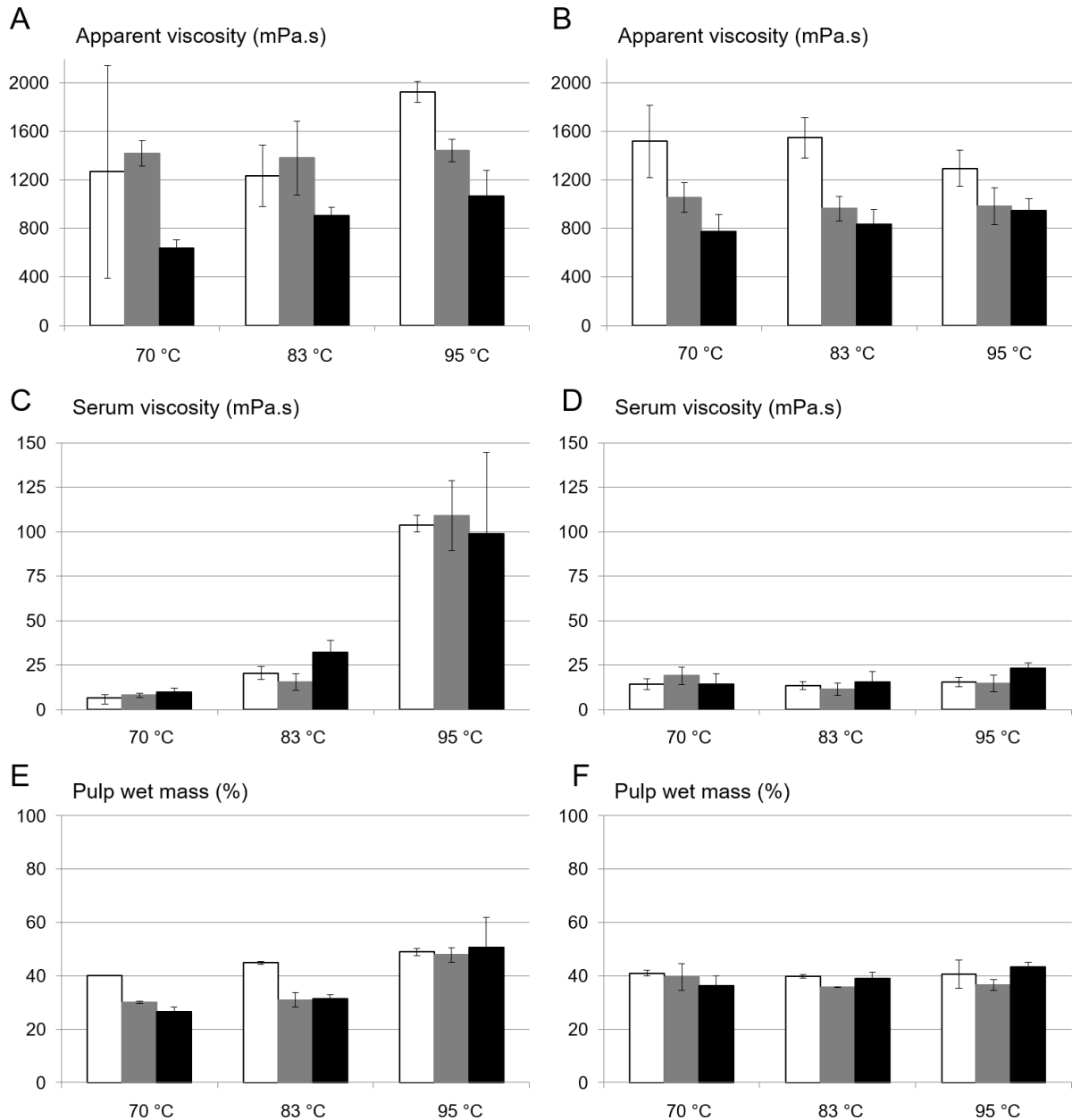
Fig. 88. Apparent viscosity at 50 s^{-1} (A, B), serum viscosity at 100 s^{-1} (C, D) and pulp wet mass (E, F) for purees obtained with different temperatures and grinding speeds at T1 (A, C, E) and T6 (B, D, F).

White bars represent purees ground at 300 rpm, grey bars purees ground at 1000 rpm and black bars purees ground at 3000 rpm.

The impact of temperature was not significant, although high temperatures seemed to increase puree's viscosity, especially at 3000 rpm. Other textural characteristics such as yield stress, G' and G" (**Table 24**) also decreased significantly with increased grinding but were not influenced by temperature. The same trend could be observed

at T6 (**Table 24**) and the effect of grinding on apparent viscosity was more evident (**Fig. 88**B). As even slow grinding speeds led to homogenous puree's textures, the range of apparent viscosity values was slightly reduced compared to T1. However, storage duration did not significantly alter textural characteristics in this experiment.

Table 24. Kruskal-Wallis *H*- and *P*-values performed on apparent puree viscosity at 50 s^{-1} (ηapp), yield stress (YS), storage (G') and loss (G'') modulus at an angular frequency of 10 rad/s, pulp wet mass (PWM), particle size d.09 (d0.9) and serum viscosity at 100 s^{-1} (ηserum).

		η_{app} 50 s^{-1}	YS	G'	G''	η_{serum} 100 s^{-1}	PWM	d0.9
		(mPa.s)	(Pa)	(Pa)	(Pa)	(mPa.s)	(%)	(μm)
T1	Temperature H	4.1	1.5	0.9	0.4	23.1	16.8	6.4
	Temperature P	0.128	0.466	0.618	0.834	**<0.001**	**< 0.001**	**0.041**
	Grinding H	10.9	19.4	21.6	22.6	0.4	4.9	15.0
	Grinding P	**0.004**	**<0.001**	**<0.001**	**<0.001**	0.825	0.087	**<0.001**
T6	Temperature H	0.04	1.8	1.0	0.4	4.5	1.1	0.8
	Temperature P	0.979	0.408	0.599	0.808	0.107	0.582	0.675
	Grinding H	19.5	20.1	22.1	23.1	1.5	6.7	23.1
	Grinding P	**<0.001**	**<0.001**	**<0.001**	**<0.001**	0.466	**0.036**	**<0.001**
Storage H		1.5	0.9	0.001	0.07	1.5	0.006	6.9
Storage P		0.223	0.346	0.979	0.789	0.216	0.938	**0.009**

2.2.3.2. Determinants of apple puree's texture

Serum viscosity

Serum viscosity was significantly altered by temperature increase at T1 (**Fig. 88**C) but not at T6 (**Fig. 88**D). Especially at T1, the colour of sera was more intense with increased grinding speed (**Fig. 89**). This might be due to small particle fragments that maintained in the serum. However, this seemed not to alter serum viscosity since the grinding speed had no significant effect on serum viscosity.
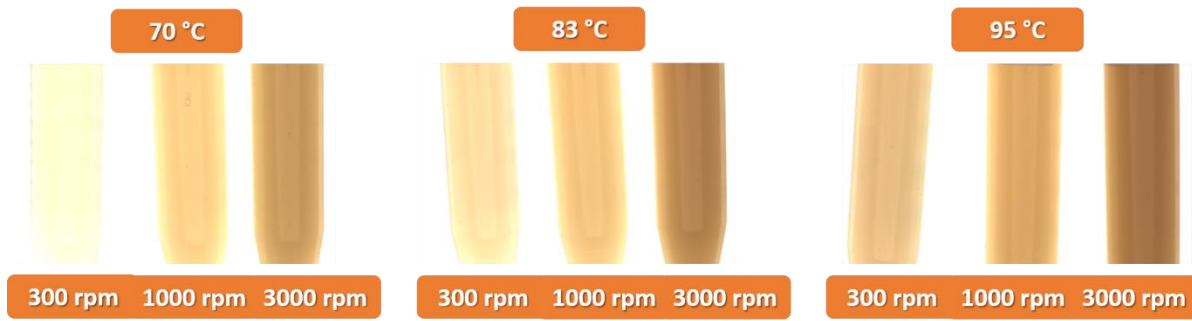
Fig. 89. Colour variations of sera prepared by different thermomechanical conditions (70, 83 or 95 °C and 300, 1000 or 3000 rpm) with apples stored for one month.

Overall, storage duration did not significantly modify serum viscosity (**Table 24**). However, the interaction storage duration x temperature had a major impact, as T1 showed lower serum viscosity values for 70 °C and impressively higher values for 95 °C than T6.

Pulp wet mass, water retention capacity and cell wall porosity

Pulp wet mass at T1 (**Fig. 88**E) was similar for purees obtained at 70 and 83 °C but significantly higher at 95 °C. Grinding speed did not induce significant differences (**Table 24**). The higher pulp wet mass of the purees obtained at 300 rpm (70 and 83 °C) must result from intact cell clusters, which did not pack as easily during centrifugation. Cell clusters are more rigid as their tissue structure is more preserved and they occupy thus more volume (Leverrier, et al., 2016; Lopez-Sanchez, et al., 2012).

At T6, temperature did not induce different PWM values (**Fig. 88**F). Grinding showed a slight significant impact on PWM but no trend could be observed. Overall, PWM was not significantly altered with storage duration. However, PWM of aged cells seemed to be higher when moderate temperatures (70 and 83 °C) and high grinding speed (1000 and 3000 rpm) were applied. With low grinding (300 rpm) or high temperature (95 °C), storage duration resulted in similar PWM.

Both at T1 and T6, WRC of the pulp (**Fig. 90**A) increased in purees obtained at 95 °C. When cells aged, WRC were higher compared to T1 in purees produced at moderate temperatures (70 and 83 °C) but similar in purees prepared at high temperatures (95 °C). T_2 relaxation times (**Fig. 90**B) showed water mobility in rehydrated pulp AIS.

296
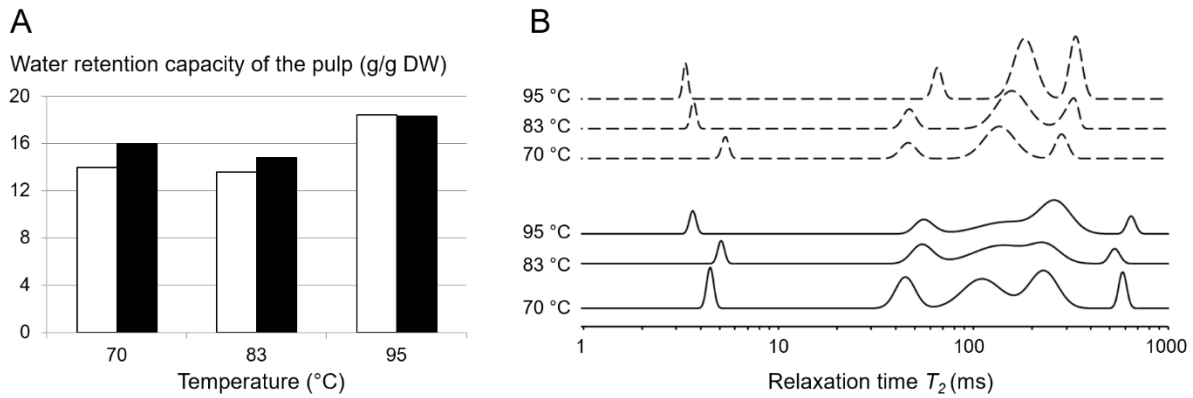
Fig. 90. Water retention capacity of the pulp (A) and relaxation times T_2 (B) for purees with different temperatures and ground at 3000 rpm at T1 (white bars or continuous lines) and T6 (black bars or dashed lines).

As the T_2 relaxation times increase, water mobility in the system also increases. This can be roughly linked to porosity of the material since an increase in T_2 relaxation times involve, among others, an increase in average pore size (Meng & Ragauskas, 2014). At T1, five environments with large distributions were detected, whereas only four, narrower environments were present at T6, indicating homogenisation of the samples at T6. The environment of the weak water mobility around 4 ms corresponded to protons that are associated with macromolecules and represent a pore size between 5 and 7.5 nm (Barron, et al., 2020). These values tended to decrease with increased temperature, indicating reduced pore size with higher temperatures. Due to the absence of repetitions, this decrease was, however, not considered significant. Environments with higher relaxation times (45–334 ms) all tended to increase with increased temperature. This partly indicated an increase in pore size of 15–120 nm (Barron, et al., 2020). Water mobility showed, mainly, higher T_2 relaxation times in aged cells. The exact values can be viewed in **Table 25**.

Similar results were obtained with fresh puree (results not shown). However, other measurements, such as Simons' stain or NMR cryoporometry (Meng & Ragauskas, 2014), should be conducted to confirm the impact of temperature on cell wall porosity.

Table 25. Relaxation times T_2 and associated proportions P_2 of the different environments a-e in the NMR spectrum for rehydrated apple pulp AIS. Values were determined by continuous analysis of the multi-exponential relaxation curves.

		T_{2a}	T_{2b}	T_{2c}	T_{2d}	T_{2e}	P_{2a}	P_{2b}	P_{2c}	P_{2d}	P_{2e}
				(ms)					(%)		
T1	70	583	227	111	45	4.5	8	32	34	18	8
	83	530	236	140	55	5.1	7	20	47	19	7
	95	643	263	150	56	3.6	7	43	30	12	7
T6	70	-	283	136	46	5.3	-	18	58	15	9
	83	-	312	158	47	3.7	-	21	59	13	8
	95	-	334	183	65	3.3	-	30	52	11	7

Particle size distribution

At T1 and T6, particle size decreased with increased grinding speed (**Fig. 91**), although to different extents (**Table 24**). At T1, particle size was influenced additionally by temperature (**Fig. 91**A). Purees prepared at low grinding speeds (300 and 1000 rpm) and moderate temperatures (70 and 83 °C) showed a bimodal distribution with a main peak around 950 µm and a shoulder, showing the presence of smaller particles. After grinding at 3000 rpm, particles showed a monomodal distribution around 480 µm for 70 °C and 360 µm for 83 °C. Particle size distributions for purees heated at 95 °C were all narrower and exhibited lower sizes for all grinding speeds, 630 µm, 315 µm and 210 µm for purees ground at 300, 1000 and 3000 rpm, respectively. Apple cells are expected to be around 200 µm in size (Espinosa-Munoz, et al., 2013; Khan & Vincent, 1990). Hence, only purees produced with maximal temperature and grinding speed (95 °C, 3000 rpm) led to individualised cells at T1. At T6 (**Fig. 91**B), particle size depended only on grinding speed (**Table 24**). Whereas purees ground at 300 rpm showed a large peak with a small shoulder, purees prepared with a grinding speed of 1000 and 3000 rpm already presented a large amount of individual cells for all temperatures.
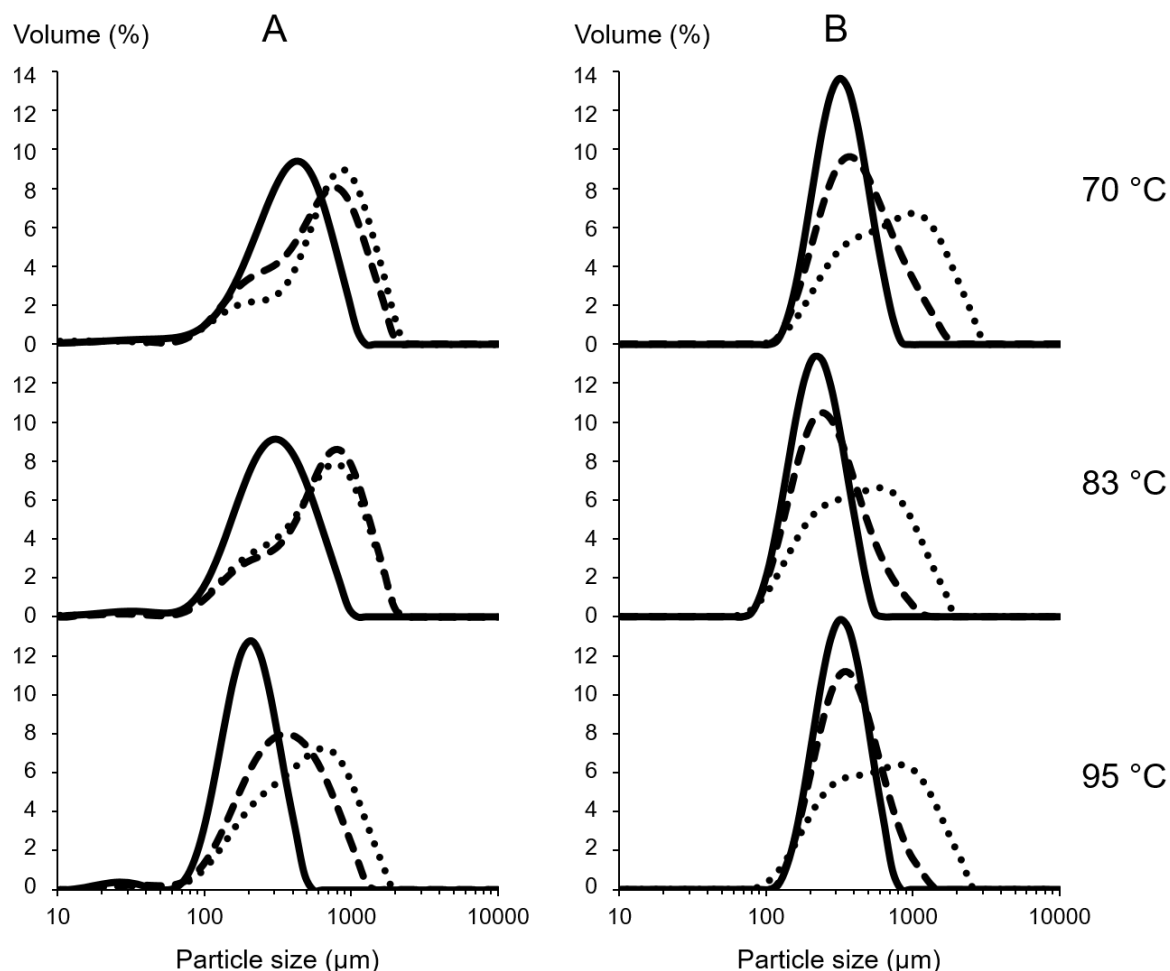
Fig. 91. Particle size distribution of purees obtained with different temperatures and grinding speeds at T1 (A) and T6 (B).

Dotted lines represent purees ground at 300 rpm, dashed lines purees ground at 1000 rpm and continuous lines purees ground at 3000 rpm.

2.2.3.3. Chemical composition of serum pectins

At T1, the amount and chemical composition of soluble pectins was significantly altered by temperature but not by grinding (**Table 26**). Serum AIS increased significantly with increased processing temperature. The amount of starch in the serum increased significantly with temperature and slightly with grinding speed. The GalA content in serum AIS also increased with temperature. All soluble pectins were highly methylated and the DM was not affected by temperature (results not shown). The ratio GalA/rhamnose estimates the proportion of HG to RG I pectins and was not altered either by temperature or by grinding. The ratio of (arabinose+galactose)/rhamnose, estimating RG I side chain branching, decreased with increased temperature.

Apparently, galactan side chains were more susceptible to temperature than arabinans since the ratio galactan/arabinan decreased when temperature increased, or pectin RG I fractions rich in arabinans were more tightly bound to the cell walls and required more degradation for solubilisation.

Interestingly, at T6, the serum AIS content was higher for 70 °C but increased much less with temperature than at T1, and its composition was stable, whatever the grinding or temperature (**Table 26**). As an exception, the ratio galactan/arabinan decreased with increased temperature but the values were less dispersed than at T1 and the overall ratio of (arabinose+galactose)/rhamnose was not modified. Starch was not detected in the serum at T6. The GalA content was higher at T6, probably due to a strong decrease in RG I side chains arabinose and galactose, leading to higher relative GalA proportion. At T1, the ratio of HG to RG I, expressed as GalA/rhamnose, was not altered either by temperature or by grinding. Although the GalA content was higher at T6, more RG I was extracted, especially by grinding.

Raw apples showed the same trends in pectin composition during post-harvest storage in terms of RG I side chain loss, GalA increase and more RG I (**Table 27**).

2.2.3.4. Macromolecular characteristics of serum pectins

Macromolecular characteristics of soluble pectins (**Table 26**) give information about molecular structure and density. At T1, molar mass was not significantly altered by temperature but showed an overall decrease when higher temperatures were applied. Intrinsic viscosity was significantly affected by temperature increase, leading to reduced values at 95 °C in spite of higher pectin concentrations. Lower intrinsic viscosities at 95 °C for comparable molar mass as 70 and 83 °C indicated more compact pectins. This was confirmed by d_{happ}, a value estimating apparent polymer density. It was similar for 70 and 83 °C but significantly higher for 95 °C. Molar mass and intrinsic viscosity were significantly lower at T6, roughly half those at T1, whereas pectin density (d_{happ}) increased by more than 2-folds. This indicated more linear but denser pectins at T6, which could be linked to higher GalA and less arabinose and galactose in these pectins (**Table 26**).

Table 26. AIS yield, composition and macromolecular characteristics of serum pectins, followed by Kruskal-Wallis *H-* and *P*-values.

Storage (months)	Temp. (°C)	Grinding (rpm)	AIS$_{serum}$ (mg/g FW)	Starch (mg/g FW)	GalA (mg/g AIS)	$\dfrac{GalA}{Rha}$	$\dfrac{Ara+Gal}{Rha}$	$\dfrac{Gal}{Ara}$	$\overline{M}_w \times 10^3$ (g/mol)	$\overline{[\eta]}_z$ (mL/g)	d_{happ} (g nm^3/mol)
1	70	300	0.9	0.1	527	73	24	1.4	311	1903	0.8
		1000	1.1	0.2	556	94	24	1.4	545	1869	0.8
		3000	1.6	0.5	470	60	26	1.3	480	1811	0.8
	83	300	2.1	0.4	554	117	22	1.2	493	1609	0.9
		1000	1.7	0.4	539	88	25	1.2	522	1760	0.9
		3000	3.0	0.6	543	93	25	1.0	455	1783	0.8
	95	300	5.3	0.5	646	74	17	0.8	406	1229	1.2
		1000	5.8	1.0	602	82	21	0.8	425	1272	1.2
		3000	6.2	1.3	577	81	22	0.8	409	1268	1.2
6*	70	300	2.1	ND	683	52	8	1.1	157	510	3.0
		1000	1.8	ND	593	26	6	1.2	188	488	3.1
		3000	3.0	ND	605	30	7	1.0	273	579	2.6
	83	300	2.4	ND	663	48	7	1.0	166	583	2.6
		1000	2.5	ND	601	26	6	0.9	204	650	2.3
		3000	3.1	ND	605	27	6	1.0	229	620	2.4

Storage (months)	Temp. (°C)	Grinding (rpm)	AIS_{serum} (mg/g FW)	Starch (mg/g FW)	GalA (mg/g AIS)	$\dfrac{GalA}{Rha}$	$\dfrac{Ara + Gal}{Rha}$	$\dfrac{Gal}{Ara}$	$\overline{M}_w \times 10^3$ (g/mol)	$\overline{[\eta]}_z$ (mL/g)	d_{happ} (g nm^3/mol)
	95	300	3.9	ND	689	67	10	0.8	159	507	3.0
		1000	3.4	ND	636	31	6	0.8	217	607	2.5
		3000	4.5	ND	619	28	6	0.8	250	636	2.4
PSD			0.8	0.5	49	28	3	0.1	50	162	0.1
1	Temperature H		20.9	10.6	9.6	3.4	7.5	22.6	5.5	18.6	18.3
	Temperature P		**<0.001**	**0.005**	**0.008**	0.184	**0.023**	**<0.001**	0.064	**<0.001**	**0.000**
	Grinding H		1.1	3.3	2.0	0.4	3.0	0.5	4.8	1.0	1.2
	Grinding P		0.572	0.190	0.361	0.804	0.220	0.798	0.089	0.614	0.556
6*	Temperature H		6.0	-	1.7	1.2	1.2	7.2	2.4	3.2	4.6
	Temperature P		0.051	-	0.430	0.561	0.561	**0.027**	0.301	0.202	0.099
	Grinding H		1.7	-	5.6	5.6	5.6	0.1	2.4	2.5	0.3
	Grinding P		0.430	-	0.061	0.061	0.061	0.957	0.301	0.288	0.875
Storage H			0.3	-	10.7	15.7	19.7	2.4	19.1	19.7	11.9
Storage P			0.596	-	**0.001**	**<0.001**	**<0.001**	0.121	**<0.001**	**<0.001**	**0.001**

* Only one repetition per sample.

Table 26 (Continuation). The ratio GalA/Rha estimated the relative amount of HG versus RG I, (Ara+Gal)/Rha estimated RG I branching and Gal/Ara the proportion of RG I side chains. Ratios were calculated using the yields of galacturonic acid (GalA) and neutral sugars arabinose (Ara), galactose (Gal) and rhamnose (Rha) content, expressed in mg/g AIS (**Table 28**). AIS and chemical composition of serum pectins were corrected for the starch content. PSD: Pooled standard deviations; ND: Not detected; FW: Fresh weight (serum); AIS: Alcohol insoluble solids; $\overline{M}_w$: Weight-average molar mass; $\overline{[\eta]}_z$: z-average intrinsic viscosity; $\overline{R}_{hz}(v)$: z-average viscometric hydrodynamic radius; d_{happ}: Apparent molecular density, calculated as $\overline{M}_w/(\frac{4}{3}\cdot\pi\cdot\overline{R}_{hz}(v)^3)$. Macromolecular characteristics were taken at the apex of the main peak.

Table 27. AIS yield, composition and macromolecular characteristics of raw apple pectins, followed by Kruskal-Wallis *H*- and *P*-values.

Storage (months)	AIS (mg/g FW)	Starch (mg/g AIS)	GalA (mg/g AIS)	$\dfrac{GalA}{Rha}$	$\dfrac{Ara + Gal}{Rha}$	$\dfrac{Gal}{Ara}$	$\overline{M}_w$ x 10^3 (g/mol)	$\overline{[\eta]}_z$ (mL/g)	d_{happ} (g nm^3/mol)
1	26	101	261	34	29	0.82	802	1224	1.2
6	27	ND	336	17	6	0.71	112	435	3.4
PSD	*2*	*12*	*11*	*3*	*3*	*0.03*	*57*	*53*	*0.1*
Storage *H*	0.4	-	3.9	3.9	3.9	3.9	3.9	3.9	3.9
Storage *P*	0.513	**-**	**0.049**	**0.049**	**0.049**	**0.049**	**0.049**	**0.049**	**0.049**

For abbreviations see **Table 26**.

AIS and chemical composition of raw apple pectins were corrected for the starch content.

Table 28. Neutral sugar composition of serum pectins, followed by Kruskal-Wallis *H*- and *P*-values.

Storage (months)	Temp. (°C)	Grinding (rpm)	Rha	Fuc	Ara	Xyl (mg/g AIS)	Man	Gal	Glc
1	70	300	7	9	73	24	ND	103	157
		1000	6	6	64	22	ND	88	163
		3000	10	6	79	20	ND	99	219
	83	300	5	5	61	15	ND	72	184
		1000	6	6	71	18	ND	85	175
		3000	6	5	73	13	ND	72	183
	95	300	9	3	84	10	ND	63	66
		1000	8	3	88	10	ND	69	111
		3000	7	3	85	10	ND	69	140
6*	70	300	13	9	48	26	ND	50	63
		1000	23	13	67	39	ND	77	91
		3000	20	10	72	32	ND	72	89
	83	300	14	10	52	33	ND	51	76
		1000	23	13	69	39	ND	65	89
		3000	22	13	71	38	ND	67	88

Storage (months)	Temp. (°C)	Grinding (rpm)	Rha	Fuc	Ara	Xyl	Man (mg/g AIS)	Gal	Glc
	95	300	10	8	55	32	ND	44	57
		1000	20	11	71	34	ND	55	70
		3000	22	10	74	33	ND	61	73
PSD			*2*	*2*	*9*	*3*	-	*12*	*40*
1	Temperature H		6.7	15.6	10.8	21.0	-	17.3	10.6
	Temperature P		**0.036**	**<0.001**	**0.005**	**<0.001**	-	**<0.001**	**0.019**
	Grinding H		0.4	1.8	1.7	0.4	-	0.3	3.4
	Grinding P		0.799	0.415	0.437	0.814	-	0.852	0.179
6*	Temperature H		1.2	3.3	1.1	1.7	-	1.9	3.3
	Temperature P		0.561	0.193	0.587	0.430	-	0.393	0.193
	Grinding H		6.0	4.4	6.5	5.7	-	5.4	3.5
	Grinding P		0.051	0.113	**0.039**	0.058	-	0.066	0.177
Storage H			18.4	16.9	4.6	19.4	-	9.8	11.7
Storage P			**<0.001**	**<0.001**	**0.033**	**<0.001**	-	**0.002**	**<0.001**

* Only one repetition per sample.

Rha: Rhamnose; Fuc: Fucose; Ara: Arabinose; Xyl: Xylose; Man: Mannose; Gal: Galactose; Glc: Glucose without starch; PSD: Pooled standard deviation. ND: Not detected. All values were corrected for the starch content.

Soluble pectins of raw apples showed the same trend as serum pectins in macromolecular characteristics during post-harvest storage, i.e. smaller molar mass and intrinsic viscosity but higher d_{happ} (**Table 27**).

Grinding had no impact on macromolecular characteristics of pectins (**Table 26**) at T1, whereas molar mass and intrinsic viscosity of pectins at T6 increased with grinding, although this trend was not significant.

Molar mass distribution of serum pectins, deriving from purees prepared at 3000 rpm and different temperatures, are presented for T1 (**Fig. 92**A) and T6 (**Fig. 92**B). For purees processed at T1 and moderate temperatures (70 °C and 83 °C), the main pectic fraction eluted at the same elution volume (~19 mL), whereas the main peak was shifted to higher elution volumes after heat treatment at 95 °C. This indicated a smaller pectin size for the samples obtained at 95 °C and confirmed that endogenous enzymes, such as pectin methylesterase and polygalacturonase, played a minor role in apples during processing. Chemical reactions were the predominant mechanism inducing pectin degradation during apple processing. In other fruits, e.g. tomatoes, enzymatic pectin degradation is marked at moderate temperatures (Lin, et al., 2005), leading to reduced puree's viscosity compared to high temperature processes (Goodman, et al., 2002).

A second peak eluting at higher elution volumes (~25 mL), which represented smaller pectin fractions, was also present and its proportion decreased with increased temperature. However, $\overline{M}_w$ (90–105 x 10^3 g/mol) and $\overline{R}_{hz}(v)$ (10–16 nm) were similar in all samples and could thus not be differentiated. At T6, processing temperature did not affect the macromolecular size of soluble pectins. Compared to T1, the main peak of all pectin chromatograms was shifted to higher elution volumes and the second peak was smaller, indicating pectin degradation during storage as observed before (Buergy, et al., 2020).

In order to estimate pectin conformation over the whole distribution, $\overline{R}_{hz}(v)$ was plotted against $\overline{M}_w$. **Fig. 92**C shows serum pectins from purees prepared at different temperatures and 3000 rpm at T1. The distributions of 70 and 83 °C were completely superposed, indicating equivalent conformation. For the same $\overline{M}_w$, $\overline{R}_{hz}(v)$ was smaller for samples heated at 95 °C. This confirmed a more compact conformation of these

pectins. Samples prepared at 95 °C and 3000 rpm were compared according to apple storage duration (**Fig. 92**D).
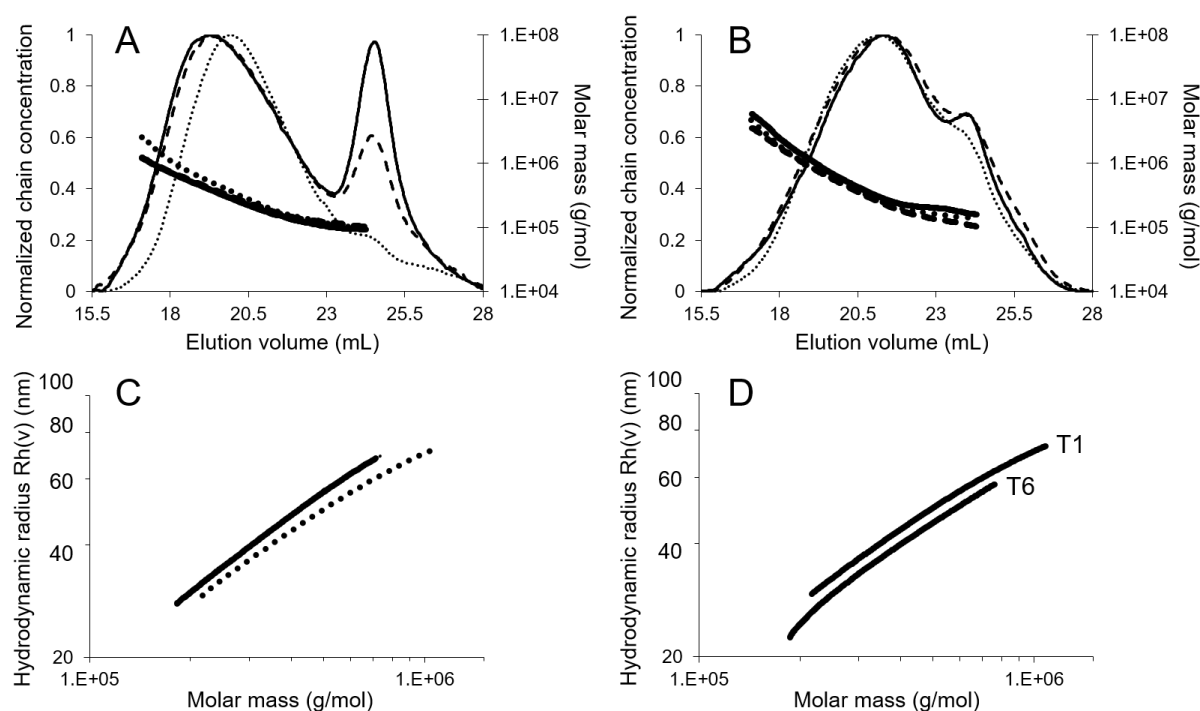
Fig. 92. Normalized chain concentration and molar mass versus elution volume of soluble pectins at T1 (A) and T6 (B) and $\overline{R}_{hz}(v)$ conformation plots (C-D) for purees prepared at 70 °C (continuous lines), 83 °C (dashed lines) and 95 °C (dotted lines) and a grinding speed of 3000 rpm.

The signal (mV) obtained by the differential refractive index detector was normalised through dividing all data points by the signal at the apex of the peak.

For the same $\overline{M}_w$, pectins were smaller after six months storage. These pectins were thus more compact, validating the conclusions reached with the values at the apex of the peak (**Table 26**). The slope of the log-log plot of $\overline{R}_{hz}(v)$ versus $\overline{M}_w$ was around 0.7 for all pectins, indicating a global similar semi-rigid structure (Smidsrød & Andresen, 1979) as expected for pectin molecules (Morris, et al., 2010). Increased compactness of pectin molecules has been linked to several reasons in literature. The DM was not significantly different between samples in this study and Diaz, et al. (2009) showed no relation between DM and pectin conformation in tomato puree. Ralet, et al. (2008) demonstrated that pectin molecules with a high number of RG I domains are more flexible. They fold thus more easily than HG and increase compact conformation in

solution. Here, more RG I domains were extracted from aged apples (T6) but not with increased temperature (**Table 26**). Nevertheless, both increased temperature and post-harvest storage caused degradation of RG I side chains in this study. Hence, pectins might also have a higher tendency to fold when they have shorter side chains because of reduced steric hindrance.

2.2.3.5. Mechanisms of pectin degradation during processing

At the natural pH of apples (circa 3.5), pectin degradation is minimal and might be due to either acid hydrolysis or β-elimination (Liu, et al., 2021). NMR was used to further investigate the mechanisms leading to pectin degradation at 95 °C. A small signal in the ^{1}H-NMR spectrum around 6 ppm indicates the presence of β-elimination products (Tjan, et al., 1974). This signal was visible in the positive control and, slightly, in the serum AIS obtained from purees heated at 95 °C (**Fig. 93**).
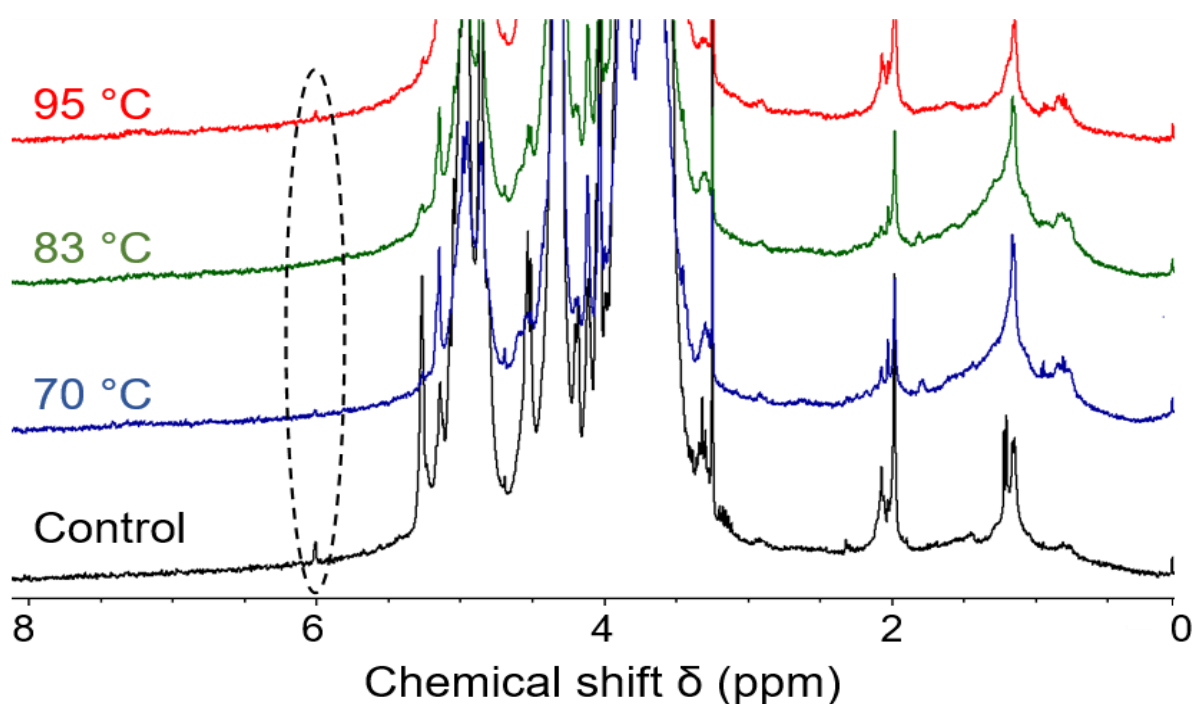
Fig. 93. ^{1}H-NMR spectrum of control and serum pectins extracted from purees at 3000 rpm with different temperatures at T1.

The control (serum pectin 95 °C, 3000 rpm) was heated at 100 °C for 30 min at pH 6 to enhance β-elimination.

2.2.4. Discussion

2.2.4.1. Relation between process conditions and puree's texture through texture determinants

Both at T1 and T6, global characteristics of puree's texture (apparent viscosity, yield stress, G' and G") were significantly influenced by grinding speed but not by temperature (**Table 24**). A principal components analysis (PCA, **Fig. 94**A-B) was conducted with texture characteristics and possible determinants of puree's texture (particle size, pulp wet mass i.e. the amount of liquid phase bound by insoluble particles, serum viscosity) for T1 and T6. The first two principal components (PC1 and PC2) explained together more than 80% of the total variance. Yield stress, G' and G" were grouped at PC1, together with particle size, indicating a strong dependence. T1 samples were more variable than T6 since they were more dispersed in the sample map. Also at T1, samples produced at 70 and 83 °C were placed together at PC1, while purees prepared at 95 °C were also explained by PC2. This led to two extremes, one at PC1 that accounted for samples ground at 300 rpm and heated at moderate temperatures (70 and 83 °C) and one at PC2, being samples heated to 95 °C.

Actually, samples could be separated according to the grinding speed along PC1 (**Fig. 94**B). Hence, large particles were related to high yield stress, G' and G". Cell clusters deform less easily than individual cells and occupy more volume in the puree, increasing rheological characteristics (Leverrier, et al., 2016; Lopez-Sanchez, et al., 2012). Serum viscosity and pulp wet mass were placed near PC2 and were thus perpendicular to the parameters mentioned before. This pointed to different response to the two input variables temperature and grinding. Indeed, in the sample map (**Fig. 94**B), PC2 separated purees produced at T1 and 95 °C, which were characterized by high serum viscosities and pulp wet masses (**Fig. 88**C and E), from purees produced at T1 and moderate temperatures (70 °C and 80 °C), while purees produced at T6 were intermediate. Apparent viscosity was less well explained in the PCA and stood alone between PC1 and PC2. This indicated some co-dependence with particle size (along PC1), and pulp wet mass and serum viscosity (along PC2).
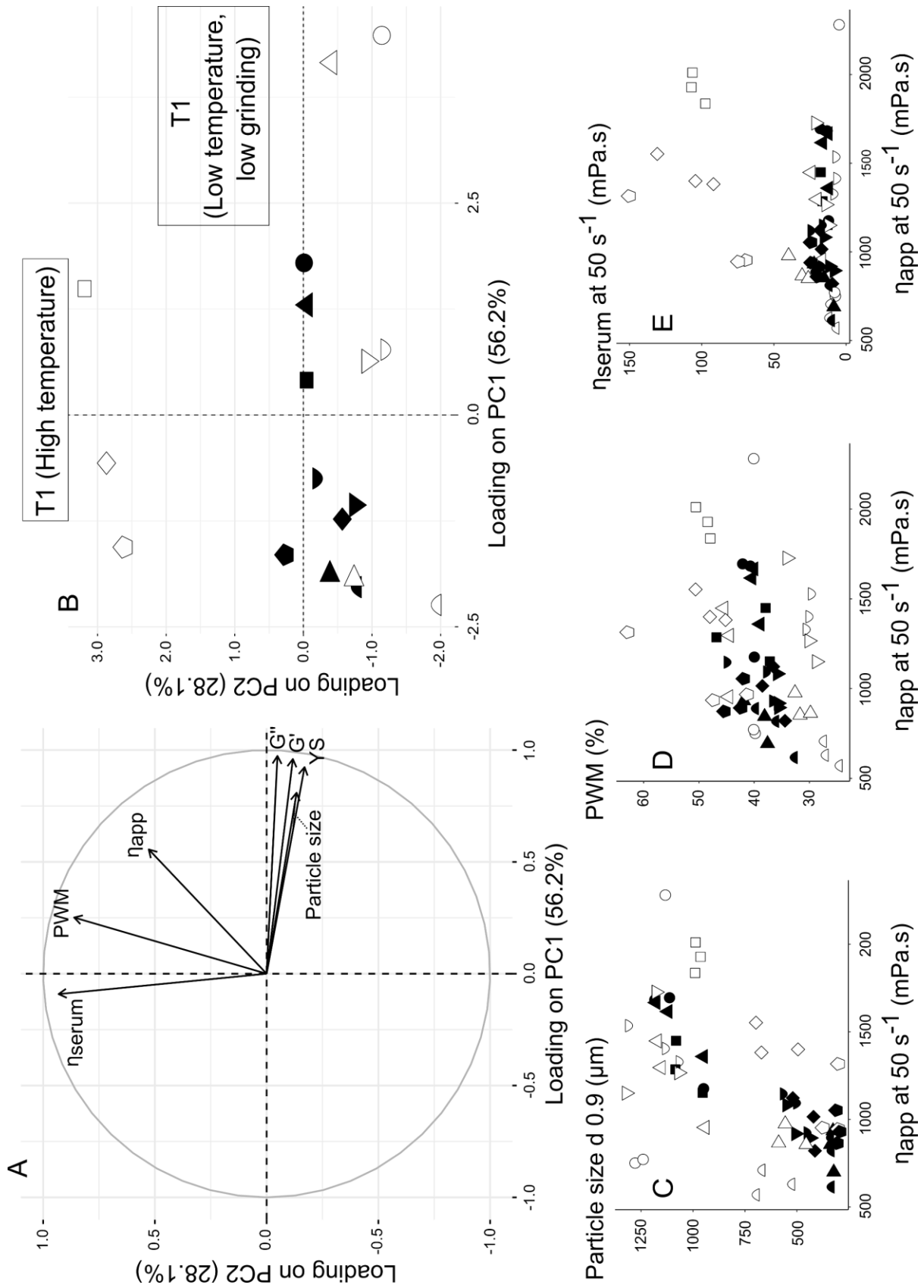
Fig. 94. Principal component analysis (PCA) (A-B) and scatterplots (C-E) of rheological characteristics and texture determinants of purees prepared with apples stored for one and six months prior to processing.

Fig. 94 (Continuation). Rheological characteristics are η_{app}: apparent viscosity of the puree at 50 s^{-1}, YS: yield stress, G' and G'': puree's storage and loss modulus, respectively, at an angular frequency of 10 rad/s) and texture determinants are particle size: particle size d 0.9, PWM: pulp wet mass, η_{serum}: serum viscosity at 100 s^{-1}. Correlation circle of variables loadings on PC1 and PC2 (A). Sample maps of scores on PC1 and PC2 (B). For more legibility, PCA was conducted on the mean value of three replications as the same patterns were obtained as for PCA with all values. Scatterplots of particle size (d 0.9) in the puree (C), pulp wet mass (D) and serum viscosity at 100 s^{-1} (E) as a function of apparent puree viscosity at 50 s^{-1}. Empty symbols represent samples at T1 and filled symbols samples at T6. 70 °C, 300 rpm (circle); 70 °C, 1000 rpm (half-circle downwards); 70 °C, 3000 rpm (half-circle upwards); 83 °C, 300 rpm (triangle); 83 °C, 1000 rpm (triangle with apex pointing downwards); 83 °C, 3000 rpm (triangle with apex pointing to the right); 95 °C, 300 rpm (square); 95 °C, 1000 rpm (lozenge); 95 °C, 3000 rpm (pentagon).

Scatterplots (**Fig. 94**C–E) confirmed correlations between puree's viscosity and particle size or pulp wet mass but not with serum viscosity. Besides, serum viscosity did not vary significantly between the samples, except for purees at T1 that were heated at 95 °C.

2.2.4.2. Relation between pectin degradation and texture determinants induced by process conditions

A detailed analysis of soluble serum pectins might explain differences observed in the factors that determine puree's texture. Pectins are solubilised during the process both from the middle lamella and cell wall (Sila, et al., 2009). The extracted amounts affect serum viscosity, particle size through altered cell adhesion and porosity of the cell wall and thus WRC and PWM. Hence, pectin structure and chemical composition might give information about the chemical processes that occur during apple processing and post-harvest storage.

At T1, particle size was not only diminished by increased grinding speed but also slightly by temperature increase (**Table 24**). Indeed, serum AIS, containing mainly soluble pectins, increased at 95 °C for T1. This indicated higher pectin solubilisation during processing from the cell wall and middle lamella, explaining reduced cell

adhesion. Pectin solubilisation was probably enhanced by pectin degradation at high temperatures. RG I side chain branching, macromolecular size and slightly molar mass decreased in serum pectins when purees were heated at 95 °C, as a consequence of acid hydrolysis of side chains and slight β-elimination of the backbone. Since RG I side chains were shown to be linked to the cellulose-xyloglucan network in the cell wall (Popper & Fry, 2005; Zykwinska, et al., 2005), pectins seemed to be less attached. This might weaken the cell wall structure and, especially, intercellular adhesion, resulting in facilitated cell separation during grinding at elevated temperatures. Former studies also showed facilitated separation of apple (Müller & Kunzek, 1998), carrot or broccoli tissue (Day, et al., 2010; Lopez-Sanchez, et al., 2011) when the raw material was heated previously to grinding but the results were not corroborated with pectin analysis.

Also at T1, PWM increased significantly in purees prepared at 95 °C (**Fig. 88**E). This was in line with WRC of the pulp (**Fig. 90**A) and might be linked to increased cell wall porosity (**Fig. 90**B). Müller and Kunzek (1998) also showed increased WRC of heat-treated cell wall material from apple parenchyma. Since temperature increase resulted in pectin degradation and thus solubilisation, the cell wall structure might be weakened, leading to increased pore sizes.

At T1, increase of serum viscosity with temperature correlated with the increased amount of solubilised pectins (measured as serum AIS) (**Fig. 95**A), while serum viscosity showed no trend with molar mass (**Fig. 95**B). Pectin conformation might also have a significant impact on serum viscosity (Diaz, et al., 2009) but it was not the case here. Starch might also slightly increase serum viscosity since a maximum concentration of about 1.3% was detected in the serum for high temperatures (**Table 26**). In fact, taking into account the gelatinisation temperature of starch in excess water around 60 °C, temperatures higher than 70 °C might be able to better solubilise starch (Singh, et al., 2005). Increased grinding also seemed to enhance starch solubilisation, probably due to increased cell wall rupture. Although amylose gels at less than 1% (Doublier & Choplin, 1989) and a 2% amylopectin solution provides a viscosity increase of 5 mPa.s (Matignon, et al., 2014), these relatively low concentrations were unlikely to explain the high increase of serum viscosity alone. Pectin solubilisation was thus identified as the main factor increasing serum viscosity, maybe in addition to starch solubilisation.
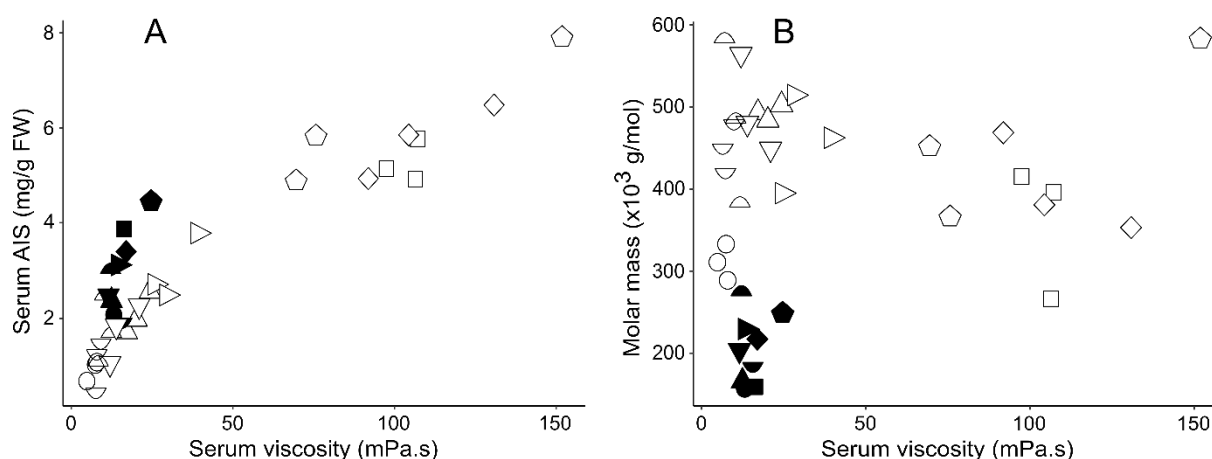
Fig. 95. Scatterplots of serum viscosity at 100 s^{-1} against serum AIS (A) and molar mass of soluble pectins at the apex of the main peak (B).

Empty symbols represent samples at T1 and filled symbols samples at T6. 70 °C, 300 rpm (circle); 70 °C, 1000 rpm (half-circle downwards); 70 °C, 3000 rpm (half-circle upwards); 83 °C, 300 rpm (triangle); 83 °C, 1000 rpm (triangle with apex pointing downwards); 83 °C, 3000 rpm (triangle with apex pointing to the right); 95 °C, 300 rpm (square); 95 °C, 1000 rpm (lozenge); 95 °C, 3000 rpm (pentagon).

2.2.4.3. Relation between pectin degradation and texture determinants induced by apple maturation x process conditions

The impact of temperature on the factors that determine puree's texture (serum viscosity, PWM, particle size) was tempered by prolonged post-harvest storage. Hence, the variability of puree's structural and textural characteristics was reduced at T6 as can be seen in PCA (**Fig. 94**B) and NMR relaxation experiments (**Fig. 90**B). This confirmed the results obtained before (Buergy, et al., 2020). At T6, cell separation was easy and pectin composition and structure were less modified by thermomechanical processes during puree production.

Purees prepared with aged apples showed significantly smaller particles (**Table 24**). In addition, grinding generated similar particle sizes no matter the temperature applied. Reduced cell adhesion was probably linked to reduced RG I side-chain branching (**Table 26**), as observed by Nara, et al. (2001) or Pena and Carpita (2004). Cell separation was thus facilitated at T6 as stated by Buergy, et al. (2020). Serum AIS, molar mass and size remained constant for all temperatures at T6, so that serum viscosity was about constant. Enzymatic reactions in aged apples (T6) and chemical

reactions during processing in fresh apples (T1) both led to pectin degradation and the impact on texture determinants were similar.

At T1, only elevated temperatures, mainly 95 °C, led to significant changes in pectin composition and structure. Since apple pectins were relatively stable at pH 3.6, only little β-elimination occurred, even at 95 °C. Hence, acid hydrolysis seemed to be the predominant reaction causing pectin degradation during apple processing. At T6, however, pectins were already degraded by endogenous enzymes and temperature did not alter pectin composition and structure in aged apples. Mechanical treatments had no significant impact on pectin degradation and solubilisation, neither at T1 nor at T6. However, in contrast to what was observed with one-month stored apples, higher grinding speed seemed to enhance the extractability of larger pectins with a higher proportion of RG I pectins (**Table 26**).

2.2.5. Conclusions

Both elevated temperatures (95 °C) and apple maturation led to pectin degradation, resulting in facilitated tissue fragmentation during processing. This affected particle size, an important determinant of puree's texture. Other parameters such as pulp wet mass and serum viscosity were also altered. Since pectin as well as puree's structure were significantly altered by temperature increase in fresh (T1) but not in aged (T6) apples, the interaction storage duration x temperature had a major impact. Mechanical treatments did not alter pectin composition and structure, neither at T1 nor at T6. However, temperature had only a limited impact on apple puree's texture, grinding being the predominant factor. This study highlighted the importance of pectin analysis in explaining phenomena at cellular level during thermomechanical processes for puree production.

Acknowledgements

Highlights

- Elevated temperature and apple maturation induced pectin degradation.

- Pectin degradation and solubilisation enhanced cell separation during processing.

- The interaction storage duration x temperature had a major impact on pectins.

- Mechanical processes altered pectin composition and structure only slightly.

- Mechanical treatments affected puree's texture more than thermal treatments.

2.3. Sensory evaluation

In this section, purees prepared by contrasted process conditions (as described in **V 2.2.**) were evaluated by a sensory panel in order to investigate how the process can be used to modulate the perceived texture. Apple variety Golden Delicious (harvest year 2019) was stored for one month at 4 °C and processed into puree by combining three temperature (70, 83 and 95 °C) and three grinding regimes (300, 1000, 3000 rpm), resulting in nine different thermomechanical processes. Since the amount of puree produced at INRAE with RoboQbo (**Fig. 96**A) was not sufficient for sensory evaluation, some more puree was produced at CTCPA using a Stephan (**Fig. 96**B).
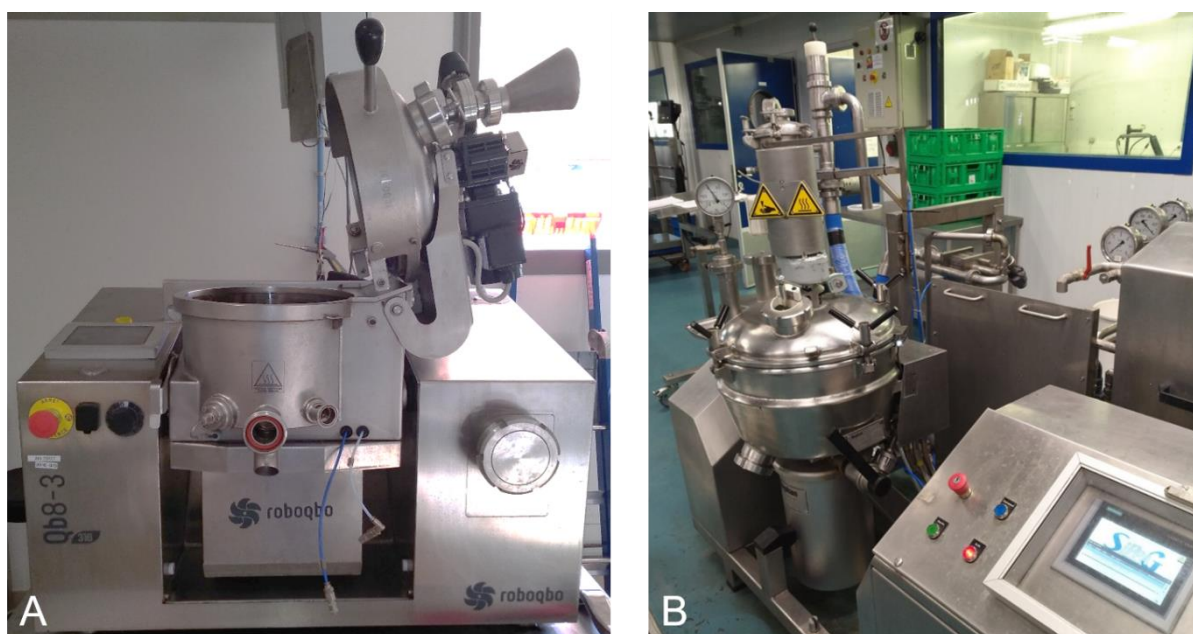
Fig. 96. Photos of a cooker-cutter for puree processing at INRAE (A) and CTCPA (B).

2.3.1. Puree preparation

The main difference between RoboQbo Qb8-3 and Stephan UM44 cooker-cutter is the tank volume, being 8 L and 44 L, respectively. A larger volume of apples (15 kg) could thus be processed with the Stephan. The minimum grinding speed also differed between the machines. While a grinding speed of 100 rpm was applied during temperature increase by RoboQbo, Stephan ground purees at 300 rpm, the minimum grinding speed, during temperature increase. Despite the fact that both RoboQbo and Stephan are able to draw vacuum, apples were processed under vacuum by RoboQbo but not by Stephan, due to a misunderstanding the day of processing.

The parameters for apple processing at INRAE and CTCPA are summarized in **Table 29**.

Table 29. Process conditions for RoboQbo (INRAE) and Stephan (CTCPA).

	RoboQbo	Stephan
Tank volume	8 L	44 L
Weight of processed apples	3 kg	15 kg
Grinding during temperature ↗	100 rpm	300 rpm
Temperature regimes	70, 83, 95 °C	70, 83, 95 °C
Grinding regimes	300, 1000, 3000 rpm	300, 1000, 3000 rpm
Cooking duration	30 min	30 min
Vacuum	Yes	No

2.3.2. Textural and structural quality traits of purees

Although processing conditions were slightly different between RoboQbo and Stephan, purees prepared with Stephan should be comparable to the well-characterised purees of the main study (cf. **V 2.2.**), which were prepared by RoboQbo.

Despite slightly higher grinding speeds during temperature increase and the fact that more apples were processed by Stephan, viscosity of the purees prepared by different cooker-cutter models did not differ significantly (**Table 30**). Viscoelastic properties (yield stress, G' and G'') as well as structural characteristics (serum viscosity, PWM and particle size) of the purees were also not significantly different.

Table 30. Comparison of textural and structural quality traits of purees prepared at two different processing sites (INRAE and CTCPA), followed by Kruskal-Wallis *H-* and *P-*values.

	Temp. (°C)	Grinding (rpm)	η_{app} (mPa.s)	YS (Pa)	G' (Pa)	G'' (Pa)	η_{serum} (mPa.s)	PWM (%)	d0.9 (µm)
INRAE	70	300	1268	95	9630	2259	7	40	1217
		1000	1421	39	3295	769	8	30	1180
		3000	637	11	1111	216	10	27	630
	83	300	1233	98	8437	2210	21	45	1090
		1000	1381	36	3037	764	16	31	1189
		3000	907	12	1312	260	32	31	531
	95	300	1925	30	3708	1101	104	49	981
		1000	1445	17	1955	522	109	48	621
		3000	1069	14	1399	362	99	51	332
CTCPA	70	300	2449	184	21418	4250	4	49	854
		1000	1056	54	4274	804	4	28	871
		3000	655	17	1042	191	5	25	1166
	83	300	1509	196	10845	2734	31	52	1071
		1000	985	57	3857	1024	20	31	1341
		3000	1002	17	1078	210	22	26	1140
	95	300	1641	27	3211	1011	78	44	987
		1000	1461	19	1815	463	67	39	910
		3000	1102	15	1273	298	79	40	403
PSD			335	13	911	228	17	4	95
Processing site *H*			0.2	3.4	1.5	0.6	0.5	0.3	0.3
Processing site *P*			0.648	0.182	0.463	0.748	0.476	0.571	0.571
Temperature *H*			4.5	8.7	1.6	0.6	31.1	14.5	8.7
Temperature *P*			0.105	**0.013**	0.463	0.748	**<0.001**	**<0.001**	**0.013**
Grinding *H*			15.2	25.1	28.2	30.1	0.3	10.3	12.7
Grinding *P*			**<0.001**	**<0.001**	**<0.001**	**<0.001**	0.843	**0.006**	**0.002**

INRAE: Institut national de recherche pour l'agriculture, l'alimentation et l'environnement; CTCPA: Centre technique de la conservation des produits agricoles; PSD: Pooled standard deviations; η_{app} : Apparent puree viscosity at 50 s^{-1}; YS: Yield stress; G' and G'': Storage and loss modulus at an angular frequency of 10 rad/s, η_{serum}: serum viscosity at 100 s^{-1}; PWM: Pulp wet mass; d0.9: Particle size d.09.

As observed before (cf. **V 2.2.**), increased temperature highly increased serum viscosity and PWM. Yield stress and particle size were slightly reduced. Intense grinding reduced both viscosity and viscoelastic properties, while serum viscosity was not altered. PWM was especially reduced by grinding in purees cooked at 70 and 83 °C. Generally, grinding led to smaller particles in all purees. Some exceptions in purees cooked at 70 and 83 °C and ground at low grinding speeds were observed, probably due to large cell clusters, which were beyond the analysis area of laser granulometry. All these findings were extensively discussed in section **V 2.2.** and thus not repeated here.

2.3.3. Quality traits of purees concerning taste and colour

Not only texture but also taste and colour (**Table 31**) of apple purees were assessed instrumentally. This included analysis of titratable acids (TA), main sugars of apples comprising glucose, fructose and sucrose and colour determination. Values obtained for TA, sugars and colour parameters L* and b* were in the same range as in literature (Lan, et al., 2020). For a*, values in literature only coincided with purees produced at INRAE, which were prepared under vacuum. Purees produced at CTCPA showed noticeably higher a* values, being in accordance with browning effects that occurred during processing without vacuum. L* values also differed, being smaller for purees prepared at CTCPA. This further emphasized the impact of enzymatic browning reactions on colour. Less sucrose was found in CTCPA purees, although the amount of other sugars were similar. Generally, temperature did not alter TA, sugars or colour of apple purees. Only b* was slightly different but no regular trend could be noticed. Grinding seemed to favour extractability of sugars and acids, since TA, glucose and fructose significantly increased with grinding. The sucrose content also increased with increased grinding speed but this was not significant. As grinding results in cell destructuration, the cell content containing sugars and acids is easily liberated. In less ground purees, several cells and cell clusters are intact so that diffusion of sugars and acids into the serum may be slower. Although samples were homogenised before analysis, this might be not enough to extract sugars and acids completely.

Table 31. Comparison of quality traits concerning taste and colour of purees prepared at two different processing sites (INRAE and CTCPA), followed by Kruskal-Wallis *H*- and *P*-values.

	Temp. (°C)	Grinding (rpm)	TA (meq/kg FW)	Glc	Frc (g/kg FW)	Suc	L*	a*	b*
INRAE	70	300	53	15	51	71	46	-4.1	13
		1000	59	18	66	67	48	-4.4	16
		3000	69	17	76	86	49	-5.8	15
	83	300	59	15	58	71	46	-4.4	14
		1000	59	17	72	75	47	-4.5	14
		3000	70	17	67	76	47	-4.3	15
	95	300	63	15	63	72	45	-3.5	15
		1000	66	18	61	64	45	-3.7	14
		3000	62	19	72	72	46	-3.9	14
CTCPA	70	300	52	17	55	53	46	0.4	18
		1000	57	18	60	56	43	0.3	15
		3000	56	22	67	57	43	0.5	15
	83	300	51	13	42	46	44	-0.1	14
		1000	62	17	55	54	43	-0.3	13
		3000	64	19	68	58	43	0.6	15
	95	300	61	14	42	42	42	-1.1	12
		1000	62	11	62	59	43	-0.5	14
		3000	65	14	64	63	43	0.0	14
PSD			5	3	8	14	1	0.4	1
Processing site *H*			1.8	0.4	3.5	11.4	16.9	19.7	0
Processing site *P*			0.176	0.523	0.060	**<0.001**	**<0.001**	**<0.001**	1
Temperature *H*			4.0	1.4	0.1	0.6	5.4	3.9	6.4
Temperature *P*			0.136	0.490	0.954	0.726	0.066	0.143	**0.041**
Grinding *H*			10.5	7.7	13.4	2.1	1.1	0.3	2.1
Grinding *P*			**0.005**	**0.022**	**0.001**	0.348	0.577	0.870	0.355

INRAE: Institut national de recherche pour l'agriculture, l'alimentation et l'environnement; CTCPA: Centre technique de la conservation des produits agricoles; PSD: Pooled standard deviations; TA: Titratable acidity; Glc: Glucose; Frc: Fructose; Suc: Sucrose; FW: Fresh weight.

2.3.4. Flash Profile analysis of purees prepared with Stephan cooker-cutter (CTCPA)

The visual aspect, textural properties as well as flavour and odour of CTCPA apple purees prepared with Stephan were evaluated by a sensory panel of 10 trained assessors. Sensory analysis was conducted by Terra'Senso (Avignon, Fracnce), a locally based sensory analysis platform, through a Flash Profile analysis. This is a descriptive sensory analysis method, during which every participant defines individual vocabulary to describe the characteristics of the different samples. The products were then ranked by the frequency of the applied vocabulary. The Flash profile has already been employed to describe apple purees and was shown to be a suitable sensory method to differentiate purees thanks to the most discriminating descriptions (Tarea, 2005).

A Generalized Procrustes Analysis (GPA) (**Fig. 97**A) was used to classify the products according to the descriptions given by the participants. Three groups of purees were obtained, which were separated along the first dimension. A first group (samples 1, 2 and 4) corresponded to purees having a crunchy and grainy texture with flesh and skin pieces. These purees were more difficult to swallow and more acid. A second group (samples 3, 6, 8 and 9) pooled more homogenous purees with creamy, velvety and melting textures. Their visual aspect was described as shiny and colourful and their flavour was sweeter than other purees. A third group (samples 5 and 7) showed intermediate characteristics.

The most important parameters to describe apple puree's texture are graininess and consistency (Espinosa-Munoz, et al., 2012; Tarea, Cuvelier, & Sieffermann, 2007). Generally, this results in two axes linking four groups in the sensory space of GPA or PCA. However, only two major groups could be distinguished along the first dimension in the sensory space of GPA (**Fig. 97**A). On the basis of the vocabulary used to evaluate the samples, these groups could be assigned to the "graininess" component of the purees.
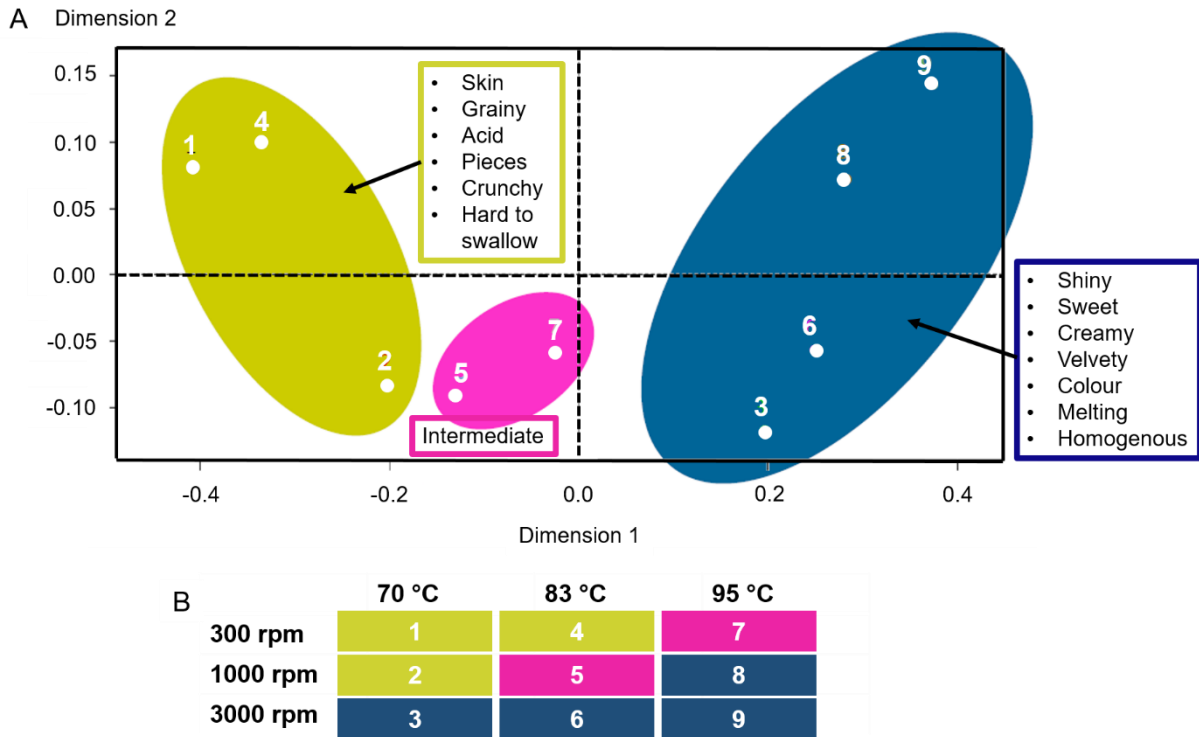
Fig. 97. Generalized Procrustes Analysis (GPA) of purees (A) and the corresponding labelling (B).

GPA was established by Terra'Senso.

The defined groups (**Fig. 97**B) corresponded well to structural characteristics of the purees prepared by different processing parameters. Purees that were produced at low grinding speed and temperature (samples 1, 2 and 4) showed "grainy" textures, reflecting the existence of big particles (**Table 30**). This is in accordance with previous studies, ascribing granular textures to particle size and proportion (Espinosa-Munoz, et al., 2012; Tarea, et al., 2007). In contrast, purees that were highly ground (samples 3, 6, 8 and 9) were described as "homogenous" and "creamy", certainly due to small particles. This effect seemed to be favoured by temperature since purees heated at 95 °C were classed in this group even when prepared at intermediate grinding. This correlated with the observation that increased temperatures favour tissue fragmentation during grinding. Textural characteristics linked to structural properties, mainly particle size, of the purees were thus well perceived by the sensory panel.

Although vocabulary used for describing the graininess of purees was similar between this study and previous ones, vocabulary was missing to describe consistency. While low consistency results in fluid and flowing purees, high consistency leads to sticky, dry and firm purees (Espinosa-Munoz, et al., 2012; Tarea, et al., 2007). This is mainly related to the pulp content in the puree as increasing pulp content increases consistency. Although the PWM was in the same range in this study and in the work from Espinosa-Munoz, et al. (2012), vocabulary to describe consistency was not used here. In this study, PWM was highest in purees with large particles (**Table 30**). Particle size thus seemed to predominate the perceived texture of apple purees. Increasing serum viscosity was reported to play a lubricant role due to the amount of solubilised pectins. Purees were thus perceived smoother and less grainy, although particle sizes were similar (Espinosa-Munoz, et al., 2012). This could not be confirmed here, since particles were always smaller when serum viscosity was increased.

In literature, another term, "moist" or "wetness", was less important than consistency and graininess but also used to describe purees (Espinosa-Munoz, et al., 2012; Tarea, et al., 2007). This parameter decreased with increasing PWM, probably due to less serum. However, this parameter did not emerge from this analysis. Although "shiny" was used to describe more homogenous purees, this might not be linked to the "wetness" of the purees since PWM was smaller in these purees.

Unlike structural data, rheological parameters show little correlations with sensory descriptors (Tarea, 2005). It seems thus difficult to predict the perception of the texture of apple purees by rheological measurements alone. Structural measurements (particle size, pulp content) are needed to complete the texture prediction. Here, small values for both viscosity and viscoelastic properties matched with more homogenous purees due to smaller particles and would thus be correlated with graininess. This highlighted the predominant impact of particle size in the purees.

While previous sensory analyses of apple purees focused only on textural and structural characteristics, also parameters describing taste and colour were included here. The panellists highlighted the "colour" of homogenous purees and described them as "shiny". However, no or only very slight differences were determined instrumentally in terms of colour between contrasted purees (**Table 31**). Interestingly, homogenous purees were classified as "sweeter" compared to granular purees that resulted more "acid". However, increased grinding favoured extraction of both sugars

and acids. In addition, percentage increase was higher for total acids than sugars. It was thus hypothesized that the visual aspect of purees highly guided the choice of vocabulary as already observed in other food products. The colour of a wine, for example, influences the perception of taste and smell since predetermined descriptions are stimulated (Brochet, 1999). In the case of apple puree, more homogenous purees could be associated with "sweeter" taste since commercial apple purees are generally sweet. In contrast, apple pieces in the puree might be associated with the acid taste of raw apples.

In conclusion, sensory evaluation of contrasted apple purees highlighted the impact of particle size on puree's texture, namely graininess. Consistency, another important parameter of apple purees, was not discriminated in this study. It was confirmed that perceived texture was better described by the puree's structure, mainly particle size, than the instrumentally obtained rheological parameters. Taste qualities were also assessed but seemed to be biased by the visual aspect of the purees.

Highlights

- Particle size seemed to predominate the perceived texture of apple purees.

- Only graininess was described, in correlation with particle size.

- Consistency was not considered by the sensory panel.

- Taste qualities seemed to be biased by the visual aspect of the purees.

---

3. General discussion

Modulation of raw material and process conditions led to a wide range of puree's textures. In this section, all data from harvest years 2016 to 2019 concerning textural (apparent viscosity, viscoelastic properties) and structural characteristics (particle size, PWM, serum viscosity) of apple purees were compared in order to assess the impact of raw material and process conditions on puree's structure. Then, the impact of structural characteristics on puree's texture was studied and the underlying mechanisms were discussed with respect to cell wall structure and pectin modifications.

3.1. Relation between structural and textural characteristics in apple purees

Several variables were selected to conduct statistical analyses. For viscosity, three values at different shear rates (50, 100, 250 s^{-1}) were chosen in order to describe the key points of the viscosity curve. Since correlations in the principal component analysis (PCA) indicated that yield tress, G' and G'' were strongly correlated (r > 0.90, **Supplementary Table S1**), only yield stress was retained as a representative of the viscoelastic properties. In this study and other ones (Espinosa-Munoz, et al., 2013; Espinosa, et al., 2011), particle size was often represented by d(0.9), which is the diameter where 90% of the volume distribution are below this value. However, other values should be included to describe particle size distribution. The volume mean diameter D[4,3] and surface mean diameter D[3,2] as well as d(0.1) and d(0.5) were thus also retained. To further describe puree's structure, pulp wet mass (PWM) and serum viscosity (value taken at 100 s^{-1} on the flow curve) were also included in the statistical analyses.

It was investigated whether raw material or process conditions (cf. **Table 5**) could differentiate samples. For this purpose, PCA was conducted and sample differentiation by their raw material characteristics (**Fig. 98**) and process conditions (**Fig. 99**) was analysed. The first two principal components (PC1 and PC2) explained together nearly 71% of the total variance. Values describing particle size (**Fig. 98**A) were grouped together and were highly correlated (r > 0.73, **Supplementary Table S1**). However,

327

they were less correlated than viscoelastic properties and that is why all values were kept. A second group was formed by η_{50}, η_{250} and yield stress. While η_{50} and yield stress were poorly correlated (r = 0.57), correlations were higher for η_{50} and η_{250} (r = 0.87) and η_{250} and yield stress (r = 0.81). Particle size as well as apparent viscosity (η_{50} and η_{250}) were grouped together and explained by PC1 and PC2. This confirmed the strong correlation between viscosity and particle size. Another variable explaining puree's viscosity, η_{100} was grouped with PWM. PWM, η_{100} and serum viscosity were poorly explained by PC1. Since viscosity values lied between particle size and PWM, they were correlated to both parameters, although slightly (**Supplementary Table S1**).

When the variables were presented using PC1 and PC3 (which explained 57% of the variation, not shown), serum viscosity was well explained by PC3 but orthogonal to yield stress. A correlation of r = -0.01 confirmed that serum viscosity and yield stress were independent variables.

Purees prepared in different harvest years 2016-2019 (**Fig. 98**B) by applying various raw material and process conditions resulted in a wide range of contrasted purees but the different years could not be differentiated by PCA. Linear discriminant analysis (LDA) also placed only 77% of samples into the correct group. Cultivars (**Fig. 98**C) were also highly mixed on the sample map. This was probably due to the different process conditions, which were applied on different cultivars in different harvest years, since previous studies (cf. **V 1.2.**) demonstrated that cultivars could produce contrasted purees. GoS could be differentiated from GS and GD2. GD1, the cultivar which was processed the most often, was highly confused with GD2 and GS. However, it could not be concluded whether this effect was caused by contrasted process conditions or by differences linked to the cultivars. Storage duration (**Fig. 98**D) resulted in a good (92%) score in the confusion matrix. PCA could differentiate samples with different storage durations on the PC1 x PC2 map, correlating with particle size. The largest particles were found at T0, followed by T1, T3, T6 and T9. While T1 could be confounded with T0, T3 and some T6, T0 was clearly separated from T3, T6 and T9. T9 was also clearly separated from other samples. Storage duration was thus confirmed to be an important parameter, which alters particle size and thus puree viscosity (cf. **V 1.1.** and **V 2.2.**).
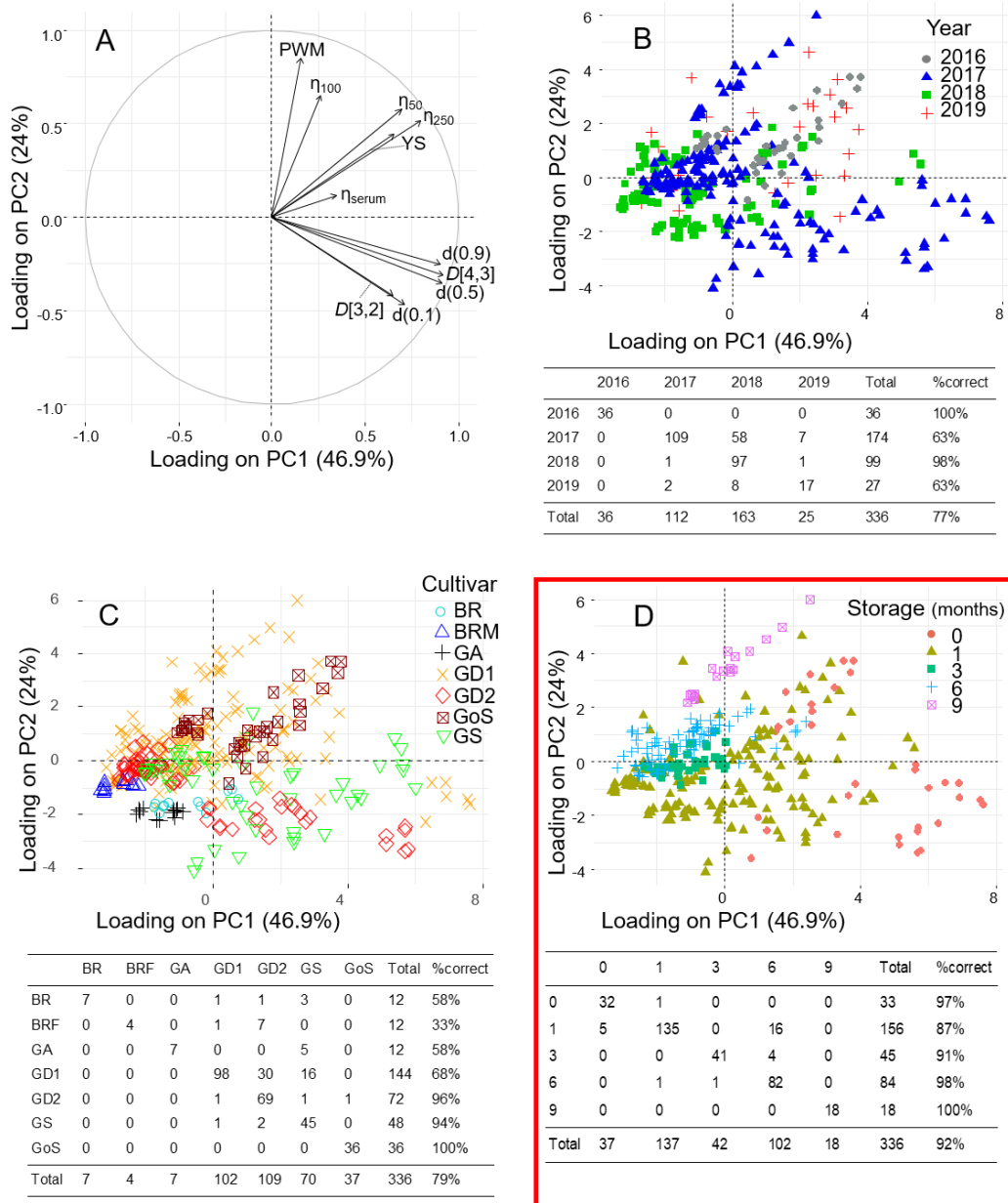
Fig. 98. Principal component analysis (PCA) of textural and structural characteristics of apple purees and corresponding confusion matrices of linear discriminant analysis (LDA) for raw material.

Correlation circle of variables loadings on PC1 (46.9%) and PC2 (24%) (A). Sample map of scores on PC1 and PC2 as function of the harvest year (B), cultivar (C) and post-harvest storage (D). η_{50}, η_{100}, η_{250}: Apparent viscosity of the puree at 50, 100 and 250 s^{-1}, respectively; YS: Yield stress of the puree; η_{serum}: Serum viscosity at 100 s^{-1}; PWM: Pulp wet mass; $D[4,3]$, $D[3,2]$, d(0.1), d(0.5) and d(0.9): Different variables explaining particle size. BR: Braeburn; BRM: Braeburn, mealy; GA: Gala; GD1: Golden Delicious, reduced fruit load; GD2: Golden Delicious, high fruit load; GoS: Golden Smoothee; GS: Granny Smith.

329

A — Temperature (°C)

	65	70	83	95	Total	%correct
65	15	0	0	3	18	83%
70	0	43	7	4	54	80%
83	0	7	6	5	18	33%
95	5	65	21	155	246	63%
Total	20	115	34	167	336	65%

B — Grinding (rpm)

	300	400	1000	3000	Total	%correct
300	11	0	7	0	18	61%
400	0	31	1	4	36	86%
1000	3	0	222	3	228	97%
3000	0	0	2	52	54	96%
Total	14	31	232	59	336	94%

C — Time (min)

	5	10	15	30	Total	%correct
5	122	5	1	64	192	64%
10	3	15	0	0	18	83%
15	1	0	70	1	72	97%
30	4	0	8	42	54	78%
Total	130	20	79	107	336	74%

D — Refining

	NR	RA	RA1	RA2	Total	%correct
NR	73	8	38	55	174	42%
RA	6	12	0	0	18	67%
RA1	7	0	32	15	54	59%
RA2	4	0	31	55	90	61%
Total	90	20	101	125	336	51%
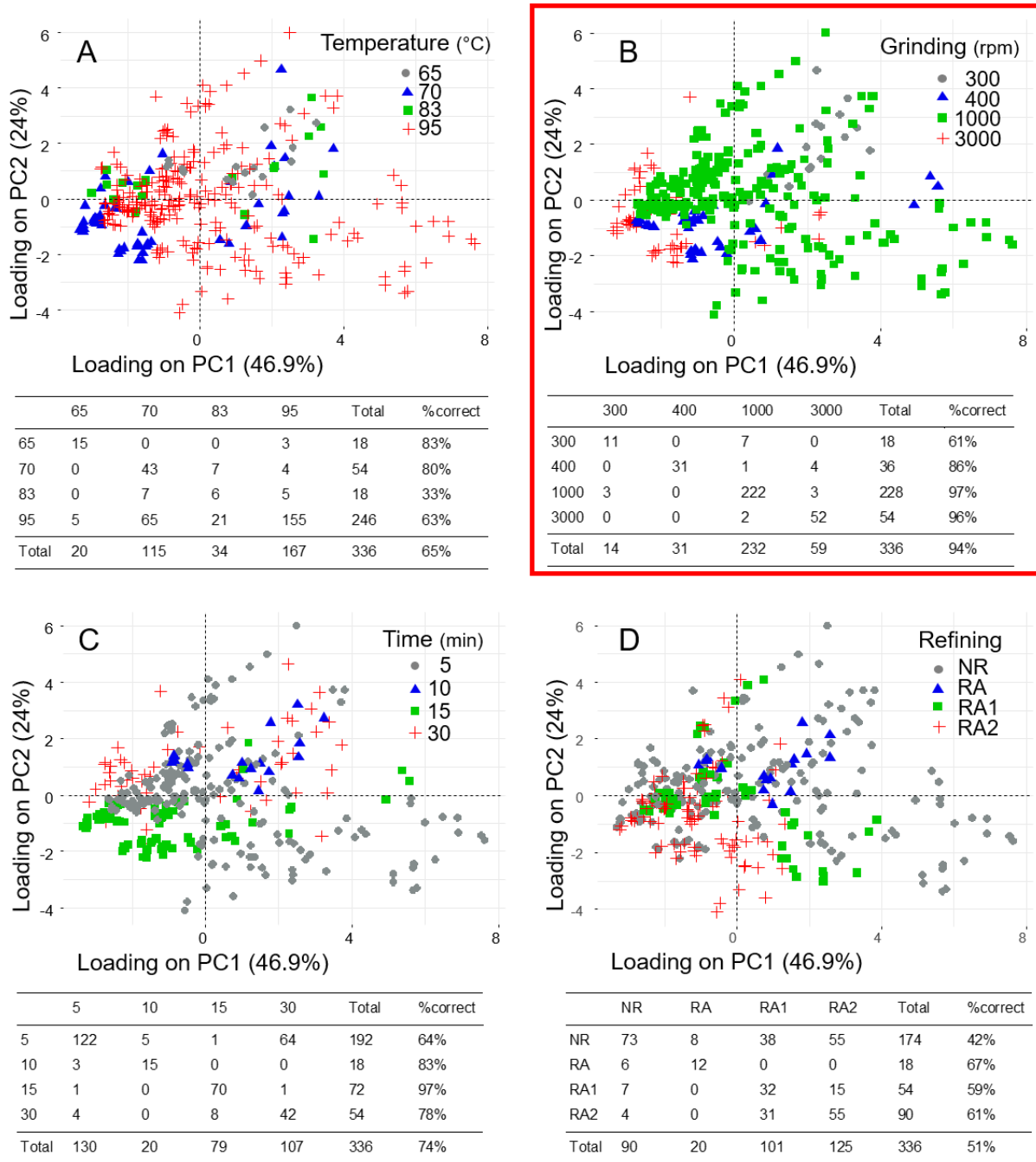
Fig. 99. Principal component analysis (PCA) of textural and structural characteristics of apple purees and corresponding confusion matrices of linear discriminant analysis (LDA) for process conditions.

Sample map of scores on PC1 (46.9%) and PC2 (24%) as function of processing temperature (A), grinding speed (B), duration (C) and refining level (D). η_{50}, η_{100}, η_{250}: Apparent viscosity of the puree at 50, 100 and 250 s^{-1}, respectively; YS: Yield stress of the puree; η_{serum}: Serum viscosity at 100 s^{-1}; PWM: Pulp wet mass; D[4,3], D[3,2], d(0.1), d(0.5) and d(0.9): Different variables explaining particle size. NR: Not refined; RA: refined (1.8 mm); RA1: refined (1.0 mm); RA2: refined (0.5 mm).

330

Temperature during process (**Fig. 99**A) failed to separate samples. Purees were mostly processed at 95 °C but were spread all over the sample map. This was probably due to the influence of storage duration since apples that were stored for several months were all processed at 95 °C but showed different puree characteristics (cf. **Fig. 98**D). Grinding speed (**Fig. 99**B) seemed to better separate samples. Although samples ground at 1000 rpm were widely spread over the sample map (in accordance with post-harvest storage), other grinding speeds (300, 400 and 3000 rpm) could be separated on the PC1 x PC2 map. This correlated with puree's viscosity, meaning that purees ground at higher speed were less viscous. This was shown to be linked to particle size, which decreased with increased grinding (cf. **V 2.1.** and **V 2.2.**). LDA confusion matrix confirmed good sample separation by grinding speed since a score of 94% was reached. Purees were only poorly separated by duration of the heat treatment (**Fig. 99**C). While purees heated for 10 and 15 min seemed to be separated on the PC1 x PC2 map, in accordance with lower viscosity for purees processed for more time, samples heated for 5 and 30 min were highly dispersed all over the sample map. The refining level (**Fig. 99**D) hardly differentiated samples since not refined and refined samples were highly mixed in the sample map and LDA showed a poor score (51%) in the confusion matrix.

It was thus evident that apple puree was a highly complex system and that puree's texture depended on several input factors, concerning both the raw material and process conditions. Hence, it was not simple to depict the effect of each variable on puree's structure and texture. However, post-harvest storage duration and grinding speed seemed to have major impact on particle size and thus puree's viscosity, no matter the harvest year and experiment. This impeded visualization of the impact of other variables on puree's structure and texture.

For better presentation and elucidation of the effect of other parameters, PCA was repeated with the same variables but only values at 1000 rpm were retained (not shown). The location of variables in the correlation circle were similar to **Fig. 98**A and samples were distributed in a similar way in the sample map. Another PCA (**Fig. 100**) was then conducted, retaining only the samples at T0 and T1, ground at 1000 rpm. PC1 and PC2 explained together nearly 75% of the total variance. PWM was explained by PC2 but stood alone (**Fig. 100**A). Values describing puree's texture (η_{50}, η_{100}, η_{250}, YS) were grouped in the correlation circle. All the different variables describing particle

331

size also formed a group. Serum viscosity was mostly explained by PC3 and thus not well represented in the plane of PC1 and PC2.
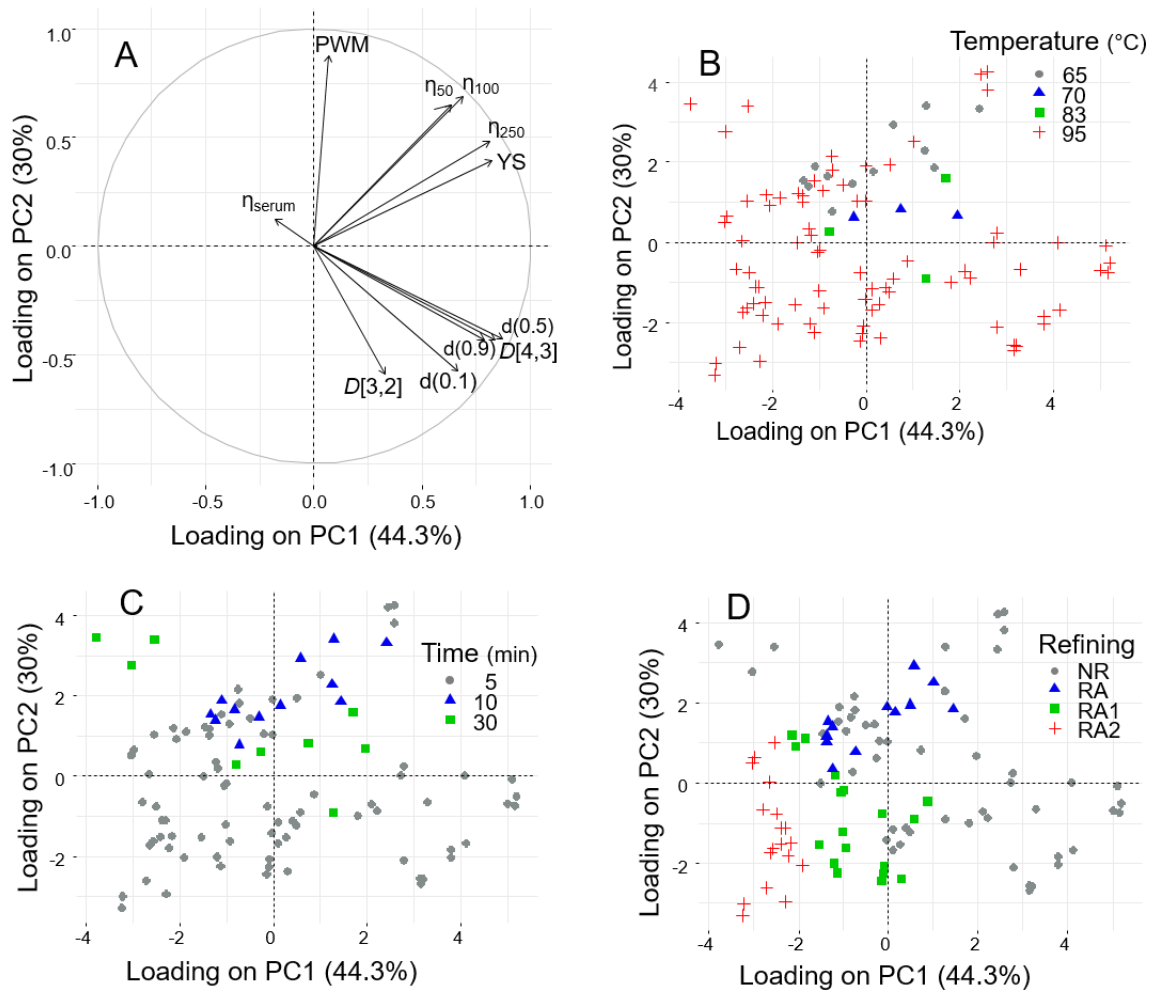
Fig. 100. Principal component analysis (PCA) of textural and structural characteristics of apple purees at T0 and T1 and ground at 1000 rpm.

Correlation circle of variables loadings on PC1 (44.3%) and PC2 (30%) (A). Sample map of scores on PC1 and PC2 as function of processing temperature (B), duration (C) and refining level (D). η_{50}, η_{100}, η_{250}: Apparent viscosity of the puree at 50, 100 and 250 s^{-1}, respectively; YS: Yield stress of the puree; η_{serum}: Serum viscosity at 100 s^{-1}; PWM: Pulp wet mass; D[4,3], D[3,2], d(0.1), d(0.5) and d(0.9): Different variables explaining particle size. NR: Not refined; RA: refined (1.8 mm); RA1: refined (1.0 mm); RA2: refined (0.5 mm).

This representation was similar to the correlation circle obtained with all the puree samples (**Fig. 98**A). Texture of apple purees at T0 and T1 thus seemed to be explained by both particle size and PWM. Although the major impact factors on puree's texture (grinding speed and post-harvest storage) were fixed in this PCA, temperature (**Fig. 100**B) and cooking duration (**Fig. 100**C) could not separate samples. NR and RA (**Fig. 100**D) could not be distinguished in the samples map. RA samples were refined by a screen opening of 1.8 mm, apparently too large to retain bigger particles such as large cell fragments. This was probably due to the deformable character of apple cells (Leverrier, et al., 2017b). However, these samples could be separated from RA1, as RA1 from RA2, according to puree's viscosity and yield stress. NR and RA samples thus resulted in high viscous purees, while refining at 1.0 mm (RA1) decreased viscosity and refining at 0.5 mm (RA2) produced the least viscous purees. Less energy was required to start these purees to flow since yield stress was lower for highly refined (less viscous) purees. Refining plays on two factors, namely PWM and particle size, since it retains cell clusters that are bigger than the sieve openings or separate them into individual cells when they pass through the sieve. Hence, both PWM and particle size decrease, leading to less viscous purees.

The correlation circle (**Fig. 101**A) of variables describing purees at T3, T6 and T9 (ground at 1000 rpm) was different from that at T0 and T1. Variables describing particle size still formed a group but they were orthogonal to variables describing viscosity and yield stress. Particle size thus seemed to be less important in purees that were prepared from apples stored for three or more months. Serum viscosity was grouped together with particle size and was thus also not important to differentiate puree's structure and texture in purees prepared from aged apples. However, PWM was grouped with puree's texture variables, mainly n_{100} and yield stress. This parameter thus seemed to gain importance in stored apples. Previous sections (cf. **V 1.1.**) showed that particle size decreased till T3 or T6 and then remained stable. PWM continued increasing and was the major factor determining puree's texture when particle size was constant. Refining (**Fig. 101**D) could not separate samples at T3, T6 and T9, further confirming constant particle sizes: Particles had reached the size of individual cells and refining was not effective. Temperature (**Fig. 101**B) and cooking duration (**Fig. 101**D) could not separate samples.
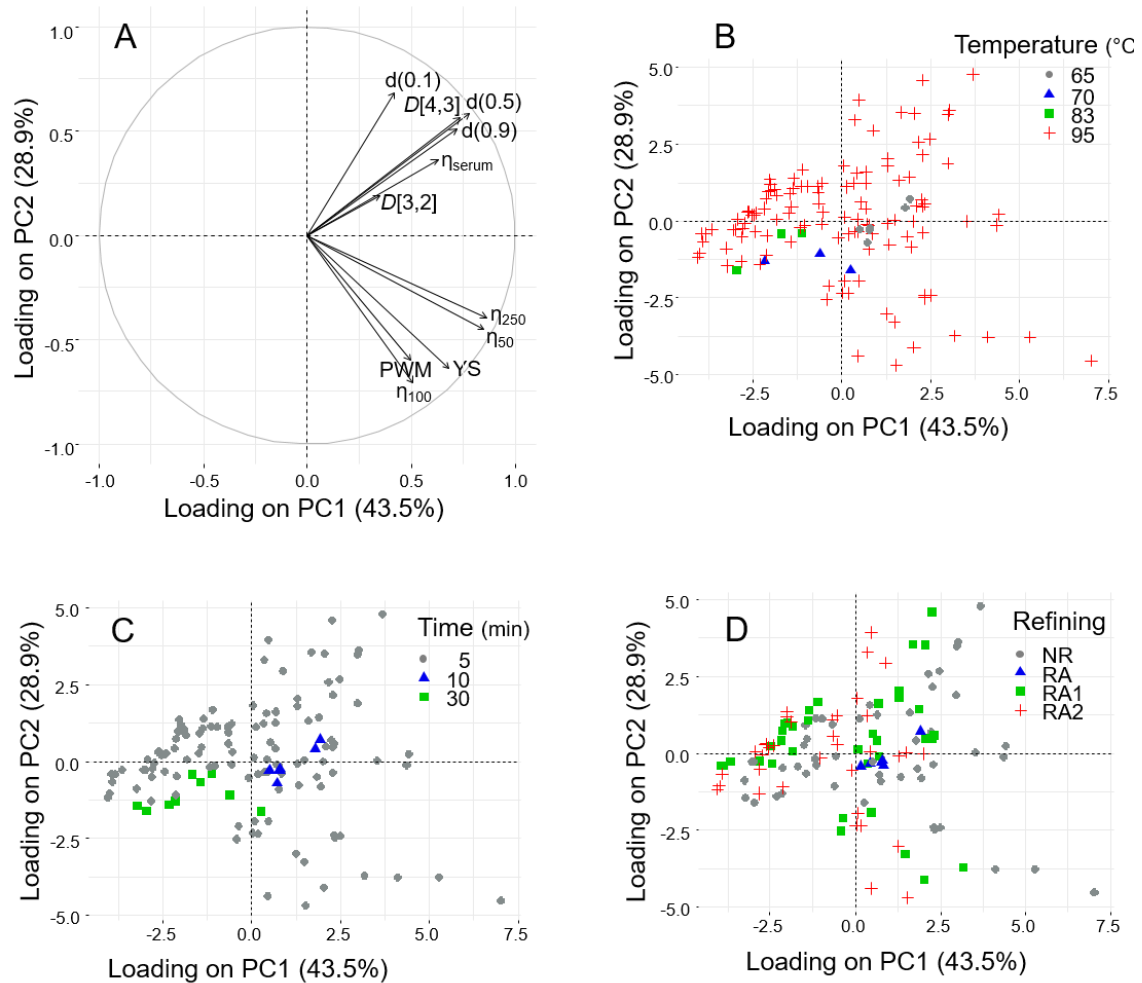
Fig. 101. Principal component analysis (PCA) of textural and structural characteristics of apple purees at T3, T6 and T9 and ground at 1000 rpm.

Correlation circle of variables loadings on PC1 (43.5%) and PC2 (28.9%) (A). Sample map of scores on PC1 and PC2 as function of processing temperature (B), duration (C) and refining level (D). η_{50}, η_{100}, η_{250}: Apparent viscosity of the puree at 50, 100 and 250 s^{-1}, respectively; YS: Yield stress of the puree; η_{serum}: Serum viscosity at 100 s^{-1}; PWM: Pulp wet mass; $D[4,3]$, $D[3,2]$, d(0.1), d(0.5) and d(0.9): Different variables explaining particle size. NR: Not refined; RA: refined (1.8 mm); RA1: refined (1.0 mm); RA2: refined (0.5 mm).

Overall, particle size was identified as the major determinant of puree's texture. As particle size was mostly affected by apple maturation and grinding speed, both parameters seemed to have major impact on puree's texture. Other input factors, such as varietal effects or temperature, were less important.

334

PWM gained in importance when particle size was constant. This effect was mainly visible in correlation with storage duration. While PWM kept increasing with apple maturity, particles had similar sizes in aged apples due to the presence of individual cells. Serum viscosity hardly had any role in explaining puree's texture.

Correlations between puree's texture and texture determinants (particle size, PWM, serum viscosity) were analysed more in detail by scatterplots (**Fig. 102**). Only few variables were retained. Apparent viscosity at 50 s^{-1} (η_{50}) was retained since it represents the approximate shear stress in mouth during mastication, as well as yield stress, which is an important viscoelastic parameter. Only one variable describing particle size distribution was kept since all these variables were correlated. The d(0.9) was chosen since the larger particles are the most influential on texture.

Yield stress and η_{50} varied in the same way, although a few points did not follow this trend. Generally, purees begun to flow at a smaller applied stress when they were less viscous. The d(0.9) values and η_{50} also increased together but several dot clouds with different slopes were visible, resulting in a low general correlation coefficient. PWM also varied in the same direction as η_{50} and values were less dispersed, resulting in a better correlation coefficient. Most samples showed low serum viscosity. Yet, some serum samples were more viscous, corresponding to GD1 and GS at T1 that were heated to 95 °C during 30 min (GD1) or 17 min (GS) and to GS at T0 that were heated at 95 °C during 5 min. However, high serum viscosity did not necessarily lead to high puree's texture.

In general, increasing particle size and PWM increased yield stress. An interesting relation was found between serum viscosity and yield stress; while yield stress was not affected by low serum viscosities, yield stress was systematically low with high serum viscosities. This might be due to the lubricant effect of highly viscous sera that was described in literature (Espinosa-Munoz, et al., 2013). The authors supposed that increased serum viscosity limits the cohesion between particles, resulting in low yield stress.
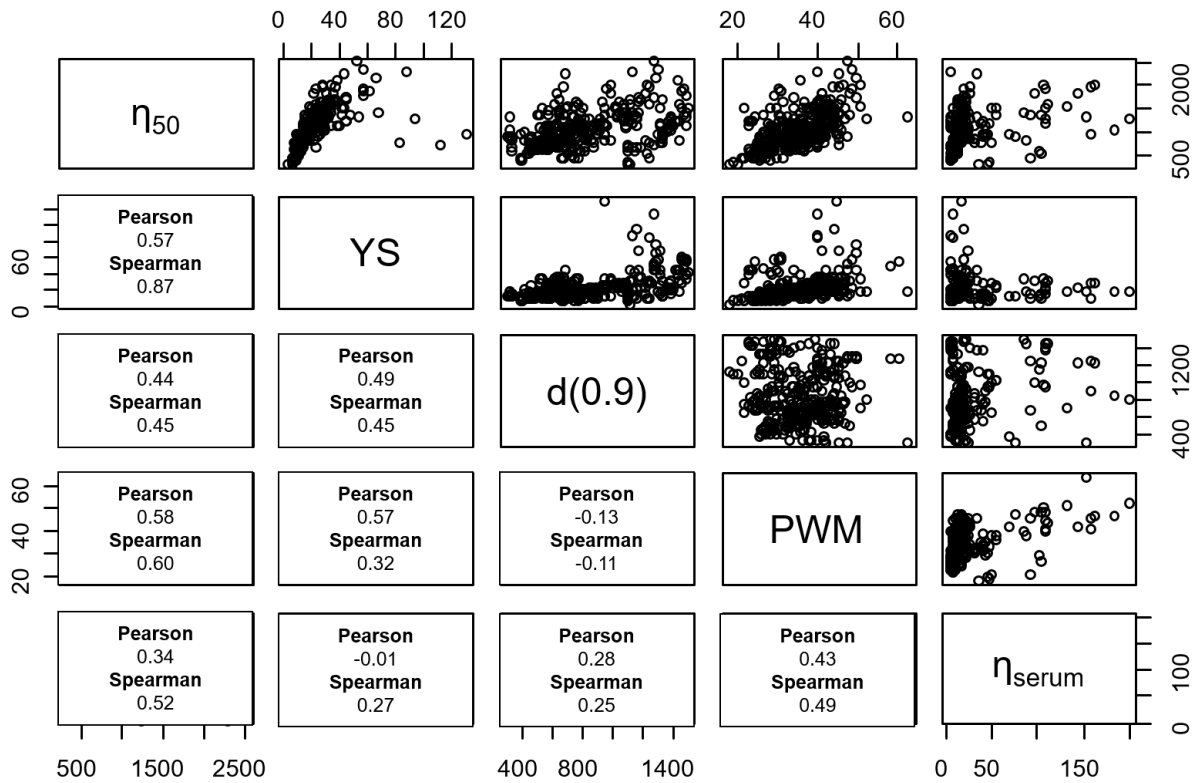
Fig. 102. Scatterplots of rheological characteristics and texture determinants of apple purees and corresponding Pearson and Spearman correlation coefficients.

η_{50}: Apparent viscosity of the puree at 50 s^{-1}; YS: Yield stress of the puree; d(0.9): Particle size d(0.9); PWM: Pulp wet mass; η_{serum}: Serum viscosity at 100 s^{-1}.

Although structural (particle size, PWM, serum viscosity) and textural (viscosity, yield stress) characteristics of apple purees sometimes varied in the same way, they were not highly correlated. This was due to several dot clouds with different slopes or dispersed points around the main cloud. It thus seemed that variations in puree's structure, induced by different input factors, were not straightforward. This is why scatterplots were redrawn using the dataset in which the main impact factors, storage duration and grinding speed (**Fig. 103**).
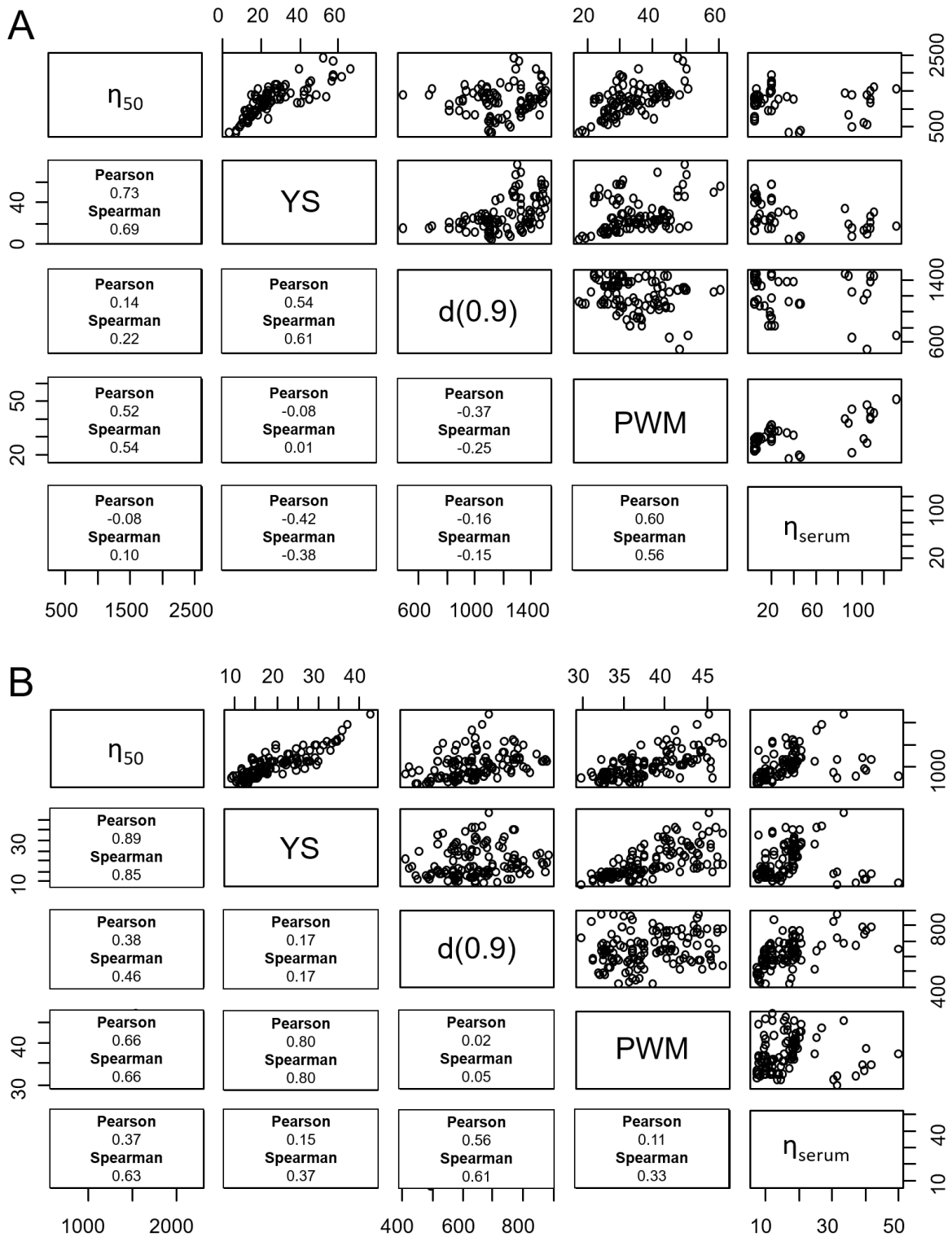
Fig. 103. Scatterplots of rheological characteristics and texture determinants of apple purees at T0 and T1 (A) and at T3, T6 and T9 (B), all ground at 1000 rpm, and corresponding Pearson and Spearman correlation coefficients.

η_{50}: Apparent viscosity of the puree at 50 s^{-1}; YS: Yield stress of the puree; d(0.9): Particle size d(0.9); PWM: Pulp wet mass; η_{serum}: Serum viscosity at 100 s^{-1}.

337

Trends were similar for samples at T0 and T1 (**Fig. 103**A) or samples at T3, T6 and T9 (**Fig. 103**B), all ground at 1000 rpm. A good correlation was detected between η_{50} and yield stress. However, particle size badly correlated to η_{50}. This was probably due to the fact that samples at related storage maturities showed similar particle sizes in the purees. Samples at T3, T6 and T9 showed moderate and good correlations between PWM and η_{50} or yield stress, respectively. Serum viscosity was not well correlated to textural characteristics of the puree and several groups were obtained. The before-mentioned lubricant effect of high viscous sera on yield stress was not confirmed.

In the literature, models were developed to predict puree´s texture by structural factors (Espinosa Brisset, 2012; Moelants, et al., 2012; Rao, 1987). However, conditions were fixed and well controlled. In this study, modelling was difficult to achieve. Although primary factors influencing puree's texture, namely apple maturity and grinding speed, were fixed, no clear correlations could be observed between the structure and texture of apple purees. Other input factors, such as cultivar or temperature, seemed to emerge. All input factors affect puree's structure differently, leading to contradictory effects, when they were linked to texture. For example, high temperature enhanced tissue fragmentation, leading to smaller particles, while PWM and serum viscosity increased.

3.2. Mechanisms on a molecular scale

The impact of several input factors on the structure of apple puree can be explained by pectin modifications. Post-harvest maturity of apples was shown to be an important factor affecting puree's texture. This was mainly due to particle size, which decreased and PWM, which increased with maturity. The previous chapters depicted a relation with pectin hydrolysis (cf. **V 1.1.** and **V 2.2.**). The focus was on serum pectins since it is the pectin fraction, which was solubilised during processing. In aged apples, serum pectins showed lower molar mass and a loss of RG I side chains, while the DM remained stable. This led to the conclusion that pectins were mainly solubilised after hydrolysis of the RG I neutral sugar side chains; RG I pectins can be linked to cellulose (Zykwinska, et al., 2005) and hemicellulose (Popper & Fry, 2005) by their side chains and their hydrolysis led to solubilisation. This would increase the porosity of the cell wall, enhancing i) water retention capacities (Guillon, et al., 1992) and thus PWM, and

ii) the access of pectinolytic enzymes to their substrates (Ng, et al., 2015). Solubilisation of HG from the middle lamella would then result in reduced cell adhesion. Tissue fragmentation is then favoured during processing, explaining why particles are smaller in purees prepared from aged apples. Interestingly, some samples showing high serum viscosity, also showed high PWM (**Fig. 102**). This highlights the relation between pectin solubilisation (increasing serum viscosity) and cell wall degradation (increasing PWM).

Like maturity, temperature showed similar effects on pectin degradation (cf. **V 2.2.**). However, samples could not be separated by this parameter in the PCAs conducted in this section. Temperature had thus no major impact on puree's structure and texture.

Besides the maturity stage of apples, grinding showed major impact on puree's structure, especially particle size. High shear intensities were shown to disrupt apple tissue without pectin degradation (cf. **V 2.1.**). However, cell separation was favoured by pectin hydrolysis, especially at low shear intensities, induced both by post-harvest storage or temperature (cf. **V 2.1.** and **V 2.2.**).

Serum viscosity hardly explained puree's texture but increased pectin solubilisation resulted in increased serum viscosity (**V 2.2.**). Hence, it indicated pectin degradation, which favoured tissue fragmentation.

Highlights

- Apple maturity and shear intensity had major impact on puree's structure.

- Particle size was identified as the major determinant of puree's texture.

- Pulp wet mass gained in importance when particle size was similar.

- Serum viscosity hardly explained puree's texture.

- Modelling was difficult due to contradictory effects on puree's structure, which emerged from the same or several input factors.

VI. Conclusions and perspectives

1. Conclusions

This thesis aimed to clarify the impact of raw material and processing on the texture of apple purees and to identify mechanisms for tissue fragmentation. This is important for industry since the processability of fruits and vegetables is poorly understood. In addition, it is not known how processing can modulate raw fruits characteristics in order to enhance puree's texture, an important quality attribute.

In contrast to previous studies, which mainly described reconstituted model systems, this study explored combined effects of raw material and processing on the structure and thus texture of apple purees. In addition, three structural levels, ranging from apple puree over its microstructure to the macromolecular scale, were analysed and correlations were pointed out. Special attention was paid to mechanical treatment. During this work, it was identified as an important parameter for texture modulation but information is missing in literature.

Apple puree is a highly complex system since texture depends from several structural factors. It could be shown that both the raw fruit and processing modulated cell wall microstructure and thus apple puree's texture. However, the alteration of one variable (e.g. prolonged cooking duration) often implicated the modification of another one (e.g. prolonged grinding). Despite numerous interactions and contradictory effects between input factors, several trends could be depicted. They are summarized in the following, grouped by the three studied scales:

1) Texture of apple purees

Since viscosity and viscoelastic properties of apple purees such as yield stress, G' and G'' all followed the same trend, "texture" was used in the following to summarize the rheological behaviour of purees.

Post-harvest maturity was the main factor influencing puree's texture. Both aged and mealy apples resulted in less viscous purees. **Cultivars** also affected puree's texture. However, individual fruit firmness could not predict puree's texture. Granny Smith was an exception since this cultivar revealed particularly high fruit and puree's textures. The effect of fruit thinning was contradictory between different studies, leading to the

assumption that different fruit sizes of the same cultivar, linked to contrasted amounts of individual cells, did not affect puree's texture.

In general, raw material altered puree's texture more than the process did. However, a combination of temperature and grinding speed could mitigate the poor performance of some cultivars as high temperature-low shear process produced more viscous purees. **Grinding** seemed to be more important than temperature as high shear intensities decreased puree's texture.

2) Microstructure of apple purees

Puree's structure could explain puree's texture. For example, large particles and high serum viscosity in purees of Granny Smith coincided with particularly viscous purees, while small particles in mealy apples led to less viscous purees.

Particle size was identified as the most important factor determining puree's texture, whereby smaller particles led to less viscous purees. Particle size also seemed to predominate the perceived texture of apple purees. In a sensory analysis of contrasted purees, the "graininess" of the purees was highlighted, knowing to be closely linked to particle size. Small particles were thus correlated with more homogenous purees. These purees were also associated with a "sweeter" taste but it seemed to be biased by the visual aspect of the purees since sugar extraction did not corroborate this observation.

The intensity of tissue fragmentation during processing determined particle size. Grinding was the main factor affecting tissue fragmentation and thus particle size, although high temperatures (95 °C) and increased post-harvest maturity enhanced tissue fragmentation additionally.

Other structural factors of the puree, i.e. the **proportion of particles** (pulp wet mass, PWM) and serum viscosity only altered puree's texture once particle size was constant. For example, PWM was the major determinant of the texture of purees prepared from aged apples. While PWM increased, particle size was constant. Hence, puree's texture increased. Not only post-harvest maturity but also high temperatures (95 °C) led to increased PWM, whereas grinding did not alter PWM.

Serum viscosity contributed very little to puree's texture. However, in apple purees showing the same particle size distribution and similar PWM, the viscosity of the continuous phase was strongly correlated with puree´s texture. Serum viscosity was mainly altered by temperature. Only 2 min at 95 °C were sufficient to increase serum viscosity, an effect that could occur during pasteurization. Prolonged heating at 95 °C, exceeding one hour, decreased serum viscosity. This might be important when purees rest for several minutes in a heated holding tank before bottling. Lower temperatures (50–83 °C) had no effect on serum viscosity.

3) Exploration of macromolecular scale (pectic polysaccharides)

Apple maturation (through enzymatic activity) and **elevated temperature** (through chemical reactions) induced **pectin degradation and solubilisation**, especially RG I side chains hydrolysis. This might decrease cell wall integrity, allowing increased solubilisation of middle lamella pectins and thus reduce cell adhesion. As a result, tissue fragmentation during grinding was favoured. Interestingly, elevated temperatures did not induce pectin degradation and solubilisation in aged apples, hinting at a maximum degradation and solubilisation during storage. Enzymatic activity in apples seemed not to be sufficient to cause pectin degradation during processing.

Decreased cell wall integrity through pectin solubilisation might result in increased cell wall porosity since more porous cells are known to retain more water (Guillon, et al., 1992). Here, an increase of water retention capacities of the cells in aged and heated apples could be linked to **higher PWM**.

Pectin solubilisation also **increased serum viscosity**. This was mainly promoted through high temperatures. A **decrease in serum viscosity** was probably due to pectin depolymerisation.

Mechanical processes had only minor impact on pectin composition and structure. However, intense grinding could disrupt cell wall tissue without pectin solubilisation.

The main results can be summarized as follows:

✓ Structural factors of the puree were linked to those of the raw material.

✓ Particle size was identified as the major determinant of puree's texture when there is no dilution or concentration of the fruit tissue.

✓ The extent of cell adhesion determined particle size more than individual cell size between apples of different cultivars or between apples produced by different agricultural practices.

✓ Other structural factors (PWM, serum viscosity) contributed to puree's texture once particle size was constant.

✓ Grinding (i.e. shear) was the main factor affecting tissue fragmentation, and thus particle size, during processing.

✓ Tissue fragmentation was additionally favoured by post-harvest maturity of the raw apples and high temperatures (95 °C) during processing.

✓ Post-harvest maturity and high temperatures led to pectin degradation, especially RG I side chain hydrolysis, and solubilisation. This enhanced tissue fragmentation during processing due to reduced cell adhesion.

2. Perspectives

The results still leave some questions. Some of them were considered in this thesis but could not be approached in detail.

Storage was shown to alter cell wall structure and thus puree's texture. However, in this study, cell wall modifications during storage were forced since apples were stored at 4 °C in normal atmosphere. The question now is how storage in low oxygen or ultra low oxygen affects cell wall microstructure and how this will affect puree's texture. It would also be of high interest for industry to understand the transition between firm apples, showing high cell adhesion, and loss of firmness. Soft apples were shown to be disrupted more easily during processing, so less energy might be required for puree production.

Apple puree's texture was also highly affected by the shear applied during processing since it decreased particle size. In this study, grinding was used to disrupt apple tissue but other techniques, such as high pressure homogenisation, exist and their potential on tissue fragmentation should be investigated in further studies.

High temperatures (95 °C) and prolonged heating duration also affected puree's structure. It would now be interesting to perform detailed kinetics in a short period of 5 to 15 min in order to quantify precisely the key moments of structure alteration.

Here, puree's structure and its impact on texture was explored after heat treatment. Hence, the cells were empty and highly deformable since the cell content has been liberated during processing. It would also be interesting to study the impact of intact cells (no heat treatment) on puree's texture to further elucidate the role of cell compressibility and cell wall rigidity in puree's texture.

Although cell deformation plays an important role in determining puree's texture (Leverrier, 2016), this aspect was not considered in this study. However, a first attempt was made to evaluate how the continuous phase could deform the particles. Tests were conducted in an "elongation flow chamber" within the laboratory for rheology and process at the CNRS (Centre National de la Recherche Scientifique) in Grenoble (France). Differences in dynamic deformation between cell clusters, individual cells and cell fragments were examined. Although cell fragments seemed to deform the most, cells tended to turn instead of deforming. In addition, cells highly aggregated in the system when the flow stopped and adapting the system would have taken up to six months. This experiment was thus abandoned in this PhD project due to lack of time, but it could be interesting to take it up in future studies.

It was hypothesized that porous cell walls increased PWM due to enhanced water retention capacities. Cell wall porosity was thus evaluated by NMR relaxation but other studies should be used to confirm the impact of apple maturity and temperature on cell wall porosity. Simons' stain (Meng & Ragauskas, 2014) was identified to be a powerful method. Here, cell wall samples are stained by a solution containing two colorants with different sizes. Then, the ratio of the adsorbed molecules provide an insight into pore size and distribution. However, the protocol is described for cellulose and needs to be adapted to cell wall samples.

Different process conditions led to more or less coloured and turbid sera. Since no small particles were detected in the serum, the colloidal state of dispersed soluble pectins should be considered.

Enzymatic activity in apples during processing was not enough to cause pectin degradation. However, the addition of pectinolytic enzymes, such as pectin methylesterase or polygalacturonase, during puree preparation could lead to differences in texture loss upon processing. This might help to understand the observed differences between apple cultivars or maturation. Slight differences in the pH value might also explain different responses of cultivars to heat treatment. This should be investigated more in detail by modulation of the pH value during puree processing.

The impact of pectin polysaccharides on structural factors of the puree could be assessed more in detail. The local distribution of pectins in the cell wall before and after processing could be assessed by Raman imaging. In addition, the structure of solubilised pectins could be further analysed by Atomic Force Microscopy (AFM). Some studies were initiated at the unit UMR5257 ICSM at CEA in Marcoule (France) but experimental setup was time-consuming and the analyses were thus not further followed.

To increase the understanding of cell wall microstructure on structural factors of the processed products and thus texture, the analyses could be extended to other fruits and vegetables.

All in all, this study deepened the understanding of tissue fragmentation and textural changes during processing, induced by pectic polysaccharides. It also provided guidelines for industry in order to handle the increasing diversity and heterogeneity of raw fruits by enlarged knowledge of how raw material and processing can be used to modulate apple puree's texture. This is a first step towards the conceptualization of innovative and more natural food products (no texturizing additives) and sustainable processing (no reconstitution).

VII. References

A

Addinsoft. (2020). *XLSTAT Statistical and Data Analysis Solution*, New York, USA. https://www.xlstat.com. (Accessed 29 April 2020).

Ahmed, J., & Ramaswamy, H. S. (2006). Viscoelastic and thermal characteristics of vegetable puree-based baby foods. *Journal of Food Process Engineering, 29*(3), 219-233.

Alba, K., Bingham, R. J., Gunning, P. A., Wilde, P. J., & Kontogiorgos, V. (2018). Pectin conformation in solution. *The Journal of Physical Chemistry B, 122*(29), 7286-7294.

Albersheim, P., Darvill, A. G., O'Neill, M. A., Schols, H. A., & Voragen, A. G. J. (1996). An hypothesis: The same six polysaccharides are components of the primary cell walls of all higher plants. In J. Visser & A. G. J. Voragen (Eds.), *Pectins and Pectinases* (Vol. 14, pp. 47-55).

Albersheim, P., Neukom, H., & Deuel, H. (1960). Splitting of pectin chain molecules in neutral solutions. *Archives of Biochemistry and Biophysics, 90*(1), 46-51.

Alvarez, M. D., Fernández, C., & Canet, W. (2004). Rheological behaviour of fresh and frozen potato puree in steady and dynamic shear at different temperatures. *European Food Research and Technology, 218*(6), 544-553.

Anantheswaran, R. C., McLellan, M. R., & Bourne, M. C. (1985). Thermal degradation of texture in apples. *Journal of Food Science, 50*(4), 1136-1138.

ANPP. (2020). Association Nationale Pommes Poires. http://lapomme.org. (Accessed 21 October 2020).

Anses. (2020). *Table de Composition Nutritionnelle des Aliments Ciqual*, www.ciqual.anses.fr. (Accessed 28 September 2020).

Anthon, G. E., Diaz, J. V., & Barrett, D. M. (2008). Changes in pectins and product consistency during the concentration of tomato juice to paste. *Journal of Agricultural and Food Chemistry, 56*(16), 7100-7105.

Anton Paar. (2020). Introduction to Rheology. https://wiki.anton-paar.com/en/basics-of-rheology/#oscilliation-tests-and-viscoelasticity. (Accessed 22 November 2020).

Aprikian, O., Duclos, V., Guyot, S., Besson, C., Manach, C., Bernalier, A., Morand, C., Remesy, C., & Demigne, C. (2003). Apple pectin and a polyphenol-rich apple concentrate are more effective together than separately on cecal fermentations and plasma lipids in rats. *Journal of Nutrition, 133*(6), 1860-1865.

Aspinall, G. O., & Fanous, H. K. (1984). Structural investigation on the non-starchy polysaccharides of apples. *Carbohydrate Polymers, 4*(3), 193-214.

Athiphunamphai, N., Bar, H. Y., Cooley, H. J., & Padilla-Zakour, O. I. (2014). Heat treatment and turbo extractor rotational speed effects on rheological and physico-chemical properties of varietal applesauce. *Journal of Food Engineering, 136*, 19-27.

Atkinson, R. G., Sutherland, P. W., Johnston, S. L., Gunaseelan, K., Hallett, I. C., Mitra, D., Brummell, D. A., Schröder, R., Johnston, J. W., & Schaffer, R. J. (2012). Down-regulation of POLYGALACTURONASE1 alters firmness, tensile strength and water loss in apple (Malus x domestica) fruit. *BMC Plant Biology, 12*(1), 129.

Auffret, A., Ralet, M. C., Guillon, F., Barry, J. L., & Thibault, J. F. (1994). Effect of grinding and experimental conditions on the measurement of hydration properties of dietary fibres. *LWT-Food Science and Technology, 27*(2), 166-172.

Axelos, M. A., & Thibault, J. F. (1991). Influence of the substituents of the carboxyl groups and of the rhamnose content on the solution properties and flexibility of pectins. *International Journal of Biological Macromolecules, 13*(2), 77-82.

Azadi, P., O'Neill, M. A., Bergmann, C., Darvill, A. G., & Albersheim, P. (1995). The backbone of the pectic polysaccharide rhamnogalacturonan I is cleaved by an endohydrolase and an endolyase. *Glycobiology, 5*(8), 783-789.

B

Bain, J. M., & Robertson, R. N. (1951). The physiology of growth in apple fruits. I. Cell size, cell number, and fruit development. *Australian Journal of Scientific Research / B, 4*(2), 75-107.

Balogh, T., Smout, C., Ly Nguyen, B., van Loey, A., & Hendrickx, M. (2004). Thermal and high-pressure inactivation kinetics of carrot pectinmethylesterase: From model system to real foods. *Innovative Food Science & Emerging Technologies, 5*(4), 429-436.

Barreiro, P., Ortiz, C., Ruiz-Altisent, M., Schotte, S., Andani, Z., Wakeling, I., & Beyt, P. K. (1998). Comparison between sensory and instrumental measurements for mealiness assessment in apples. A collaborative test. *Journal of Texture Studies, 29*(5), 509-525.

Barringer, S. A., Azam, A. T. M. S., Heskitt, B., & Sastry, S. (1998). On-line prediction of Bostwick consistency from pressure differential in pipe flow for ketchup and related tomato products. *Journal of Food Processing and Preservation, 22*(3), 211-220.

Barron, C., Devaux, M.-F., Foucat, L., Falourd, X., Looten, R., Joseph-Aimé, M., Durand, S., Bonnin, E., Lapierre, C., Saulnier, L., Rouau, X., & Guillon, F. (2020). Enzymatic degradation of maize shoots: Monitoring of chemical and physical changes reveals different saccharification behaviors. *Biotechnology for Biofuels, Ahead of Print.*

Bartley, I. M. (1978). Exo-polygalacturonase of apple. *Phytochemistry, 17*(2), 213-216.

Bazzocco, S., Mattila, I., Guyot, S., Renard, C. M., & Aura, A. M. (2008). Factors affecting the conversion of apple polyphenols to phenolic acids and fruit matrix to short-chain fatty acids by human faecal microbiota in vitro. *European Journal of Nutrition, 47*(8), 442-452.

Beckman, C. H. (2000). Phenolic-storing cells: Keys to programmed cell death and periderm formation in wilt disease resistance and in general defence responses in plants? *Physiological and Molecular Plant Pathology, 57*(3), 101-110.

Belović, M., Pajić-Lijaković, I., Torbica, A., Mastilović, J., & Pećinar, I. (2016). The influence of concentration and temperature on the viscoelastic properties of tomato pomace dispersions. *Food Hydrocolloids, 61*, 617-624.

Ben, J., & Gaweda, M. (1985). Changes of pectic compounds in jonathan apples under various storage conditions. *Acta Physiologiae Plantarum, 7*(2), 45-54.

Bidhendi, A. J., & Geitmann, A. (2016). Relating the mechanics of the primary plant cell wall to morphogenesis. *Journal of Experimental Botany, 67*(2), 449-461.

Billy, L., Mehinagic, E., Royer, G., Renard, C., Arvisenet, G., Prost, C., & Jourjon, F. (2008). Relationship between texture and pectin composition of two apple cultivars during storage. *Postharvest Biology and Technology, 47*(3), 315-324.

Bisulca, C., Nascimbene, P., Elkin, L., & Grimaldi, D. (2012). Variation in the deterioration of fossil resins and implications for the conservation of fossils in amber. *American Museum Novitates*, 1-19.

Blum, P. (1997). *Physical Properties Handbook*. Texas A&M University.

Blumenkrantz, N., & Asboe-Hansen, G. (1973). New method for quantitative-determination of uronic acids. *Analytical Biochemistry, 54*(2), 484-489.

Bondonno, N. P., Bondonno, C. P., Ward, N. C., Hodgson, J. M., & Croft, K. D. (2017). The cardiovascular health benefits of apples: Whole fruit vs. isolated compounds. *Trends in Food Science & Technology, 69*, 243-256.

Bonnin, E., Garnier, C., & Ralet, M. C. (2014). Pectin-modifying enzymes and pectin-derived materials: applications and impacts. *Applied Microbiology and Biotechnology, 98*(2), 519-532.

Bonnin, E., Le Goff, A., van Alebeek, G., Voragen, A. G. J., & Thibault, J. F. (2003). Mode of action of Fusarium moniliforme endopolygalacturonase towards acetylated pectin. *Carbohydrate Polymers, 52*(4), 381-388.

Bordenave, M. (1996). Analysis of pectin methyl esterases. In H. F. Linskens (Ed.), *Plant Cell Wall Analysis* (pp. 80-165). Berlin, Germany: Springer-Verlag.

Bourles, E., Mehinagic, E., Courthaudon, J. L., & Jourjon, F. (2009). Impact of vacuum cooking process on the texture degradation of selected apple cultivars. *Journal of Food Science, 74*(9), E512-E518.

Box, G. E. P., Hunter, W. G., & Hunter, J. S. (1978). *Statistics for Experimenters: An Introduction to Design, Data Analysis, and Model Building*. New York: John Wiley and Sons.

Boyer, J., & Liu, R. H. (2004). Apple phytochemicals and their health benefits. *Nutrition Journal, 3*(1), 5.

Brahem, M., Eder, S., Renard, C. M. G. C., Loonis, M., & Le Bourvellec, C. (2017a). Effect of maturity on the phenolic compositions of pear juice and cell wall effects on procyanidins transfer. *LWT-Food Science and Technology, Volume 85*, 380-384.

Brahem, M., Renard, C. M. G. C., Gouble, B., Bureau, S., & Le Bourvellec, C. (2017b). Characterization of tissue specific differences in cell wall polysaccharides of ripe and overripe pear fruit. *Carbohydrate Polymers, 156*, 152-164.

Brett, C. T., & Waldron, K. W. (1996). *Physiology and biochemistry of plant cell walls* (Vol. 2). United Kingdom: Chapman & Hall.

Brochet, F. (1999). The taste of wine in consciousness. *Journal International des Sciences de la Vigne et du Vin: Special Issue Wine Tasting*, 19-22.

Brookfield, P., Murphy, P., Harker, R., & MacRae, E. (1997). Starch degradation and starch pattern indices; interpretation and relationship to maturity. *Postharvest Biology and Technology, 11*(1), 23-30.

Broxterman, S. E., & Schols, H. A. (2018). Interactions between pectin and cellulose in primary plant cell walls. *Carbohydrate Polymers, 192*, 263-272.

Brummell, D., Lashbrook, C., & Bennett, A. (1994). Plant endo-1,4 β-D glucanase: structure, properties and physiological function. In M. Himmel, J. Baker & R. Overend (Eds.), *Enzymatic Conversion of Biomass for Fuels Production* (pp. 100-129): American Chemical Society.

Brummell, D. A. (2006). Cell wall disassembly in ripening fruit. *Functional Plant Biology, 33*(2), 103-119.

Brummell, D. A., & Harpster, M. H. (2001). Cell wall metabolism in fruit softening and quality and its manipulation in transgenic plants. *Plant Molecular Biology, 47*(1), 311-339.

Buergy, A. (2017). Impact of Storage and Process on the Cell Wall Composition of Apple Purees. *Master's Thesis* (Technical University of Munich, INRA UMR408 SQPOV).

Buergy, A., Rolland-Sabaté, A., Leca, A., & Renard, C. M. G. C. (2020). Pectin modifications in raw fruits alter texture of plant cell dispersions. *Food Hydrocolloids, 107*, 105962.

Burchard, W. (1983). Static and dynamic light scattering from branched polymers and biopolymers. In *Light Scattering from Polymers. Advances in Polymer Science* (Vol. 48, pp. 1-124). Berlin, Heidelberg: Springer.

C

Caelles, C., Delseny, M., & Puigdomenech, P. (1992). The hydroxyproline-rich glycoprotein gene from Oryza sativa. *Plant Molecular Biology, 18*(3), 617-619.

Caffall, K. H., & Mohnen, D. (2009). The structure, function, and biosynthesis of plant cell wall pectic polysaccharides. *Carbohydrate Research, 344*(14), 1879-1900.

Cámara Hurtado, M., Greve, L. C., & Labavitch, J. M. (2002). Changes in cell wall pectins accompanying tomato (Lycopersicon esculentum Mill.) paste manufacture. *Journal of Agricultural and Food Chemistry, 50*(2), 273-278.

Cardenas-Perez, S., Mendez-Mendez, J. V., Chanona-Perez, J. J., Zdunek, A., Guemes-Vera, N., Calderon-Dominguez, G., & Rodriguez-Gonzalez, F. (2017). Prediction of the nanomechanical properties of apple tissue during its ripening process from its firmness, color and microstructural parameters. *Innovative Food Science & Emerging Technologies, 39*, 79-87.

Carpita, N. C., & Gibeaut, D. M. (1993). Structural models of primary-cell walls in flowering plants - Consistency of molecular-structure with the physical-properties of the walls during growth. *Plant Journal, 3*(1), 1-30.

Carrington, C., Greve, L. C., & Labavitch, J. M. (1993). Cell wall metabolism in ripening fruit (VI. Effect of the antisense polygalacturonase gene on cell wall changes accompanying ripening in transgenic tomatoes). *Plant Physiology, 103*(2), 429-434.

Castro, A., Bergenståhl, B., & Tornberg, E. (2013). Effect of heat treatment and homogenization on the rheological properties of aqueous parsnip suspensions. *Journal of Food Engineering, 117*(3), 383-392.

Ceci, L., & Lozano, J. (1998). Determination of enzymatic activities of commercial pectinases for the clarification of apple juice. *Food Chemistry, 61*(1), 237-241.

Chan, S. Y., Choo, W. S., Young, D. J., & Loh, X. J. (2017). Pectin as a rheology modifier: Origin, structure, commercial production and rheology. *Carbohydrate Polymers, 161*, 118-139.

Chen, E. M. W., & Mort, A. J. (1996). Nature of sites hydrolyzable by endopolygalacturonase in partially-esterified homogalacturonans. *Carbohydrate Polymers, 29*(2), 129-136.

Christiaens, S., Mbong, V. B., Van Buggenhout, S., David, C. C., Hofkens, J., Van Loey, A. M., & Hendrickx, M. E. (2012). Influence of processing on the pectin structure-function relationship in broccoli puree. *Innovative Food Science & Emerging Technologies, 15*, 57-65.

Christiaens, S., Van Buggenhout, S., Houben, K., Fraeye, I., Van Loey, A. M., & Hendrickx, M. E. (2011). Towards a better understanding of the pectin structure-function relationship in broccoli during processing: Part I-macroscopic and molecular analyses. *Food Research International, 44*(6), 1604-1612.

Chu, C. L. G., & Wilson, K. (2000). Evaluating maturity of empire, idared and spartan apples. In *FactSheet ISSN 1198-712X ©Queen´s Printer for Ontario.*

Chylińska, M., Szymańska-Chargot, M., & Zdunek, A. (2014). Imaging of polysaccharides in the tomato cell wall with Raman microspectroscopy. *Plant Methods, 10*(1), 14.

Coenen, G. J., Bakx, E. J., Verhoef, R. P., Schols, H. A., & Voragen, A. G. J. (2007). Identification of the connecting linkage between homo- or xylogalacturonan and rhamnogalacturonan type I. *Carbohydrate Polymers, 70*(2), 224-235.

Colin-Henrion, M., Cuvelier, G., & Renard, C. M. G. C. (2007). Texture of pureed fruit and vegetable foods. *Steward Postharvest Review*, 1-14.

Colin-Henrion, M., Mehinagic, E., Renard, C. M. G. C., Richomme, P., & Jourjon, F. (2009). From apple to apple sauce: Processing effects on dietary fibres and cell wall polysaccharides. *Food Chemistry, 117*(2), 254-260.

Cornille, A., Gladieux, P., Smulders, M. J., Roldán-Ruiz, I., Laurens, F., Le Cam, B., Nersesyan, A., Clavel, J., Olonova, M., Feugey, L., Gabrielyan, I., Zhang, X. G., Tenaillon, M. I., & Giraud, T. (2012). New insight into the history of domesticated apple: secondary contribution of the European wild apple to the genome of cultivated varieties. *PLoS Genetics, 8*(5), e1002703.

Cosgrove, D. J. (2005). Growth of the plant cell wall. *Nature Reviews Molecular Cell Biology, 6*(11), 850-861.

Cosgrove, D. J. (2016). Catalysts of plant cell wall loosening. *F1000Research, 5*, F1000 Faculty Rev-1119.

Cosgrove, D. J., & Jarvis, M. C. (2012). Comparative structure and biomechanics of plant primary and secondary cell walls. *Frontiers in Plant Science, 3*(204).

Crelier, S., Robert, M., Claude, J., & Juillerat, M. A. (2001). Tomato (Lycopersicon esculentum) pectin methylesterase and polygalacturonase behaviors regarding heat- and pressure-induced inactivation. *Journal of Agricultural and Food Chemistry, 49*, 5566-5575.

Cros, S., Garnier, C., Axelos, M. A., Imberty, A., & Perez, S. (1996). Solution conformations of pectin polysaccharides: Determination of chain characteristics by small angle neutron scattering, viscometry, and molecular modeling. *Biopolymers, 39*(3), 339-352.

Cullen, P. J., Duffy, A. P., & O'Donnell, C. P. (2001). On-line rheological charcterization of pizza sauce using tube viscometry. *Journal of Food Process Engineering, 24*(3), 145-159.

Cummings, J. H. (1983). Fermentation in the human large intestine - Evidence and implications for health. *Lancet, 1*(8335), 1206-1209.

Cybulska, J., Zdunek, A., Psonka-Antonczyk, K. M., & Stokke, B. T. (2013). The relation of apple texture with cell wall nanostructure studied using an atomic force microscope. *Carbohydrate Polymers, 92*(1), 128-137.

D

Daas, P. J. H., Meyer-Hansen, K., Schols, H. A., De Ruiter, G. A., & Voragen, A. G. J. (1999). Investigation of the non-esterified galacturonic acid distribution in pectin with endopolygalacturonase. *Carbohydrate Research, 318*(1), 135-145.

Dairou, V., & Sieffermann, J. M. (2002). A comparison of 14 jams characterized by conventional profile and a quick original method, the Flash Profile. *Journal of Food Science, 67*(2), 826-834.

Darvill, A., McNeil, M., Albersheim, R., & Delmer, D. (1980). *The biochemistry of plants* (Vol. 1). New York: Academic.

Day, L., Xu, M., Oiseth, S. K., Lundin, L., & Hemar, Y. (2010). Dynamic rheological properties of plant cell-wall particle dispersions. *Colloids and Surfaces B: Biointerfaces, 81*(2), 461-467.

De Roeck, A., Duvetter, T., Fraeye, I., Plancken, I. V. d., Sila, D. N., Loey, A. V., & Hendrickx, M. (2008). Effect of high pressure/high temperature processing on chemical pectin conversions in relation to fruit and vegetable texture. *Food Chemistry, 115*(1), 207-213.

De Vries, J. A., Rombouts, F. M., Voragen, A. G. J., & Pilnik, W. (1982). Enzymic degradation of apple pectins. *Carbohydrate Polymers, 2*(1), 25-33.

De Vries, J. A., Voragen, A. G. J., Rombouts, F. M., & Pilnik, W. (1981). Extraction and purification of pectins from Alcohol Insoluble Solids from ripe and unripe apples. *Carbohydrate Polymers, 1*(2), 117-127.

Del Rio, D., Costa, L. G., Lean, M. E., & Crozier, A. (2010). Polyphenols and health: What compounds are involved? *Nutrition, Metabolism & Cardiovascular Diseases, 20*(1), 1-6.

Den Ouden, F. W. C., & Van Vliet, T. (1997). Particle size distribution in tomato concentrate and effects on rheological properties. *Journal of Food Science, 62*, 565-567.

Denes, J. M., Baron, A., & Drilleau, J. F. (2000). Purification, properties and heat inactivation of pectin methylesterase from apple (cv Golden Delicious). *Journal of the Science of Food and Agriculture, 80*(10), 1503-1509.

Denne, P. M. (1963). Fruit development and some tree factors affecting it. *New Zealand Journal of Botany, 1*(3), 265-294.

Dheilly, E., Le Gall, S., Guillou, M. C., Renou, J. P., Bonnin, E., Orsel, M., & Lahaye, M. (2016). Cell wall dynamics during apple development and storage involves hemicellulose modifications and related expressed genes. *BMC Plant Biology, 16*.

Dhingra, D., Michael, M., Rajput, H., & Patil, R. T. (2012). Dietary fibre in foods: A review. *Journal of Food Science and Technology, 49*(3), 255-266.

Diaz, J. V., Anthon, G. E., & Barrett, D. M. (2009). Conformational changes in serum pectins during industrial tomato paste production. *Journal of Agricultural and Food Chemistry, 57*(18), 8453-8458.

Dick-Pérez, M., Zhang, Y., Hayes, J., Salazar, A., Zabotina, O. A., & Hong, M. (2011). Structure and interactions of plant cell-wall polysaccharides by two- and three-dimensional magic-angle-spinning solid-state NMR. *Biochemistry, 50*(6), 989-1000.

Dobias, J., Voldrich, M., & Curda, D. (2006). Heating of canned fruits and vegetables: Deaeration and texture changes. *Journal of Food Engineering, 77*(3), 421-425.

Doublier, J. L., & Choplin, L. (1989). A rheological description of amylose gelation. *Carbohydrate Research, 193*, 215-226.

Downing, D. L. (1989). *Processed apple products* (1st ed.). New York: Van Nostrand Reinhold.

Dubois, M., Gilles, K. A., Hamilton, J. K., Rebers, P. A., & Smith, F. (1956). Colorimetric method for determination of sugars and related substances. *Analytical Chemistry, 28*(3), 350-356.

Duden. (2017). http://www.duden.de/rechtschreibung/Kelch11. (Accessed 11 September 2017).

Dunn, O. J. (1964). Multiple comparisons using rank sums. *Technometrics, 6*(3), 241-252.

Duran, L., & Costell, E. (1982). Rheology of apricot puree: Characterization of flow. *Journal of Texture Studies, 13*, 43-58.

Duvetter, T., Sila, D. N., Van Buggenhout, S., Jolie, R., Van Loey, A., & Hendrickx, M. (2009). Pectins in processed fruit and vegetables: Part I - Stability and catalytic activity of pectinases. *Comprehensive Reviews in Food Science and Food Safety, 8*(2), 75-85.

E

Ebel, R., C., Proebsting, E., L., & Patterson, M., E. (1993). Regulated deficit irrigation may alter apple maturity, quality, and storage life. *Journal of Horticultural Science, 28*(2), 141-143.

Ebermann, R., & Elmadfa, I. (2011). *Lehrbuch Lebensmittelchemie und Ernährung* (2nd ed.). Wien, New York: Springer.

Einstein, A. (1906). Eine neue Bestimmung der Moleküldimensionen. *Annalen der Physik, 324*(2), 289-306.

Einstein, A. (1911). Berichtigung zu meiner Arbeit: „Eine neue Bestimmung der Moleküldimensionen". *Annalen der Physik, 339*(3), 591-592.

Eisele, T., & Drake, S. (2005). The partial compositional characteristics of apple juice from 175 apple varieties. *Journal of Food Composition and Analysis, 18*, 213-221.

Ella Missang, C., Maingonnat, J. F., Renard, C. M. G. C., & Audergon, J.-M. (2012). Apricot cell wall composition: Relation with the intra-fruit texture heterogeneity and impact of cooking. *Food Chemistry, 133*(1), 45-54.

Englyst, H., Wiggins, H. S., & Cummings, J. H. (1982). Determination of the non-starch polysaccharides in plant-foods by gas-liquid-chromatography of constituent sugars as alditol acetates. *Analyst, 107*(1272), 307-318.

Esau, K. (1977). *Anatomy of seed plants* (2nd ed.). New York: John Wiley & Sons Ltd.

Espinosa-Munoz, L., Renard, C. M. G. C., Symoneaux, R., Biau, N., & Cuvelier, G. (2013). Structural parameters that determine the rheological properties of apple puree. *Journal of Food Engineering, 119*(3), 619-626.

Espinosa-Munoz, L., Symoneaux, R., Renard, C. M. G. C., Biau, N., & Cuvelier, G. (2012). The significance of structural properties for the development of innovative apple puree textures. *LWT-Food Science and Technology, 49*(2), 221-228.

Espinosa Brisset, L. C. (2012). Texture de la Purée de Pomme : Influence de la Structure sur les Propriétés Rhéologiques et la Perception Sensorielle - Effet du Traitement Mécanique. *Doctoral thesis* (AgroParisTech).

Espinosa, L., To, N., Symoneaux, R., Renard, C. M. G. C., Biau, N., & Cuvelier, G. (2011). Effect of processing on rheological, structural and sensory properties of apple puree. In G. Saravacos, P. Taoukis, M. Krokida, V. Karathanos, H. Lazarides, N. Stoforos, C. Tzia & S. Yanniotis (Eds.), *11th International Congress on Engineering and Food* (Vol. 1, pp. 513-520). Amsterdam: Elsevier Science Bv.

Eurostat. (2017). Where are our Fruit and Veg produced? https://ec.europa.eu/eurostat/web/products-eurostat-news/-/DDN-20170728-1. (Accessed 13 November 2020).

F

FAO. (2018). http://www.fao.org/faostat/en/#data/QC. (Accessed 13 September 2020).

Featherstone, S. (2016). Canning of fruit. In S. Featherstone (Ed.), *A Complete Course in Canning and Related Processes* (14th ed., Vol. 3, pp. 85-134). Cambridge: Woodhead Publishing.

Filippov, M. P., & Kohn, R. (1975). Determination of esterification degree of carboxyl groups of pectin with methanol by means of infrared spectroscopy. *Chemické Zvesti, 29*(1), 88-91.

Fischer, M., & Amado, R. (1994). Changes in the pectic substances of apples during development and postharvest ripening. Part 1: Analysis of the alcohol insoluble residue. *Carbohydrate Polymers, 25*(3), 161-166.

Fischer, M., Arrigoni, E., & Amado, R. (1994). Changes in the pectic substances of apples during development and postharvest ripening. Part 2: Analysis of the pectic fractions. *Carbohydrate Polymers, 25*(3), 167-175.

Fischer, R. L., & Bennett, A. B. (1991). Role of cell wall hydrolases in fruit ripening. *Annual Review of Plant Physiology and Plant Molecular Biology, 42*(1), 675-703.

Fishman, M. L., Cooke, P. H., Chau, H. K., Coffin, D. R., & Hotchkiss, A. T., Jr. (2007). Global structures of high methoxyl pectin from solution and in gels. *Biomacromolecules, 8*(2), 573-578.

Fishman, M. L., Gillespie, D. T., Sondey, S. M., & Barford, R. A. (1989). Characterization of pectins by size exclusion chromatography in conjunction with viscosity detection. *Journal of Agricultural and Food Chemistry, 37*(3), 584-591.

Fishman, M. L., Pfeffer, E. P., Barford, A. R., & Doner, W. L. (1984). Studies of pectin solution properties by high-performance size exclusion chromatography. *Journal of Agricultural and Food Chemistry, 32*(2), 372–378.

Foodbay. (2020). https://foodbay.com/en/bbs/brands/roboqbo/kuttery/serija-qbo/qb8-3?lt=1. (Accessed 7 November 2020).

Foucat, L., & Lahaye, M. (2014). A subzero 1H NMR relaxation investigation of water dynamics in tomato pericarp. *Food Chemistry, 158*, 278-282.

Fraeye, I., De Roeck, A., Duvetter, T., Verlent, I., Hendrickx, M., & Van Loey, A. (2007). Influence of pectin properties and processing conditions on thermal pectin degradation. *Food Chemistry, 105*(2), 555-563.

Fraga, C. G., Oteiza, P. I., & Galleano, M. (2018). Plant bioactives and redox signaling: (–)-Epicatechin as a paradigm. *Molecular Aspects of Medicine, 61*, 31-40.

FranceAgriMer. (2015). La Pomme en 2014-2015. https://www.rnm.franceagrimer.fr. (Accessed 21 October 2020).

FranceAgriMer. (2017). La Pomme en 2016-2017. https://www.rnm.franceagrimer.fr. (Accessed 21 October 2020).

Fricke, W., Jarvis, M. C., & Brett, C. T. (2000). Turgor pressure, membrane tension and the control of exocytosis in higher plants. *Plant, Cell & Environment, 23*(9), 999-1003.

Fujino, T., Sone, Y., Mitsuishi, Y., & Itoh, T. (2000). Characterization of cross-links between cellulose microfibrils, and their occurrence during elongation growth in pea epicotyl. *Plant Cell Physiology, 41*(4), 486-494.

G

Gálvez-López, D., Laurens, F., Devaux, M. F., & Lahaye, M. (2012). Texture analysis in an apple progeny through instrumental, sensory and histological phenotyping. *Euphytica, 185*(2), 171-183.

Gawkowska, D., Cybulska, J., & Zdunek, A. (2018). Structure-related gelling of pectins and linking with other natural compounds: A review. *Polymers, 10*(7), 762.

Geshi, N., Jørgensen, B., & Ulvskov, P. (2004). Subcellular localization and topology of β(1 → 4)galactosyltransferase that elongates β(1 → 4)galactan side chains in rhamnogalacturonan I in potato. *Planta, 218*(5), 862-868.

Gibson, L. J. (2012). The hierarchical structure and mechanics of plant materials. *Journal of the Royal Society Interface, 9*(76), 2749-2766.

Gidley, M. J. (2013). Hydrocolloids in the digestive tract and related health implications. *Current Opinion in Colloid & Interface Science, 18*, 371–378.

Gidley, M. J., & Yakubov, G. E. (2019). Functional categorisation of dietary fibre in foods: Beyond 'soluble' vs 'insoluble'. *Trends in Food Science & Technology, 86*, 563-568.

Gierlinger, N., Keplinger, T., & Harrington, M. (2012). Imaging of plant cell walls by confocal Raman microscopy. *Nature Protocols, 7*(9), 1694-1708.

Goffinet, M. C., Robinson, T. L., & Lakso, A. N. (1995). A comparison of 'Empire' apple fruit size and anatomy in unthinned and hand-thinned trees. *Journal of Horticultural Science, 70*(3), 375-387.

Goodman, C. L., Fawcett, S., & Barringer, S. A. (2002). Flavor, viscosity, and color analyses of hot and cold break tomato juices. *Journal of Food Science, 67*(1), 404-408.

Gower, J. C. (1975). Generalized procrustes analysis. *Psychometrika, 40*(1), 33-51.

Grant, G. T., Morris, E. R., Rees, D. A., Smith, P. J. C., & Thom, D. (1973). Biological interactions between polysaccharides and divalent cations: The egg-box model. *FEBS Letters, 32*(1), 195-198.

Grasdalen, H., Einar Bakøy, O., & Larsen, B. (1988). Determination of the degree of esterification and the distribution of methylated and free carboxyl groups in pectins by 1H-NMR spectroscopy. *Carbohydrate Research, 184*, 183-191.

Green, J. W. (1967). The glycofuranosides. In M. L. Wolfrom & R. S. Tipson (Eds.), *Advances in Carbohydrate Chemistry* (Vol. 21, pp. 95-142): Academic Press.

Gregson, C. M., & Lee, T.-C. (2003). Evaluation of numerical algorithms for the instrumental measurement of bowl-life and changes in texture over time for ready-to-eat breakfast cereals. *Journal of Texture Studies, 33*(6), 505-528.

Greve, L. C., Shackel, K. A., Ahmadi, H., McArdle, R. N., Gohlke, J. R., & Labavitch, J. M. (1994). Impact of heating on carrot firmness: Contribution of cellular turgor. *Journal of Agricultural and Food Chemistry, 42*(12), 2896-2899.

Gross, K. C., & Sams, C. E. (1984). Changes in cell wall neutral sugar composition during fruit ripening: a species survey. *Phytochemistry, 23*(11), 2457-2461.

Guiavarc'h, Y., Sila, D., Duvetter, T., van Loey, A., & Hendrickx, M. (2003). Influence of sugars and polyols on the thermal stability of purified tomato and cucumber pectinmethylesterases: A basis for TTI development. *Enzyme and Microbial Technology, 33*(5), 544-555.

Guillemin, F., Guillon, F., Bonnin, E., Devaux, M. F., Chevalier, T., Knox, J. P., Liners, F., & Thibault, J. F. (2005). Distribution of pectic epitopes in cell walls of the sugar beet root. *Planta, 222*(2), 355-371.

Guillon, F., Barry, J.-L., & Thibault, J.-F. (1992). Effect of autoclaving sugar-beet fibre on its physico-chemical properties and its in-vitro degradation by human faecal bacteria. *Journal of the Science of Food and Agriculture, 60*(1), 69-79.

Guillon, F., & Champ, M. (2000). Structural and physical properties of dietary fibres, and consequences of processing on human physiology. *Food Research International, 33*, 233-245.

Guyot, S., Marnet, N., Laraba, D., Sanoner, P., & Drilleau, J.-F. (1998). Reversed-phase HPLC following thiolysis for quantitative estimation and characterization of the four main classes of phenolic compounds in different tissue zones of a French cider apple variety (Malus domestica Var. Kermerrien). *Journal of Agricultural and Food Chemistry, 46*(5), 1698-1705.

Gwanpua, S. G., Van Buggenhout, S., Verlinden, B. E., Christiaens, S., Shpigelman, A., Vicent, V., Kermani, Z. J., Nicolai, B. M., Hendrickx, M., & Geeraerd, A. (2014). Pectin modifications and the role of pectin-degrading enzymes during postharvest softening of Jonagold apples. *Food Chemistry, 158*, 283-291.

Gwanpua, S. G., Verlinden, B. E., Hertog, M., Nicolai, B. M., Hendrickx, M., & Geeraerd, A. (2016). Slow softening of Kanzi apples (Malus x domestica L.) is associated with preservation of pectin integrity in middle lamella. *Food Chemistry, 211*, 883-891.

H

Harker, F., & Hallett, I. (1992). Physiological changes associated with development of mealiness of apple fruit during cool storage. *HortScience, 27*(12), 1291-1294.

Heredia, A., Guillen, R., Jimenez, A., & Fernandez-Bolanos, J. (1993). Plant cell wall structure. *Revista Española de Ciencia y Tecnología de Alimentos, 33*(2), 113-131.

Heredia, A., Jimenez, A., & Guillen, R. (1995). Composition of plant cell walls. *Zeitschrift für Lebensmittel-Untersuchung und -Forschung, 200*(1), 24-31.

Hervé du Penhoat, C., Gey, C., Pellerin, P., & Perez, S. (1999). An NMR solution study of the mega-oligosaccharide, rhamnogalacturonan II. *Journal of Biomolecular NMR, 14*(3), 253-271.

Hobson, G. E. (1962). Determination of polygalacturonase in fruits. *Nature, 195*(4843), 804-&.

Hou, J., Sun, Y., Chen, F., Yu, L., Mao, Q., Wang, L., Guo, X., & Liu, C. (2016). Analysis of microstructures and macrotextures for different apple cultivars based on parenchyma morphology. *Microscopy Research and Technique, 79*(4), 304-312.

Hourdet, D., & Muller, G. (1991). Solution properties of pectin polysaccharides. 2. Conformation and molecular-size of high galacturonic acid content isolated pectin chains. *Carbohydrate Polymers, 16*(2), 113-135.

Hurtado, M. C., Greve, L. C., & Labavitch, J. M. (2002). Changes in cell wall pectins accompanying tomato (Lycopersicon esculentum Mill.) paste manufacture. *Journal of Agricultural and Food Chemistry, 50*(2), 273-278.

I

Imaizumi, T., Szymanska-Chargot, M., Pieczywek, P. M., Chylinska, M., Koziol, A., Ganczarenko, D., Tanaka, F., Uchino, T., & Zdunek, A. (2017). Evaluation of pectin nanostructure by atomic force microscopy in blanched carrot. *LWT-Food Science and Technology, 84*, 658-667.

Ishii, T. (1995). Isolation and characterization of acetylated rhamnogalacturonan oligomers liberated from bamboo shoot cell-walls by driselase. *Mokuzai Gakkaishi, 41*(6), 561-572.

Ishii, T. (1997). O-acetylated oligosaccharides from pectins of potato tuber cell walls. *Plant Physiology, 113*(4), 1265-1272.

Ishii, T., Matsunaga, T., Pellerin, P., O'Neill, M. A., Darvill, A., & Albersheim, P. (1999). The plant cell wall polysaccharide rhamnogalacturonan II self-assembles into a covalently cross-linked dimer. *Journal of Biological Chemistry, 274*(19), 13098-13104.

Ishii, T., & Ono, H. (1999). NMR spectroscopic analysis of the borate diol esters of methyl apiofuranosides. *Carbohydrate Research, 321*(3), 257-260.

Iwai, H., Masaoka, N., Ishii, T., & Satoh, S. (2002). A pectin glucuronyltransferase gene is essential for intercellular attachment in the plant meristem. *Proceedings of the National Academy of Sciences of the United States of America, 99*(25), 16319-16324.

J

Jackson, J. E. (2003). *Biology of Apple and Pears*. Cambridge: Cambridge University Press.

Jarvis, M. C. (1984). Structure and properties of pectin gels in plant-cell walls. *Plant Cell and Environment, 7*(3), 153-164.

Jarvis, M. C. (2011). Plant cell walls: Supramolecular assemblies. *Food Hydrocolloids, 25*(2), 257-262.

Jarvis, M. C., Briggs, S. P. H., & Knox, J. P. (2003). Intercellular adhesion and cell separation in plants. *Plant Cell and Environment, 26*(7), 977-989.

Jarvis, M. C., & McCann, M. C. (2000). Macromolecular biophysics of the plant cell wall: Concepts and methodology. *Plant Physiology and Biochemistry, 38*(1-2), 1-13.

Jiménez, A. J., Labavitch, J. M., & Moreno, A. H. (1994). Changes in the cell-wall of olive fruit during processing. *Journal of Agricultural and Food Chemistry, 42*(5), 1194-1199.

Jolliffe, I. T. (2002). *Principal Component Analysis* (2nd ed.). New York: Springer.

K

Khan, A. A., & Vincent, J. F. V. (1990). Anisotropy of apple parenchyma. *Journal of the Science of Food and Agriculture, 52*(4), 455-466.

Kikuchi, A., Edashige, Y., Ishii, T., & Satoh, S. (1996). A xylogalacturonan whose level is dependent on the size of cell clusters is present in the pectin from cultured carrot cells. *Planta, 200*(4), 369-372.

Kim, D. M., Smith, N. L., & Lee, C. Y. (1993). Apple cultivar variations in response to heat-treatment and minimal processing. *Journal of Food Science, 58*(5), 1111-&.

Kirby, A. R., Gunning, A. P., & Morris, V. J. (1995). Atomic-force microscopy in food research - A new technique comes of age. *Trends in Food Science & Technology, 6*(11), 359-365.

Knee, M. (1973). Polysaccharide changes in cell-walls of ripening apples. *Phytochemistry, 12*(7), 1543-1549.

Knox, J. P. (1997). The use of antibodies to study the architecture and developmental regulation of plant cell walls. *International Review of Cytology, 171*, 79-120.

Knox, J. P. (2008). Revealing the structural and functional diversity of plant cell walls. *Current Opinion in Plant Biology, 11*(3), 308-313.

Kobayashi, M., Matoh, T., & Azuma, J. (1996). Two chains of rhamnogalacturonan II are cross-linked by borate-diol ester bonds in higher plant cell walls. *Plant Physiology, 110*(3), 1017-1020.

Kohn, R., & Luknár, O. (1977). Intermolecular calcium ion binding on polyuronates-polygalacturonate and polyguluronate. *Collection of Czechoslovak Chemical Communications, 42*, 731-744.

Komalavilas, P., & Mort, A. J. (1989). The acetylation at O-3 of galacturonic acid in the rhamnose-rich portion of pectins. *Carbohydrate Research, 189*, 261-272.

Koziol, A., Cybulska, J., Pieczywek, P. M., & Zdunek, A. (2017). Changes of pectin nanostructure and cell wall stiffness induced in vitro by pectinase. *Carbohydrate Polymers, 161*, 197-207.

Krall, S. M., & McFeeters, R. F. (1998). Pectin hydrolysis: Effect of temperature, degree of methylation, pH, and calcium on hydrolysis rates. *Journal of Agricultural and Food Chemistry, 46*(4), 1311-1315.

Kravtchenko, T. P., Arnould, I., Voragen, A. G. J., & Pilnik, W. (1992). Improvement of the selective depolymerization of pectic substances by chemical β-elimination in aqueous solution. *Carbohydrate Polymers, 19*(4), 237-242.

Kruskal, W. H., & Wallis, W. A. (1952). Use of ranks in one-criterion variance analysis. *Journal of the American Statistical Association, 47*(260), 583-621.

Kunzek, H., Kabbert, R., & Gloyna, D. (1999). Aspects of material science in food processing. Changes in plant cell walls of fruits and vegetables. *Zeitschrift für Lebensmittel-Untersuchung und -Forschung, 208*(4), 233-250.

Kunzek, H., Opel, H., & Senge, B. (1997). Rheological examination of material with cellular structure. 2. Creep and oscillation measurements of apple material with cellular structure. *Zeitschrift für Lebensmittel-Untersuchung und -Forschung, 205*(3), 193-203.

Kyomugasho, C., Christiaens, S., Shpigelman, A., Van Loey, A. M., & Hendrickx, M. E. (2015). FT-IR spectroscopy, a reliable method for routine analysis of the degree of methylesterification of pectin in different fruit- and vegetable-based matrices. *Food Chemistry, 176*, 82-90.

L

Lahaye, M., Bouin, C., Barbacci, A., Le Gall, S., & Foucat, L. (2018). Water and cell wall contributions to apple mechanical properties. *Food Chemistry, 268*, 386-394.

Lahaye, M., Falourd, X., Laillet, B., & Le Gall, S. (2020). Cellulose, pectin and water in cell walls determine apple flesh viscoelastic mechanical properties. *Carbohydrate Polymers, 232*, 115768.

Lairon, D., Arnault, N., Bertrais, S., Planells, R., Clero, E., Hercberg, S., & Boutron-Ruault, M. C. (2005). Dietary fiber intake and risk factors for cardiovascular disease in French adults. *American Journal of Clinical Nutrition 82*(6), 1185-1194.

Lakso, A. N., Robinson, T. L., & Pool, R. M. (1989). Canopy microclimate effects on patterns of fruiting and fruit development in apples and grapes. In C. J. Wright (Ed.), *Manipulation of Fruiting* (pp. 263-192). London: Butterworth.

Lan, W., Jaillais, B., Leca, A., Renard, C. M. G. C., & Bureau, S. (2020). A new application of NIR spectroscopy to describe and predict purees quality from the non-destructive apple measurements. *Food Chemistry, 310*, 125944.

Lane, M. D. (2015). Introduction to statistics. *Online Statistics Education: A Multimedia Course of Study (http://onlinestatbook.com/). (Accessed 4 November 2020)*.

Lapsley, K. G., Escher, F. E., & Hoehn, E. (1992). The cellular structure of selected apple varieties. *Food Structure, 11*, 339-349.

Le Bourvellec, C., Bouchet, B., & Renard, C. M. (2005). Non-covalent interaction between procyanidins and apple cell wall material. Part III: Study on model polysaccharides. *Biochimica et Biophysica Acta, 1725*(1), 10-18.

Le Bourvellec, C., Bouzerzour, K., Ginies, C., Regis, S., Ple, Y., & Renard, C. M. G. C. (2011). Phenolic and polysaccharidic composition of applesauce is close to that of apple flesh. *Journal of Food Composition and Analysis, 24*(4-5), 537-547.

Le Bourvellec, C., Guyot, S., & Renard, C. M. G. C. (2009). Interactions between apple (Malus x domestica Borkh.) polyphenols and cell walls modulate the extractability of polysaccharides. *Carbohydrate Polymers, 75*(2), 251-261.

Lê, S., Josse, J., & Husson, F. (2008). FactoMineR: An R package for multivariate analysis. *Journal of Statistical Software, 25*(1), 1-18.

Lecain, S., Ng, A., Parker, M. L., Smith, A. C., & Waldron, K. W. (1999). Modification of cell-wall polymers of onion waste—Part I. Effect of pressure-cooking. *Carbohydrate Polymers, 38*(1), 59-67.

Lee, K. W., Kim, Y. J., Kim, D.-O., Lee, H. J., & Lee, C. Y. (2003). Major phenolics in apple and their contribution to the total antioxidant capacity. *Journal of Agricultural and Food Chemistry, 51*(22), 6516-6520.

Leszczuk, A., Chylinska, M., & Zdunek, A. (2019). Distribution of arabinogalactan proteins and pectins in the cells of apple (Malus x domestica) fruit during post-harvest storage. *Annals of Botany, 123*(1), 47-55.

Leszczuk, A., Chylińska, M., Zięba, E., Skrzypek, T., Szczuka, E., & Zdunek, A. (2018). Structural network of arabinogalactan proteins (AGPs) and pectins in apple fruit during ripening and senescence processes. *Plant Science, 275*, 36-48.

Leverrier, C. (2016). Relations Structure/Propriétés des Suspensions de Particules Végétales. *Doctoral thesis* (Université Paris-Saclay, AgroParisTech).

Leverrier, C., Almeida, G., Espinosa-Munoz, L., & Cuvelier, G. (2016). Influence of particle size and concentration on rheological behaviour of reconstituted apple purees. *Food Biophysics, 11*(3), 235-247.

Leverrier, C., Almeida, G., Menut, P., & Cuvelier, G. (2017a). Design of model apple cellls suspensions: Rheological properties and impact of the continuous phase. *Food Biophysics, 12*(3), 383-396.

Leverrier, C., Moulin, G., Cuvelier, G., & Almeida, G. (2017b). Assessment of deformability of soft plant cells by 3D imaging. *Food Structure, 14*, 95-103.

Levigne, S., Thomas, M., Ralet, M.-C., Quéméner, B., & Thibault, J. F. (2002). Determination of the degrees of methylation and acetylation of pectins using a C18 column and internal standards. *Food Hydrocolloids, 16*, 547-550.

Limberg, G., Korner, R., Buchholt, H. C., Christensen, T., Roepstorff, P., & Mikkelsen, J. D. (2000). Analysis of pectin structure part 1 - Analysis of different de-esterification mechanisms for pectin by enzymatic fingerprinting using endopectin lyase and endopolygalacturonase II from A-niger. *Carbohydrate Research, 327*(3), 293-307.

Lin, D. H., Lopez-Sanchez, P., & Gidley, M. J. (2015). Binding of arabinan or galactan during cellulose synthesis is extensive and reversible. *Carbohydrate Polymers, 126*, 108-121.

Lin, D. H., Lopez-Sanchez, P., & Gidley, M. J. (2016). Interactions of pectins with cellulose during its synthesis in the absence of calcium. *Food Hydrocolloids, 52*, 57-68.

Lin, H. J., Qin, X. M., Aizawa, K., Inakuma, T., Yamauchi, R., & Kato, K. (2005). Chemical properties of water-soluble pectins in hot- and cold-break tomato pastes. *Food Chemistry, 93*(3), 409-415.

Liu, X., Renard, C. M. G. C., Rolland-Sabaté, A., Bureau, S., & Le Bourvellec, C. (2021). Modification of apple, beet and kiwifruit cell walls by boiling in acid conditions: Common and specific responses. *Food Hydrocolloids, 112*, 106266.

Löfgren, C., Guillotin, S., Evenbratt, H., Schols, H., & Hermansson, A.-M. (2005). Effects of calcium, pH, and blockiness on kinetic rheological behavior and microstructure of HM pectin gels. *Biomacromolecules, 6*(2), 646-652.

Lopez-Sanchez, P., Chapara, V., Schumm, S., & Farr, R. (2012). Shear elastic deformation and particle packing in plant cell dispersions. *Food Biophysics, 7*(1), 1-14.

Lopez-Sanchez, P., & Farr, R. (2012). Power laws in the elasticity and yielding of plant particle suspensions. *Food Biophysics, 7*(1), 15-27.

Lopez-Sanchez, P., Martinez-Sanz, M., Bonilla, M. R., Sonni, F., Gilbert, E. P., & Gidley, M. J. (2020). Nanostructure and poroviscoelasticity in cell wall materials from onion, carrot and apple: Roles of pectin. *Food Hydrocolloids, 98*, 105253.

Lopez-Sanchez, P., Martinez-Sanz, M., Bonilla, M. R., Wang, D., Gilbert, E. P., Stokes, J. R., & Gidley, M. J. (2017). Cellulose-pectin composite hydrogels: Intermolecular interactions and material properties depend on order of assembly. *Carbohydrate Polymers, 162*, 71-81.

Lopez-Sanchez, P., Martinez-Sanz, M., Bonilla, M. R., Wang, D. J., Walsh, C. T., Gilbert, E. P., Stokes, J. R., & Gidley, M. J. (2016). Pectin impacts cellulose fibre architecture and hydrogel mechanics in the absence of calcium. *Carbohydrate Polymers, 153*, 236-245.

Lopez-Sanchez, P., Nijsse, J., Blonk, H. C. G., Bialek, L., Schumm, S., & Langton, M. (2011). Effect of mechanical and thermal treatments on the microstructure and rheological properties of carrot, broccoli and tomato dispersions. *Journal of the Science of Food and Agriculture, 91*(2), 207-217.

Lötter, J. D. V., Beukes, D. J., & Weber, H. W. (1985). Growth and quality of apples as affected by different irrigation treatments. *Journal of Horticultural Science, 60*(2), 181-192.

Lukhmana, N., Kong, F., Kerr, W. L., & Singh, R. K. (2018). Rheological and structural properties of tart cherry puree as affected by particle size reduction. *LWT-Food Science and Technology, 90*, 650-657.

M

Mafra, I., Lanza, B., Reis, A., Marsilio, V., Campestre, C., Angelis, M., & Coimbra, M. (2001). Effect of ripening on texture, microstructure and cell wall polysaccharide composition of olive fruit (Olea europaea). *Physiologia plantarum, 111*, 439-447.

Manach, C., Williamson, G., Morand, C., Scalbert, A., & Rémésy, C. (2005). Bioavailability and bioefficacy of polyphenols in humans. I. Review of 97 bioavailability studies. *American Journal of Clinical Nutrition, 81*(1 Suppl), 230s-242s.

Marigheto, N., Venturi, L., & Hills, B. (2008). Two-dimensional NMR relaxation studies of apple quality. *Postharvest Biology and Technology, 48*(3), 331-340.

Market Resarch Future. (2019). *Fruit Puree Market Research Report- Forecast to 2023*, https://www.marketresearchfuture.com/reports/fruit-puree-market/. (Accessed 15 January 2020).

Martinez-Sanz, M., Mikkelsen, D., Flanagan, B. M., Gidley, M. J., & Gilbert, E. P. (2017). Multi-scale characterisation of deuterated cellulose composite hydrogels reveals evidence for different interaction mechanisms with arabinoxylan, mixed-linkage glucan and xyloglucan. *Polymer, 124*, 1-11.

Martinez, M. V., & Whitaker, J. R. (1995). The biochemistry and control of enzymatic browning. *Trends in Food Science & Technology, 6*(6), 195-200.

Massiot, P., Baron, A., & Drilleau, J. F. (1996). Effect of storage of apple on the enzymatic hydrolysis of cell wall polysaccharides. *Carbohydrate Polymers, 29*(4), 301-307.

Massiot, P., & Renard, C. M. G. C. (1997). Composition, physico-chemical properties and enzymatic degradation of fibres prepared from different tissues of apple. *LWT-Food Science and Technology, 30*(8), 800-806.

Mastersizer 2000. (2007). User manual. *Malvern Instruments.*

Matignon, A., Ducept, F., Sieffermann, J.-M., Barey, P., Desprairies, M., Mauduit, S., & Michon, C. (2014). Rheological properties of starch suspensions using a rotational rheometer fitted with a starch stirrer cell. *Rheologica Acta, 53*(3), 255-267.

McAtee, P. A., Hallett, I. C., Johnston, J. W., & Schaffer, R. J. (2009). A rapid method of fruit cell isolation for cell size and shape measurements. *Plant Methods, 5.*

McCann, M. C., Wells, B., & Roberts, K. (1990). Direct visualization of cross-links in the primary plant cell wall. *Journal of Cell Science, 96*(2), 323.

McQueen-Mason, S., & Cosgrove, D. J. (1994). Disruption of hydrogen bonding between plant cell wall polymers by proteins that induce wall extension. *Proceedings of the National Academy of Sciences, 91*(14), 6574.

McQueen-Mason, S. J., & Cosgrove, D. J. (1995). Expansin mode of action on cell walls (Analysis of wall ydrolysis, stress relaxation, and binding). *Plant Physiology, 107*(1), 87.

Mebatsion, H. K., Verboven, P., Ho, Q. T., Verlinden, B., Mendoza, F., Nguyen, T. A., & Nicolaï, B. (2006). Modeling fruit microstructure using an ellipse tessellation algorithm. *Computer Modeling in Engineering and Sciences, 14*(1), 1-14.

Meng, X., Foston, M., Leisen, J., DeMartini, J., Wyman, C. E., & Ragauskas, A. J. (2013). Determination of porosity of lignocellulosic biomass before and after pretreatment by using Simons' stain and NMR techniques. *Bioresource Technology, 144*, 467-476.

Meng, X., & Ragauskas, A. J. (2014). Recent advances in understanding the role of cellulose accessibility in enzymatic hydrolysis of lignocellulosic substrates. *Current Opinion in Biotechnology, 27*, 150-158.

Mercado, J. A., Matas, A. J., & Posé, S. (2019). Fruit and vegetable texture: Role of their cell walls. In *Encyclopedia of Food Chemistry* (Vol. 3, pp. 1-7).

Mezger, T. G. (2014). *The Rheology Handbook* (4th ed.). Hanover: European Coatings TECH FILES.

Micheli, F. (2001). Pectin methylesterases: Cell wall enzymes with important roles in plant physiology. *Trends in Plant Science, 6*(9), 414-419.

Milić, B., Tarlanović, J., Keserović, Z., Zorić, L., Blagojević, B., & Magazin, N. (2017). The growth of apple central fruits as affected by thinning with NAA, BA and naphthenic acids. *Erwerbs-Obstbau, 59*(3), 185-193.

Missaire, F., Qiu, C. G., & Rao, M. A. (1990). Yield stress of structured and unstructured food suspensions. *Journal of Texture Studies, 21*(4), 479-490.

Moelants, K., Cardinaels, R., Jolie, R., Tina, V., Buggenhout Sandy, V., Zumalacarregui, L., van Loey, A., Moldenaers, P., & Hendrickx, M. (2012). Relation between particle properties and rheological characteristics of carrot-derived suspensions. *Food and Bioprocess Technology, 6*.

Moelants, K., Cardinaels, R., Van Buggenhout, S., van Loey, A., Moldenaers, P., & Hendrickx, M. (2014a). A review on the relationships between processing, food structure, and rheological properties of plant-tissue-based food suspensions. *Comprehensive Reviews in Food Science and Food Safety, 13*, 241-260.

Moelants, K. R. N., Cardinaels, R., Jolie, R. P., Verrijssen, T. A. J., Van Buggenhout, S., Van Loey, A. M., Moldenaers, P., & Hendrickx, M. E. (2014b). Rheology of concentrated tomato-derived suspensions: Effects of particle characteristics. *Food and Bioprocess Technology*.

Moelants, K. R. N., Jolie, R. P., Palmers, S. K. J., Cardinaels, R., Christiaens, S., Van Buggenhout, S., Van Loey, A. M., Moldenaers, P., & Hendrickx, M. E. (2013). The effects of process-induced pectin changes on the viscosity of carrot and tomato sera. *Food and Bioprocess Technology, 6*(10), 2870-2883.

Mohnen, D. (2008). Pectin structure and biosynthesis. *Current Opinion in Plant Biology, 11*(3), 266-277.

Morris, G. A., Foster, T. J., & Harding, S. E. (2002). A hydrodynamic study of the depolymerisation of a high methoxy pectin at elevated temperatures. *Carbohydrate Polymers, 48*(4), 361-367.

Morris, G. A., & Ralet, M.-C. (2012). The effect of neutral sugar distribution on the dilute solution conformation of sugar beet pectin. *Carbohydrate Polymers, 88*(4), 1488-1491.

Morris, G. A., Ralet, M.-C., Bonnin, E., Thibault, J.-F., & Harding, S. E. (2010). Physical characterisation of the rhamnogalacturonan and homogalacturonan fractions of sugar beet (Beta vulgaris) pectin. *Carbohydrate Polymers, 82*(4), 1161-1167.

Morris, V. J., Gunning, A. P., Kirby, A. R., Round, A., Waldron, K., & Ng, A. (1997). Atomic force microscopy of plant cell walls, plant cell wall polysaccharides and gels. *International Journal of Biological Macromolecules, 21*(1-2), 61-66.

Morris, V. J., Mackie, A. R., Wilde, P. J., Kirby, A. R., Mills, E. C. N., & Gunning, A. P. (2001). Atomic force microscopy as a tool for interpreting the rheology of food biopolymers at the molecular level. *LWT-Food Science and Technology, 34*(1), 3-10.

Mortensen, M., Thybo, A. K., Bertram, H. C., Andersen, H. J., & Engelsen, S. B. (2005). Cooking effects on water distribution in potatoes using nuclear magnetic resonance relaxation. *Journal of Agricultural and Food Chemistry, 53*(15), 5976-5981.

Müller-Maatsch, J., Caligiani, A., Tedeschi, T., Elst, K., & Sforza, S. (2014). Simple and validated quantitative (1)H NMR method for the determination of methylation, acetylation, and feruloylation degree of pectin. *Journal of Agricultural and Food Chemistry, 62*(37), 9081-9087.

Müller, S., & Kunzek, H. (1998). Material properties of processed fruit and vegetables - I. Effect of extraction and thermal treatment on apple parenchyma. *Zeitschrift für Lebensmittel-Untersuchung und -Forschung, 206*(4), 264-272.

Musse, M., Quellec, S., Cambert, M., Devaux, M.-F., Lahaye, M., & Mariette, F. (2009). Monitoring the postharvest ripening of tomato fruit using quantitative MRI and NMR relaxometry. *Postharvest Biology and Technology, 53*(1), 22-35.

Mutenda, K. E., Korner, R., Christensen, T., Mikkelsen, J., & Roepstorff, P. (2002). Application of mass spectrometry to determine the activity and specificity of pectin lyase A. *Carbohydrate Research, 337*(13), 1217-1227.

Mutter, M., Beldman, G., Pitson, S. M., Schols, H. A., & Voragen, A. G. J. (1998). Rhamnogalacturonan α-D-galactopyranosyluronohydrolase: An enzyme that specifically removes the terminal nonreducing galacturonosyl residue in rhamnogalacturonan regions of pectin. *Plant Physiology, 117*(1), 153-163.

Mutter, M., Beldman, G., Schols, H. A., & Voragen, A. G. (1994). Rhamnogalacturonan alpha-L-rhamnopyranohydrolase. A novel enzyme specific for the terminal nonreducing rhamnosyl unit in rhamnogalacturonan regions of pectin. *Plant Physiology, 106*(1), 241-250.

N

Nara, K., Kato, Y., & Motomura, Y. (2001). Involvement of terminal-arabinose and -galactose pectic compounds in mealiness of apple fruit during storage. *Postharvest Biology and Technology, 22*(2), 141-150.

Ndeh, D., Rogowski, A., Cartmell, A., Luis, A. S., Baslé, A., Gray, J., Venditto, I., Briggs, J., Zhang, X., Labourel, A., Terrapon, N., Buffetto, F., Nepogodiev, S., Xiao, Y., Field, R. A., Zhu, Y., O'Neill, M. A., Urbanowicz, B. R., York, W. S., Davies, G. J., Abbott, D. W., Ralet, M.-C., Martens, E. C., Henrissat, B., & Gilbert, H. J. (2017). Complex pectin metabolism by gut bacteria reveals novel catalytic functions. *Nature, 544*(7648), 65-70.

Neal, G. E. (1965). Changes occurring in the cell walls of strawberries during ripening. *Journal of the Science of Food and Agriculture, 16*(10), 604-611.

Ng, A., & Waldron, K. W. (1997). Effect of cooking and pre-cooking on cell-wall chemistry in relation to firmness of carrot tissues. *Journal of the Science of Food and Agriculture, 73*(4), 503-512.

Ng, J. K. T., Schröder, R., Brummell, D. A., Sutherland, P. W., Hallett, I. C., Smith, B. G., Melton, L. D., & Johnston, J. W. (2015). Lower cell wall pectin solubilisation and galactose loss during early fruit development in apple (Malus x domestica) cultivar 'Scifresh' are associated with slower softening rate. *Journal of Plant Physiology, 176*, 129-137.

Ng, J. K. T., Schröder, R., Sutherland, P. W., Hallett, I. C., Hall, M. I., Prakash, R., Smith, B. G., Melton, L. D., & Johnston, J. W. (2013). Cell wall structures leading to cultivar differences in softening rates develop early during apple (Malus x domestica) fruit growth. *BMC Plant Biology, 13*.

Nobile, P. M., Wattebled, F., Quecini, V., Girardi, C. L., Lormeau, M., & Laurens, F. (2011). Identification of a novel α-L-arabinofuranosidase gene associated with mealiness in apple. *Journal of Experimental Botany, 62*(12), 4309-4321.

Nunan, K. J., & Scheller, H. V. (2003). Solubilization of an arabinan arabinosyltransferase activity from mung bean hypocotyls. *Plant Physiology, 132*(1), 331.

Nunes, C., Castro, S., Saraiva, J., Coimbra, M., Hendrickx, M., & van Loey, A. (2006). Thermal and high-pressure stability of purified pectin methylesterase from plums (Prunus domestica). *Journal of Food Biochemistry, 30*, 138-154.

O

O'Neill, M. A., Albersheim, P., & Darvill, A. G. (1990). Carbohydrates. In P. M. Dey (Ed.), *Methods in Plant Biochemistry* (Vol. 2, pp. 415-441). London: Academic press.

O'Neill, M. A., Eberhard, S., Albersheim, P., & Darvill, A. G. (2001). Requirement of borate cross-linking of cell wall rhamnogalacturonan II for Arabidopsis growth. *Science, 294*(5543), 846-849.

O'Neill, M. A., Ishii, T., Albersheim, P., & Darvill, A. G. (2004). Rhamnogalacturonan II: Structure and function of a borate cross-linked cell wall pectic polysaccharide. *Annual Review of Plant Biology, 55*, 109-139.

O'Neill, M. A., Warrenfeltz, D., Kates, K., Pellerin, P., Doco, T., Darvill, A. G., & Albersheim, P. (1996). Rhamnogalacturonan-II, a pectic polysaccharide in the walls of growing plant cell, forms a dimer that is covalently cross-linked by a borate ester - In vitro conditions for the formation and hydrolysis of the dimer. *Journal of Biological Chemistry, 271*(37), 22923-22930.

O'Neill, M. A., & York, W. S. (2003). The composition and structure of plant primary cell walls. In J. K. C. Rose (Ed.), *The Plant Cell Wall* (pp. 1–54): Blackwell Publishing, CRC Press.

Obro, J., Harholt, J., Scheller, H. V., & Orfila, C. (2004). Rhamnogalacturonan I in Solanum tuberosum tubers contains complex arabinogalactan structures. *Phytochemistry, 65*(10), 1429-1438.

Oey, I., Lille, M., van Loey, A., & Hendrickx, M. (2008). Effect of high-pressure processing on colour, texture and flavour of fruit- and vegetable-based food products: A review. *Trends in Food Science & Technology, 19*, 320-328.

Oszmianski, J., & Wojdylo, A. (2008). Polyphenol content and antioxidative activity in apple purees with rhubarb juice supplement. *International Journal of Food Science and Technology, 43*(3), 501-509.

P

Padayachee, A., Day, L., Howell, K., & Gidley, M. J. (2017). Complexity and health functionality of plant cell wall fibers from fruits and vegetables. *Critical Reviews in Food Science and Nutrition, 57*(1), 59-81.

Pagliuso, D., Grandis, A., Igarashi, E. S., Lam, E., & Buckeridge, M. S. (2018). Correlation of apiose levels and growth rates in duckweeds. *Frontiers in Chemistry, 6*, 291.

Paniagua, C., Kirby, A. R., Gunning, A. P., Morris, V. J., Matas, A. J., Quesada, M. A., & Mercado, J. A. (2017a). Unravelling the nanostructure of strawberry fruit pectins by endo-polygalacturonase digestion and atomic force microscopy. *Food Chemistry, 224*, 270-279.

Paniagua, C., Pose, S., Morris, V. J., Kirby, A. R., Quesada, M. A., & Mercado, J. A. (2014). Fruit softening and pectin disassembly: An overview of nanostructural pectin modifications assessed by atomic force microscopy. *Annals of Botany, 114*(6), 1375-1383.

Paniagua, C., Santiago-Domenech, N., Kirby, A. R., Gunning, A. P., Morris, V. J., Quesada, M. A., Matas, A. J., & Mercado, J. A. (2017b). Structural changes in cell wall pectins during strawberry fruit development. *Plant Physiology and Biochemistry, 118*, 55-63.

Patova, O. A., Golovchenko, V. V., & Ovodov, Y. S. (2014). Pectic polysaccharides: Structure and properties. *Russian Chemical Bulletin, 63*(9), 1901-1924.

Pavel, E. W., & Dejong, T. M. (1995). Seasonal patterns of nonstructural carbohydrates of apple (Malus pumila Mill.) fruits: Relationship with relative growth rates and contribution to solute potential. *Journal of Horticultural Science, 70*(1), 127-134.

Pearson-Education. (2005). https://images.slideplayer.com/33/8252225/slides/slide_22.jpg. (Accessed 29 September 2020).

Pena, M. J., & Carpita, N. C. (2004). Loss of highly branched arabinans and debranching of rhamnogalacturonan I accompany loss of firm texture and cell separation during prolonged storage of apple. *Plant Physiology, 135*(3), 1305-1313.

Percy, A. E., Melton, L. D., & Jameson, P. E. (1997). Xyloglucan and hemicelluloses in the cell wall during apple fruit development and ripening. *Plant Science, 125*(1), 31-39.

Pérez, S., & Bertoft, E. (2010). The molecular structures of starch components and their contribution to the architecture of starch granules: A comprehensive review. *Starch - Stärke, 62*(8), 389-420.

Pérez, S., Mazeau, K., & Hervé du Penhoat, C. (2000). The three-dimensional structures of the pectic polysaccharides. *Plant Physiology and Biochemistry, 38*(1), 37-55.

Pitson, S. M., Mutter, M., van den Broek, L. A., Voragen, A. G., & Beldman, G. (1998). Stereochemical course of hydrolysis catalysed by alpha-L-rhamnosyl and alpha-D-galacturonosyl hydrolases from Aspergillus aculeatus. *Biochemical and Biophysical Research Communications, 242*(3), 552-559.

Plaza, L., Duvetter, T., Plancken, I. V. d., Meersman, F., Loey, A. V., & Hendrickx, M. (2008). Influence of environmental conditions on thermal stability of recombinant Aspergillus aculeatus pectinmethylesterase. *Food Chemistry, 111*(4), 912-920.

Popper, Z. A., & Fry, S. C. (2005). Widespread occurrence of a covalent linkage between xyloglucan and acidic polysaccharides in suspension-cultured angiosperm cells. *Annals of Botany, 96*(1), 91-99.

Popper, Z. A., & Fry, S. C. (2008). Xyloglucan-pectin linkages are formed intra-protoplasmically, contribute to wall-assembly, and remain stable in the cell wall. *Planta, 227*(4), 781-794.

Pose, S., Kirby, A. R., Mercado, J. A., Morris, V. J., & Quesada, M. A. (2012). Structural characterization of cell wall pectin fractions in ripe strawberry fruits using AFM. *Carbohydrate Polymers, 88*(3), 882-890.

Posé, S., Kirby, A. R., Paniagua, C., Waldron, K. W., Morris, V. J., Quesada, M. A., & Mercado, J. A. (2015). The nanostructural characterization of strawberry pectins in pectate lyase or polygalacturonase silenced fruits elucidates their role in softening. *Carbohydrate Polymers, 132*, 134-145.

Posé, S., Paniagua, C., Matas, A. J., Gunning, A. P., Morris, V. J., Quesada, M. A., & Mercado, J. A. (2018). A nanostructural view of the cell wall disassembly process during fruit ripening and postharvest storage by atomic force microscopy. *Trends in Food Science & Technology*.

Postnova. (2020). PN3621 Multi-Angle Light Scattering Detector. https://www.postnova.com/product/modules/pn3000-detectors/10-pn3621-mals-detector.html. (Accessed 22 November 2020).

Pye, K., & Blott, S. J. (2004). Particle size analysis of sediments, soils and related particulate materials for forensic purposes using laser granulometry. *Forensic Science International, 144*(1), 19-27.

Q

Qiu, C. G., & Rao, M. (1989). Effect of disperse phase on the slip coefficient of applesauce in a concentric cylinder viscometer. *Journal of Texture Studies, 20*, 57-70.

Quarmby, A. R., & Ratkowsky, D. A. (1988). Free-choice flavour and odour profiling of fish spoilage: Does it achieve its objective? *Journal of the Science of Food and Agriculture, 44*(1), 89-98.

R

R Core Team. (2018). R: A language and environment for statistical computing. *R Foundation for Statistical Computing*, Vienna, Austria. https://www.R-project.org/. (Accessed 14 March 2018).

Ralet, M. C., Crepeau, M. J., Buchholt, H. C., & Thibault, J. F. (2003). Polyelectrolyte behaviour and calcium binding properties of sugar beet pectins differing in their degrees of methylation and acetylation. *Biochemical Engineering Journal, 16*(2), 191-201.

Ralet, M. C., Crepeau, M. J., Lefebvre, J., Mouille, G., Hofte, H., & Thibault, J. F. (2008). Reduced number of homogalacturonan domains in pectins of an Arabidopsis mutant enhances the flexibility of the polymer. *Biomacromolecules, 9*(5), 1454-1460.

Ralet, M. C., Tranquet, O., Poulain, D., Moise, A., & Guillon, F. (2010). Monoclonal antibodies to rhamnogalacturonan I backbone. *Planta, 231*(6), 1373-1383.

Ralet, M. C., Williams, M. A. K., Tanhatan-Nasseri, A., Ropartz, D., Quemener, B., & Bonnin, E. (2012). Innovative enzymatic approach to resolve homogalacturonans based on their methylesterification pattern. *Biomacromolecules, 13*(5), 1615-1624.

Rao, M. A. (1977). Rheology of liquid food - A review. *Journal of Texture Studies, 8*(2), 135-168.

Rao, M. A. (1987). Predicting the flow of food suspensions of plant origin. *Food technology, 41*(3), 85-89.

Rao, M. A. (1992). The structural approach to rheology of plant food dispersions. *Revista Española de Ciencia y Tecnología de Alimentos, 32*(1), 3-17.

Rao, M. A. (2007). Rheological behavior of processed fluid and semisolid foods. In M. A. Rao (Ed.), *Rheology of Fluid and Semisolid Foods: Principles and Applications* (pp. 223-337). Boston, MA: Springer US.

Rao, M. A., Cooley, H. J., Nogueira, J. N., & McLellan, M. R. (1986). Rheology of apple sauce - effect of apple cultivar, firmness, and processing parameters. *Journal of Food Science, 51*(1), 176-179.

Raschka, S. (2014). Linear Discriminant Analysis – Bit by Bit. https://sebastianraschka.com/Articles/2014_python_lda.html. (Accessed 5 November 2020).

Raven, P. H., Evert, R. F., & Eichhorn, S. E. (1999). *Biology of Plants* (6th ed.). New York: W.H. Freeman & Co Ltd.

Ray, S., Vigouroux, J., Quémener, B., Bonnin, E., & Lahaye, M. (2014). Novel and diverse fine structures in LiCl–DMSO extracted apple hemicelluloses. *Carbohydrate Polymers, 108*, 46-57.

Redgwell, R. J., Fischer, M., Kendal, E., & MacRae, E. A. (1997). Galactose loss and fruit ripening: high-molecular-weight arabinogalactans in the pectic polysaccharides of fruit cell walls. *Planta, 203*(2), 174-181.

Rees, D. A., & Wight, A. W. (1971). Polysaccharide conformation. Part VII. Model building computations for α-1,4 galacturonan and the kinking function of L-rhamnose residues in pectic substances. *Journal of the Chemical Society B: Physical Organic*(0), 1366-1372.

Renard, C. M. G. C. (1989). Etude des Polysaccharides Pariétaux de la Pomme. Extraction et Caractérisation par des Méthodes Chimiques et Enzymatiques. *Doctoral thesis* (Université de Nantes).

Renard, C. M. G. C. (2005a). Effects of conventional boiling on the polyphenols and cell walls of pears. *Journal of the Science of Food and Agriculture, 85*, 310-318.

Renard, C. M. G. C. (2005b). Variability in cell wall preparations: Quantification and comparison of common methods. *Carbohydrate Polymers, 60*(4), 515-522.

Renard, C. M. G. C., Baron, A., Guyot, S., & Drilleau, J. F. (2001). Interactions between apple cell walls and native apple polyphenols: quantification and some consequences. *International Journal of Biological Macromolecules, 29*(2), 115-125.

Renard, C. M. G. C., Crepeau, M. J., & Thibault, J. F. (1999). Glucuronic acid directly linked to galacturonic acid in the rhamnogalacturonan backbone of beet pectins. *European Journal of Biochemistry, 266*(2), 566-574.

Renard, C. M. G. C., & Ginies, C. (2009). Comparison of the cell wall composition for flesh and skin from five different plums. *Food Chemistry, 114*(3), 1042-1049.

Renard, C. M. G. C., Le Quere, J. M., Bauduin, R., Symoneaux, R., Le Bourvellec, C., & Baron, A. (2011). Modulating polyphenolic composition and organoleptic properties of apple juices by manipulating the pressing conditions. *Food Chemistry, 124*(1), 117-125.

Renard, C. M. G. C., & Thibault, J. F. (1993). Structure and properties of apple and sugar-beet pectins extracted by chelating-agents. *Carbohydrate Research, 244*(1), 99-114.

Renard, C. M. G. C., Voragen, A. G. J., Thibault, J. F., & Pilnik, W. (1990). Studies on apple protopectin: I. Extraction of insoluble pectin by chemical means. *Carbohydrate Polymers, 12*(1), 9-25.

Renard, C. M. G. C., Voragen, A. G. J., Thibault, J. F., & Pilnik, W. (1991). Studies on apple protopectin. IV: Apple xyloglucans and influence of pectin extraction treatments on their solubility. *Carbohydrate Polymers, 15*(4), 387-403.

Renard, C. M. G. C., Weightman, R. M., & Thibault, J. F. (1997). The xylose-rich pectins from pea hulls. *International Journal of Biological Macromolecules, 21*(1-2), 155-162.

Ridley, B. L., O'Neill, M. A., & Mohnen, D. A. (2001). Pectins: Structure, biosynthesis, and oligogalacturonide-related signaling. *Phytochemistry, 57*(6), 929-967.

Rihouey, C., Morvan, C., Borissova, I., Jauneau, A., Demarty, M., & Jarvis, M. (1995). Structural features of CDTA-soluble pectins from flax hypocotyls. *Carbohydrate Polymers, 28*(2), 159-166.

Rimbach, G., Möhring, J., & Erbersdobler, H. F. (2010). *Lebensmittel-Warenkunde für Einsteiger* (1st ed.). Heildelberg: Springer.

Robertson, J. A., de Monredon, F. D., Dysseler, P., Guillon, F., Amado, R., & Thibault, J.-F. (2000). Hydration properties of dietary fibre and resistant starch: A European collaborative study. *LWT-Food Science and Technology, 33*(2), 72-79.

Rolland-Sabaté, A. (2017). High-performance size-exclusion chromatography coupled with on-line multi-angle laser light scattering (HPSEC-MALLS). In M. Masuelli & D. Renard (Eds.), *Advances in Physicochemical Properties of Biopolymers: Part 1*: Bentham ebooks.

Rolland-Sabaté, A., Colonna, P., Potocki-Véronèse, G., Monsan, P., & Planchot, V. (2004). Elongation and insolubilisation of α-glucans by the action of Neisseria polysaccharea amylosucrase. *Journal of Cereal Science, 40*(1), 17-30.

Rolland-Sabate, A., Guilois, S., Jaillais, B., & Colonna, P. (2011). Molecular size and mass distributions of native starches using complementary separation methods: Asymmetrical Flow Field Flow Fractionation (A4F) and Hydrodynamic and Size Exclusion Chromatography (HDC-SEC). *Analytical and Bioanalytical Chemistry, 399*(4), 1493-1505.

Rondeau-Mouro, C., Defer, D., Leboeuf, E., & Lahaye, M. (2008). Assessment of cell wall porosity in Arabidopsis thaliana by NMR spectroscopy. *International Journal of Biological Macromolecules, 42*, 83-92.

Root, W., & Barrett, D. M. (2005). Apples and apple processing. In D. M. Barrett, L. P. Somogyi & H. S. Ramaswamy (Eds.), *Processing Fruits: Science and Technology* (Vol. 2). Boca Raton: CRC Press.

Rosenbohm, C., Lundt, I., Christensen, T. I., & Young, N. G. (2003). Chemically methylated and reduced pectins: preparation, characterisation by 1H NMR spectroscopy, enzymatic degradation, and gelling properties. *Carbohydrate Research, 338*(7), 637-649.

Round, A. N., Rigby, N. M., MacDougall, A. J., & Morris, V. J. (2010). A new view of pectin structure revealed by acid hydrolysis and atomic force microscopy. *Carbohydrate Research, 345*(4), 487-497.

Round, A. N., Rigby, N. M., MacDougall, A. J., Ring, S. G., & Morris, V. J. (2001). Investigating the nature of branching in pectin by atomic force microscopy and carbohydrate analysis. *Carbohydrate Research, 331*(3), 337-342.

S

Saeman, J. F., Moore, W. E., Mitchell, R. L., & Millett, M. A. (1954). Techniques for the determination of pulp constituents by quantitative paper chromatography. *Tappi, 37*(8), 336-343.

Sakamoto, T., & Thibault, J. F. (2001). Exo-arabinanase of Penicillium chrysogenum able to release arabinobiose from alpha-1,5-L-arabinan. *Applied and Environmental Microbiology, 67*(7), 3319-3321.

Schaffer, R. J., Friel, E. N., Souleyre, E. J., Bolitho, K., Thodey, K., Ledger, S., Bowen, J. H., Ma, J. H., Nain, B., Cohen, D., Gleave, A. P., Crowhurst, R. N., Janssen, B. J., Yao, J. L., & Newcomb, R. D. (2007). A genomics approach reveals that aroma production in apple is controlled by ethylene predominantly at the final step in each biosynthetic pathway. *Plant Physiology, 144*(4), 1899-1912.

Schijvens, E. P. H. M., van Vliet, T., & van Dijk, C. (1998). Effect of processing conditions on the composition and rheological properties of applesauce. *Journal of Texture Studies, 29*(2), 123-143.

Schols, H. A., Bakx, E. J., Schipper, D., & Voragen, A. G. J. (1995). A xylogalacturonan subunit present in the modified hairy regions of apple pectin. *Carbohydrate Research, 279*, 265-279.

Schols, H. A., & Voragen, A. G. J. (1996). Complex pectins: Structure elucidation using enzymes. In J. Visser & A. G. J. Voragen (Eds.), *Progress in Biotechnology* (Vol. 14, pp. 3-19): Elsevier.

Selvendran, R. R. (1985). Developments in the chemistry and biochemistry of pectic and hemicellulosic polymers. *Journal of Cell Science*, 51-88.

Selvendran, R. R., & O'Neill, M. A. (1987). Isolation and analysis of cell walls from plant material. *Methods of Biochemical Analysis, 32*, 25-153.

Shackel, K. A., Greve, C., Labavitch, J. M., & Ahmadi, H. (1991). Cell turgor changes associated with ripening in tomato pericarp tissue. *Plant Physiology, 97*(2), 814-816.

Shama, F., & Sherman, P. (1973). Identification of stimuli controlling the sensory evaluation of viscosity II. Oral methods. *Journal of Texture Studies, 4*(1), 111-118.

Showalter, A. M. (1993). Structure and function of plant cell wall proteins. *The Plant Cell, 5*(1), 9-23.

Shpigelman, A., Kyomugasho, C., Christiaens, S., Van Loey, A. M., & Hendrickx, M. E. (2014). Thermal and high pressure high temperature processes result in distinctly different pectin non-enzymatic conversions. *Food Hydrocolloids, 39*, 251-263.

Sila, D. N., Doungla, E., Smout, C., Van Loey, A., & Hendrickx, M. (2006a). Pectin fraction interconversions: Insight into understanding texture evolution of thermally processed carrots. *Journal of Agricultural and Food Chemistry, 54*(22), 8471-8479.

Sila, D. N., Smout, C., Elliot, F., Van Loey, A., & Hendrickx, M. (2006b). Non-enzymatic depolymerization of carrot pectin: Toward a better understanding of carrot texture during thermal processing. *Journal of Food Science, 71*(1), E1-E9.

Sila, D. N., Smout, C., Satara, Y., Truong, V., Loey, A. V., & Hendrickx, M. (2007). Combined thermal and high pressure effect on carrot pectinmethylesterase stability and catalytic activity. *Journal of Food Engineering, 78*(3), 755-764.

Sila, D. N., Smout, C., Vu Son, T., Loey, A., & Hendrickx, M. (2005). Influence of pretreatment conditions on the texture and cell wall components of carrots during thermal processing. *Journal of Food Science, 70*(2), E85-E91.

Sila, D. N., van Buggenhout, S., Duvetter, T., Fraeye, I., de Roeck, A., van Loey, A., & Hendrickx, M. (2009). Pectins in processed fruits and vegetables: Part II - Structure-function relationships. *Comprehensive Reviews in Food Science and Food Safety, 8*(2), 86-104.

Simha, R. (1940). The influence of Brownian movement on the viscosity of solutions. *The Journal of Physical Chemistry, 44*(1), 25-34.

Simpson, B. K. (2012). *Food Biochemistry and Food Processing* (2nd ed. Vol. 2). Iowa – West Sussex – Oxford: Wiley-Blackwell.

Singh, N., Inouchi, N., & Nishinari, K. (2005). Morphological, structural, thermal, and rheological characteristics of starches separated from apples of different cultivars. *Journal of Agricultural and Food Chemistry, 53*(26), 10193-10199.

Smidsrød, O., & Andresen, I. L. (1979). *Biopolymerkjemi.* Trondheim, Norway: Tapir Press.

Smith, L. G. (2001). Plant cell division: Building walls in the right places. *Nature Reviews Molecular Cell Biology, 2*(1), 33-39.

Smith, W. H. (1950). Cell-multiplication and cell-enlargement in the development of the flesh of the apple fruit. *Annals of Botany, 14*(1), 23-38.

Somerville, C., Bauer, S., Brininstool, G., Facette, M., Hamann, T., Milne, J., Osborne, E., Paredez, A., Persson, S., Raab, T., Vorwerk, S., & Youngs, H. (2004). Toward a systems approach to understanding plant-cell walls. *Science, 306*(5705), 2206-2211.

Sorochan, V. D., Dzizenko, A. K., Bodin, N. S., & Ovodov, Y. S. (1971). Light-scattering studies of pectic substances in aqueous solution. *Carbohydrate Research, 20*(2), 243-249.

Soukup, A. (2014). Selected simple methods of plant cell wall histochemistry and staining for light microscopy. In V. Žárský & F. Cvrčková (Eds.), *Plant Cell Morphogenesis. Methods in Molecular Biology (Methods and Protocols)* (Vol. 1080, pp. 25-40). Totowa, NJ: Humana Press.

Sterling, C. (1963). Texture in cell-wall polysaccharides in food. In R. M. Leitch & D. N. Rhodes (Eds.), *Recent Advances in Food Science, Biochemistry and Biophysics in Food Research* (pp. 259-279). London: Butterworths.

Sterling, J. D., Quigley, H. F., Orellana, A., & Mohnen, D. (2001). The catalytic site of the pectin biosynthetic enzyme alpha-1,4-galacturonosyltransferase is located in the lumen of the Golgi. *Plant Physiology, 127*(1), 360-371.

Stokes, D. J. (2001). Characterisation of soft condensed matter and delicate materials using environmental scanning electron microscopy (ESEM). *Advanced Engineering Materials, 3*, 126-130.

Stokes, J. R. (2012). 'Oral' rheology. In J. Chen & L. Engelen (Eds.), *Food Oral Processing: Fundamentals of Eating and Sensory Perception* (pp. 227–264): Wiley-Blackwell.

Stolle-Smits, T., Beekhuizen, J., Recourt, K., Voragen, A., & Cees, D. (2000). Preheating effects on the textural strength of canned green beans. 1. Cell wall chemistry. *Journal of Agricultural and Food Chemistry, 48*, 5269-5277.

Sun, J., Chu, Y. F., Wu, X., & Liu, R. H. (2002). Antioxidant and antiproliferative activities of common fruits. *Journal of Agricultural and Food Chemistry, 50*(25), 7449-7454.

Szczesniak, A. S., & Kahn, E. L. (1971). Consumer awareness of and attitudes to food texture- I: Adults. *Journal of Texture Studies, 2*(3), 280-295.

Szymańska-Chargot, M., Chylińska, M., Pieczywek, P. M., Rösch, P., Schmitt, M., Popp, J., & Zdunek, A. (2016). Raman imaging of changes in the polysaccharides distribution in the cell wall during apple fruit development and senescence. *Planta, 243*, 935-945.

T

Tarea, S. (2005). Etude de la Texture de Suspensions de Particules Molles Concentrées. Relations entre la Structure, la Rhéologie et la Perception Sensorielle : Application aux Purées de Pommes et Poires et Mise au Point de Milieux Modèles. *Doctoral thesis* (ENSIA, AgroParisTech).

Tarea, S., Cuvelier, G., & Sieffermann, J. M. (2007). Sensory evaluation of the texture of 49 commercial apple and pear purees. *Journal of Food Quality, 30*(6), 1121-1131.

Taylor, N. G. (2008). Cellulose biosynthesis and deposition in higher plants. *New Phytologist, 178*(2), 239-252.

Thakur, B. R., Singh, R. K., & Handa, A. K. (1997). Chemistry and uses of pectin - A review. *Critical Reviews in Food Science and Nutrition, 37*(1), 47-73.

Tharanathan, R. N., Changala Reddy, G., Muralikrishna, G., Susheelamma, N. S., & Ramadas Bhat, U. (1994). Structure of a galactoarabinan-rich pectic polysaccharide of native and fermented blackgram (Phaseolus mungo). *Carbohydrate Polymers, 23*(2), 121-127.

Thermo Scientific. (2017). Rheology Solutions for Cosmetics and Personal Care Products. https://assets.thermofisher.com/TFS-Assets/MSD/Application-Notes/ANC003-rheology-solutions-cosmetics-personal-care-products-compendium.pdf. (Accessed 14 Novemver 2020).

Thibault, J. F., Renard, C. M. G. C., Axelos, M. A. V., Roger, P., & Crepeau, M. J. (1993). Studies of the length of homogalacturonic regions in pectins by acid hydrolysis. *Carbohydrate Research, 238*, 271-286.

Thompson, J. E., & Fry, S. C. (2000). Evidence for covalent linkage between xyloglucan and acidic pectins in suspension-cultured rose cells. *Planta, 211*(2), 275-286.

Tjan, S. B., Voragen, A. G. J., & Pilnik, W. (1974). Analysis of some partly and fully esterified oligogalactopyranuronic acids by P.M.R. spectrometry at 220 MHz. *Carbohydrate Research, 34*(1), 15-32.

Toivonen, P. M. A., & Brummell, D. A. (2008). Biochemical bases of appearance and texture changes in fresh-cut fruit and vegetables. *Postharvest Biology and Technology, 48*(1), 1-14.

Tomás-Barberán, F. A., Selma, M. V., & Espín, J. C. (2016). Interactions of gut microbiota with dietary polyphenols and consequences to human health. *Current Opinion in Clinical Nutrition & Metabolic Care, 19*(6), 471-476.

Tucker, G. A., Robertson, N. G., & Grierson, D. (1982). Purification and changes in activities of tomato pectinesterase isoenzymes. *Journal of the Science of Food and Agriculture, 33*(4), 396-400.

Tukey, H. B., & Young, J. O. (1942). Gross morphology and histology of developing fruit of the apple. *Botanical Gazette, 104*(1), 3-25.

Tyl, C., & Sadler, G. D. (2017). pH and titratable acidity. In S. S. Nielsen (Ed.), *Food Analysis* (pp. 389-406). Cham: Springer International Publishing.

V

Van Buren, J. P. (1979). The chemistry of texture in fruits and vegetables. *Journal of Texture Studies, 10*(1), 1-23.

Velasco, R., Zharkikh, A., Affourtit, J., Dhingra, A., Cestaro, A., Kalyanaraman, A., Fontana, P., Bhatnagar, S. K., Troggio, M., Pruss, D., Salvi, S., Pindo, M., Baldi, P., Castelletti, S., Cavaiuolo, M., Coppola, G., Costa, F., Cova, V., Dal Ri, A., Goremykin, V., Komjanc, M., Longhi, S., Magnago, P., Malacarne, G., Malnoy, M., Micheletti, D., Moretto, M., Perazzolli, M., Si-Ammour, A., Vezzulli, S., Zini, E., Eldredge, G., Fitzgerald, L. M., Gutin, N., Lanchbury, J., Macalma, T., Mitchell, J. T., Reid, J., Wardell, B., Kodira, C., Chen, Z., Desany, B., Niazi, F., Palmer, M., Koepke, T., Jiwan, D., Schaeffer, S., Krishnan, V., Wu, C., Chu, V. T., King, S. T., Vick, J., Tao, Q., Mraz, A., Stormo, A., Stormo, K., Bogden, R., Ederle, D., Stella, A., Vecchietti, A., Kater, M. M., Masiero, S., Lasserre, P., Lespinasse, Y., Allan, A. C., Bus, V., Chagné, D., Crowhurst, R. N., Gleave, A. P., Lavezzo, E., Fawcett, J. A., Proost, S., Rouzé, P., Sterck, L., Toppo, S., Lazzari, B., Hellens, R. P., Durel, C. E., Gutin, A., Bumgarner, R. E., Gardiner, S. E., Skolnick, M., Egholm, M., Van de Peer, Y., Salamini, F., & Viola, R. (2010). The genome of the domesticated apple (Malus × domestica Borkh.). *Nature Genetics, 42*(10), 833-839.

Verhertbruggen, Y., Walker, J. L., Guillon, F., & Scheller, H. V. (2017). A comparative study of sample preparation for staining and immunodetection of plant cell walls by light microscopy. *Frontiers in Plant Science, 8.*

Vetter, S., & Kunzek, H. (2003). The influence of the sequential extractions on the structure and the properties of single cell materials from apples. *European Food Research and Technology, 217*(5), 392-400.

Vidal, S., Doco, T., Williams, P., Pellerin, P., York, W. S., O'Neill, M. A., Glushka, J., Darvill, A. G., & Albersheim, P. (2000). Structural characterization of the pectic polysaccharide rhamnogalacturonan II: Evidence for the backbone location of the aceric acid-containing oligoglycosyl side chain. *Carbohydrate Research, 326*(4), 277-294.

Vincken, J. P., Beldman, G., & Voragen, A. G. J. (1994). The effect of xyloglucans on the degradation of cell-wall-embedded cellulose by the combined action of cellobiohydrolase and endoglucanases from Trichoderma viride. *Plant Physiology, 104*(1), 99-107.

Vincken, J. P., de Keizer, A., Beldman, G., & Voragen, A. G. (1995). Fractionation of xyloglucan fragments and their interaction with cellulose. *Plant Physiology, 108*(4), 1579-1585.

Vincken, J. P., Schols, H. A., Oomen, R., McCann, M. C., Ulvskov, P., Voragen, A. G. J., & Visser, R. G. F. (2003). If homogalacturonan were a side chain of rhamnogalacturonan I. Implications for cell wall architecture. *Plant Physiology, 132*(4), 1781-1789.

Visser, J., & Voragen, A. G. J. (1996). *Pectins and Pectinases* (1st ed. Vol. 14): Elsevier Science.

Voiniciuc, C., Pauly, M., & Usadel, B. (2018). Monitoring polysaccharide dynamics in the plant cell wall. *Plant Physiology, 176*(4), 2590.

Volz, R. K., Harker, F. R., & Lang, S. (2003). Firmness decline in `Gala' apple during fruit development. *Journal of the American Society for Horticultural Science, 128*(6), 797-802.

Voragen, A. G. J., Coenen, G.-J., Verhoef, R. P., & Schols, H. A. (2009). Pectin, a versatile polysaccharide present in plant cell walls. *Structural Chemistry, 20*(2), 263.

Voragen, A. G. J., Pilnik, W., Thibault, J.-F., Axelos, M. A. V., & Renard, C. M. G. C. (1995). Pectins. In A. M. Stephen (Ed.), *Food Polysaccharides and their Applications*. New York: Dekker.

Voragen, A. G. J., Schols, H. A., & Pilnik, W. (1986a). Determination of the degree of methylation and acetylation of pectins by HPLC. *Food Hydrocolloids, 1*(1), 65-70.

Voragen, F. G. J., Schols, H. A., & Pilnik, W. (1986b). Structural features of the hemicellulose polymers of apples. *Zeitschrift für Lebensmittel-Untersuchung und -Forschung, 183*(2), 105-110.

W

Waldron, K. W., Parker, M. L., & Smith, A. C. (2003). Plant cell walls and food quality. *Comprehensive Reviews in Food Science and Food Safety, 2*(4), 101-119.

Waldron, K. W., Smith, A. C., Parr, A. J., Ng, A., & Parker, M. L. (1997). New approaches to understanding and controlling cell separation in relation to fruit and vegetable texture. *Trends in Food Science & Technology, 8*(7), 213-221.

Wang, D. D., Yeats, T. H., Uluisik, S., Rose, J. K. C., & Seymour, G. B. (2018). Fruit softening: Revisiting the role of pectin. *Trends in Plant Science, 23*(4), 302-310.

Wang, T., Park, Y. B., Cosgrove, D. J., & Hong, M. (2015). Cellulose-pectin spatial contacts are inherent to never-dried Arabidopsis primary cell walls: Evidence from solid-state nuclear magnetic resonance. *Plant Physiology, 168*(3), 871.

Wang, T., Zabotina, O., & Hong, M. (2012). Pectin-cellulose interactions in Arabidopsis primary cell wall from two-dimensional magic-angle-spinning solid-state NMR. *Biochemistry, 51*.

Wang, X., Ouyang, Y., Liu, J., Zhu, M., Zhao, G., Bao, W., & Hu, F. B. (2014). Fruit and vegetable consumption and mortality from all causes, cardiovascular disease, and cancer: Systematic review and dose-response meta-analysis of prospective cohort studies. *British Medical Journal, 349*, g4490.

Whitney, S. E. C., Gidley, M. J., & McQueen Mason, S. J. (2000). Probing expansin action using cellulose/hemicellulose composites. *The Plant Journal, 22*(4), 327-334.

WHO. (2003). Diet, nutrition and the prevention of chronic diseases. Report of a joint FAO/WHO Expert Consultation. *WHO Technical Report Series, No. 916*.

Wickham, H. (2016). *ggplot2: Elegant Graphics for Data Analysis*. New York: Springer.

Willats, G. T., Steele-King, W. G., McCartney, C., Orfila, L., Marcus, C. S., & Knox, P. (2000). Making and using antibody probes to study plant cell walls. *Plant Physiology and Biochemistry, 38*(1-2), 27-36.

Willats, W. G. T., Orfila, C., Limberg, G., Buchholt, H. C., van Alebeek, G., Voragen, A. G. J., Marcus, S. E., Christensen, T., Mikkelsen, J. D., Murray, B. S., & Knox, J. P. (2001). Modulation of the degree and pattern of methyl-esterification of pectic homogalacturonan in plant cell walls - Implications for pectin methyl esterase action, matrix properties, and cell adhesion. *Journal of Biological Chemistry, 276*(22), 19404-19413.

Williams, A. A., & Langron, S. P. (1984). The use of free-choice profiling for the evaluation of commercial ports. *Journal of the Science of Food and Agriculture, 35*(5), 558-568.

Wills, R. B. H., McGlasson, W. B., Graham, D., & Joyce, D. C. (2007). *Postharvest: An introduction to physiologyand handling of fruits, vegetables and ornamentals* (5th ed.). UK: UNSW Press, CAB International.

Wilson, W. D., Jarvis, M. C., & Duncan, H. J. (1989). In-vitro digestibility of kale (Brassica oleracea) secondary xylem and parenchyma cell walls and their polysaccharide components. *Journal of the Science of Food and Agriculture, 48*(1), 9-14.

Winisdorffer, G., Musse, M., Quellec, S., Barbacci, A., Le Gall, S., Mariette, F., & Lahaye, M. (2015). Analysis of the dynamic mechanical properties of apple tissue and relationships with the intracellular water status, gas distribution, histological properties and chemical composition. *Postharvest Biology and Technology, 104*, 1-16.

Wink, M. (1997). Compartmentation of secondary metabolites and xenobiotics in plant vacuoles. In R. A. Leigh & D. Sanders (Eds.), *Advances in Botanical Research Incorporating Advances in Plant Pathology: The Plant Vacuole* (Vol. 25, pp. 141-169).

Winning, H., Viereck, N., Nørgaard, L., Larsen, J., & Engelsen, S. B. (2007). Quantification of the degree of blockiness in pectins using 1H NMR spectroscopy and chemometrics. *Food Hydrocolloids, 21*(2), 256-266.

Wismer, P. T., Proctor, J. T. A., & Elfving, D. C. (1995). Benzyladenine affects cell division and cell size during apple fruit thinning. *Journal of the American Society for Horticultural Science, 120*(5), 802-807.

Wojdyło, A., Oszmiański, J., & Laskowski, P. (2008). Polyphenolic compounds and antioxidant activity of new and old apple varieties. *Journal of Agricultural and Food Chemistry, 56*(15), 6520-6530.

Wolf, S., Mouille, G., & Pelloux, J. (2009). Homogalacturonan methyl-esterification and plant development. *Molecular Plant, 2*(5), 851-860.

Wu, J., Gao, H., Zhao, L., Liao, X., Chen, F., Wang, Z., & Hu, X. (2007). Chemical compositional characterization of some apple cultivars. *Food Chemistry, 103*(1), 88-93.

Wu, Q. D., Szakacsdobozi, M., Hemmat, M., & Hrazdina, G. (1993). Endopolygalacturonase in apples (Malus domestica) and its expression during fruit ripening. *Plant Physiology, 102*(1), 219-225.

Wyatt, P. (1993). Light scattering and the absolute characterization of macromolecules. *Analytica Chimica Acta, 272*(1), 1-40.

X

Xia, Z., Dayong, D., Jing, M., Zhe, J., Xun, Z., & Feng, X. (2015). Ultrastructure and topochemistry of plant cell wall by transmission electron microscopy. In F. E. Xu & K. Maaz (Eds.), *The Transmission Electron Microscope* (2nd ed.): INTECH.

Y

Yapo, B. M. (2011). Pectic substances: From simple pectic polysaccharides to complex pectins-A new hypothetical model. *Carbohydrate Polymers, 86*(2), 373-385.

Yapo, B. M., Lerouge, P., Thibault, J.-F., & Ralet, M.-C. (2007). Pectins from citrus peel cell walls contain homogalacturonans homogenous with respect to molar mass, rhamnogalacturonan I and rhamnogalacturonan II. *Carbohydrate Polymers, 69*(3), 426-435.

Yi, J., Kebede, B. T., Hai Dang, D. N., Buvé, C., Grauwet, T., Van Loey, A., Hu, X., & Hendrickx, M. (2017). Quality change during high pressure processing and thermal processing of cloudy apple juice. *LWT-Food Science and Technology, 75*, 85-92.

Yoshioka, H., Aoba, K., & Kashimura, Y. (1992). Molecular weight and degree of methoxylation in cell-wall polyuronide during softening in pear and apple fruit. *Journal of the American Society for Horticultural Science, 117*(4), 600-606.

Yoshioka, H., Kashimura, Y., & Kaneko, K. (1995). β-D-galactosidase and α-L-arabinofuranosidase activities during the softening of apples. *Journal of the Japanese Society for Horticultural Science, 63*(4), 871-878.

Z

Zareie, H., Gökmen, V., & Javadipour, I. (2003). Investigating network, branching, gelation and enzymatic degradation in pectin by atomic force microscopy. *Journal of Food Science and Technology-mysore, 40*(2), 169-172.

Zdunek, A., Koziol, A., Pieczywek, P. M., & Cybulska, J. (2014). Evaluation of the nanostructure of pectin, hemicellulose and cellulose in the cell walls of pears of different texture and firmness. *Food and Bioprocess Technology, 7*(12), 3525-3535.

Zhang, C., Li, P., Zhang, Y., Lu, F., Li, W., Kang, H., Xiang, J.-f., Huang, Y., & Liu, R. (2016). Hierarchical porous structures in cellulose: NMR relaxometry approach. *Polymer, 98*, 237-243.

Zhang, J., Cui, J. H., Xiao, L., & Wang, Z. W. (2014). The combination of atomic force microscopy and sugar analysis to evaluate alkali-soluble Canna edulis Ker pectin. *Food Chemistry, 156*, 64-71.

Zhang, Y., Li, P., & Cheng, L. (2010). Developmental changes of carbohydrates, organic acids, amino acids, and phenolic compounds in 'Honeycrisp' apple flesh. *Food Chemistry, 123*(4), 1013-1018.

Zimet, P., & Livney, Y. D. (2009). Beta-lactoglobulin and its nanocomplexes with pectin as vehicles for ω-3 polyunsaturated fatty acids. *Food Hydrocolloids, 23*(4), 1120-1126.

Zimm, B. H. (1948). Apparatus and methods for measurement and interpretation of the angular variation of light scattering; Preliminary results on polystyrene solutions. *Journal of Chemical Physics, 16*, 1099-1116.

Zykwinska, A., Gaillard, C., Buléon, A., Pontoire, B., Garnier, C., Thibault, J.-F., & Ralet, M.-C. (2007). Assessment of in vitro binding of isolated pectic domains to cellulose by adsorption isotherms, electron microscopy, and X-ray diffraction methods. *Biomacromolecules, 8*(1), 223-232.

Zykwinska, A. W., Ralet, M.-C., Garnier, C. D., & Thibault, J.-F. (2005). Evidence for in vitro binding of pectin side chains to cellulose. *Plant Physiology, 139*(1), 397-407.

VIII. Supplementary data

Supplementary Table S1. Correlation table of principal component analysis of textural and structural characteristics of apple purees comprising harvest 2016–2019 with G' and G''.

	η_{50}	η_{100}	η_{250}	YS	G'	G''	η_{serum}	PWM	d(0.9)	d(0.5)	d(0.1)	D[3,2]	D[4,3]
η_{50}	1	0.58	0.87	0.57	0.58	0.59	0.34	0.58	0.44	0.37	0.32	0.39	0.41
η_{100}	0.58	1	0.48	0.34	0.35	0.31	0.04	0.45	0.02	-0.03	-0.03	0.10	-0.02
η_{250}	0.87	0.48	1	0.81	0.79	0.81	0.26	0.49	0.58	0.51	0.40	0.42	0.54
YS	0.57	0.34	0.81	1	0.93	0.90	-0.01	0.32	0.49	0.42	0.29	0.21	0.45
G'	0.58	0.35	0.79	0.93	1	0.99	-0.07	0.44	0.35	0.22	0.07	0.07	0.27
G''	0.59	0.31	0.81	0.90	0.99	1	0.01	0.48	0.38	0.24	0.07	0.09	0.30
η_{serum}	0.34	0.04	0.26	-0.01	-0.07	0.01	1	0.44	0.28	0.31	0.27	0.24	0.31
PWM	0.58	0.45	0.49	0.50	0.44	0.48	0.44	1	-0.13	-0.13	-0.22	-0.11	-0.17
d(0.9)	0.44	0.02	0.58	0.42	0.35	0.38	0.28	-0.13	1	0.95	0.74	0.73	0.98
d(0.5)	0.37	-0.03	0.51	0.29	0.22	0.24	0.31	-0.21	0.95	1	0.89	0.76	0.99
d(0.1)	0.32	-0.03	0.40	0.21	0.07	0.07	0.27	-0.22	0.76	0.89	1	0.74	0.85
D[3,2]	0.39	0.10	0.42	0.45	0.07	0.09	0.24	-0.11	0.73	0.76	0.74	1	0.74
D[4,3]	0.41	-0.02	0.54	0.32	0.27	0.30	0.31	-0.17	0.98	0.99	0.85	0.74	1

η_{50}, η_{100}, η_{250}: Apparent viscosity of the puree at 50, 100 and 250 s^{-1}, respectively; YS: Yield stress of the puree; G': Storage modulus; G'': Loss modulus; η_{serum}: Serum viscosity at 100 s^{-1}; PWM: Pulp wet mass; D[4,3], D[3,2], d(0.1), d(0.5) and d(0.9): Different variables explaining particle size.
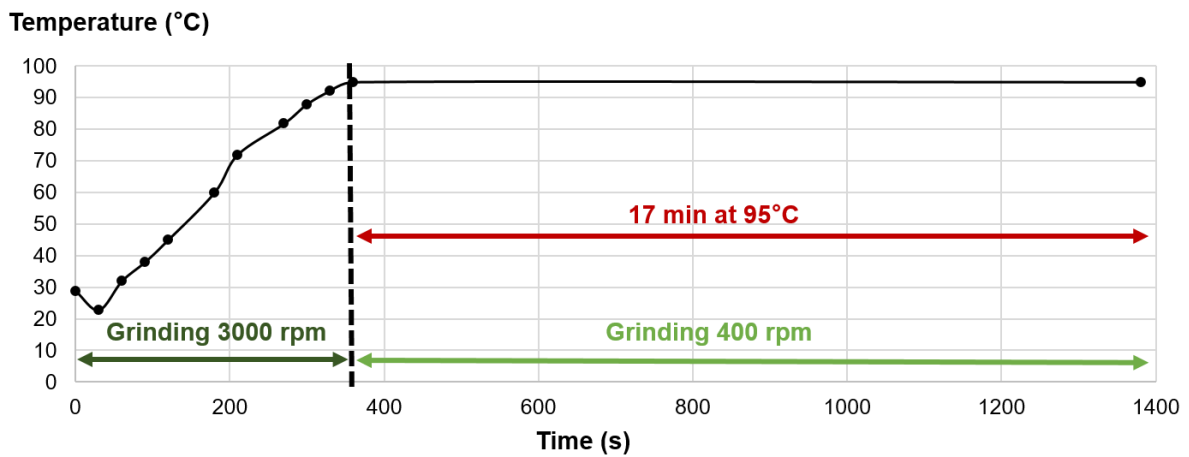
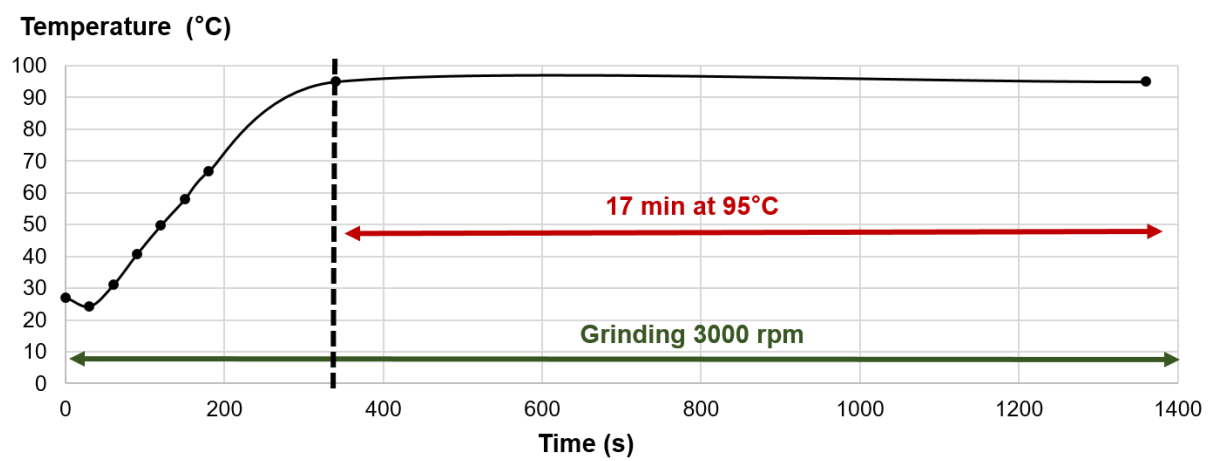**Supplementary Fig. S1.** Processing curve 70 °C – 400 rpm.
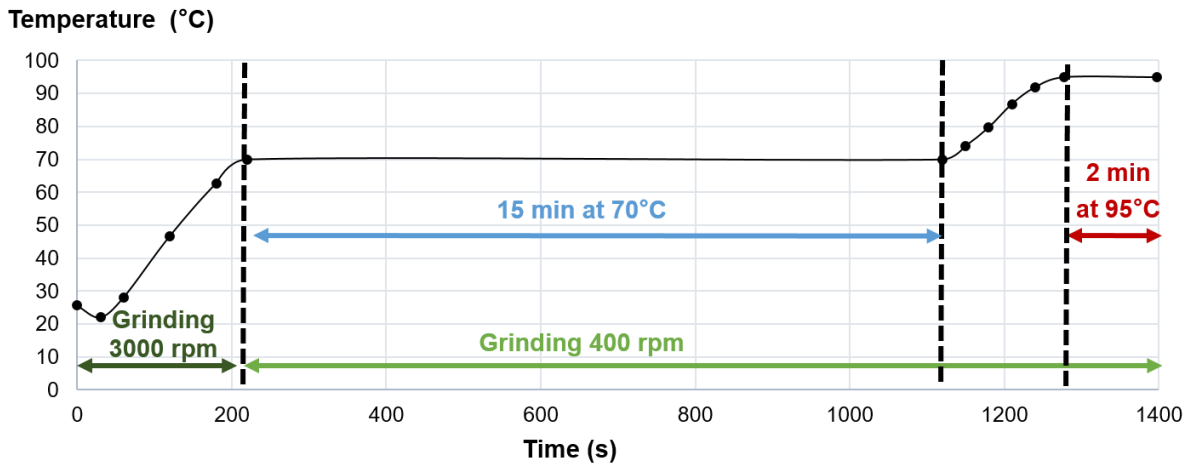
Supplementary Fig. S2. Processing curve 70 °C – 3000 rpm.
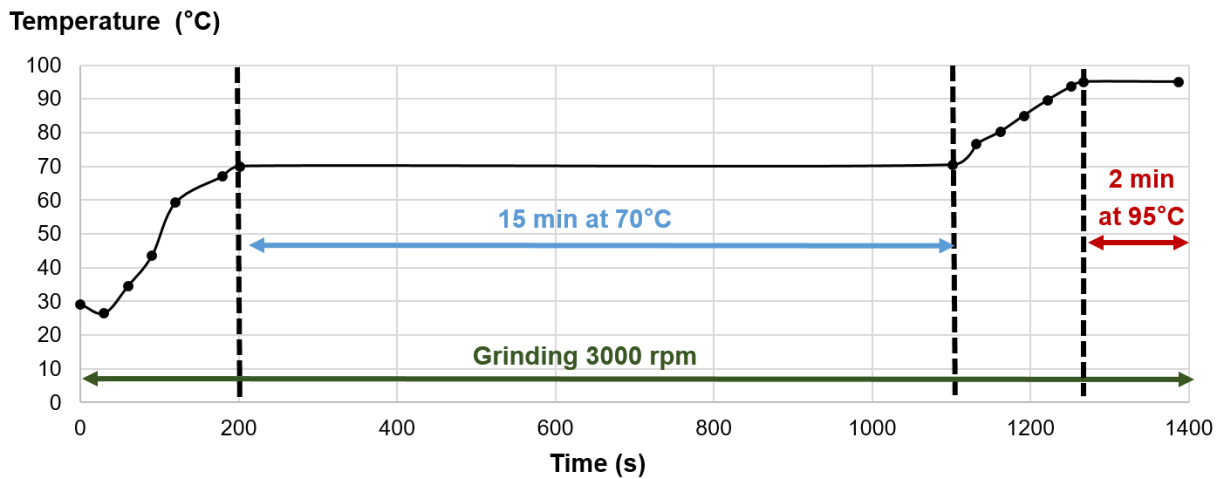
Supplementary Fig. S3. Processing curve 95 °C – 400 rpm.

Supplementary Fig. S4. Processing curve 95 °C – 3000 rpm.

Résumé

L'objectif de cette thèse était de comprendre comment les caractéristiques structurales des pommes peuvent être liées aux facteurs structurels des purées après cuisson et fragmentation tissulaire. Les caractéristiques structurales du fruit ont été modulées par les cultivars, les pratiques culturales et la maturation, et les conditions du procédé (thermique : 50–95 °C et mécanique : 100–3000 tr/min) ont été modulées grâce à un cuiseur-broyeur. La structure de la purée (volume occupé par les particules, taille des particules, viscosité du sérum) et la texture (viscosité, seuil d'écoulement, G' et G") ont ensuite été analysées et comparées entre les matières premières et les conditions du procédé. Les pectines ont été extraites et leur composition chimique ainsi que leur structure ont été corrélées à la structure de la purée. La taille des particules s'est montré être le déterminant majeur de la texture des purées en absence de dilution ou de concentration. Le degré d'adhésion cellulaire (défini par la structure et la composition des pectines) a eu un impact plus important sur la taille des particules que la taille des cellules individuelles (définie par les cultivars ou les pratiques culturales). D'autres facteurs structuraux, tels que la viscosité du sérum ou la quantité de pulpe, n'ont contribué à la texture des purées qu'à taille de particules constante. La fragmentation tissulaire, déterminant la taille des particules pendant le procédé, a été principalement affectée par l'intensité du cisaillement. Le stockage post-récolte des pommes et des températures élevées (95 °C) ont induit une dégradation et une solubilisation des pectines, en particulier par l'hydrolyse des chaînes latérales des rhamnogalacturonanes I. Cela a réduit l'adhésion cellulaire et la fragmentation tissulaire a ainsi été favorisée. Ces résultats ont permis d'approfondir la compréhension de la fragmentation tissulaire et des changements de texture au cours du procédé ce qui permettra de fournir des directives à l'industrie pour mieux gérer la diversité et l'hétérogénéité des fruits pendant le procédé de transformation des fruits en purée.

Malus x domestica Borkh., Purée, Rhéologie, Maturation, Traitement thermique, Fragmentation tissulaire, Polysaccharides pariétaux

Abstract

The objective of this thesis was to understand how structural characteristics in raw apples can be linked to structural factors in purees after cooking and tissue fragmentation. Structural characteristics of the fruit were modulated by cultivars, agricultural practices and maturation, and process conditions (thermal: 50–95 °C and mechanical: 100–3000 rpm) were modulated in a cooker-cutter during processing. Puree's structure (volume occupied by particles, particle size, serum viscosity) and texture (viscosity, yield stress, G' and G") were then analysed and compared between raw materials and process conditions. Pectins were extracted and their chemical composition and structure were correlated to puree's structure. Particle size appeared to be the most important determinant of puree's texture when there is no dilution or concentration of the fruit tissue. The extent of cell adhesion (defined by pectin structure and composition) determined particle size more than individual cell size (defined by varietal effects or agricultural practices). Other structural factors only contributed to puree's texture once particle size was constant. Tissue fragmentation, determining particle size during processing, was principally affected by shear intensity. Post-harvest maturity of the raw apples and high temperatures (95 °C) induced pectin degradation, especially rhamnogalacturonan I side chain hydrolysis, and solubilisation. This led to reduced cell adhesion and tissue fragmentation was additionally favoured. The results deepened the understanding of tissue fragmentation and textural changes during processing and provided guidelines for industry to manage diversity and heterogeneity of raw fruits during processing.

Malus x domestica Borkh., Puree, Rheology, Maturation, Heat processing, Tissue fragmentation, Cell wall polysaccharides

AVIGNON UNIVERSITÉ